1982

Fluorescence line narrowing spectrometry of polycyclic aromatic hydrocarbons in organic glasses

Johnie Charles Brown
Iowa State University

Brown, Johnie Charles

FLUORESCENCE LINE NARROWING SPECTROMETRY OF POLYCYCLIC AROMATIC HYDROCARBONS IN ORGANIC GLASSES

Iowa State University PH.D. 1982

PLEASE NOTE:

In all cases this material has been filmed in the best possible way from the available copy. Problems encountered with this document have been identified here with a check mark __√__.

1. Glossy photographs or pages ____√____
2. Colored illustrations, paper or print ____√____
3. Photographs with dark background _____
4. Illustrations are poor copy _____
5. Pages with black marks, not original copy _____
6. Print shows through as there is text on both sides of page _____
7. Indistinct, broken or small print on several pages _____
8. Print exceeds margin requirements _____
9. Tightly bound copy with print lost in spine _____
10. Computer printout pages with indistinct print _____
11. Page(s) _____ lacking when material received, and not available from school or author.
12. Page(s) _____ seem to be missing in numbering only as text follows.
13. Two pages numbered _____. Text follows.
14. Curling and wrinkled pages _____
15. Other _____

Fluorescence line narrowing spectrometry of polycyclic aromatic hydrocarbons in organic glasses

by

Johnie Charles Brown

A Dissertation Submitted to the
Graduate Faculty in Partial Fulfillment of the
Requirements for the Degree of
DOCTOR OF PHILOSOPHY

Department: Chemistry
Major: Analytical Chemistry

Approved:

Signature was redacted for privacy.

In Charge of Major Work

Signature was redacted for privacy.

For the Major Department

Signature was redacted for privacy.

For the Graduate College

Iowa State University
Ames, Iowa

1982

TABLE OF CONTENTS

LIST OF FIGURES

LIST OF TABLES

GLOSSARY OF ABBREVIATIONS USED

A	Anthracene
Å	Angstrom (0.1 nm)
1-AP	1-Alkylpyrene
BaP	B(a)P, Benzo(a)pyrene
BeP	B(e)P, Benzo(e)pyrene
BghiP	B(ghi)P, Benzo(ghi)perylene
BkF	Benzo(k)fluoranthene
C	Capacitance in Farads
c	Concentration
CC-GC	Capillary Column Gas Chromatography
CC-GC/MS	Capillary Column GC/MS
cm^{-1}	Inverse centrimeters or wavenumbers
DBP	3,4,9,10-Dibenzpyrene
DBrA	9,10-Dibromoanthracene
DMA	9,10-Dimethylanthracene
EtOH	Ethanol
FLN	Fluorescence Line Narrowing (or Narrowed)
FLNS	Fluorescence Line Narrowing Spectrometry
GC	Gas Chromatography
GC/MS	Gas Chromatography/Mass Spectrometry
HPLC	High Performance Liquid Chromatography
I_o	Incident (excitation) beam intensity
I_f	Fluorescence intensity
IR	Infrared radiation

L	Laser line
LESS	Laser Excited Shpolskii Spectrometry
MA	9-Methylanthracene
MI	Matrix Isolation
MI-FT-IR	Matrix Isolation-Fourier Transform-Infrared
MI-IR	Matrix Isolation-Infrared
MP	1-Methylpyrene
MTHF	Methyltetrahydrofuran
nm	Nanometers
O	Origin line
(0,0)	Origin line
P	Pyrene
PA	9-Phenylanthracene
PAH	Polycyclic Aromatic Hydrocarbons
Pe	Perylene
PSB	Phonon Side Band
Q	Charge in Coulombs
R	Raman line
RMP	Resonant Multiphoton Photoionization
SF	Scale Factor
U	Unidentified or Unknown Peak
uv	Ultraviolet Radiation
Δv	Electrical potential difference in volts
XEOL	X-Ray Excited Optical Luminescence
ZPL	Zero Phonon Line

Ω	Resistance in Ohms
μf	Microfarads
λ_{ex}	Excitation Wavelength
?	Structure of uncertain origin
$\Delta\nu$	Linewidth in wavenumbers

I. INTRODUCTION

A. Preamble

This dissertation is concerned with the description of a new fluorescence-based analytical method for the differentiation and quantitation of closely related pollutant species in complex mixtures. The technique, fluorescence line narrowing spectrometry (FLNS) of impurity species embedded in organic glasses, is shown to be a powerful tool for the determination of polycyclic aromatic hydrocarbons (PAHs). Although only PAH analysis is considered here, the reader will appreciate that FLNS using glassy hosts should be applicable to any class of fluorescent compounds. This generality results from the underlying physics of the fluorescence line narrowing phenomenon itself and from the large number of glasses available for testing.

B. Definition of Problem

Analysis of PAH compounds presents an important problem to modern scientists largely because the occurrence of PAHs is not well understood. Their notoriety arises from the fact that many of the PAHs are known to induce or promote cancer. Indeed, they constitute one of the largest and most potent classes of chemical carcinogens (1). However, PAH species occur throughout the biosphere and are routinely metabolized by plants and microorganisms. The presence of PAH material in the soil is important. In fact, several PAHs have been shown to act as growth factors in plants. Curiously, those species most potent at promoting plant growth are also most dangerous to mammals (1).

Of particular concern, now that human civilization covers much of the earth, is the generation of PAH concentrations far higher than the natural background.[1] Many human activities, especially those involving the pyrolysis or imperfect combustion of organic material, produce large amounts of many PAH compounds. Given that our use of fuels such as solvent refined coal and others which are derived by pyrolytic processes from fossil organic material is projected to increase substantially, PAH production and the concomitant threat to public health and the environmert can also be expected to grow. The need to develop methods which possess the power required for PAH analysis is, therefore, becoming increasingly urgent.

Intelligent assessment of the ramifications of environmental PAH material is an exceedingly formidable task. There exists a great number of PAH species, including parent compounds (distinguished by the size, number, and arrangement of aromatic rings) and a myriad of substitutional derivatives. Real samples frequently contain hundreds of these individual PAH species along with vast quantities of other organic material. For example, 153 PAHs have been identified in the brown tar condensed from tobacco and marijuana smokes (2), while 122 PAH species have been extracted from airborne particulates (3). It is not sufficient to characterize the PAH content of these mixtures in such a coarse grained manner as determination of the amounts of material with various numbers of rings.

---

[1]Natural soils contain PAHs at concentrations between 10 and 0.1 parts per million (ppm, mg/kg) while most natural waters contain between 0.01 and 1.0 parts per billion (ppb, μg/ℓ) total PAH (1).

PAH species with only subtle structural dissimilarities can display marked differences in biological activity. This arises as a manifestation of the extreme geometric specificity exhibited by the enzyme systems of living organisms. For example, benzo(a)pyrene is highly carcinogenic while its otherwise similar structural isomer, benzo(e)pyrene, is far less dangerous. Likewise, 5-methylchrysene is among the most potent of known carcinogens while the parent, chrysene, and the remaining five methyl isomers are all relatively innocuous (4,5). In addition, the potency and low natural abundance of individual PAH species make their occurrence important at or below the ppb (10^{-9} g ml^{-1}) concentration level. Thus, a satisfactory analytical technique must permit determination of many individual PAH compounds at low concentrations in very complex mixtures.

Considerable effort has been expended by many investigators in attempts to develop methods for PAH analysis. In the next chapter, several of the most prominent methodologies are discussed with the intent of underscoring the need for a more powerful analytical tool. To this end, a set of ideal attributes, against which the power of PAH analysis techniques can be gauged, is delineated. The first two of these attributes are actually requirements which must be met by any technique applied to this problem. The other three qualities complete a list of the five most desirable attributes to be possessed by any ideal method. This list of attributes, along with brief explanations, follows on a separate page for easy reference during later discussions.

In addition to possession of the delineated attributes, a new analytical methodology will have greater impact on the scientific community if it is applicable to a number of different classes of analyte species.

How well FLNS in glasses fares in this regard as well as in satisfying the requirements for solution of the PAH analysis problem will be carefully considered throughout this dissertation.

C. Ideal Attributes

To solve the PAH analysis problem (or any other pollutant analysis problem involving a large class of highly potent compounds), it is desirable to employ a technique that has:

(i) high selectivity -- allowing differentiation of essentially any chosen species in complex mixtures which may include many closely-related isomers.

(ii) high sensitivity -- with the low detection limits and large working range required for sensitive determination of many compounds over a wide range of concentrations in a single sample.

(iii) quantitative response -- allowing direct absolute quantitation, preferably without recourse to internal standards, standard additions or extensive preparation,

(iv) practicality -- providing the capability for routine analysis for many species in many samples without exhausting expensive supplies or requiring a highly skilled and specialized operator,

(v) nondestructive measurements -- facilitating attributes ii, iii, and iv by enhancing flexibility and allowing determination of the compounds of interest in any order with observation times commensurate with good signal-to-noise ratios.

II. REVIEW

A. Chromatography

Gas chromatography (GC) and high performance liquid chromatography (HPLC) combined with a host of detectors have become a panacea in recent years. The analytical literature is replete with papers devoted to the development and application of these techniques. However, the large number of compounds, and the great chemical and physical similarity between the many isomeric species within the PAH class, present a particularly thorny problem to chromatographers. The partition coefficients on which chromatographic separations are based are nearly identical for many structural isomers. Early chromatographic techniques, therefore, only allowed for determination of the few species for which interferences were minor. The more successful of these techniques, as referred to in the 1970 World Health Organization review (1), were rather elaborate and resulted only in dubious quantitation of one or a few species in real samples, due to severe interference problems.

In more recent years, chromatographic separation techniques have undergone significant improvement. Improved separation of closely related species, however, often involves the use of special low capacity chromatographic columns. For this reason, separation of structurally similar species requires that they first be separated from the rest of the sample matrix. One technique reported to be in routine use (6) involves the following procedure: two liquid/liquid extractions steps to isolate the neutral organic phase; gel permeation chromatography to

select the multi-ring compounds; thin layer chromatography to separate and concentrate the PAH fraction; and injection into a high resolution packed GC column under programmed heating to obtain the final chromatogram. Despite the complexity of this procedure, only partial resolution of geometric isomers such as anthracene and phenanthrene is obtained. Consequently, this method is practical only for such simple problems as the one for which it was developed.[2]

At the present time, the most powerful separation technique (from the standpoint of attribute i) is capillary column-gas chromatography (CC-GC). Many of the strengths and limitations of CC-GC are illustrated in a recent paper by Lee et al. (7). In this work, a 1 hr. and 40 min. CC-GC chromatogram is presented which demonstrates resolution of most of the constituents in a 209 component artificial PAH mixture. However, substitutional[3] isomers were not resolved. Nonetheless, differences in their retention indices were measured which indicate that their separation should be achievable with a column of sufficient length and a longer analysis time.

---

[2]This technique is used to compare the PAH contents of extracts of the particulates collected by a standard smoking machine from various cigarette tobacco blend and filter combinations.

[3]Substitutional isomers have the same parent and the same substituent group but differ in the position at which the substituent is attached.

Application of CC-GC to the PAH fraction of a natural mixture produces a profusion of resolved and partially resolved chromatographic peaks (2,3). The shear number of peaks and the fact that their positions shift with age of the column, sample composition, and other factors make identification of the analyte peaks an arduous task. In actual analyses, this job is facilitated by the use of internal standards (7) and/or standard additions (8). Utilization of these techniques and sufficiently long capillary columns, in principle, allows for the determination of any species.

However, there are trade-offs which make CC-GC by itself impractical for solution of the PAH analysis problem (7-9). The heavy loading required for determination of minor constituents in natural mixtures results in rapid degradation of the expensive CC-GC columns (7,8). Most CC-GC techniques are destructive, lacking the advantages noted in attribute v. The recompense for GC is the one picogram detection limits[4] afforded by flame ionization detectors (8,9). This, together with preconcentration or dilution during the preseparation steps, yields an excellent working range and partially compensates for many of the shortcomings.

Greatly enhanced selectivities are obtained by combining chromatographic separations with detectors which themselves are specific. For

---

[4]One picogram (10^{-12} grams) corresponds to a concentration of one ppb in a typical injection volumn of one microliter (9).

example, modern HPLC instruments for PAH analysis employ detectors which provide resolution based on molecular electronic absorption and luminescence properties (10,11). For the most part, however, HPLC is being relegated to use as a preseparation tool for more specific methods (8,10,12). In GC, such exotic selective detectors as rotationally cooled fluorescence (13) and matrix isolation infrared, Raman, and fluorescence spectrometries (14-16) are now being evaluated for use in PAH analysis, vide infra.

To date, gas chromatography/mass spectrometry (GC/MS), particularly when capillary columns are employed (CC-GC/MS), has been the most successful of the chromatography/selective detector combinations for addressing the PAH problem (2.3,8). The characteristic mass fragmentation pattern of each molecular species facilitates the assignment of CC-GC peaks. Frequently, selective ion monitoring[5] of the GC effluent can allow for rapid and simple determination of one or a few compounds per injection (8). However, compounds that are very similar and difficult to separate also tend to fractionate in much the same manner. Differentiation, therefore, often requires information contained in a complete mass scan. The sophisticated instrumentation required to obtain mass scans of each peak in the GC effluent and the extensive data handling system needed to present these data in a useable form make the

---

[5]This involves setting the mass spectrometer to pass only ions of a mass characteristic for the species being determined.

CC-GC/MS system that would be needed for PAH analysis extremely expensive, about one half million dollars (8). In the hands of an expert, this tool should allow for the determination of essentially any molecular species from complex mixtures. The fact that the GC-MS data may contain information leading to the identification of compounds, whose presence in the sample were not previously suspected, is a major advantage.

Because of its applicability to a wide variety of problems, CC-GC/MS will probably continue to be the most widely used high resolution technique. However, its complexity and expense detract from its desirability as a routine method for the high resolution analysis of PAHs in complex mixtures. The development of simpler methods which still have the delineated attributes is, therefore, highly desirable.

B. Spectroscopy

1. General comments

Analytical methods which utilize detectors that are more selective than mass spectrometers hold the most promise as replacements for CC-GC/MS in routine PAH analysis. Many of the highly selective physical techniques under investigation involve molecular electronic and vibrational spectroscopy. These techniques have a great potential for specificity since the spectroscopic transitions of molecules are highly dependent upon their structure. Each PAH species has a unique spectrum (17). However, classical spectroscopic methods usually produce broad band spectra which meld into informationless continua for all but the

most simple mixtures. As already pointed out, it is not practical to separate PAH species completely from real mixtures for identification and quantitation. The techniques discussed in the following subsections, therefore, are considered primarily because of their potential for increased specificity.

2. Gas phase spectroscopy

The broad bands in the spectra of polyatomic molecules in the gaseous phase are largely caused by unresolved rotational and overlapping sequence bands (18,19). Rotationally cooled fluorescence spectroscopy (13) is one promising technique for alleviating some of the spectral congestion and circumventing this selectivity problem. To obtain narrowed fluorescence bands, the proposed analytical method involves expension of a GC effluent through a "supersonic" nozzle. Collisions with the translationally cooled carrier gas lead to a marked rotational cooling of the analyte molecules ($\leq$ 2K). Laser excitation of molecules in the supersonic jet affords fluorescence bands as sharp as a few wavenumbers. These narrow spectral linewidths should allow resolution of the fluorescence lines, thus providing a unique fingerprint for each species. Computer routines should allow deconvolution of the signals from species that elute together, thereby decreasing the demands on GC resolution.

Another novel gas phase technique utilizes resonant multiphoton photoionization (RMP) (19,20). By taking advantage of the high peak powers of pulsed lasers and sensitive current measurement instrumentation, detection limits on the order of one femptogram (10^{-15} g) are

possible (20). The signal most often used is the one arising from two photon ionization by a single laser beam. Selectivity arises from the fact that the first photon must be resonant with a real intermediate vibronic state and the second photon absorbed by the same molecule must result in ionization. High specificity for the PAH class can be achieved. However, complex mixtures of PAHs cannot be resolved since the broad gas phase absorption bands and the similar ionization energies result in signals from a large fraction of the species present.

The greatest promise for this technique lies with its low detection limits. A one femptogram detection limit would allow determination of species down to the parts per trillion concentration level in a one microliter GC injection volume. This makes the RMP technique very attractive as a sensitive detector for high resolution CC-GC. The ability to reject signals from other classes of compounds is in itself valuable. Even greater specificity and resolving power may be achieved by incorporating ion mobility measurements (20) or rotational cooling into the CC-GC/RMP methodology.

Both of the techniques described in this subsection are in the initial stages of development and show great potential. Neither has been shown to possess the attributes of an ideal PAH analysis technique in actual practice. However, the high degree of discrimination between unseparated species with a single laser wavelength makes GC/rotationally cooled fluorescence especially attractive.

Most of the attention in the last ten years has been focused on condensed (solid or liquid) phase spectroscopies. The remaining

methodologies in this chapter are all based on condensed phase spectroscopies and are presented in approximate order of increasing power for PAH analysis.

3. Vibrational spectroscopy

Infra-red absorption (IR) and Raman vibrational transitions of organic molecules in room temperature solutions give rise to relatively sharp spectral bands, 20-30 cm^{-1} as opposed to 200 cm^{-1} for their electronic counterparts.[6] These spectroscopies alone, however, cannot solve the PAH analysis problem. This results, in part, because the fundamental vibrational frequencies of molecules span only the narrow range between about 200 and 4,000 cm^{-1}. Another problem is that IR and conventional, nonresonant, Raman spectroscopies yield signals from every molecule in a mixture. Furthermore, for a molecule with N atoms, there are 3N-6 fundamental vibrations, roughly half of which will appear in a given IR or Raman spectrum. The spectral congestion that these three intrinsic properties portend prevents achievement of the required selectivity, cf., attribute i.

Raman and IR methods for PAH analysis that utilize low temperature matrix isolation (MI) techniques (vide infra) for increased spectral resolution are under investigation. These MI-IR and MI-Raman methods yield bandwidths on the order of 2.0 cm^{-1} (4,16,21). It has been shown

---

[6]All spectral bandwidths are expressed as the full width at half the maximum peak height (FWHM).

(4,16) that this allows the differentiation of even closely related substitutional isomers as long as there are no more than six or seven species present in the mixture. The necessity for chromatographic separation when using these techniques is, therefore, firmly established. When these techniques are used as chromatographic detectors, the line rich spectra become an asset, facilitating the identification and further differentiation of partially separated species (4,16,21).

Chromatography utilizing MI-IR or MI-Raman as detectors is not likely to rival GC-MS as a PAH analysis tool. Utilization of the most sensitive Fourier transform techniques in MI-IR (MI-FT-IR) yields detection limits only in the fractional microgram range (21). Likewise, MI-Raman is reported to have detection limits on the order of nanograms (16). The one picogram detection limit of GC/MS (8) makes it three to six orders of magnitude more sensitive, cf., attribute ii.

4. Electronic molecular absorption

The lowest electronically excited singlet states of organic molecules range in energy from the ultra-violet (uv) at about 50,000 cm^{-1} to the near infra-red at about 10,000 cm^{-1}. The spectral coverage of uv-visible spectroscopy is, thereby, roughly ten times that for vibrational spectroscopy. Since the vibronic spectra of individual PAH species are dispersed throughout the uv-visible region (17), the possibility exists that uv-visible spectroscopy may provide greater selectivity than IR or Raman methods. However, the most obvious way to probe the vibronic transitions of PAHs, room-temperature solution absorption spectrometry, suffers from two major problems.

First, classical absorption is calculated from transmittance and involves the measurement of small changes in large signals. Even the best instrumental methods cannot completely eliminate contributions by source noise. Because of this, transmittance methods suffer from a limited dynamic range[7], cf., attribute ii. The second drawback is the fact that classical techniques do not address the thermal or solutional broadening problem. These phenomena account for the greater than 200 cm^{-1} bandwidths which preclude the utilization of classical absorption techniques for the resolution of complex mixtures. Hence, these techniques are only used as rather nonselective HPLC detectors in PAH analysis. Typical applications involve measuring the absorbance of HPLC effluents in the 200-300 nanometer (nm) wavelength region where most PAHs absorb strongly.

5. Classical luminescence

The vibronic transitions observed in absorption can be probed with vastly improved sensitivity by using the photoexcitation technique. For fluorescent species, e.g., virtually all PAHs, the wavelength of an

---

[7] A reasonable lower limit for measurable absorbance is about 0.01 (22). Combined with a reasonable maximum PAH absorptivity of 10^5 (17), this indicates a detection limit of about 10^{-7} molar or 20 ppb in a one centimeter cell. An upper absorption limit of 2.0 corresponds to a concentration of about 4 ppm which yields only a two decade working range.

excitation beam can be scanned while monitoring the total luminescence from the sample. This photoexcitation spectrum will have peaks in emission at wavelengths corresponding to maximum absorptions of the excitation beam. Since luminescence signals are measured as differences from zero, source noise is not as important allowing extremely low detection limits. Richardson and Ando (23), for example, reported detection limits for pyrene, a common PAH, at less than one part-per-trillion (pptr, 10^{-3} ppb) when a laser was used to excite luminescence.

Luminescence methods are much more flexible than simple transmittance techniques. In addition to photoexcitation spectra, the analyst can scan the luminescence spectra at fixed excitation wavelengths to obtain dispersed luminescence spectra. A dispersed luminescence spectrum will generally be comprised of higher and lower energy portions due, respectively, to fluorescence and phosphorescence. Vibronic transitions for the former and latter originate, in almost all cases, from the zero-point vibrational level of the lowest excited singlet (S_1) and triplet (T_1) states, respectively. These transitions terminate at various vibrational sublevels of the ground state. The energies of the transitions and the lifetime of the emitting states are highly species dependent (17).

Luminescence techniques thus provide three modes of selectivity: selective excitation whereby a specific vibronic absorption band is irradiated; selective observation utilizing the dispersed luminescence spectrum; and temporal resolution whereby species are distinguished on the basis of their radiative lifetimes. Combining this great potential

for selectivity with the sensitivity resulting from the high fluorescence and/or phosphorescence quantum yields of many PAHs (17), one can understand why the development of new PAH analysis techniques based on molecular luminescence is so attractive.

It should be emphasized, however, that the same mechanisms which broaden absorption transitions also produce broad bands in luminescence. The vibronic bands are so broad ($\sim$ 300 cm^{-1}) that the usefulness of room temperature solution techniques for PAH analysis is quite limited. The most popular utilization of broad-band luminescence is as a sensitive HPLC detector which allows the knowledgeable analyst to deconvolute some overlapping chromatographic peaks (10). However, this situation would be expected to change when techniques for circumventing the broadening problem are employed.

6. Synchronously scanned luminescence

One recently publicized technique for PAH analysis involves an elegant utilization of two of the selectivity modes inherent in luminescence methods. This methodology, synchronously scanned luminescence (24-26), is based upon selection of a wavelength difference which corresponds to the difference in energies between a prominent absorption and a prominent luminescence transition for a particular species. By simultaneously scanning both excitation and emission while maintained this fixed wavelength difference between the two light beams, it is possible to produce spectra that are much less complicated. For a single compound, the spectrum can be as simple as a single

slightly narrowed peak (24,25) instead of the band rich spectra produced by other dispersed luminescence techniques.

This simple technique cannot solve the aforementioned PAH analysis problem in spite of its advantages over more conventional luminescence techniques. The increased luminescence structure for mixtures which is produced by the simplified spectra of each component has been used to demonstrate the presence of a compound in an unseparated natural mixture (25). Also the individual species in a few five and six component artificial mixtures have been resolved and quantitated (24,25). However, the energy differences between strong transitions turn out to be shared by many PAH species due to structural and thus vibrational similarities (26). This and the still broad bands result in many interferences in any complex mixture (26). Synchronously scanned luminescence may find its greatest application as a field portable technique for tracing the sources of PAH contaminations.

C. Low Temperature Solid State Luminescence

1. General comments

The room temperature vibronic spectroscopic techniques, just described, do not address the problem of thermal broadening. Fluorescence line narrowing spectroscopy and the other methods to be reviewed in the following pages, all deal with this problem (to a greater or lesser extent) by utilizing low temperature solid state spectroscopic matrices. These methods differ in the way that they deal with

inhomogeneous line broadening and in their applicability to the solution of the PAH analysis problem.

2. Matrix isolation

Wehry and his colleagues have been investigating applications of matrix isolation (MI) spectroscopic techniques to PAH analysis (4,14,21, 27-30). MI methods usually require that the PAH sample be first separated from any solvent and then vaporized and deposited along with a large excess of "inert" gas as a solid "matrix" on an optical surface within a cryostat. Temperatures below 20K are used to eliminate the effect of thermal broadening. High dilution with the inert gas, usually N_2 or Ar, eliminates strong interactions between analyte molecules.

These experimental conditions result in narrowing of the vibronic bands observed for the PAH species being analyzed. The actual amount of band narrowing will be limited by the disorder in the matrix. Disorder results in a wide range of possible environments for the analyte molecules embedded in the host and results in observation of what is referred to as site inhomogeneous line broadening (31). For the matrices used in PAH analysis, disorder is considerable resulting in bandwidths of 70 to 90 cm^{-1} when classical light sources are employed (27-29). In other types of matrices, these same vibronic transitions can be considerably sharper, vide infra (31).

However, this threefold improvement in linewidths, as compared to room temperature spectra, results in a corresponding increase in selectivity. The MI-dispersed-luminescence technique has been

demonstrated to be capable of allowing determination of six common PAHs in an artificial mixture (27). The same paper reports qualitative identification of three major constituents in a natural PAH fraction via this method (27). As would be expected, vide supra, improvements in selectivity are also gained by utilizing both temporal resolution (29) and selective excitation into the narrowed absorption bands (14, 28). Another advantage is that once the sample is in the matrix, sensitivities of about one part in 10^{11} and a five order of magnitude linear working range can be achieved (28), cf., attribute ii. Also, luminescence in the matrix is nondestructive with the accompanying advantages described in attribute v.

MI-luminescence spectrometry utilizing broad band excitation is not the answer to the PAH analysis problem. The luminescence bands are still too broad to allow the spectral interferences to be reduced to the requisite level for direct analysis of natural samples. For example, differentiation of closely related substitutional isomers is probably not possible. Quantitation of minor constituents which luminesce in the same region as more intense signals would also be difficult. Thus, the requirement listed as attribute i is not met. Quantitation schemes utilizing internal standards are necessary (28) to compensate for irreproducible deposition of sample components, cf., attribute iii. Also, considerable skill may be required to lay down a useful sample matrix, cf., attribute iv. Nevertheless, these techniques are certainly powerful enough to warrant continuing investigations, especially in light of their potential as GC detectors (14,27).

3. Mixed crystal

It has long been known that some of the vibronic bands in the spectra of PAH species can be greatly narrowed by the employment of suitable single crystal host matrices (13,31-33). At matrix temperatures below about 15K, thermal broadening is negligible (a few cm^{-1}). Incorporation of the guest PAH molecules into specific well-defined "sites" within the host crystal minimizes inhomogeneous broadening. Vibronic transitions associated with the lowest excited singlet state (S_1) of the guest PAH can thereby be as sharp as a few cm^{-1} in these systems. With few exceptions, it is only the S_1 state of π-electron molecules (such as the PAHs) which fluoresce with reasonable quantum yields (17). In suitable mixed crystal systems, excitation of any electronic state of either impurity or host will result in radiationless transitions to the zero-point vibrational level of the S_1 state of the impurity. It is possible in mixed crystal systems, therefore, to observe fluorescence from the guest with linewidths on the order of a few cm^{-1} even when using classical broad band excitation.

Unfortunately, this technique for obtaining very sharp line fluorescence is not applicable as an analytical method due to severe problems associated with mixed crystal sample preparation. In order for the guest to be accepted into the host lattice, there must be a close match between the physical dimensions of the two types of molecules. Also, the S_1 system for the host must lie above the S_1 system for the guest. A different host, thus, is required for almost every analyte.

Even with a suitable host, sample preparation time is usually unacceptably long, several hours at least.

4. Shpolskii effect

Another low temperature solid state spectroscopic method allows observation of sharp line luminescence without single crystal preparation. Known as the Shpolskii effect, this technique was originally characterized and used by the physical spectroscopists as a widely applicable way to obtain high resolution spectra of polyatomic molecules (34-36). To observe this effect, the compound of interest is dissolved in an n-alkane solvent with linear molecular dimensions which match the length of at least one side of the rigid portion of the impurity molecule. The sample is then cooled to liquid nitrogen temperatures or below so that the guest molecules are incorporated into the lattice of n-alkane microcrystals. Ideally, the impurity molecules will occupy only one or a few well-defined "sites" within the crystal lattice. As described in the preceding subsection, the crystalline media can lead to a minimization of inhomogeneous broadening. As a result, observation of both absorption and luminescence spectra consisting of small groups of sharp "quasilines" for each vibronic transition is possible.

Several papers have been published on analytical applications of the Shpolskii effect. Kirkbright and DeLima in 1974 (37) reviewed earlier analytical work and characterized the luminescence spectra of twenty-three PAH species in several solvents at 77K. Their work illustrates many of the qualitative and quantitative aspects of the Shpolskii technique. The one very promising aspect of this methodology

is the line rich spectra which facilitate unambiguous identification of individual PAH species. However, several solvents had to be used since no single n-alkane matrix could be found which would produce the Shpolskii effect for all of the PAH species of interest. To some extent, this adds another mode of selectivity, i.e., the solvents which cause the analyte to exhibit the Shpolskii effect aid in its identification. The issue is not that simple, however, since the degree of mismatch was observed to produce a distribution of linewidths ranging from broad band to quasilines as narrow as instrument resolution and the thermal broadening at 77K would allow.

Use of the Shpolskii effect as reported by Kirkbright and DeLima requires the analyst to contend with the above and several other inherent problems (37). The spectra of mixtures, for example, are extremely complicated due to the overlapping line rich spectra of the constituent species. With classical broad band excitation, the determination of eight individual species in an artificial mixture was shown to be just barely possible (37), cf., attribute i. Interestingly, these authors (37) proposed the utilization of tunable narrow-line dye lasers to take advantage of the sharp quasilinear absorption spectra for highly selective excitation. This method for obtaining greatly simplified spectra from mixtures in Shpolskii matrices is the crux of a new Shpolskii technique (38) to be reviewed at the end of this chapter.

Quantitation and prediction of the location of the best analytical line are also problems. The relative intensities of the quasilines for a species not only can shift with differences in solution composition,

but they also depend on the microscopic details of sample formation. Difficulties can also arise from irreproducible exclusion of the analyte molecules from the n-alkane microcrystals and from aggregate formation. In addition, the opaque microcrystalline matrices make it difficult to excite and collect luminescence reproducibly. Kirkbright and DeLima (37) found it necessary to utilize a combined internal standard-standard additions method to achieve quantitation with a working range of more than two decades in concentration, cf., attributes ii and iii. Recent analytical Shpolskii methods attempt to minimize irreproducible exclusion of the analyte and aggregate formation, vide infra, by either employing very rapid cooling rates (37) or by depositing the Shpolskii matrix from the vapor phase (30).

From the long list of problems, it seems obvious that the Shpolskii technique, as described by Kirkbright and DeLima (37), cannot alone solve the PAH analysis problem. One recent paper (39) reports an interesting but complicated application of the Shpolskii effect as a detector for HPLC.

5. XEOL

X-ray excited optical luminescence (XEOL) (40-42) is another Shpolskii technique which must be covered in any review of PAH analysis methods. Excitation of the n-alkane lattice with x-rays followed by a complex energy transfer process results in the population of the luminescent states of PAH species in a Shpolskii matrix (42). XEOL detection limits are in the fractional ppb range (42), a one to two

order of magnitude improvement over those reported by Kirbright and DeLima (37).

On the negative side, XEOL still suffers from most of the problems outlined in the preceding subsection. In addition, x-ray bombardment causes the PAHs to photodecompose so that the technique does not possess attribute v. XEOL of complex natural samples is little better than a survey tool allowing for the identification of major luminescent species only (41). However, the technique has been used successfully to quantitate individual species in HPLC fractions from a natural sample (38). In this author's opinion, though, the analyst would not choose HPLC/XEOL as a routine PAH analysis method if either of the following two techniques were available.

D. Laser Pumped Low Temperature Solid State Luminescence

Only two techniques remain to be discussed. Both are new and both depend upon the use of tunable narrow-line laser systems. Both methods should allow qualitative and quantitative determination of any or all of the fluorescent PAH species in natural samples with a minimum amount of preseparation. One technique, FLNS, will be discussed throughout the remainder of this thesis. The other, laser excited Shpolskii spectroscopy (LESS), is being developed by another group within this laboratory (38,43) and will be briefly described below

The LESS technique involves incorporation of the sample into an n-alkane Shpolskii matrix. However, the utilization of narrow-line

laser excitation makes this method much more powerful than the Shpolskii techniques discussed earlier. The narrow laser line can be used to greatly enhance selective excitation as predicted earlier (37). Also, as it turns out, the site selection process causes excitation into a single absorption quasiline to produce luminescence spectra that contain a single sharp line at each vibronic transition rather than the multiplet produced by broad-band excitation.

The improved selective excitation and the simplification of individual species luminescence allow this technique to produce spectra for a single component in a natural mixture which resemble a spectrum taken of that component by itself. Both groups investigating laser excited luminescence from Shpolskii matrices (30,38,43) have utilized temperatures in the 15 to 16K range in order to fully realize the advantages of optical site selection spectroscopy.

Optical site selection allows luminescence to be excited only from those analyte molecules which are contributing to the absorption quasiline overlapped by the laser. Other analyte molecules in the n-alkane matrix occupy different sites within the microcrystals which result in different transition energies. Normally, the molecules contributing to absorption quasilines other than the one overlapped by the laser will not be excited and will not luminesce. The single sharp line at each luminescence transition results because only molecules in identical sites are being excited.

It is not necessary for the absorption band to be sharp in order to excite narrow line fluorescence with a narrow line excitation source.

Under the conditions used by the above investigators, a species in the matrix that is not experiencing the Shpolskii effect can emit fluorescence lines just as sharp as those for species which can fit into the n-alkane crystals and experience the Shpolskii effect. This fact has been known since the early papers on fluorescence line narrowing (FLN) by Personov et al. (44) and Bykovskaya et al. (45). Since the Shpolskii effect is not required, it seems logical to abandon the n-alkane matrices with all of their inherent problems and to do optical site selection in a better host. This is, in fact, what is done in FLNS from organic glasses which was published as an analytical method for PAHs by this group in 1978 (46).

As would be expected from the preceding argument, FLNS and LESS share the ability to produce sharp line fluorescence spectra. By abandoning the polycrystalline Shpolskii matrices, FLNS gains many advantages for quantitative analysis (46,47). By utilizing the Shpolskii effect, LESS can be more selective producing cleaner looking spectra for species in complex mixtures because of great enhancements in the absorption of the chosen species. The LESS method should also produce sharp line phosphorescence for some species. This is not normally possible for FLNS.

The arguments about which technique best satisfies the attributes of an ideal analytical technique will continue after this dissertation is published. The full power of both techniques has yet to be realized. More comparisons will be made near the end of this report after a more thorough discussion of the theory and practice of FLNS has been

presented. Before continuing, however, two points must be kept in mind. Both LESS (43) and FLNS (47) have been shown to be capable of allowing determination of several PAH species in unseparated SRC-II[8] samples. Secondly, FLNS is the more general technique.

---

[8]SRC-II is the product from one of the experimental solvent refined coal liquification processes. This material is very high in PAHs.

III. THEORY OF FLNS

A. Physical Aspects

The phenomenon of fluorescence line narrowing or optical site selection spectroscopy was first reported by Szabo in 1970 (48). In this early paper it was reported that narrow line ruby laser excitation, at temperatures below about 80K (to prevent "spectral diffusion"), produced narrow line fluorescence from Cr^{3+} in a cooled ruby sample. Under these experimental conditions, the fluorescence bands were narrowed to about 0.7 cm^{-1} from the broad band excited value of 15 cm^{-1}.

In 1972, Personov et al. (44) reported a similar effect for organic compounds. At sufficiently low temperatures, laser excitation was found to produce lines as narrow as 1.0 cm^{-1} in the fluorescence spectrum of perylene whether in microcrystalline n-undecane or glassy ethanol matrices. That sharp lines were produced, irrespective of the host used, when perylene was excited in the vicinity of its S_1 absorption origin with a narrow line excitation source was an important observation.

FLNS, for the first time, gave spectroscopists a tool for studying sharp line spectra of many polyatomic molecules without the need for finding suitable crystalline hosts (44,45,49-51). In fact, this technique could be used to study simplified and/or higher resolution spectra for molecules already in either Shpolskii (30,38,43,52) or mixed crystal (53,54) systems. During the last ten years, a rather clear understanding of the mechanism of FLNS has emerged. Much of this

theory was presented by McColgin (55) and reviewed more recently by Kohler (56). Before presenting a development of the analytical aspects of FLNS in organic glasses, it is useful to review briefly the physical aspects of this phenomenon as gleaned from the FLNS literature (13, 44-59).

Solid state media are most often chosen for high resolution vibronic spectroscopy because they are the easiest known scheme for maintaining temperatures low enough to minimize the effects of thermal broadening. With the molecules of interest dissolved in a solid matrix held at low temperature ($\lesssim$ 20K), it is possible to keep the phonon populations low enough to minimize[9] coupling between the vibronic states of the guest and phonon states of the host medium. If the excited vibronic states of the host lie higher in energy than the excited states of interest in the guest, so that coupling between individual molecules is also minimized, it is possible for molecules of the impurity to interact independently with electromagnetic radiation.

There are important interactions between these "isolated" molecules in solid state media and electromagnetic radiation. Figure 1 is presented as a basis from which to discuss these interactions. The solid lines represent the electronic energy levels as labeled. The dashed lines depict the molecular vibrations that build on the electronic

---

[9]This interaction cannot be entirely eliminated as evidenced by the phonon side bands that occur even in the sharpest low temperature solid state spectra, vide infra.

Figure 1. Schematic representation of the lower electronic energy levels of a hypothetical PAH molecule

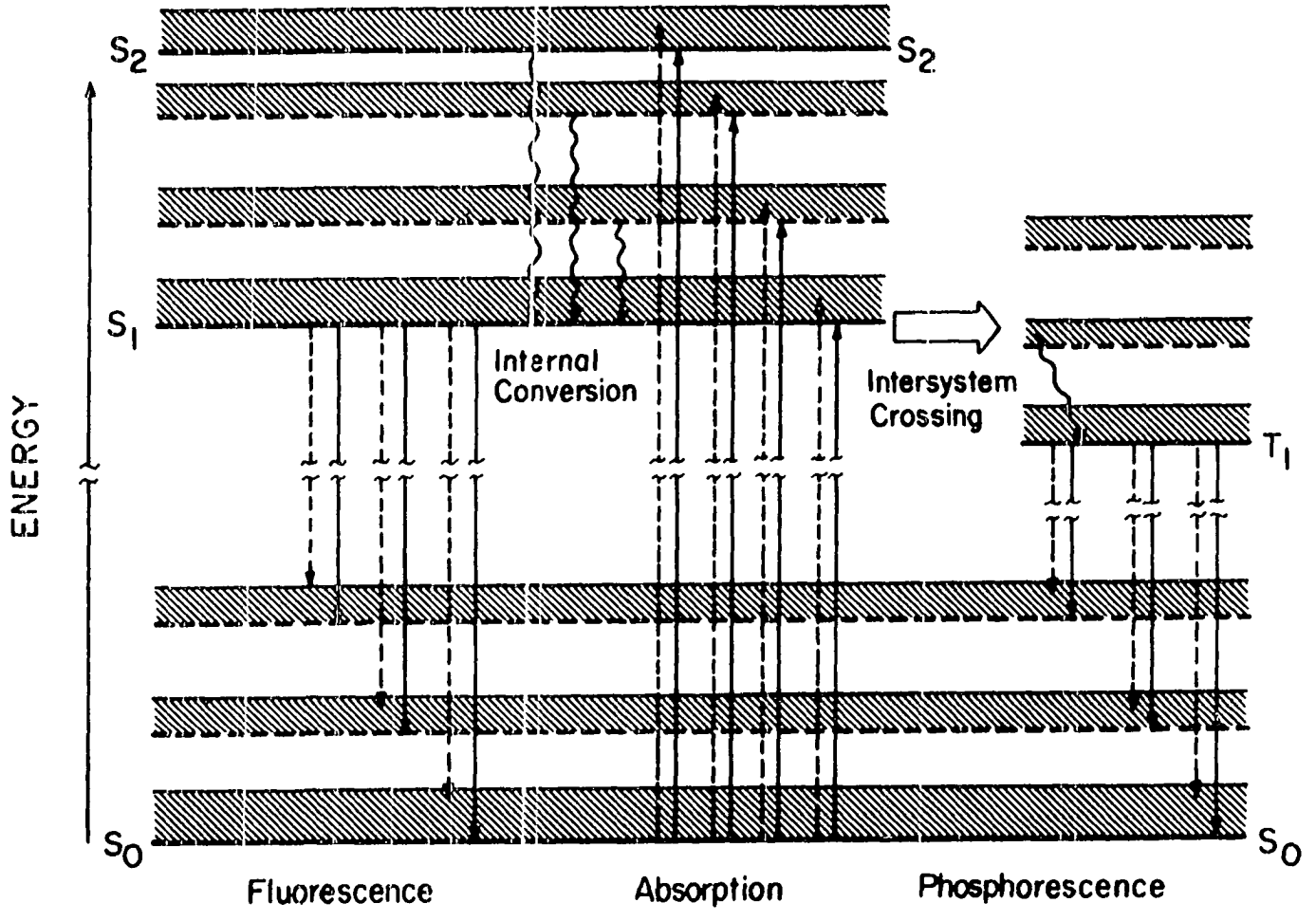
ENERGY
S2
S2
S1
Internal
Conversion
Intersystem
Crossing
T1
S0
S0
Fluorescence
Absorption
Phosphorescence

states. In the solid state at low temperatures, all analyte molecules are normally in the zero point vibrational level of the ground electronic state, S_0. Absorption transitions from this level to any of the higher levels represented by the solid or dashed lines can take place just as with a molecule in free space.

After excitation, a molecule in a solid state medium relaxes within picoseconds to the zero point vibrational level of the S_1 electronic state. From this point, the molecule can relax to S_0 via nonradiative processes, can fluoresce by making radiative transitions to the vibrational levels of S_0, or can phosphoresce after undergoing intersystem crossing to the lowest triplet state, T_1. The radiative transitions involving the states just described do not produce spectral bands which are infinitely sharp even for a single molecule. By the Heisenberg Uncertainty principle, the spectral bands have a width related to the initial and final state lifetimes.

The host medium plays an important part in the solid state spectroscopy of a molecule. Each molecule interacts with the crystal field or electrostatic environment imposed on it by the surrounding host molecules. The energy level spacings, depicted in Figure 1, are very sensitive to the electrostatic environment of the molecule. This susceptability is manifest as a shift in the transition energies to values often different from those of the molecule in free space. Any difference in electrostatic environment can cause a different energy shift for the vibronic transitions. It is by making the electrostatic environments for each molecule nearly identical that mixed crystal,

Shpolskii, and to a certain extent matrix isolation techniques achieve narrow lines. The disorder in any solid state matrix, especially in mismatched crystalline hosts or glassy hosts, results in a range of transition energies. This site inhomogeneous line broadening can result in vibronic spectral bands with widths greater than 100 cm^{-1} in the worst cases.

The host has another important role in the spectroscopy of molecules in the solid state. Phonons[10] in the host carry away the energy from vibrational relaxation of the analyte molecules. These site vibrations also can be involved in the vibronic transitions of the guest molecule. The dashed areas above each of the vibronic energy levels in Figure 1 represent excited states which include vibrations. It should be noted that the appearance of these phonon states is somewhat analogous to the existence of rotational states in gas phase spectroscopy.

The cryogenic heat bath rapidly removes the phonon energy, as mentioned earlier, and limits thermal broadening. Absorption transitions, therefore, start from close to the zero phonon level of the initial state and can terminate either at the corresponding level of an excited vibronic state or at the phonon band associated with that

---

[10]Although the periodic lattice required by the formal definition of a phonon is not present in a glass, researchers in the field of FLNS have generalized the "phonon" to include excited intermolecular vibrational states in both crystalline and glassy media.

vibronic state. This gives rise to two components in the spectral band associated with the transition. There is a sharp,[11] linewidth $\lesssim 1\ cm^{-1}$, line associated with the transition directly to the excited virbonic state without involving the creation of host phonons. This structure is called a zero phonon line (ZPL). The upper state of the absorption transition can also involve any one of the many possible phonon states of the host. This second type of transition gives rise to diffuse phonon side bands (PSBs). Both spectral components can often be observed for each vibronic transition of the guest molecule.

Very similar processes are involved in luminescence transitions for the guest molecule. As all of the internal conversion and intersystem crossing relaxation processes are taking place, the excess energy is dissipated as phonons to the heat bath. Before luminescence takes place, the molecule will usually have relaxed to the zero point vibrational level of either the S_1 or T_1 electronic state. From this point, radiationless decay or luminescence transitions can take place. Again, the luminescence transitions can be either directly into a vibrational level in S_0 giving rise to a ZPL, or into one of the many phonon states associated with the vibrational state giving rise to a PSB.

---

[11] For the isolated molecule, the zero phonon absorption transitions will remain sharp as long as they are into reasonably low vibronic levels. The increased density of states as one excites near or above S_2 often results in coupling between nearly coincident states and in broadened transitions.

In the Franck-Condon approximation, the fluorescence spectrum originating from the zero-point vibrational level of the S_1 state is predicted to be the mirror image of the absorption spectrum of this state. This mirror symmetry is frequently observed. The PSBs associated with the transitions appear on the low and high energy sides of the ZPL in luminescence and absorption, respectively. A summary of the ideas presented thus far appears in Figure 2. This figure depicts the contribution of a single molecule in its site within the host to the inhomogeneously broadened profiles that would be observed for a real sample containing many such molecules. The spectral components from the hypothetical single molecule/site are shown under idealized absorption, fluorescence, and phosphorescence profiles to illustrate the structures associated with the transitions depicted in Figure 1. Note the approximate mirror symmetry between absorption and luminescence.

The bands observed in the spectra from real samples are actually ensembles made up of the spectra from many such independently acting molecules in their associated sites. The only variation between systems that give narrow bands and those that give broad bands involves the amount of site inhomogeneous line broadening. For all of the following discussions, the media are assumed to be completely disordered producing vibronic spectral bands in absorption with 100 cm^{-1} or greater bandwidths. One such inhomogeneously broadened band is shown in Figure 3 with several of the contributing single site contributions drawn in. The bands would be expected to be gaussian with the greatest number of sites producing molecular vibronic transitions near an energy

Figure 2. The hypothetical contribution of a single molecule in a solid state host to the site inhomogeneous broad bands of the compound's absorption, fluorescence and phosphorescence spectra

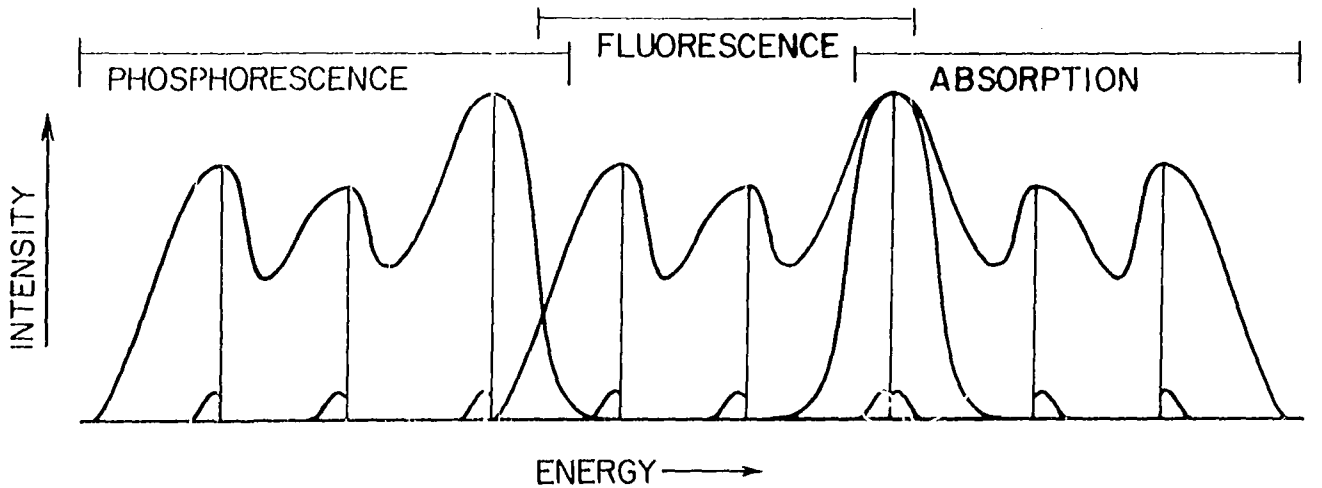
FLUORESCENCE
PHOSPHORESCENCE
ABSORPTION
INTENSITY
ENERGY

Figure 3. The inhomogeneously broadened bands in solid state absorption and luminescence transitions are actually ensembles of sharp components arising from independently acting molecules in their associated sites

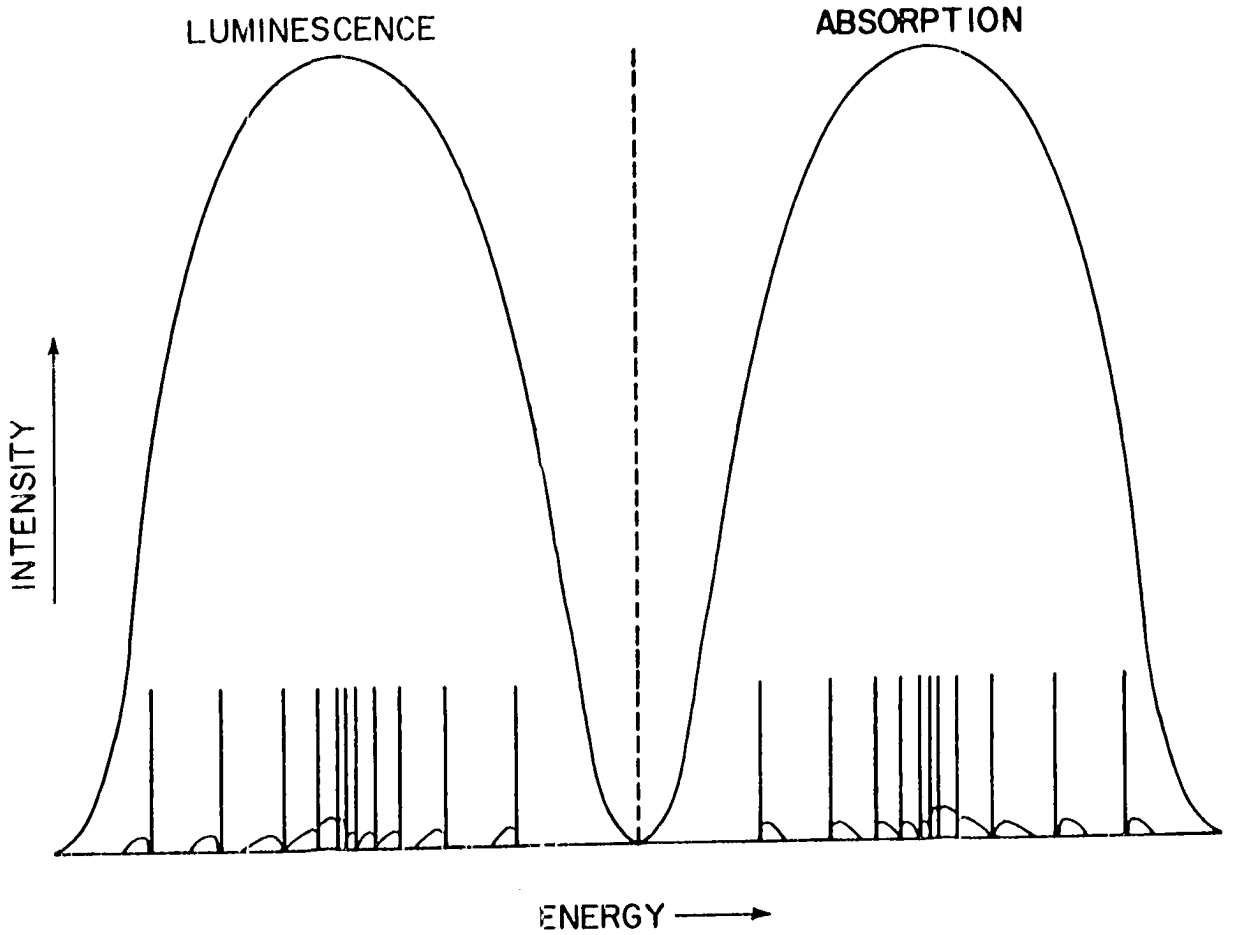
LUMINESCENCE
ABSORPTION
INTENSITY
ENERGY

that represents the most probable energy for the particular transition in the particular host.

FLNS is based on the observation that, under certain conditions, a fraction of the total number of molecules in the ensemble can be selected which will fluoresce with spectral components similar to those for the hypothetical single site. The sites are persistent on the time scale of fluorescence. Thus, the molecules can absorb and luminesce within an unchanged electrostatic environment. By exciting into the inhomogeneously broadened absorption band with a narrow line excitation source, only those sites (analyte molecules in their associated site within the host) with absorption energies overlapped by the excitation line will absorb. The "isochromat" thus prepared can remain pure in fluorescence yielding greatly narrowed bands. Narrow line fluorescence composed of sharp ZPLs and diffuse PSBs have been observed both in photoexcitation[12] (57) and in fluorescence as shown in Figure 4.

Several conditions are necessary for the isochromat prepared by narrow line excitation to produce useful narrow line fluorescence. The energy released by vibrational relaxation must not be so great as to produce local heating. This excess energy increases the phonon

---

[12]Note that the observation of photoexcitation spectra with sharp ZPLs and higher energy diffuse PSBs while monitoring a fluorescence transition as described in reference (57) does not indicate a lessening of inhomogeneous broadening by the media -- a caveat for the laser excited Shpolskii luminescence investigators.

Figure 4. Line narrowed fluorescence spectrum of pyrene

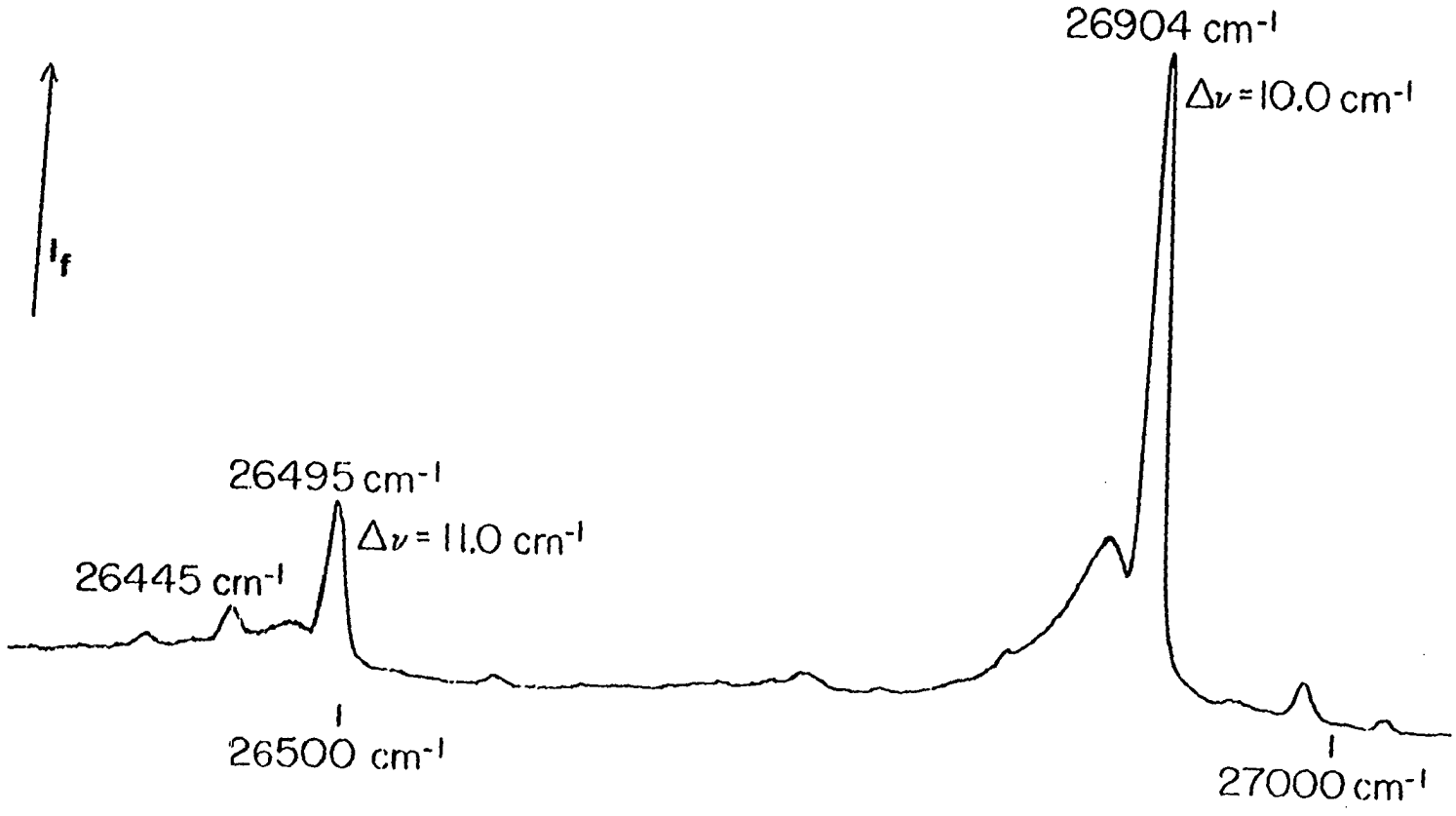
26904 cm-1
Δν = 10.0 cm-1
If
26495 cm-1
Δν = 11.0 cm-1
26445 cm-1
26500 cm-1
27000 cm-1

population which both increases electron-phonon coupling and increases the likelihood of site geometry changes. These processes yield broadened spectra. Also, the narrow excitation region must be situated within the inhomogeneously broadened absorption profile so as to excite only one or a few isochromats. In a highly congested region of a molecular spectrum, many absorption transitions for guest molecules in energetically different sites may be excited by a single monochromatic beam.

The greatest degree of line narrowing will take place, therefore, if excitation is into either the origin or one of the low lying vibrational bands of S_1. Under these excitation conditions, both spectral congestion and excess vibrational energy are minimized. These effects can be easily observed in Figure 5 where the lower spectrum was excited at a higher energy. Note that the lower spectrum is more than three times as intense and has broad bands indicating a loss of FLN. Further evidence of these phenomena are discussed in reference 58.

Other conditions necessary for useful narrow line fluorescence involve the media. The identity of the solvent may be important along with the low temperature and rigidity required for minimization of phonon sidehand intensity. The very existence of the PSB indicates interaction between the excited states of the guest and the surrounding site. The shape and intensity of the PSB has been shown not only to depend on the host, but upon the relative energy of the selected isochromat within the ensemble (59). In extreme cases, the PSB may be so intense as to preclude observation of the ZPL (55).

Figure 5. The fluorescence line narrowing effect decreases as molecules are excited higher into their vibronic manifold

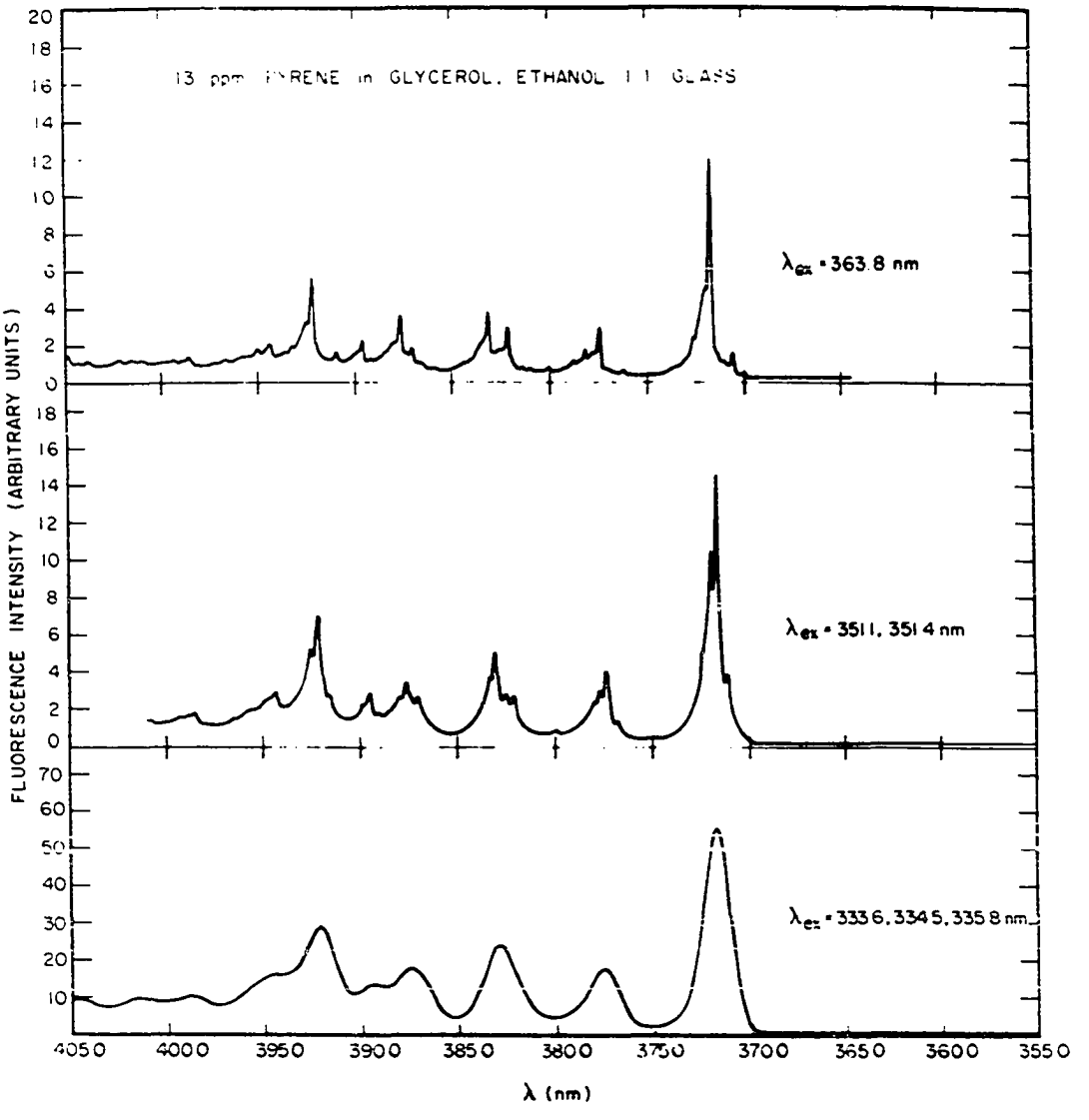
13 ppm PYRENE in GLYCEROL, ETHANOL 1:1 GLASS
λ_{ex} = 363.8 nm
λ_{ex} = 351.1, 351.4 nm
λ_{ex} = 333.6, 334.5, 335.8 nm
FLUORESCENCE INTENSITY (ARBITRARY UNITS)
λ (nm)
4050
4000
3950
3900
3850
3800
3750
3700
3650
3600
3550

The chosen medium must also be a good solvent for the molecule being determined. The guest molecules must be completely solvated and dispersed within the host. Otherwise, intermolecular energy transfer and the formation of new states by coupling between molecules will result in loss of line narrowing. Matrices, especially crystalline matrices, which seem to be good solvents for a species at room temperature, may allow aggregates to form as the matrix is cooled. In other cases, the room temperature solution may be largely composed of dimers, trimers, and other oligomeric associations which persist as the sample is cooled. The mechanisms and effects of aggregate formation are discussed in the literature for both Shpolskii (60,61) and glassy matrices (62). As will be illustrated in a later chapter, the important aspect of aggregate formation is the resulting occurrence of broad structure in fluorescence spectra that cannot be narrowed by FLNS techniques.

Another very important physical aspect of FLNS must be considered before continuing. The sites making up the isochromat are selected because they are energetically equivalent in absorption, i.e., they overlap the narrow excitation line. This is not to say that the sites are geometrically equivalent. Nor does this mean that all of the sites selected must have the same luminescence transition energies. In fact, due to relatively large differences in the electronic geometries of the singlet and triplet states, line narrowed phosphorescence for PAH species following $S_0 \rightarrow S_1$ excitation in a disordered matrix has not been observed. Vibrational fluorescence lines are also somewhat broadened since they involve transitions into excited vibrational states which may interact

differently with geometrically inequivalent sites. This latter effect, though observable (cf., Figure 33), is of minor importance for analytical FLNS.

Any time the energetic and geometric processes of absorption and luminescence are essentially equivalent, line narrowing should be possible. All of the FLNS literature cited earlier in this chapter concerns $S_1 \rightarrow S_0$ fluorescence transitions following $S_0 \rightarrow S_1$ absorption transitions. Line narrowed phosphorescence is, in fact, possible following direct excitation into the T_1 electronic state. Several papers have been published noting the appearance of line narrowed phosphorescence after using this more compatible method of selecting the isochromat (63-65).

Line narrowed fluorescence has frequently been observed for PAH compounds. FLN has also been demonstrated for organic dyes (55), chlorophylls (51), porphin (51), and heterocyclic compounds (55) in organic media. Similarly, FLN has been observed for Cr^{3+} in ruby (48), for trace inorganic species in microcrystalline percipitates (66), and for both transition metal and rare-earth ions in inorganic glasses (67, 68). On the basis of the general nature of the mechanisms of FLN and in light of the widespread success reported in the literature, it seems that FLN should be possible for most luminescent molecular and ionic species in many solid state matrices.

B. Analytical Aspects

1. Laser excited analytical FLNS

Lasers are not required for FLNS, as has been documented in several publications (57,59). However, lasers are the most practical means of obtaining useful intensities in high resolution FLNS. In fact, it is the advent of dependable, commercially available, tunable dye laser systems which has made FLNS an analytical practical technique.

The first analytical application of FLNS was published by this group in 1978 (46). Among the most important characteristics of FLNS is that it obviates the need for the ensemble narrowing effects of mixed crystal, matrix isolation, and Shpolskii techniques. This leads to several important advantages for FLNS as an analytical technique. Consideration of the analytical aspects of this method along with the demonstrated results of their application shows that FLNS in organic glasses using a pulsed tunable dye laser and gated detection system provides the power demanded by the PAH analysis problem.

2. Organic glasses

Organic glasses are the most promising systems in which to do analytical fluorescence line narrowing spectrometry. The term organic glass, as used throughout this dissertation, refers to a special case within the usual definition of a glassy medium. A glassy medium is any solid state medium with no crystalline or long range ordered structure.

Extensive cracking and the formation of microcrystalline inclusions can make glassy media nearly as opaque as Shpolskii matrices. The organic glasses needed to realize the full analytical potential of FLNS are solvents or mixtures of solvents which form optically clear media at cryogenic temperatures, cf., Figure 6.

The lack of crystal growth as glasses form alleviates many of the quantitative problems associated with other cryogenic spectroscopic matrices. There is no concern that the guest molecules will be excluded irreproducibly to the interstices as crystals grow. In fact, there should be no innate segregation mechanisms since glasses form as the viscosity increases with cooling. Also, the direct incorporation of the sample into the liquid solvent mixture before cooling eliminates analyte losses during the vapor phase deposition step required in matrix isolation techniques.

The lack of ensemble narrowing mechanisms due to the disorder in glasses is an advantage. When choosing the exact excitation wavelength, flexibility or even some uncertainty is allowed by the lack of any sharp structure in the absorption bands. Small changes in solvent composition which cause small shifts in the energy of spectral bands have little effect on FLNS signals from glasses. This is true because the differences in absorption caused by small shifts of the narrow excitation line relative to the broad absorption bands are negligible. In a Shpolskii matrix, the excitation laser line must be coincident with one of the sharp absorption quasilines for maximum sensitivity. A small change in solvent composition or cooling conditions can have a dramatic

Figure 6. Photograph of a 4:5 water in glycerol glass immersed in liquid nitrogen

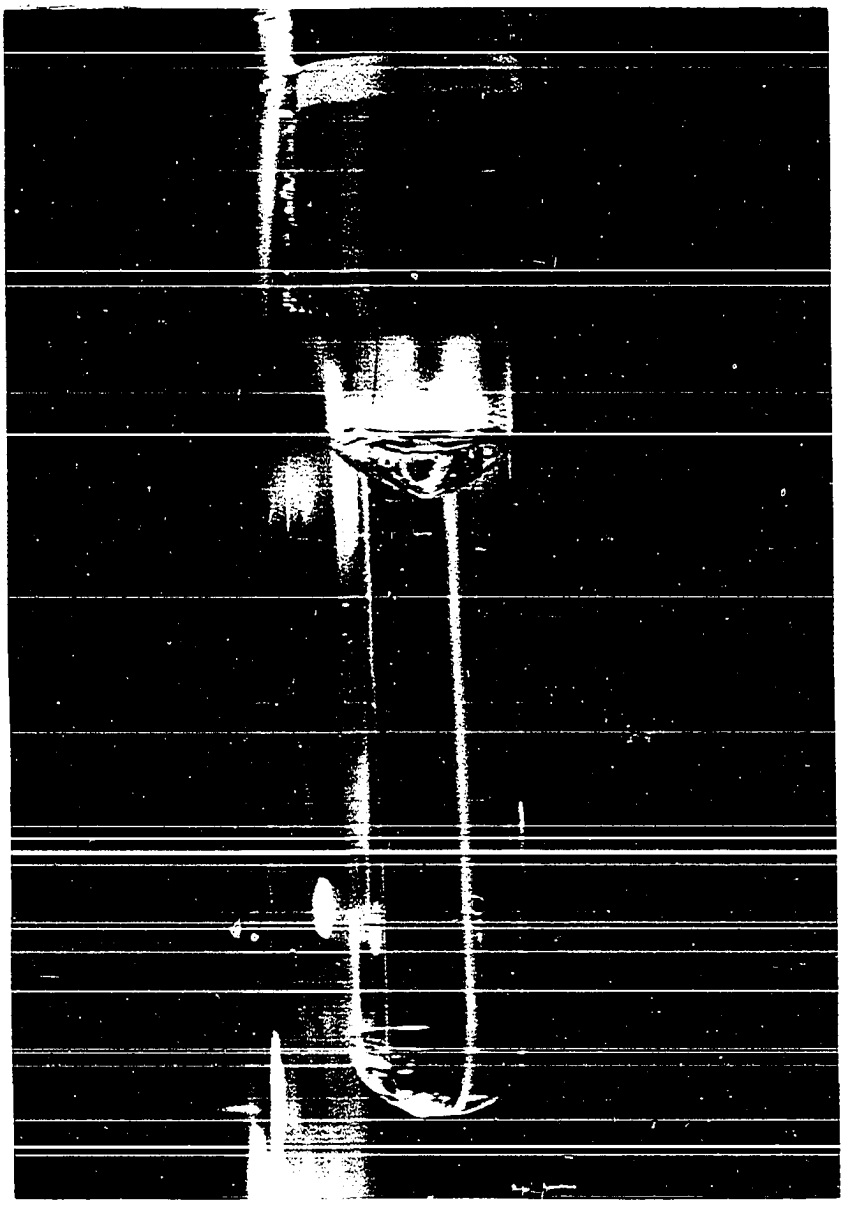

effect on the intensity of a quasiline, thus markedly influencing the observed fluorescence intensity (37).

The high optical quality of organic glasses provides advantages that cannot be achieved with the other cryogenic media. The highly defined collimation of laser excitation sources can be utilized for fine focusing through the clear glass samples. The small sharply defined fluorescing volume produced can be efficiently and reproductibly collected and imaged onto the slits of the emission monochromator. Once the optical paths of the excitation and luminescence beams have been established, the exact position and orientation of the sample has very little effect on excitation or collection efficiency. This sharply defined cylindrical emission region fixed in space by the focused laser beam contrasts sharply with the diffuse spot of emission produced on the surface of opaque Shpolskii matrices by the scattered excitation beam.

Optically clear glasses also allow for higher rejection of scattered light from the excitation beam. Most of the unwanted scatter from an organic glass sample occurs at the surfaces where the excitation beam enters and exits the sample. The image from the fluorescing region in a glass can be so well defined that occluders can be used to prevent light from the sides of the sample from entering the monochromator. The reduction in scatter from the excitation beam allows spectra such as the one in Figure 7 to be possible. The signal-to-noise ratio is improved and lower detection limits facilitated. Sensitivity is further enhanced by the small image that can be obtained The image of the fluorescing

Figure 7. Pyrene excited with the 330 nm series of argon ion laser lines at 4.2 K in the water/glycerol glass. Note the very low intensities of the scattered laser lines

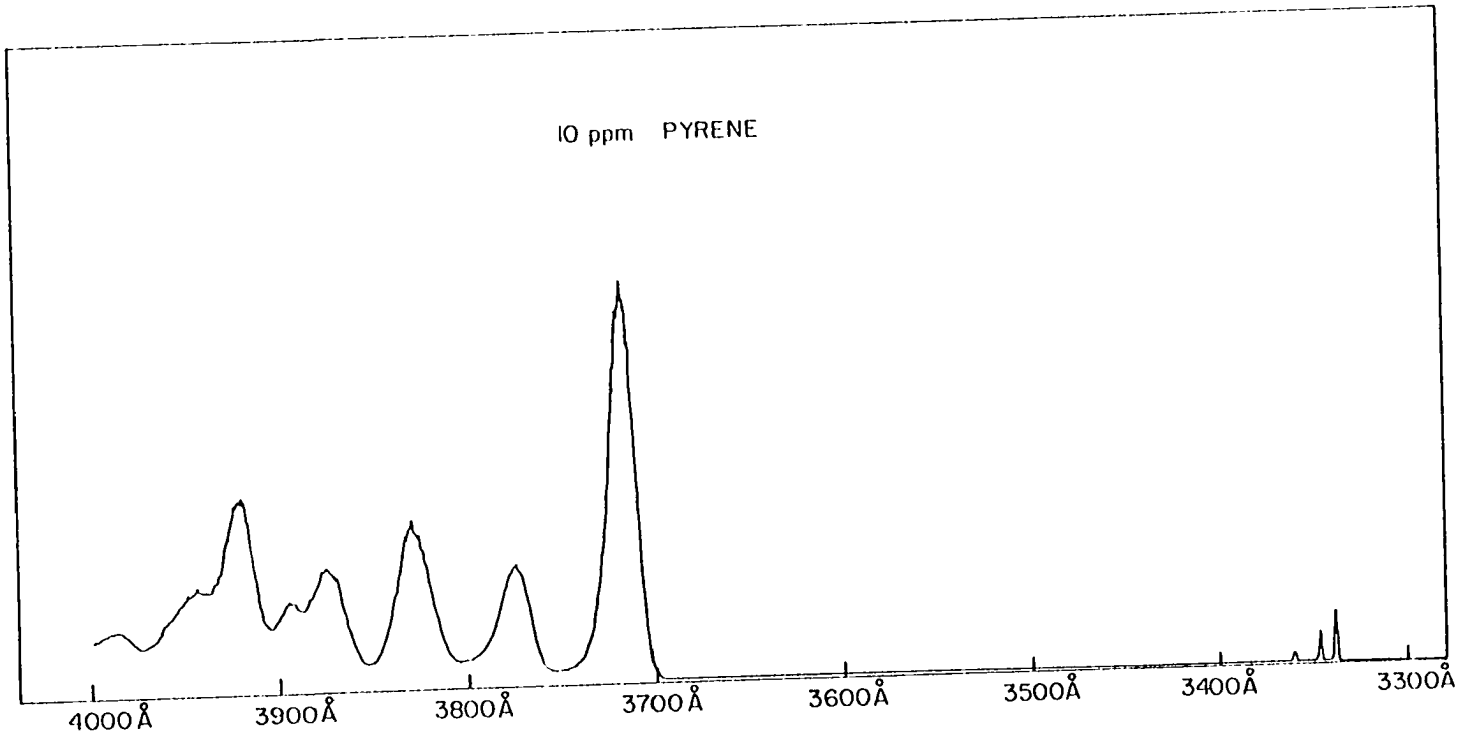
10 ppm PYRENE
4000 Å
3900 Å
3800 Å
3700 Å
3600 Å
3500 Å
3400 Å
3300 Å

region excited by a focused laser beam in an organic glass can approach the width of the monochromator slits at reasonable resolutions. These characteristics of glasses allow very efficient observation of fluorescence signals as is not possible with opaque or translucent matrices.

No other cryogenic sampling medium has all of the advantages listed above. Now that the superior qualities of organic glasses as spectroscopic sample media have been presented, it is necessary to discuss some of the details associated with their application.

Organic glasses used for analytical FLNS must form without producing "snows" and without cracking. The formation of snowy microcrystalline inclusions within the glass occurs when one or more of the solvent constituents is incompatible with the rest of the glass. The incompatible component in an otherwise good glass is usually introduced with the sample or sample extract. The problem can be alleviated by using a different solvent to extract the sample, by evaporating the sample solvent before dissolving the sample in the glass mixture, or by choosing a different glass. Although no recent exhaustive work could be found, it is the experience and feeling of the writer that any sample solvent can be incorporated into some suitable glass forming mixture.

Cracking occurs as a result of mechanical stress whether inherent in the glass itself or imposed by the container. As a glass solvent mixture is cooled, a temperature gradient is established from the center of the sample cell to the surface. If the gradient becomes too large due to a rapid cooling rate, the outer shell of solvent becomes rigid

while the warmer material in the center is still shrinking. The explosive release of this strain often causes the glasses to shatter. Evidence of this could frequently be heard echoing down the halls during some stages of this research.

In other situations, the glass seems to be incompatible with the chosen container. Some glasses used in these investigations split the sample cell each time they formed. Other glasses had a tendency to pull away from the sample cell wall upon cooling. This often results in a translucent sample surface as well as four extra surfaces from which to scatter the excitation beam. Perhaps most disappointing were those glass mixtures which formed good glasses at 77K (boiling nitrogen, a convenient glass testing temperature), but which consistently and explosively cracked as the temperature was lowered toward 4.2K where actual analyses were run. This latter problem occurs because some solvent mixtures can undergo appreciable changes in density below the temperature at which they become rigid.

In spite of the bothersome problems that the researcher encounters while searching for new glasses, it must be emphasized that there should exist an infinite number of possible "good" organic glass mixtures. Once a compatible glass and cell have been chosen for a problem, they can be used routinely with no further difficulty as long as a certain maximum cooling rate is not exceeded. Several glasses were used during the course of the investigations described herein and will be characterized later.

3. Qualitative attributes of FLNS

The description of FLNS presented in the physical aspects section of this chapter does not illustrate the analytical potential of this technique. It was shown that a judicious choice of excitation energies makes it possible to excite sharp ZPLs from molecules in low temperature solid state matrices. The advantages of choosing organic glasses as the analytical media have also been presented. The features of FLNS which make the technique useful for determination of species in complex mixtures are considered next. Following this are discussions of the instrumentation and actual demonstrative experiments.

A given molecule will produce sharp ZPLs under FLN conditions for only a relatively small range of excitation energies. Obviously, excitation lines with wavelengths longer than the origin band cannot excite the molecule. Excitation lines at more than 1000 cm^{-1} to higher energy (about 20 nm to shorter wavelength) than the origin band excite only broad band fluorescence for reasons already given. It is hoped that the following description of what is to be expected from excitation of a sample containing hundreds of species is reasonably clear.

Three regions will appear in the dispersed fluorescence spectrum of a complex mixture under FLNS conditions. All three regions are seen in the 363.8 nm laser excited luminescence spectrum of a soot extract in 4:5 water/glycerol at 4.2 K shown in Figure 8. Region I, near and coincident with the laser wavelength, is an area of intense Raman and Rayleigh scattering and resonant fluorescence. Since any compound

Figure 8. FLN spectrum from a naturally complex mixture. The three characteristic regions of fluorescence are illustrated

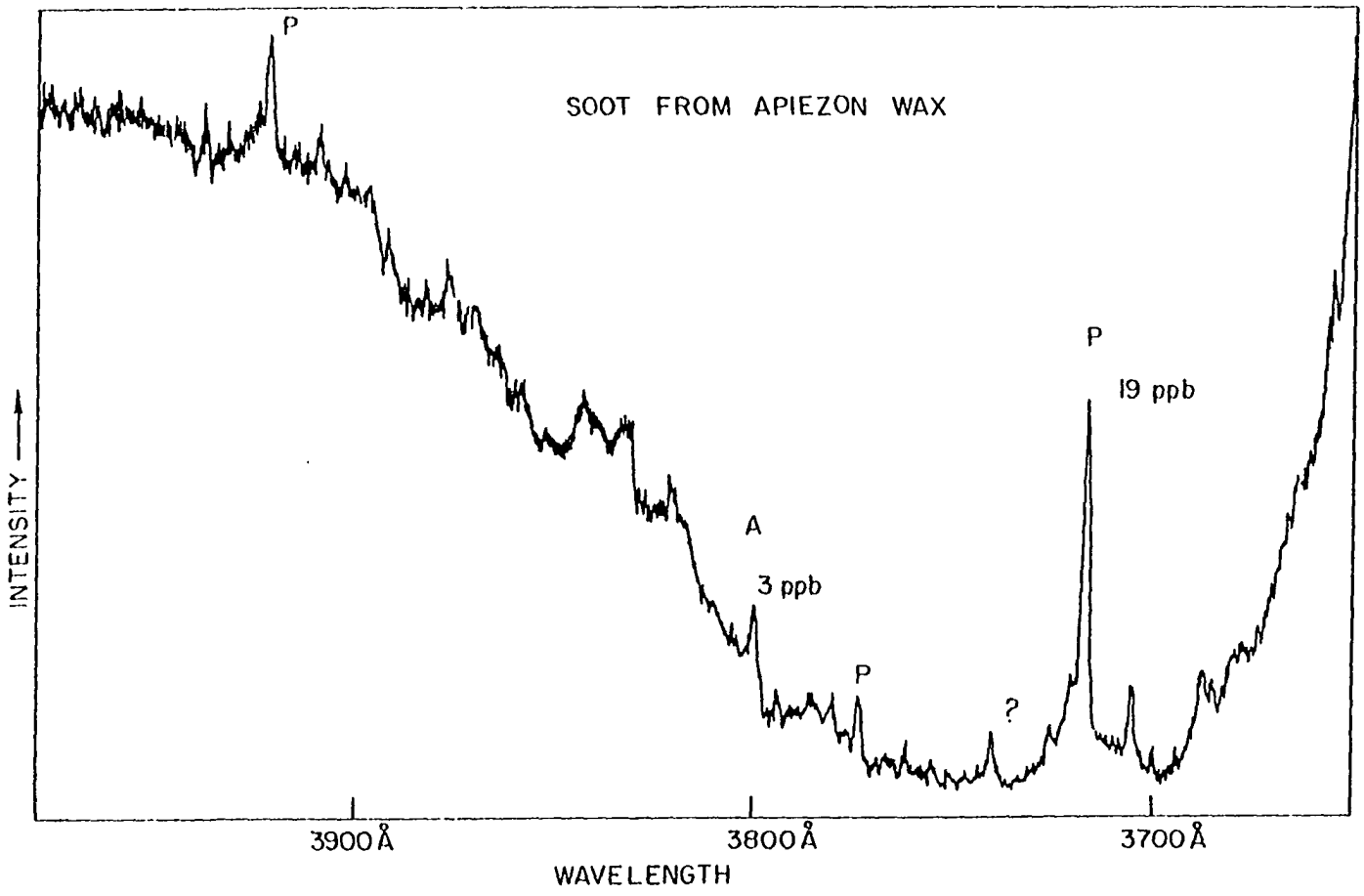
SOOT FROM APIEZON WAX
P
A
3 ppb
P
?
P
19 ppb
INTENSITY
3900 Å
3800 Å
3700 Å
WAVELENGTH

whose (0,0) absorption overlaps the laser line can emit in resonance with the pump beam, even temporal resolution to remove Raman and Rayleigh scattering will not make region I useful for the analysis of mixtures.

The other two regions are of greater analytical importance. Region II is a region of relatively low fluorescence intensity between the more intense regions I and III. The intensity in region II is low because in the mixture only those species which happen to be excited in or just above their origins can fluoresce in this region. In region III, however, essentially any molecule in the mixture with possible emission lines more than 20 nm longer in wavelength than the laser will be excited. All excited species with origin bands in region III will give rise primarily to broad band fluorescence, the superposition of which is the intense featureless luminescence in this region.

The three regions will in general follow the laser wavelength as it is tuned through the 300-500 nm region where PAH origins are usually located. At excitation wavelengths very high or very low in this region, the intensity of region I will decrease and region III will build more slowly. Thus, region II will appear to be more pronounced at either longer or shorter wavelengths than it would near 400 nm where the density of PAH origins is maximized. This behavior would be expected for other classes of compounds also.

Fortuitously, the region of lowest total fluorescence intensity, region II, coincides with the region where maximum fluorescence line narrowing (FLN) can occur. As shown in Figure 8 and other spectra which

follow, much of the fluorescence in region II is comprised of sharp ZPLs and accompanying PSBs. It is also fortuitous that region III is featureless enough that vibrations building on sharp origin lines in region III can often be observed. The pronounced pyrene line in Figure 8 at 392 nm is a good example of this.

The three regions should appear to some extent in all mixture spectra. For many of the spectra in later chapters, regions I and III are very pronounced. However, for a major fluorescent species, the sharp line fluorescence in region II can dominate regions I and III. Spectra where this is the case appear in later chapters. Regions I and III can be decreased by temporal resolution, vide infra. As will be shown in the following paragraphs, however, the existence of regions I and III do not greatly affect the analytical utility of FLNS.

Under ideal FLN excitation conditions for a single molecular species in a complex mixture, only one or two ZPLs may appear in region II. Other lines in region III may be impossible to use due to the extreme intensity of region III. The 392 nm pyrene line in Figure 8 is more an exception than the rule due to the high concentration of pyrene in this sample and the relatively low excitation wavelength. In what follows, it will be shown that one intense ZPL in region II suffices for unambiguous identification and quantitation of a single species in a complex mixture.

Our experiments have shown that for a given species there is a limited number of excitation regions within the inhomogeneously broadened origin and low lying vibrational absorption bands that will allow

the observation of intense FLN spectra with most of the intensity concentrated into sites belonging to a single isochromat. The first step in developing a technique (using FLNS) to determine a species requires that one or more of these ideal excitation wavelengths be found for that molecule. Within approximately an 0.5 nm region about these ideal wavelengths, the excitation wavelength can usually be changed without drastically altering the appearance of the FLN spectrum. Within these ideal excitation regions, the single intense ZPL associated with each fluorescence transition can be seen to move as the excitation wavelength is changed. The energy difference between the excitation line and the ZPL in question is a constant reflecting the characteristic energy differences between the absorption and fluorescence transitions involved for the molecule in question.

The energy differences maintained between the molecule's fluorescence ZPLs and the laser are as unique as that molecule's vibrational spectrum. In addition, the molecule's ideal excitation regions are characteristic of that molecule. The occurrence of a ZPL for a species is exactly determined by the spectral location of the excitation line and an energy difference characteristic to that molecule.

The availability of more than one ideal excitation wavelength can be used to advantage since their associated FLN spectra can be used to identify interferences and frequently eliminate them. This follows since regions I, II, and III shift with excitation wavelength and it is improbable that the molecule of interest and the interfering species will have active vibrations which are all identical in frequency. The

linewidth of the ZPLs determines, in part, the extent to which the frequencies must differ in order that an interference be eliminated. In this regard, FLN linewidths can be decreased to about 1 cm^{-1} (by narrowing the laser profile and increasing the resolution of the emission monochrometer).

For molecules with weak fluorescence origins, excitation into the (0,0) rather than a (0,1) band may be advisable. Such excitation increases the probability that more than one intense ZPL will be observed in region II. In addition, one can tune over a much wider range (than previously stated) within the absorption origin without causing a deterioration of the FLN spectrum. This additional tuning capability is obviously important for partial or complete elimination of an interference.

The approaches outlined for elimination of interferences underscore the flexibility of the FLN technique. Ideally, the analyst should have the capability of analyzing for each molecule under several FLN excitation conditions. However, it is germane to note that the author encountered only one case of interference while studying 18 different PAHs in several types of samples. For all molecules excitation was into a low lying vibrational subband of the S_1 state. The interference was subsequently eliminated.

We consider next certain aspects of our procedure for the analysis of a specific compound. First, standard FLN spectra for the appropriate glass are obtained for at least two ideal excitation wavelengths. Although any of these excitation wavelengths will suffice for

identification of the compound in a real mixture, the excitation wavelength chosen for quantitative measurements is the one yielding the "cleanest" FLN spectrum. For reasons already discussed, the presence of hundreds of species in a real mixture does not alter the ideal excitation wavelengths determined for the compound of interest when it is the only species in the glass.

The procedure for selecting excitation wavelengths is best illustrated with the aid of Figures 9-12. Figure 9 shows the transmittance spectrum of perylene in the S_1 region. The intense origin at about 22,700 cm^{-1} and several vibronic bands are discernable. The marked points on the spectrum indicate the excitation wavelengths used to excite the FLN spectra shown in Figure 10. In each of the three spectra, there are lines due to excitation of groups of sites comprising different isochromats. These isochromats arise because the excitation line overlaps several broad absorption bands. Excitation at points A, B and C results in a FLN spectrum characterized by four, five and three multiplet components, respectively. The spectra illustrate that as the excess vibrational energy created by excitation decreases, there is a tendency for one ZPL to dominate. This is consistent with the fact that vibrational congestation increases with increasing excess vibrational energy.

The spectrum of perylene when excited at 23,015 cm^{-1} is shown at the top of Figure 11. This corresponds to excitation at a point just to the low energy side of the first vibrational peak in Figure 9. Note that the trend indicated in Figure 10 has continued to the point that

Figure 9. Transmittance spectrum of perylene

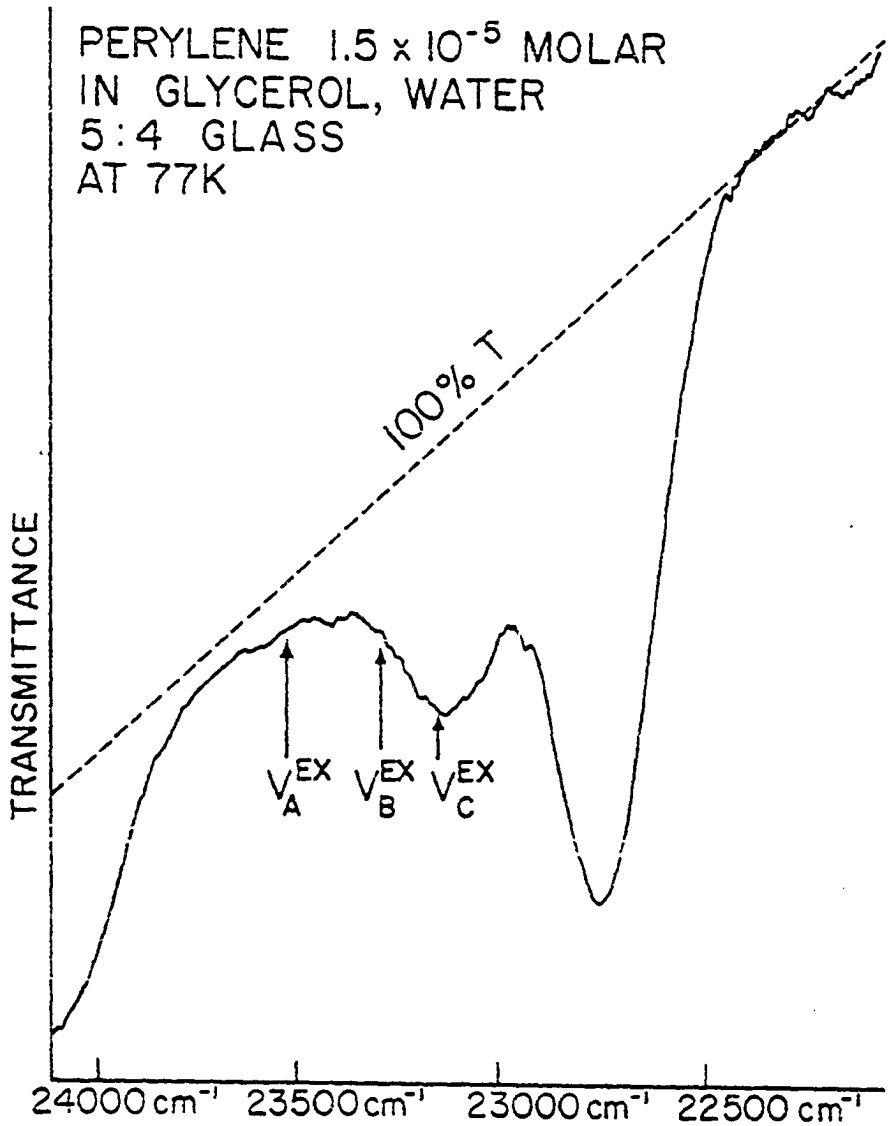
PERYLENE 1.5 x 10⁻⁵ MOLAR
IN GLYCEROL, WATER
5:4 GLASS
AT 77K
100% T
TRANSMITTANCE
V_A^{EX}
V_B^{EX}
V_C^{EX}
24000 cm⁻¹
23500 cm⁻¹
23000 cm⁻¹
22500 cm⁻¹

Figure 10. Perylene fluorescence excited with dye laser at the points marked in Figure 9. O stands for origin. The truncated line at the right is the laser line

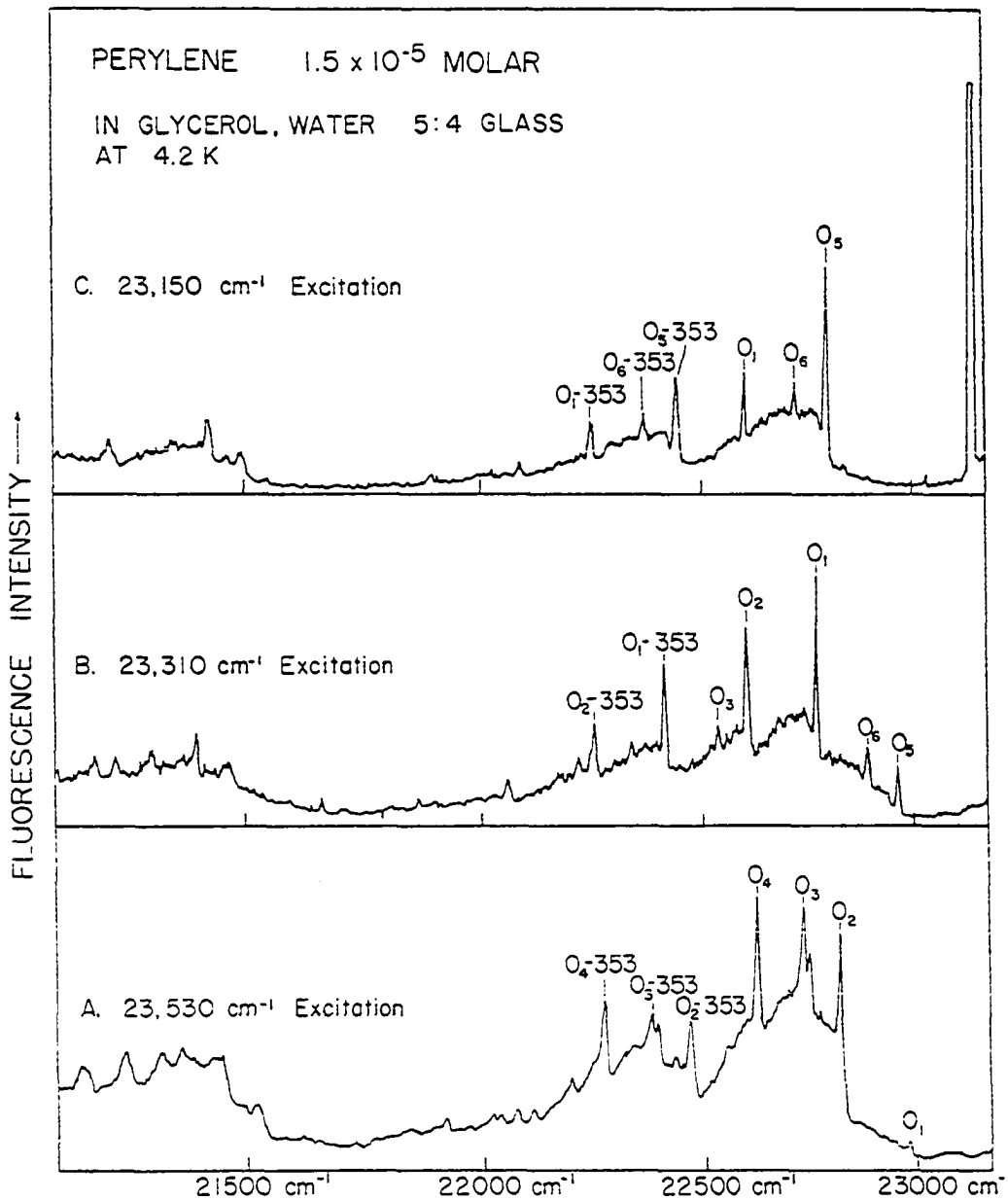
PERYLENE 1.5 x 10⁻⁵ MOLAR
IN GLYCEROL, WATER 5:4 GLASS
AT 4.2 K
C. 23,150 cm⁻¹ Excitation
O₁-353
O₆-353
O₅-353
O₁
O₆
O₅
B. 23,310 cm⁻¹ Excitation
O₂-353
O₁-353
O₃
O₂
O₁
O₆
O₅
A. 23,530 cm⁻¹ Excitation
O₄-353
O₃-353
O₂-353
O₄
O₃
O₂
O₁
FLUORESCENCE INTENSITY
21500 cm⁻¹
22000 cm⁻¹
22500 cm⁻¹
23000 cm⁻¹

there is only one strong isochromat contributing to each fluorescence transition. Figure 11, spectrum A, further illustrates the point made with Figure 7 in that the perylene origin ZPL is nearly as intense as the scattered laser line.

The resolution of the mixture in spectra A and B of Figure 11 illustrates in practice how FLNS can be used to differentiate species. In spectrum A, the laser is at too low an energy to excite benzo[a]-pyrene(BaP). Hence, only perylene emission is visible. Spectrum B is excited with a laser line absorbed by both molecules. At this high energy of excitation, BaP fluoresces with a spectrum containing one prominent ZPL and a broad phonon and multisite side band. The perylene emission in the same spectrum is dominated by broad structure and would be buried in region III of a more complicated mixture.

Spectrum C is included to show for BaP how the lower excitation energy affects the phonon structure. Still, however, the spacing between the laser and the dominent ZPL of BaP has remained the same. This indicates that sites in the same vibronic absorption band are still being excited with greatest efficiency.[13] This same behavior is illustrated in Figure 10 where the origin lines are numbered in the order of their appearance as the laser frequency is lowered.

---

[13]The dramatic decrease in phonon structure observed as the excitation line is tuned to the low energy side of an absorption band (inhomogeneously broadened) has been documented and explanations proposed in reference 57.

Figure 11. A and B are FLNS spectra excited from an artificial mixture. The bottom spectrum shows benzo(a)pyrene at a different excitation wavelength. 4345 Å corresponds to 23015 cm^{-1}

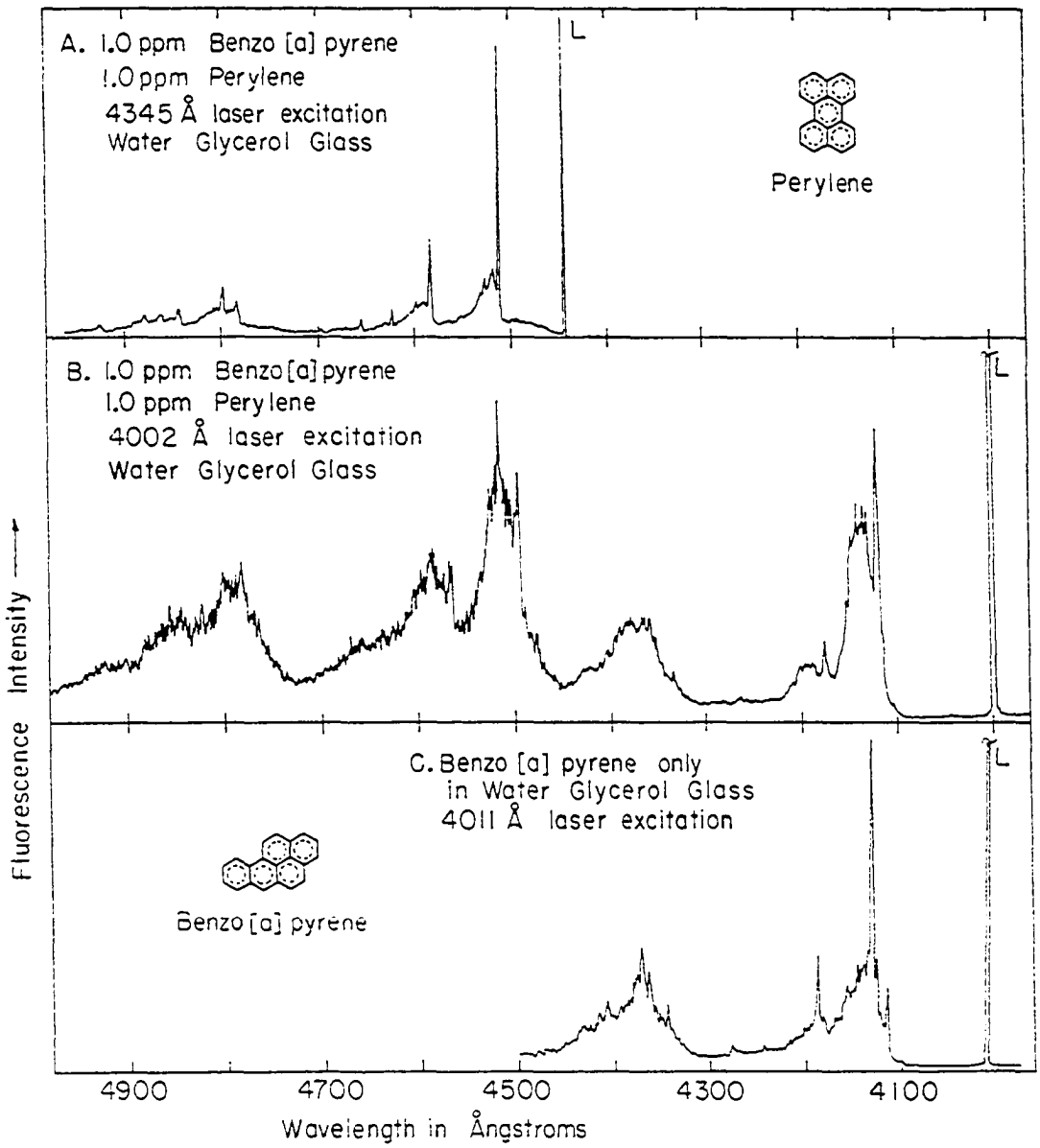
A. 1.0 ppm Benzo [a] pyrene
1.0 ppm Perylene
4345 Å laser excitation
Water Glycerol Glass
L
Perylene
B. 1.0 ppm Benzo[a] pyrene
1.0 ppm Perylene
4002 Å laser excitation
Water Glycerol Glass
L
C. Benzo [a] pyrene only
in Water Glycerol Glass
4011 Å laser excitation
L
Benzo [a] pyrene
Fluorescence Intensity
4900
4700
4500
4300
4100
Wavelength in Ångstroms

4. Quantitative aspects of FLNS

The position of the chosen analytical fluorescence line relative to the laser excitation line allows for identification of a species. The intensity of the analytical line is proportional to the concentration of the compound. For one-photon absorption and in the absence of saturation effects, the relationship between concentration and observed fluorescence intensity is:

$$I_f = kE_I\phi I_o\varepsilon\ell C \qquad (1)$$

I_f = Fluorescence intensity

k = Proportionality constant

E_I = Instrumental efficiency

ϕ = Fluorescence quantum yield

I_o = Excitation beam intensity

ε = Absorption coefficient

ℓ = Path length of collected region

C = Concentration of fluorescing species

In actual experiments, k, E_I, ϕ, ε and ℓ are fixed for a given species after initial setup and can be combined into one constant. Thus, equation (1) can be written:

$$I_f = KI_oC \qquad (2)$$

with

$$K = kE_I\phi\varepsilon\ell \qquad (2)$$

To simplify the equation still further, the excitation beam intensity can be factored out to give equation (3)

$$\frac{I_f}{I_o} = KC \tag{3}$$

From this relationship, it can be seen that linear calibration curves result from plotting $\frac{I_f}{I_o}$ versus C. By measuring normalized fluorescence intensity, I_f/I_o, at one or more concentrations, the concentration of an unknown can be determined.

FLNS has an important quantitative advantage over broad band techniques. The spectral sharpness of the ZPL allows many of the sources of noise encountered in broad band techniques to be eliminated. Instead of measuring all of the light passing through the monochromator at the analytical wavelength, the intensity of the sharp analytical line can be measured independently of much of the background. Most scattered light backgrounds are broad compared to the analytical ZPL so that a baseline for the ZPL can be extrapolated which excludes this noise contribution. In addition, with FLNS a higher instrumental resolution is used without sacrificing sensitivity, vide infra. This allows for many of the sharp solvent Raman and impurity lines to be excluded from the quantitative measurement of the FLNS signal. Figure 12 illustrates the difference between classical and FLNS signal quantitation. In classical methods, the unknown is quantitated by measuring all of the light that passes through the monochromator when it is set near the peak of the emission band. Without the use of a

Figure 12. Comparison of FLNS and broad band quantitation techniques: a) scattered light and instrument background, b) solvent and impurity fluorescence and Raman signals, and c) extrapolated background for analytical ZPL; $\delta\lambda$ = bandpass of emission monochromater

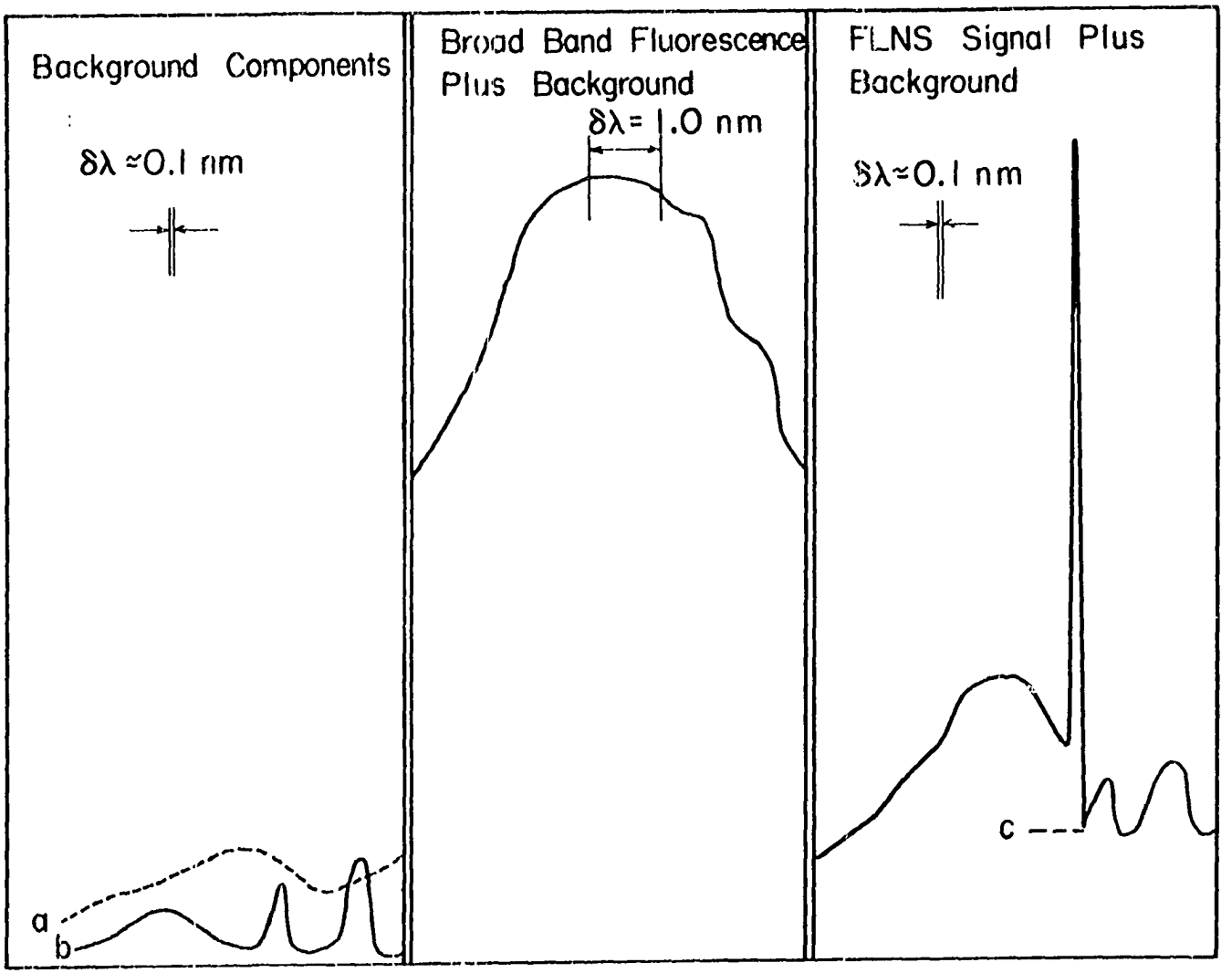
Background Components
δλ ≈0.1 nm
a
b
Broad Band Fluorescence
Plus Background
δλ = 1.0 nm
FLNS Signal Plus
Background
δλ≈0.1 nm
c

carefully formulated blank, there is no way to subtract out the ever present background contributions. On the other hand, in FLNS the ZPL can be distinguished from these background contributions even when at sub-part-per-billion concentrations the solvent emission lines and the total background may be several times as intense as the analytical line.

Optimization of sensitivity in analytical FLNS requires more than indiscriminate reliance upon the relationship described in equation (1). The ability to detect the analytical ZPL depends on its height above the statistical noise in the broad background and upon the ability of the analyst to distinguish a sharp ZPL from structure in the background. Maintaining the same integrated fluorescence intensity while increasing spectral resolution can aid in the achievement of both of these requirements. The capacity for efficient imaging of a very small excited volume of the sample onto the narrow slits of a high resolution monochromator is very important. Organic glasses are necessary for taking full advantage of the sharp ZPLs of FLNS for the best possible detection limits.

For maximum sensitivity, the best relationship between integrated intensity and peak height occurs when the linewidth of the laser and the bandpass of the monochromator are approximately equal. Increasing the resolution of the monochromator beyond that required to reproduce the true spectral distribution of the excitation laser line only serves to decrease the amount of light passed by the monochromator which decreases the observed intensity of the ZPL. Decreasing the resolution,

beyond the minimum required for reproduction of the approximate line-shapes of the sharp ZPLs increases the throughput. However, beyond a certain point the ZPLs will be instrumentally broadened to the point that they cannot be distinguished from other structure in the background at low analyte concentrations.

Ultra-narrow line lasers are not required for a FLNS solution of the PAH analysis problem. At an instrumental resolution of 10 cm^{-1}, as many as 50 ZPLs can be resolved in region II of a mixture spectrum. The fluorescence origins for most PAH compounds are distributed between 300 and 600 nanometers. A conservative estimate with a minimum excitation wavelength spacing of 1.0 nm, gives more than 15,000 resolution elements in which to determine several hundred PAH species. The qualitative schemes described in the preceding subsection allow an even more encouraging resolution prediction.

The implication of this review of the qualitative aspects of FLNS is that although this is a very high resolution technique, high selectivity is achievable with moderate instrumental resolutions. Monochromators capable of 0.10 nm (less than 10 cm^{-1}) resolution are quite common and can be quite efficient, e.g., an f-number of 5.3 or lower. Also, tunable dye lasers with linewidths better than 0.10 nm are relatively simple, inexpensive, and readily available. A dye laser designed specifically for such low resolution operation can be made quite efficient so that high output powers can be obtained at very reasonable pump energies.

To demonstrate the very low detection limits (cf., attribute ii) achievable with FLNS, consider Figures 13 and 14. These spectra were taken with the pulsed-dye laser/gated-detection system to be described in the instrumentation chapter. The resolution of the monochromator was 0.10 nm and the linewidth of the laser not less than 0.03 nm for these experiments. Figure 13 shows spectra for perylene (Pe) and 1-methylpyrene (MP) in a water/glycerol (4:5) glass at concentration levels of 20 parts per trillion (0.02 ppb). Perylene has a particularly high fluorescence quantum yield and can be seen to have a very good signal-to-noise ratio (S/N) at this concentration. Detection limits near one pptr for perylene are easily projected from this figure. The MP spectrum is not quite as pleasing due in part to instrumentation problems to be described later.

The spectrum on the left in Figure 14 is of pyrene at 20 pptr. In this case also, the analytical ZPL is quite plainly visible well above the detection limit. The vertical axis in both Figures 13 and 14 are normalized fluorescence intensity, I_f/I_o, as shown in equation (3). All three spectra, perylene 1-methylpyrene and pyrene, were taken from an artificial mixture containing pyrene, 1-methylpyrene, benzo[e]pyrene, anthracene, benzo[a]pyrene, and perylene. Several instrumental improvements could be made to increase signal-to-noise (S/N) greatly as will be explained later. Although these spectra are quite impressive, they by no means depict the best that FLNS can achieve.

To demonstrate the quantitative response of FLNS, cf. attribute iii, we discuss now some data obtained in our earliest experiments.

Figure 13. FLN spectra of perylene and 1-methylpyrene near their detection limits

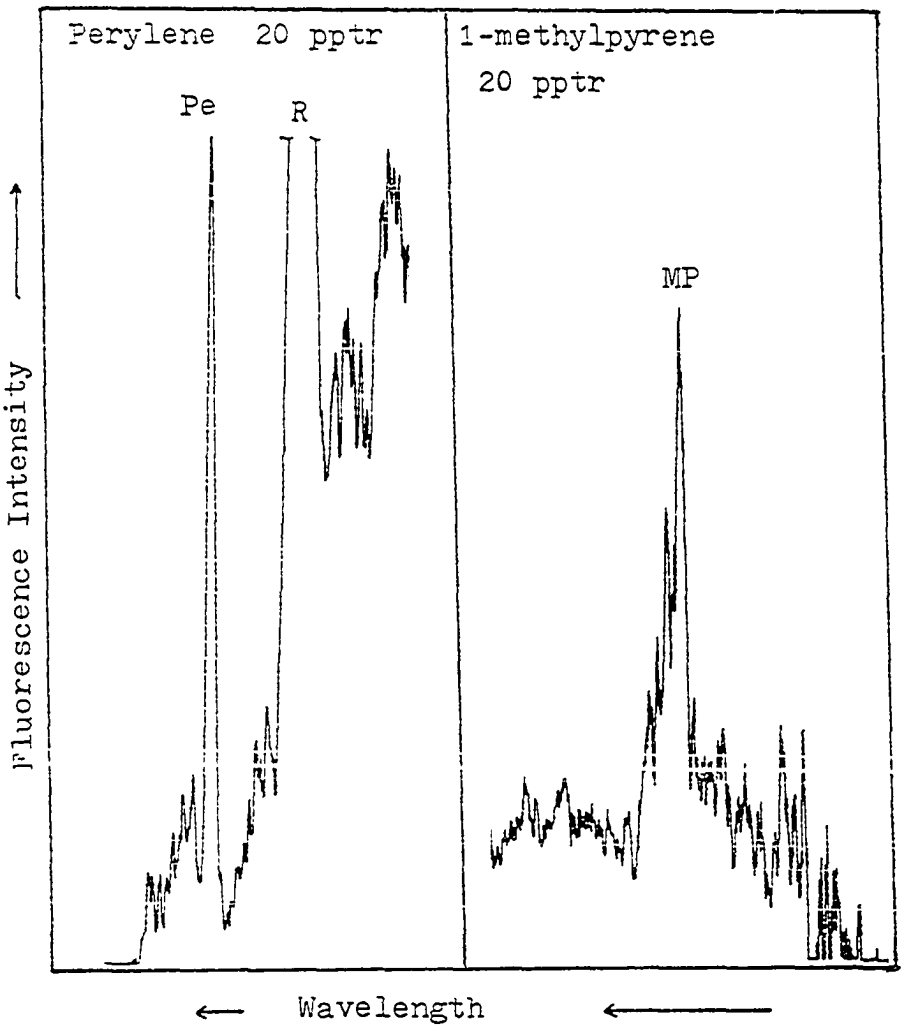
Perylene 20 pptr
Pe
R
1-methylpyrene
20 pptr
MP
Fluorescence Intensity
Wavelength

Figure 14. FLN spectrum of pyrene near the detection limit and spectrum of solvent blank under identical conditions

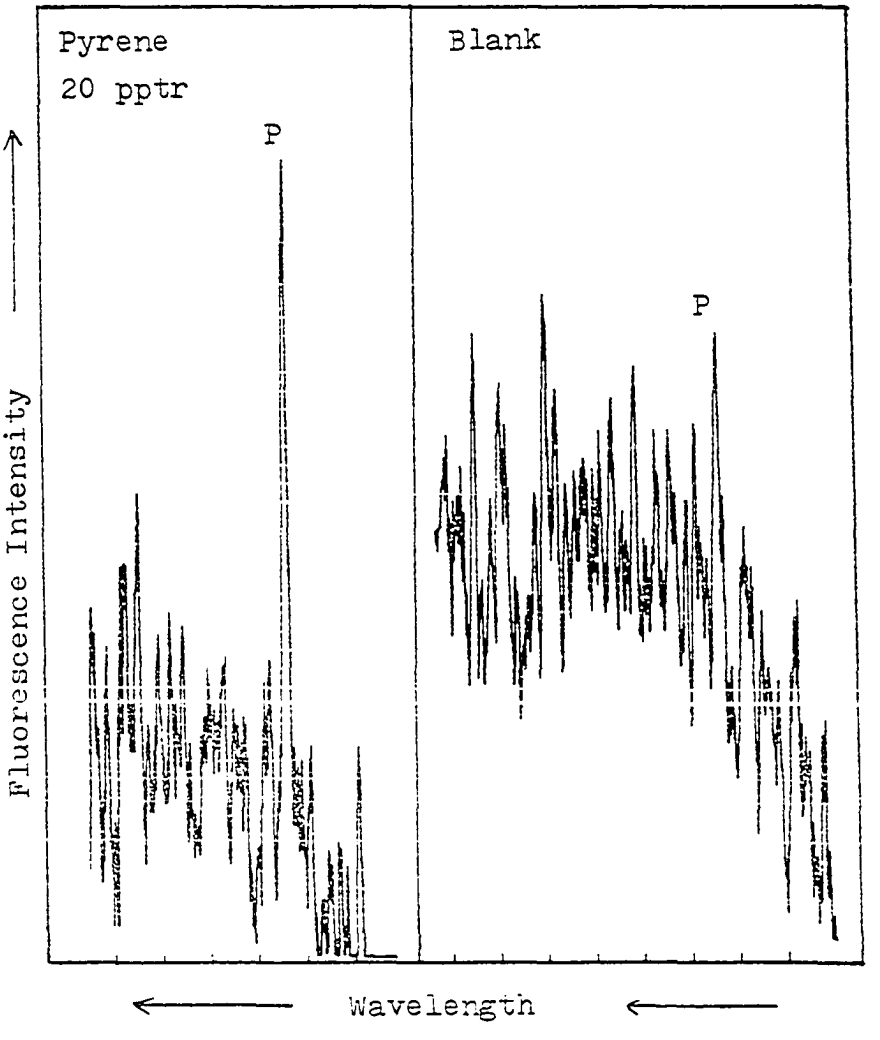
Pyrene
20 pptr
P
Blank
P
Fluorescence Intensity
Wavelength

Anthracene and pyrene can both be made to give analytically useful ZPLs in region II via excitation with the 363.8 nm argon ion laser line, as shown in Figure 15. A comparison of corresponding ZPL intensities for the two pyrene and the two anthracene concentrations shows not only that the two compounds are easily resolved, but that the unadjusted ZPL intensities are proportional to concentration.

To test this simple absolute intensity quantitation scheme, several mixture samples containing pyrene and anthracene were made spanning more than three decades in concentration. At least four spectra were taken from a minimum of two different glasses at each concentration except the lowest. Figures 16 and 17 show the resulting calibration curves. In this early experiment, it was assumed that the laser intensity, I_0 in equation (3), was constant. The calibration curves, therefore, are unnormalized intensity, I_f, versus concentration. The logarithmic scales are necessary for a meaningful display of the data. With the data forming its own error bars on the curves, it can be seen that the absolute quantitation scheme works well. The relationship is linear with an average deviation of about 8% at each concentration. This reproducibility occurs in spite of the fact that these data were taken in independent experiments, requiring several complete realignments during a seven day period. The only deviation from linearity occurs at the highest concentrations where aggregate formation and reabsorption, also called the "innerfilter effect", begin to become a problem.

The spectra from which points a and b on Figure 17 were taken are shown in Figure 18. Spectrum a in Figure 18 shows that the pyrene

Figure 15. FLN spectra of pyrene and anthracene excited with the argon ion laser

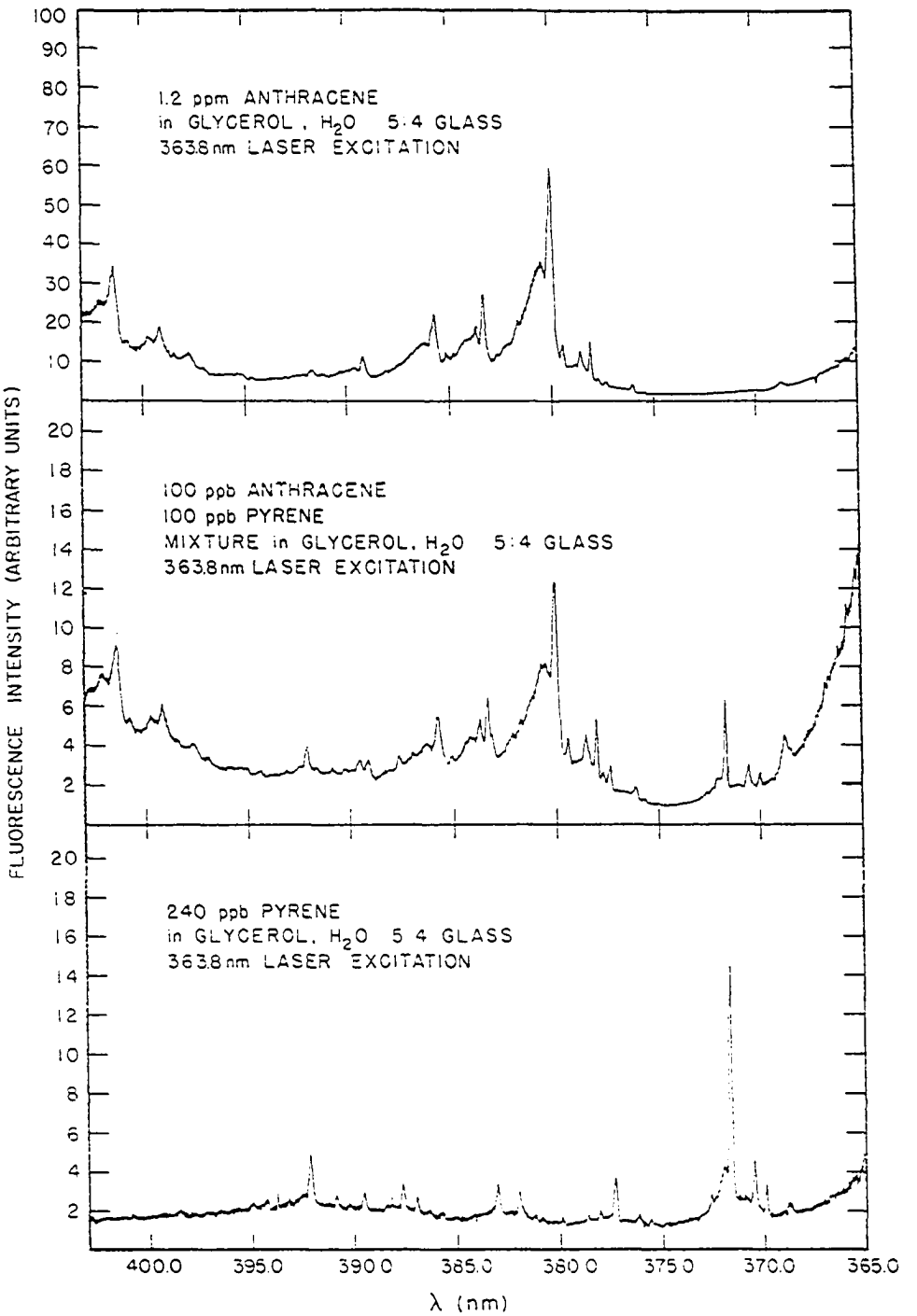
1.2 ppm ANTHRACENE
in GLYCEROL, H_2O 5:4 GLASS
363.8nm LASER EXCITATION
100 ppb ANTHRACENE
100 ppb PYRENE
MIXTURE in GLYCEROL, H_2O 5:4 GLASS
363.8nm LASER EXCITATION
240 ppb PYRENE
in GLYCEROL, H_2O 5 4 GLASS
363.8nm LASER EXCITATION
FLUORESCENCE INTENSITY (ARBITRARY UNITS)
400.0 395.0 390.0 385.0 380.0 375.0 370.0 365.0
λ (nm)

Figure 15. Anthracene calibration curve

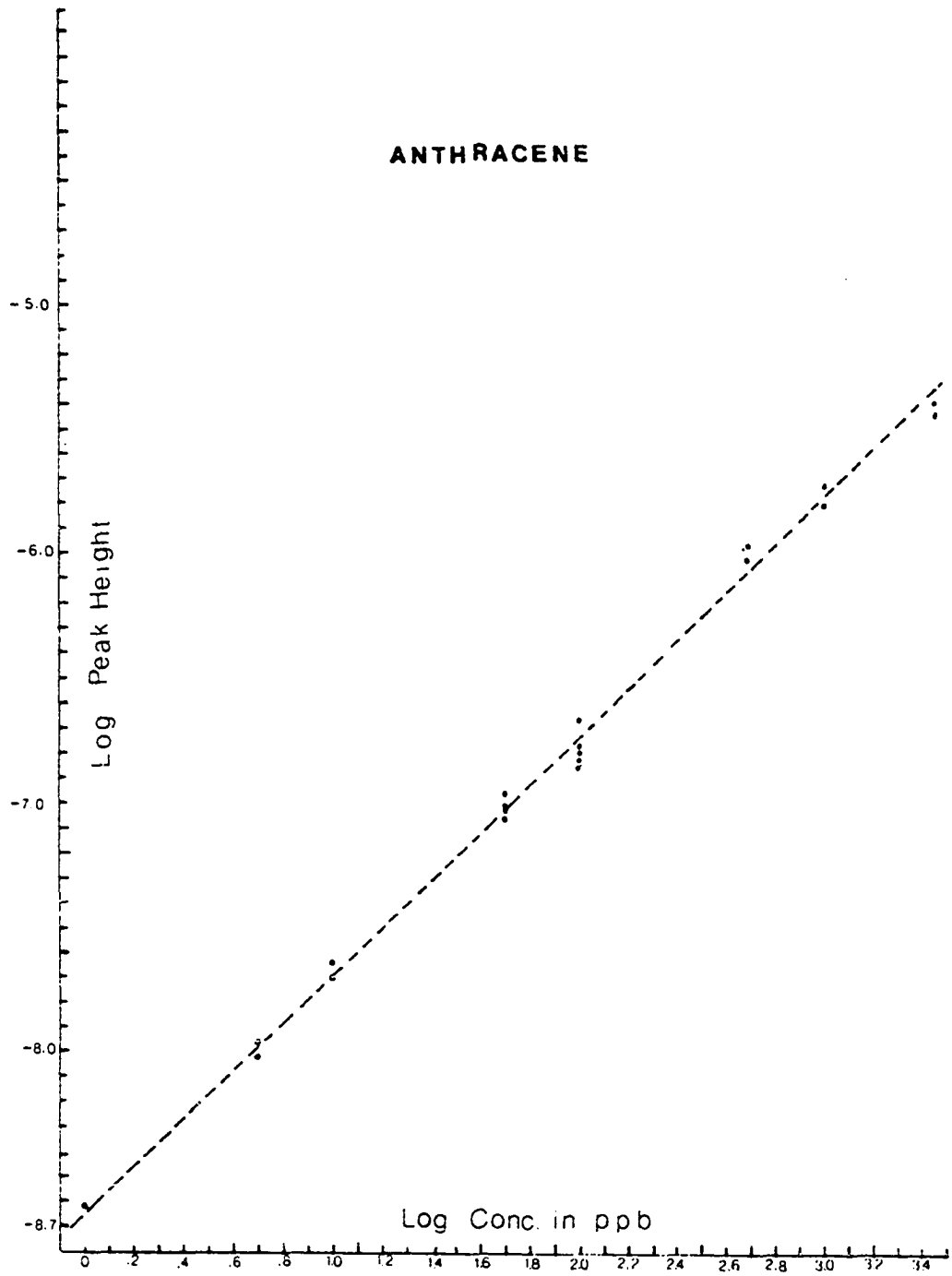
ANTHRACENE
-5.0
-6.0
-7.0
-8.0
-8.7
Log Peak Height
Log Conc. in ppb
0
.2
.4
.6
.8
1.0
1.2
1.4
1.6
1.8
2.0
2.2
2.4
2.6
2.8
3.0
3.2
3.4

Figure 17. Pyrene calibration curve

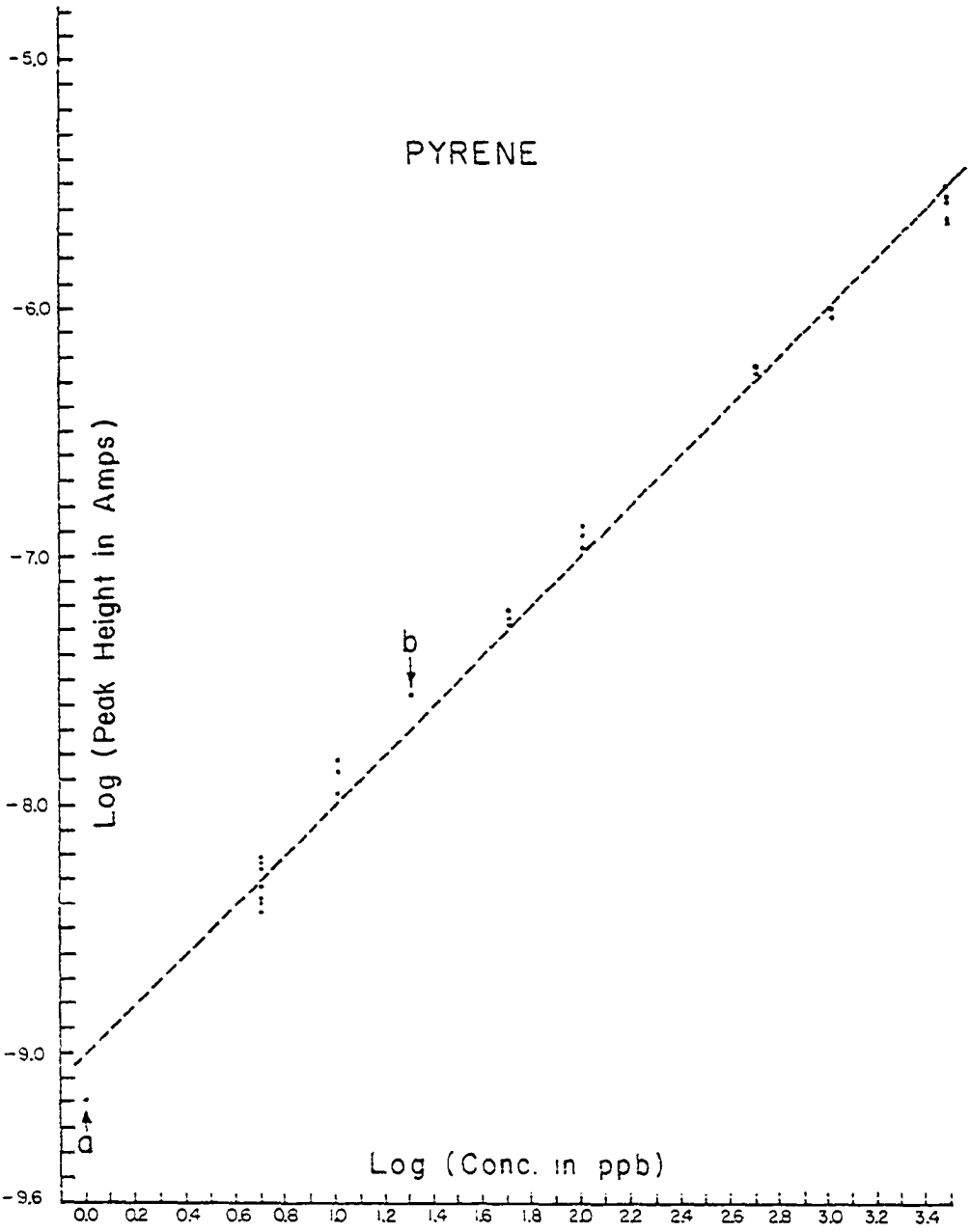
PYRENE
Log (Peak Height in Amps)
Log (Conc. in ppb)
-5.0
-6.0
-7.0
-8.0
-9.0
-9.6
a
b
0.0
0.2
0.4
0.6
0.8
1.0
1.2
1.4
1.6
1.8
2.0
2.2
2.4
2.6
2.8
3.0
3.2
3.4

signal in the artificial mixture is still quite large at one ppb, even with the rather primitive instrumentation used in these early experiments. Spectrum b was included to test for interferences. A sample of cigarette tar condensate was prepared and diluted so as to avoid a high absorbancy. At the very high dilution required, no pyrene signal could be seen. A sample of this diluted tar was spiked to 20 ppb with pyrene and included with the quantitation experiment samples. As can be seen in Figure 17, this point, b, falls on the calibration curve within the error established by standards. This indicates that there are no major interferences to be found for pyrene even in samples that contain many complex alkaloid species.

By way of review of the foregoing ideas and data, the following is a description of the steps involved in determining individual PAHs in a complex natural mixture. Step one involves direct incorporation of the sample (or a sample extract that is high in PAH) into the liquid glass solvent mixture. The overall dilution of the sample during this initial step must be great enough to decrease the total optical density at both the excitation and emission wavelengths of interest to acceptable levels, below 0.1 for a less than 10% error. The high dilution also helps ensure that individual analyte molecules are isolated within the solvent matrix, so that no aggregate formation will occur. The second step involves cooling the sample and one or more standards to cryogenic temperatures, 4.2 K for all work presented herein. FLNS spectra are then taken for each species of interest in the sample and for the corresponding species in the standard mixture under identical conditions

Figure 18. The spectra from which points a and b on Figure 17 were taken. Vertical and horizontal axes are at different dispersions in the two spectra

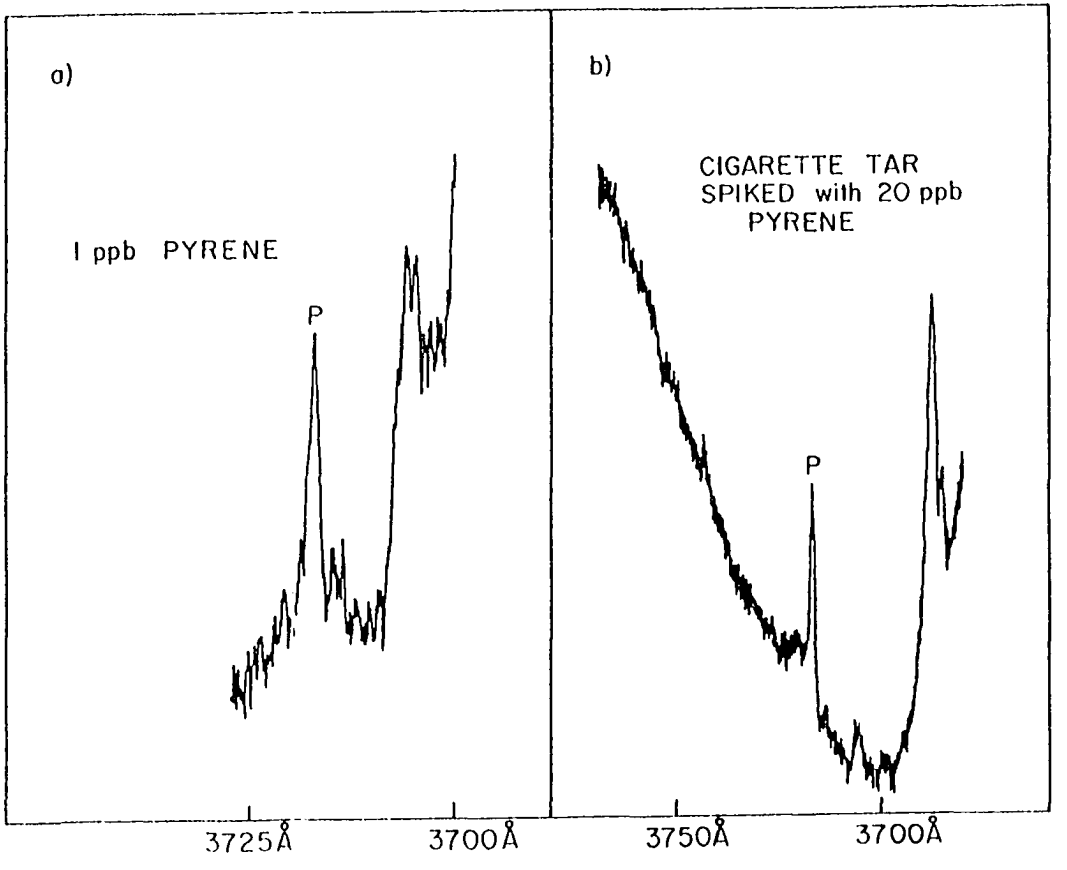
a)
1 ppb PYRENE
P
3725Å
3700Å
b)
CIGARETTE TAR
SPIKED with 20 ppb
PYRENE
P
3750Å
3700Å

of alignment and excitation wavelength. The ratios of analytical ZPL peak heights extrapolated above background for the standard and unknown are calculated. These numbers are multiplied by the standard concentration and the dilution factor to give the concentrations in the original sample or extract. The actual equations used are presented after a consideration of instrumental factors.

5. Temporal resolution

As already alluded to, temporal resolution of molecular luminescence is a powerful tool for the analytical chemist. Phosphorescence is generally longer lived than fluorescence which is longer lived than instantaneous Raman and Rayleigh scattering. Among PAHs, different species can have significantly dissimilar fluorescence lifetimes ranging from less than one nanosecond up to several hundred nanoseconds (17). For some analytical fluorescence techniques, these facts are of little value since the continuous excitation sources and steady state measurements cannot detect the different lifetimes. The most versatile moderate resolution lasers for FLNS, however, are pulsed nitrogen, eximer, or YAG laser pumped dye laser systems. The added analytical power imparted by the proper use of these pulsed excitation sources is explained and demonstrated in this subsection.

Excited electronic or vibronic states decay radiatively and non-radiatively (e.g., internal conversion or intersystem crossing). Focusing our attention on fluorescence, we note that it is well known that in the condensed phase the fluorescence generally decays exponentially following the preparation of an excited state population,

i.e., according to exp(-kt) with t, the time, measured relative to the time at which the excitation source is "shuttered". The radiative lifetime τ is the inverse of k, the radiative rate constant.

Values of τ for many PAH species are listed in reference 17. The exact values are not important since they undergo changes, albeit usually modest, with the medium. The important point is that the fluorescence lifetimes for the PAHs vary from less than one nanosecond to several hundreds of nanoseconds. This has several implications when pulsed laser excitation is utilized in FLNS.

The laser employed for most of the work in this dissertation produces a pulse about five nanoseconds in duration. The very short lived luminescence processes such as Raman and Rayleigh scattering and short lived (< 1 ns) fluorescence would be observed to follow the temporal profile of the laser. Emission from species with intermediate lifetimes, between 10 and 20 ns, can be seen to increase in intensity as the laser pulse evolves to its maximum intensity and then decay with a slower exponential tail than that of the laser. The fluorescence intensity of long lived species would be seen to increase throughout the laser pulse and to decrease with an even longer exponential tail.

Figure 19 illustrates the above and suggests a simple scheme for temporal resolution. Obviously, an ungated detection system would collect all of the emission. A gated detection system allows emission to be collected for specific intervals of time, thus selectively enhancing the contribution of one temporal component at a time, as shown in Figure 19. A gate opening at or before the beginning of the laser pulse and remaining open only during its duration is biased towards

Figure 19. Idealized decay of luminescence from short, intermediate and long lived excited states. All decay after about 7 ns is exponential. The laser profile is divided by a large factor with a temporal profile modeled after the laser used herein

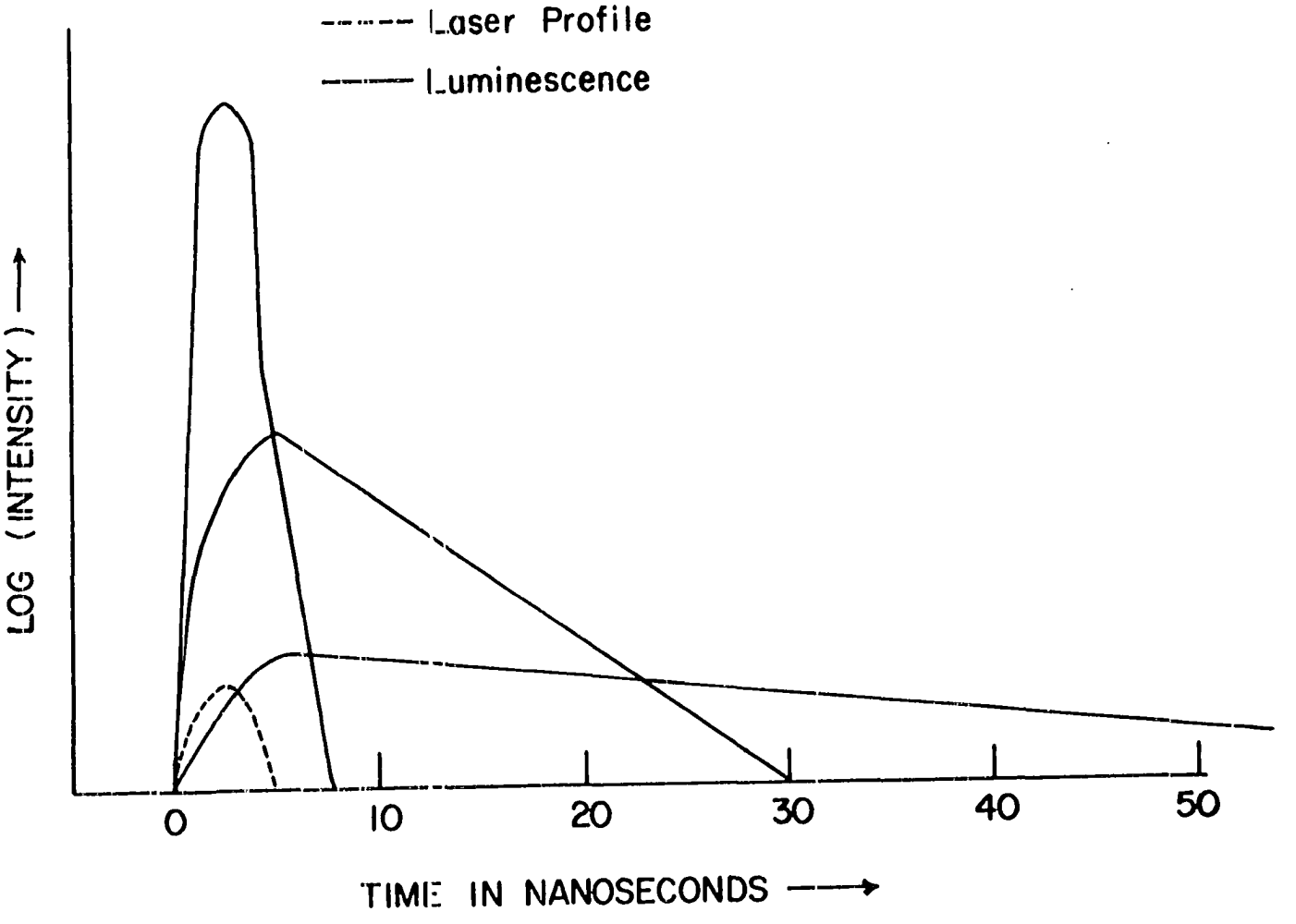
Laser Profile
Luminescence
LOG (INTENSITY) ⟶
0
10
20
30
40
50
TIME IN NANOSECONDS ⟶

short lived species. The intermediate and long lived luminescence signals would be greatly discriminated against since most of their integrated intensity occurs over times longer than the laser pulse. A gate opening at 5 ns and closing at ≈ 30 ns would "see" mostly fluorescence from PAHs with intermediate lifetimes -- the short lived states would have undergone substantial decay prior to the opening or the gate. Finally, a "late" gate opening ≈ 40 ns after termination of the pulse and left open indefinitely significantly accentuates the fluorescence intensities of long lived species.

Figures 20 and 21 illustrate the above effects and why the instrumentation described in the next chapter is capable of temporal resolution. All three of the spectra in Figures 20 and 21 were obtained from a mixture containing 200 ppb each of pyrene, 1-methylpyrene, benzo[e]pyrene, anthracene, benzo[a]pyrene and perylene with excitation of 363.5 nm. This excitation wavelength yields acceptable FLNS for pyrene and anthracene, but not for 1-methylpyrene (note the complex multiplet structure in its spectrum). This wavelength does not excite benzo[e]pyrene and results in the occurrence of benzo[a]pyrene and perylene fluorescence in region III. Figure 20 shows spectral regions I and II for this mixture where all temporal components are collected. The top spectrum in Figure 21 shows the early and intermediate fluorescence which is composed mostly of anthracene, $\tau \cong 4.9$ ns (17). The lines due to pyrene and 1-methylpyrene are even weaker than the Raman line marked in the early gated spectrum. The lower spectrum in Figure 21 shows a late "wide open" gate.

Figure 20. All temporal components in luminescence of a mixture

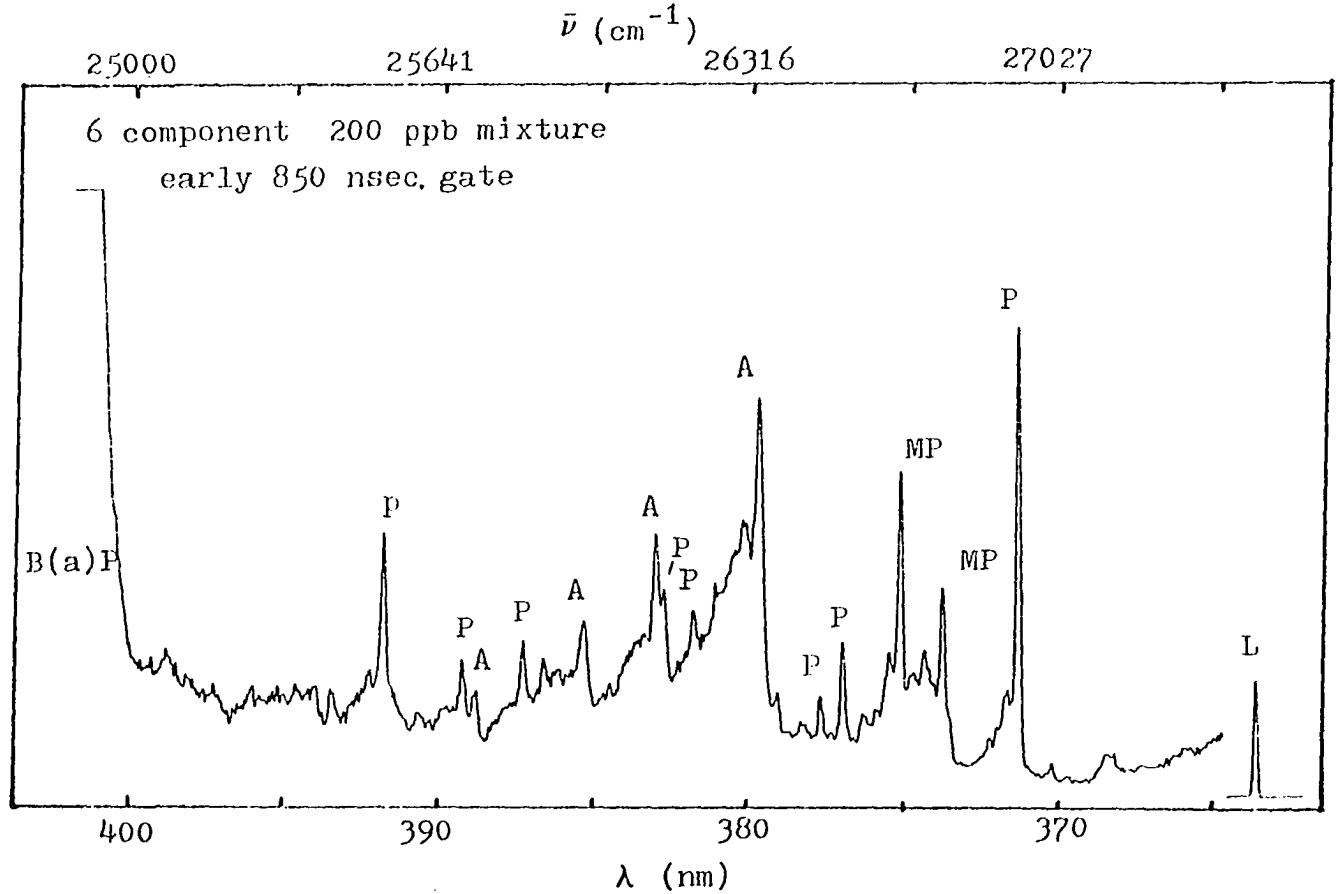
$\bar{\nu}$ (cm^{-1})
25000
25641
26316
27027
6 component 200 ppb mixture
early 850 nsec. gate
B(a)P
P
P
A
P
A
A
P
P
A
P
P
MP
MP
P
L
400
390
380
370
λ (nm)

Figure 21. Early and late temporally resolved FLN spectra from mixture in Figure 20

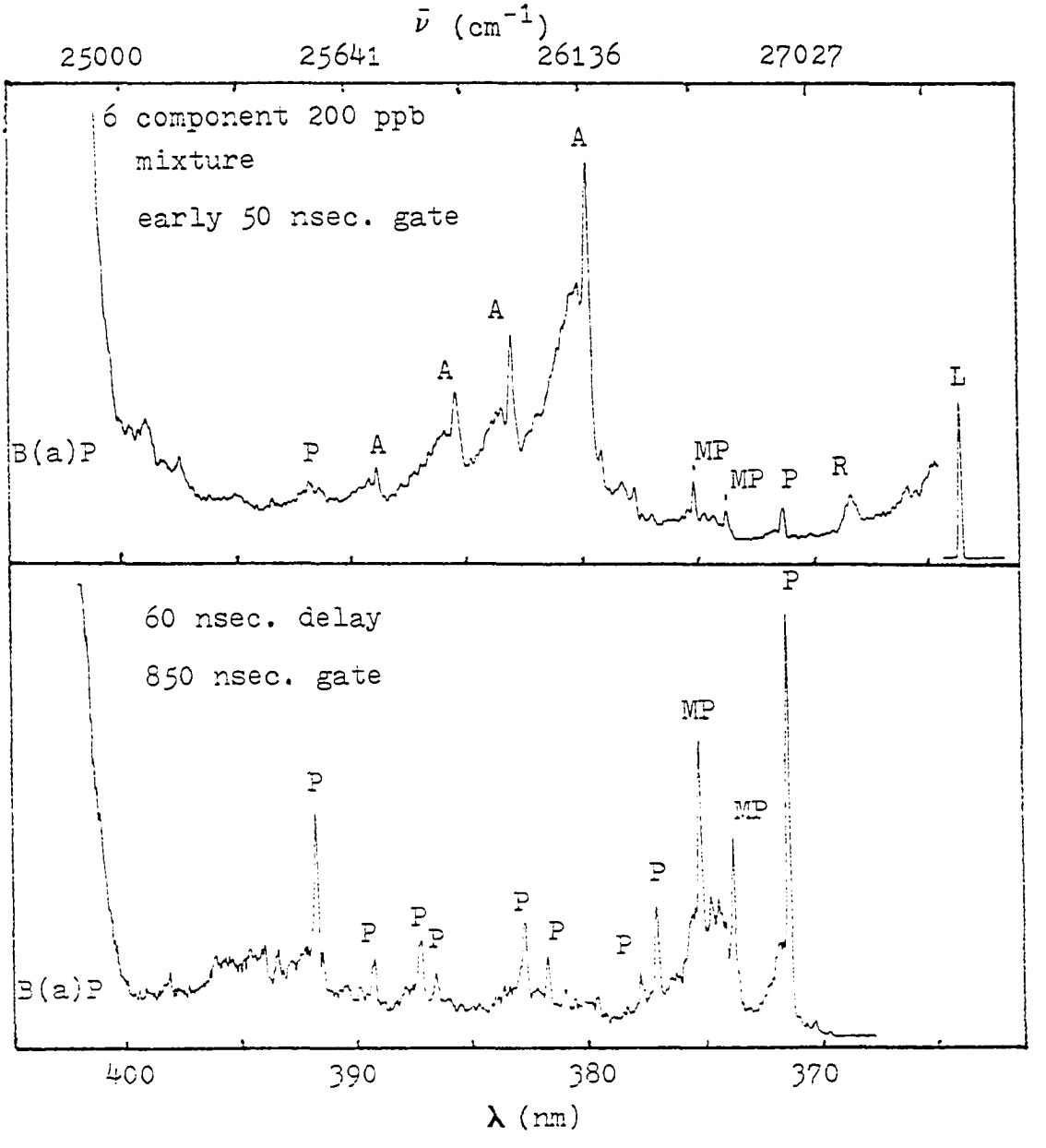
$\bar{\nu}$ (cm^{-1})
25000
25641
26136
27027
6 component 200 ppb
mixture
early 50 nsec. gate
B(a)P
P
A
A
A
A
MP
MP
P
R
L
60 nsec. delay
850 nsec. gate
B(a)P
P
P
P
P
P
P
P
P
MP
MP
P
400
390
380
370
λ (nm)

It is readily seen that the only bands appearing in this spectrum are due to pyrene, $\tau \simeq 400$ ns, and 1-methylpyrene which has a similar radiative lifetime. Note also that the sensitivity of the top and bottom spectra of Figure 21 are identical.

In the FLNS analysis of complex mixtures, temporal resolution has been found to be very useful. As will be seen later, region II of a complex mixture can be complicated when high sensitivity is utilized for the analysis of a minor constituent. By optimizing the time resolution and other parameters for each analyte, the complexity of region II (for each analyte) can be minimized. We note that several spectra (low concentration) in this dissertation reveal one of the most bothersome sources of interference -- solvent Raman emission. For example, in the perylene spectrum of Figure 13, such Raman bands are major features in region II where the analytical FLNS lines appear. Raman scattering, being instantaneous (following the temporal profile of the laser pulse) can be eliminated from the FLNS spectra of intermediate and long lived PAHs by gating.

In summary, temporal resolution, although not essential to FLNS, yields definite advantages. Its implementation when using pulsed excitation lasers is relatively straightforward and requires little additional expense. The characteristics of FLNS presented in this chapter demonstrate its promise as a technique for determining individual PAH species at concentrations between saturation and the pptr level in complex mixtures. The following chapters deal with the instrumentation and results of actual FLNS analyses.

IV. INSTRUMENTATION

A. Physical Arrangement

Two different types of instrumentation were used in this work. Early work including the pyrene and anthracene calibration data shown earlier utilized a Control Corporation[14] Model 553 argon ion laser. With uv optics, this laser lases cw[15] at 363.8, 351.4, 351.1, 335.8, 334.5 and 333.6 nm. The 363.8 line or any of the others was selected with a double prism and mirror arrangement situated in front of the laser. Both 60° quartz prisms were situated so as to approximate Brewsters angle in the polarized laser output. The mirror was used to align the desired beam through the opening of an iris diaphragm at the sample. A cooled EMI 9558QB photomultiplier tube wired for analog high gain current detection, vide infra, along with conventional current amplifier and strip chart output were used to display the dispersed fluorescence. Sample configuration and monochromator used were the same as for the pulsed laser instrumentation described below.

The cw laser instrumentation, although very simple, was not of much use for general FLNS analyses. Of the many compounds investigated, only pyrene and anthracene yielded acceptable FLN with the 363.8 nm excitation line. Triphenylene exhibited FLN when excited with the 330 nm excitation

---

[14] Orlando, Florida.

[15] The abbreviation cw (continuous wave) referes to the laser output power which is approximately constant in time.

lines. As shown in the Theory chapter, realization of the full power of FLNS requires utilization of a tunable laser system. Thus, once the analysis of the pyrene and anthracene mixtures had shown that FLNS in glasses allows for absolute quantitation (46), attention was focused on the design and construction of new instrumentation.

Figure 22 shows a block diagram of the instrumentation used during the final stages of this research. The argon ion laser, although included, was not actually used in any recorded experiments. The glass samples were placed either two or three at a time into the optical tail section of a Pope Scientific[16] glass liquid helium cryostat. The three liter double nested dewar was constructed so that no liquid nitrogen bubbles could interfere with either the excitation or luminescence optical paths. The dewar was equipped with quartz windows and a quartz inner tail section so that uv excitation could be utilized.

The fluorescence was excited with a Molectron Corporation[17] DL200 dye laser pumped with the output of a Molectron UV-14 nitrogen laser. The dye laser output was collimated near the laser and brought to the correct orientation for FLNS excitation with two front surface mirrors. A long focal length lens (50-100 cm) situated after the second mirror was used for final beam steering and to obtain a very fine focus through

---

[16]Manomonee Falls, Wisconsin

[17]Sunnyvale, California.

Figure 22. Block diagram of FLNS instrumentation

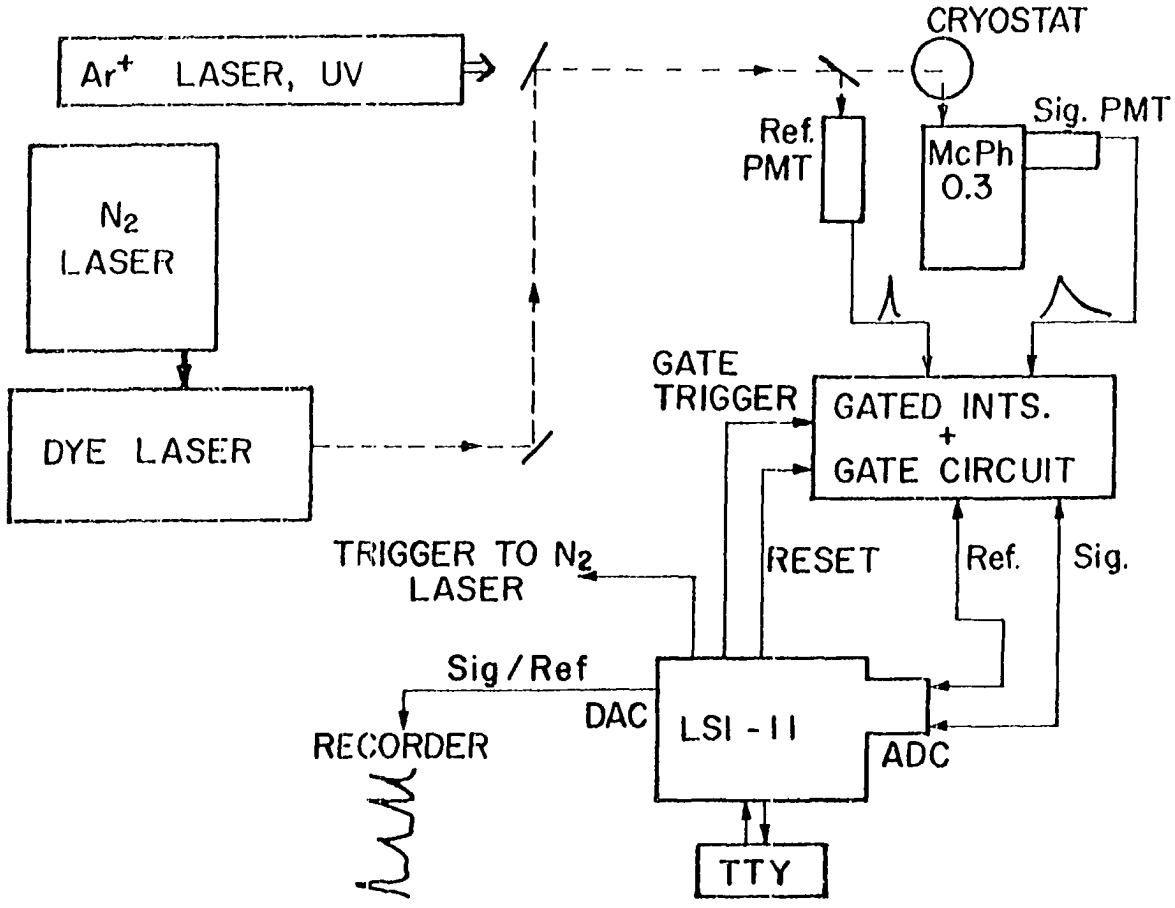
CRYOSTAT
Ar+ LASER, UV
Ref. PMT
Sig. PMT
McPh 0.3
N2 LASER
DYE LASER
GATE TRIGGER
GATED INTS. + GATE CIRCUIT
TRIGGER TO N2 LASER
RESET
Ref.
Sig.
Sig/Ref
DAC
LSI-11
ADC
RECORDER
TTY

the imaging region of the collection optics. A microscope slide beam splitter was positioned between this lens and the cryostat to split off a small fraction of the excitation beam for generation of a reference signal.

The fluorescence was collected at right angles to the excitation beam and imaged onto the entrance slit of a McPherson, model 218, 1/3 meter monochromator. The two quartz lenses used to collect and image the fluorescence were adjusted so as to match the f = 5.3 specification of the monochromator. The collection efficiency of the monochromator was greatly improved by rotating it 90° in a plane perpendicular to the collection optical axis. This made it possible for the line defined by the fluorescence image from the glass to be oriented parallel to the entrance slit. This horizontal slit orientation, as opposed to the conventional vertical orientation, was adapted very early on because it facilitated more than an order of magnitude improvement in signal. The grating of the monochromator could be scanned at several speeds to produce the necessary dispersed fluorescence spectra. The light passing through the exit slit of the monochromator was converted to an electrical signal by a rugged high gain photomultiplier tube (PMT), vide infra.

Figure 22 includes a block diagram of the electrical signal and control circuitry. The signals from the reference and signal PMTs were trapped on a set of gated integraters and sent to the analog to digital (ADC) input card on the DEC[18] LSI-11 laboratory computer. The computer

---

[18]Digital Equipment Corporation, Merrimack, New Hampshire.

also controlled the resetting and triggering of the gated integraters and the firing of the laser system. The digitized responses from the signal and reference channels were then converted, under program control, to a response on a strip chart recorder via a digital to analog converter (DAC). The PMTs, the gated integraters. and the computer control and display functions represented in the block diagram are each very important and as such are discussed separately in more detail in the following sections.

B. Photomultiplier Considerations

The pulsed nature of the nitrogen laser pumped dye laser system necessitates the use of special pulse response PMT configurations. A PMT amplifies the photoelectrons that are ejected from the photocathode by a fraction ($\sim$10%) of the incident photons. The original photoelectron is accelerated in an electric field toward the first "dynode" in an electron multiplier chain. The kinetic energy gained by the electron results in the emission of three to five secondary electrons by the dynode surface after impact. These secondary electrons are likewise accelerated toward the next dynode where they are again multiplied. The RCA 931-A PMT has ten such stages of amplification and the Amperex 2232-B has twelve stages. The final stage in each tube is an anode which collects the electrons emitted by the last dynode to produce a charge pulse of 10^6-10^8 electrons for each photoelectron emitted from the cathode.

For normal cw operation, where the photons arrive at rates of less than 10^6 per second, the output current is less than 10^{14} electrons per second or 0.02 milliamperes. The voltage divider that maintains the voltages between the dynodes can easily supply this current without noticeably affecting the interdynode voltages. Typical cw PMT configurations draw less than one milliamp from the high voltage power supply and distribute the high voltage evenly down the dynode chain for maximum gain. The current passed by each dynode surface increases geometrically as one approaches the anode until the last dynode which passes the entire output current of the tube.

For photon counting applications, some of the overall tube gain is sacrificed by proportionally increasing the potential differences between the last two or three dynodes. This voltage increase, coupled with the use of capacitors to supply the current while maintaining a constant voltage, allows the tube to give a faster response to charge pulses passing down the dynode chain. The higher electric field strength near the end of a photon counting dynode chain allows the electrons to be drawn away from the dynode surfaces faster, thus reducing space charging effects. Typical photon counting tubes can recover fast enough to allow temporal resolution of two or more photons in ten nanoseconds. Such currents (about 10^{15} electrons per second or 0.16 microamperes) cannot be maintained for long or the capacitors discharge, the final dynode voltages decrease, and the response of the tube deteriorates.

The pulses from the nitrogen laser pumped dye laser used in this experiment are only of five to seven nanoseconds duration. In light of the above description of normal cw PMT configurations, problems become apparent. Photon counting techniques would allow one to count zero, one or two photons per laser pulse -- a very poor dynamic range! Current detection with high gain tube configurations fares only a little better since the dynode/divider chain combination used can only respond linearly to short duration pulses that result in less than about one milliampere peak current which allows response only up to about ten photons per pulse. At ten photons per pulse, the statistical uncertainty is 32% which indicates an unacceptable signal-to-noise problem.

PMTs for pulsed light detection must be wired with special pulse response divider chains and used in an analog detection mode as opposed to pulse counting. These pulse response divider chains are highly "tapered", i.e., the interstage voltage increases as the secondary electrons travel down the dynode chain. This lowers the overall tube gain, but vastly increases the ability of the last few dynodes to carry large currents without space charging. All or most of the dynodes, especially near the end, are decoupled with capacitors large enough to supply all of the required current with no change in dynode potential. Also, to insure that the capacitors recharge rapidly, the divider chain is made to carry more current. The dividers used in this research dissipate enough I^2R power to make the tube housings warm to the touch ($I = \sim 3$ milliamperes).

Besides the design of the voltage divider chain, the choice of tubes is also quite important. Many photomultiplier tubes are designed for highest possible gain with no regard for high current response. For the widest dynamic range, the PMTs used must respond linearly to the highest possible currents. The tube used to monitor fluorescence must at the same time give a measurable signal at very low light levels. According to manufacturers specifications, the Amperex PM-2232/B PMT used with the voltage divider shown in Figure 23 can respond linearly up to 350 milliamperes with a gain of about 7×10^6. This allows measurement of from zero to about 1500 photons in a ten nanosecond pulse. Notice that the divider is highly tapered and that the last four dynodes are decoupled with large capacitors. The resistor and capacitor network at the negative high voltage input is a radio frequency filter for the high voltage input line and the magnetic shield.

The expensive high gain Amperex tube just described is not necessary for the reference PMT application. The reference signal split off from the incident laser beam can be made arbitrarily large up to levels where one laser shot vaporizes the PMT cathode. Laser intensity variations of more than one order of magnitude can be discounted by the data handling routine as misfires. Thus, the tube used for reference can have lower gain and a lower dynamic range.

The best compromise between performance and cost appears to be the RCA 931A PMT. Using a divider constructed very much like that proposed in reference 69, the RCA 931A responds linearly to peak currents in excess of 60 milliamperes with a gain of just less than 10^6. The gain

Figure 23. Base wiring diagram for PM 2232/B used in FLNS experiments -- based on standard "B" divider voltage ratios supplied by Amperex Corporation

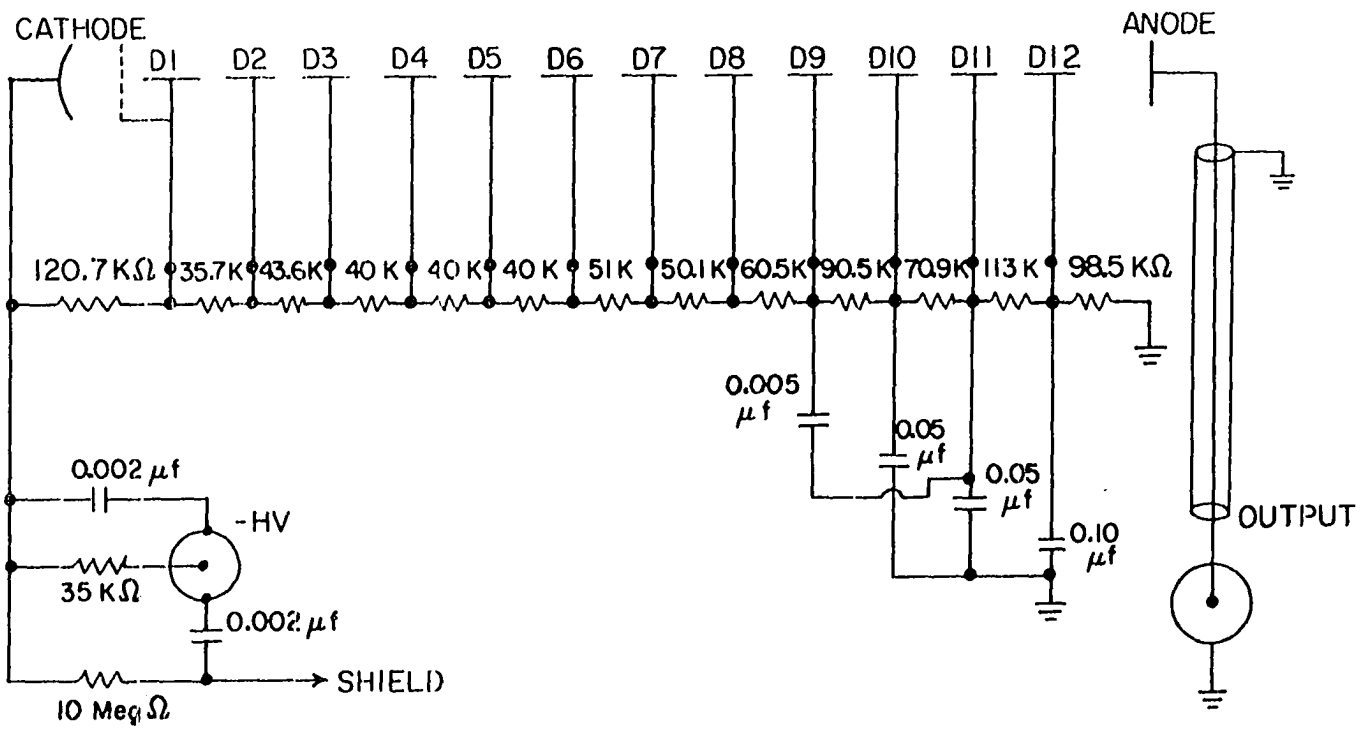
CATHODE
D1
D2
D3
D4
D5
D6
D7
D8
D9
D10
D11
D12
ANODE
120.7 KΩ
35.7K
43.6K
40 K
40 K
40 K
51 K
50.1K
60.5K
90.5K
70.9K
113 K
98.5 KΩ
0.005 μf
0.05 μf
0.05 μf
0.10 μf
0.002 μf
-HV
35 KΩ
0.002 μf
SHIELD
10 Meg Ω
OUTPUT

need not be so high. For this reason, some experimentation was done with abbreviated dynode chains which involve electrically tying the last several dynodes to the anode (70-72). Although these designs allow the tube to respond linearly to more photons, the peak currents produced were decreased. Therefore, due to the need for the largest possible signals in the electrically noisy laboratory environment, this experimentor chose to use a modification of the literature design.[19] A rather extensive review of the considerations involved in choosing a detector for pulsed optical signals was presented by Lytle in 1974 (73).

C. Charge Sensitive Gated Integrator

The radiative lifetimes of most PAH fluorescent states are less than 100 nanoseconds. For optimal performance, the laser is fired at rates of about 25 Hertz (Hz). Therefore, the signal is present for only 1/400,000 of the time, i.e., the detection electronics can respond to noise 400,000 times longer than signal. Because of the heat generated by high pulse response divider chains, tube noise may be substantial. Thus, standard cw current amplification techniques look very unattractive. The multiple excitation perylene data shown in Figure 10 was taken with a conventional current amplifier and a pulsed laser.

---

[19]The resistance values proposed by Harris, Lytle and McCain (69) were increased by a factor of four to account for the lower duty cycles in this experiment. Also, the resistances of the last three dynodes were increased progressively to give the divider chain slightly more taper.

However, this particular sample was so strongly fluorescent that the yellow solution looked blue in room light. Also, this experiment used a refrigerated high gain PMT. No other spectra could be obtained this way indicating a pressing need for a gated detection system.

As a first step in this direction (monitoring of a signal only during its "on" time), a commercial boxcar integrator[20] was applied to this pulsed fluorescence problem. With the fast pulses produced by this experiment, the boxcar seemed to have a dynamic range that was even more restricted than that of the PMT. This very unsatisfying state of affairs is brought on by the fact that the boxcar integrator terminates the signal from the PMT anode and converts the current to a voltage. The commercial instrument then depends upon the ability of a voltage following circuit to respond to the rapidly changing voltages at the termination resistor. The finite setting time of the voltage follower, the wide range of rapidly changing voltages produced by the terminated currents, and the voltage oscillations produced when the very low impedence signal from the PMT encounters all of the stray capacitance and inductance problems inherent in PAR's design (70) cause many noise and dynamic range problems. Added to this, the PAR boxcar's trigger mechanism is so slow that our laboratory computer had to be used to simultaneously trigger the laser and the boxcar more than one microsecond before the event. The reaction of this investigator to all

---

[20]A Princeton Applied Research Model 164 boxcar integrater.

these shortcomings was to relegate the boxcar to use as a very pretty bookend.

Using the laboratory computer, a pair of $125.00 gated integrator boards, and a handful of inexpensive integrated circuits, a gated detection system that is vastly superior to the $9,000 PAR boxcar was assembled. This detector is based on the decision that the best way to handle signals from the low impedence "ideal" current source represented by the PMT anode is to treat them as currents, not voltages. This simplifies the instrumentation, thus, reducing sensitivity to stray capacitance and inductance. The gated integrator design used for most of the pulsed work presented in this thesis is sketched in Figure 24.

The function of this circuit is quite easy to understand. The gate driver circuitry supplies complimentary signals to the bases of the two D-MOS FET gate transitors. With the gate in the false state, transistor G1 is turned on hard and transistor G2 is turned off. Thus, in the false state all current from the PMT anode is shorted to ground and none can get through G2 to the analyzing capacitor, C_a. With the gate in the true state, transistor G1 is turned off and G2 turned on so that all current from the PMT is accumulated as charge on the analyzing capacitor.

The charge that is accumulated on the analyzing capacitor is expressed as a voltage by the analyzing capacitor following the simple rule:

$$\Delta V = \frac{Q}{C} \qquad (4)$$

Figure 24. Schematic diagram of gated charge sensitive integrator used for detection of pulsed fluorescence

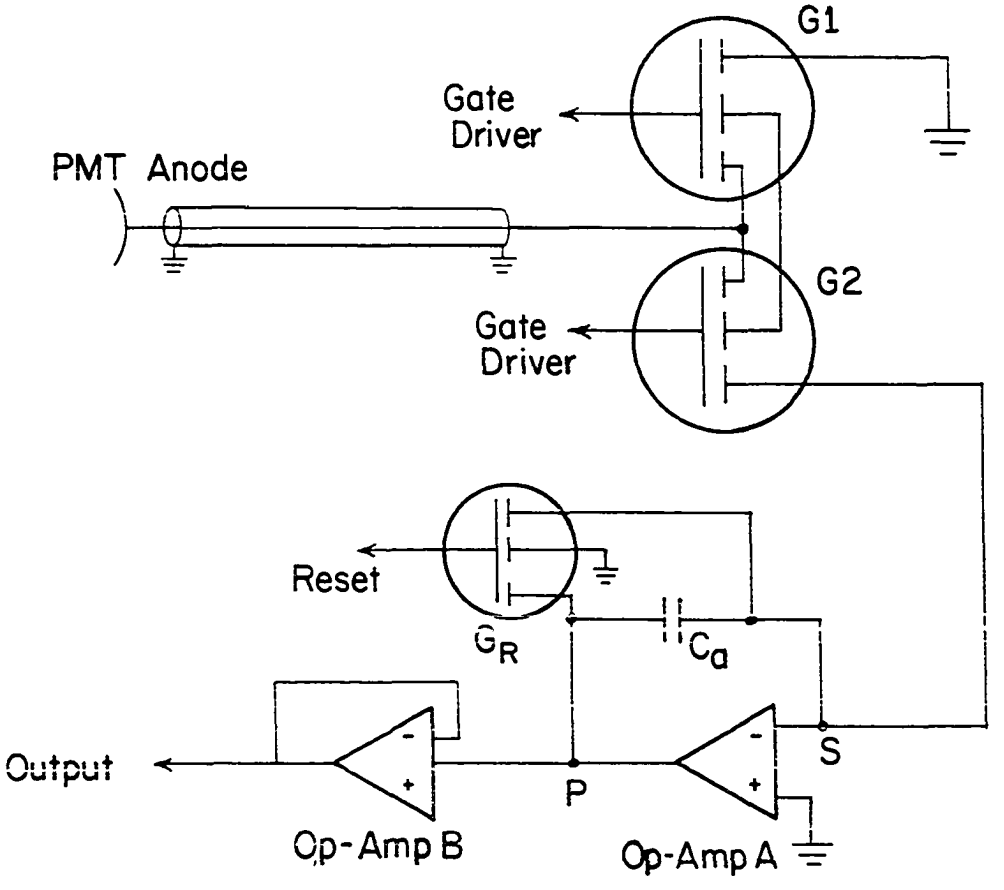
G1
Gate
Driver
PMT Anode
G2
Gate
Driver
Reset
G_R
C_a
Output
P
S
Op-Amp B
Op-Amp A

ΔV = Voltage difference across the capacitor

Q = Charge on the capacitor

C = Capacitance in farads of the analyzing capacitor

As the charge accumulates on the analyzing capacitor, operational amplifier A changes its voltage output to keep the potential at the summing point, s, at ground. Even if op-amp A cannot slew its output fast enough to keep up with a rapidly accumulating charge, when the gate goes false the charge is trapped. The op-amp will eventually display the signal predicted by equation (4). This design eliminates the need for impossibly fast voltage followers.

The remaining elements in Figure 24 complete the circuit. Operational amplifier, op-amp B, is necessary to isolate the analyzing capacitor from the output line. This supplies line driving capability and prevents feedback from the voltage detection circuitry. Once the current of interest has been gated onto the analyzing capacitor and the circuitry given time to settle, the output displays a DC level equal to ΔV in equation (4). Once the data have been read, in this case by the ADC input of the LSI-11, the analyzing capacitor, C_a, can be zeroed by temporarily shorting the two plates together via a signal opening G_R, the reset gate. Alternately, more than one shot can be accumulated on the analyzing capacitor before it is read and reset. Multiple shot accumulation may, in fact, have some advantages when looking at small signals. However, in all of the pulse spectra that appear in this dissertation, only single shots were allowed to accumulate at the integrator.

The sequence of events that occurs each time the laser fires is shown in Figure 25. Two trigger pulses are generated simultaneously by a single computer instruction at a parallel interface. The two coincident trigger signals are transmitted to the experiment via a pair of 75182/75183 differential line driver/receiver integrated circuit based cards and ribbon cables. One trigger line triggers the laser. The second triggers a 74121 integrated circuit implemented delay circuit. This delay can be changed with a variable resistor (a potentiometer, Pot) to trigger a 74121 gate circuit at any time before, during or after the firing of the laser at about 1.5 microseconds after the original trigger. The gate width can, likewise, be varied with an adjustable resistor so that temporal resolution as described in a earlier chapter can be utilized.

The gate driver circuit, the current gate the integrator, and the reset gate are contained on the commercial Evans Associates[21] model 4130 gated integrator module. Two of these modules are used, one for the signal PMT and one for the reference PMT as depicted in Figure 26. The analyzing capacitors, C_a, were chosen for each channel so that the maximum linear response from the tube gives a three-to-five volt response from the integrator. This optimizes the dynamic range since the maximum response of the integrators is 5 volts and the maximum value that can be converted by the ADC is also 5 volts. The ADC does a 12 bit

---

[21] Berkeley, California.

Figure 25. Temporal relationship between control logic, laser and fluorescence signals

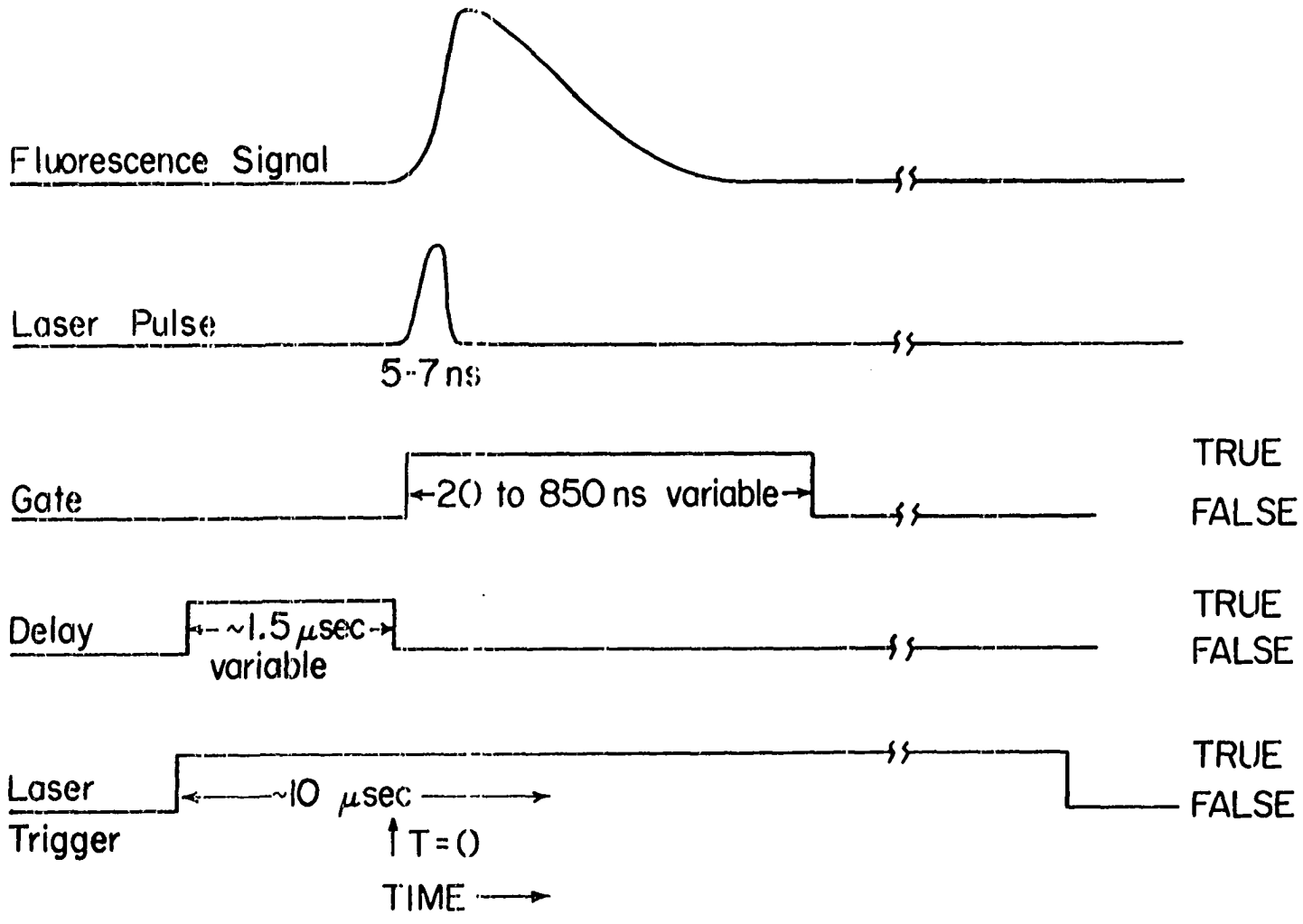
Fluorescence Signal
Laser Pulse
5-7 ns
Gate
←20 to 850 ns variable→
TRUE
FALSE
Delay
←~1.5 μsec→
variable
TRUE
FALSE
Laser
Trigger
←~10 μsec→
T=0
TIME →
TRUE
FALSE

Figure 26. Signal and reference channels

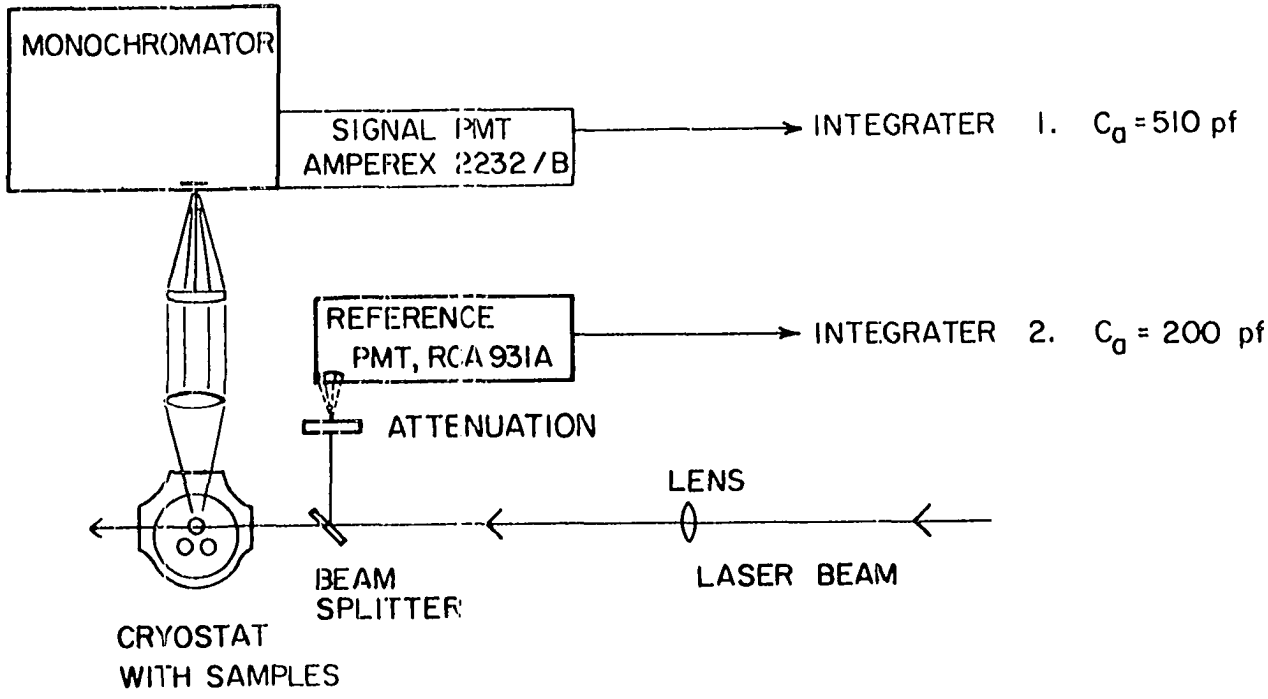
MONOCHROMATOR
SIGNAL PMT
AMPEREX 2232/B
INTEGRATER 1. C_a = 510 pf
REFERENCE
PMT, RCA 931A
INTEGRATER 2. C_a = 200 pf
ATTENUATION
LENS
BEAM
SPLITTER
LASER BEAM
CRYOSTAT
WITH SAMPLES

conversion which, when the gains of the tubes are considered, gives about a one photon per bit sensitivity on both channels. This one photon detection limit and three decade dynamic range is thus common to all three steps in the conversion of photons to digital signal.

Before continuing with a description of the computer program, it is important to note that the Evans integrator modules are not used precisely in the configuration they were in when they were purchased. The modules are designed for general purpose applications and contain much circuitry that is not used in this application. One such circuit is an op-amp wired in parallel with the input shown in Figure 24. This circuit is included so that high impedence signals can be measured as voltages. To prevent large current errors from being introduced by offset errors in this op-amp, the conductor connecting it to the input of the gate is removed. Also, all resistors in series with the input must be removed, or at least reduced to below about ten ohms, to prevent distortion of the temporal profile required for temporal resolution. The circuits as they exist on the Evans cards are prone to leaky gate problems. Large signals tend to confuse the states of the gates. Proposals have been made to change the 0 volts and +6 volts off and on levels to something like -5 volts and +12 volts (70). Although this idea was not implemented in this work, the substrates of the D-MOS FET were disconnected from ground and tied to each other since this is reported to both decrease the charge injection caused by changing the state of the gate and to slightly improve the off to on resistance ratio (70). A vastly improved integrator in terms of gate speed, gate

leakage, and noise minimization could be built by careful design using the most modern electronic components (70).

D. Computer Control and Data Reduction

As mentioned several times in preceding sections of this chapter and shown in Figures 22 and 25, the laboratory computer is a very important part of the instrumentation used in these investigations. The LSI-11 computer in our laboratory was assembled from individual components by this investigator and several other members of Professor G. J. Small's research group before serious work on pulsed laser excited fluorescence was begun. The total hardware cost for this quite powerful computer was less than $6,000. For these investigations, no commercial software was purchased. Programming involved either machine code entry via firmware implimented ODT (octal debugging technique) or down-loading from an assembler program resident at the campus computer center. A short program,[22] supplied by Dennis Jensen at the Ames Laboratory Instrumentation Services department, could be loaded via paper tape to provide easy communication on the campus time sharing network via the Teletype[23] 43 console of our computer. This program provided for interaction with the Stanford WYLBUR text editing and remote job entry capabilities of the campus computer center's time sharing system. Once

---

[22]ALVIN version 2.8 or version 3.0.

[23]Teletype Corporation, Skokie, Illinois.

a program had been edited and assembled successfully, using WYLBUR, a hexadecimal load module could be down-loaded into the memory of the LSI-11 via interactions between ALVIN and WYLBUR over the phone.

The final version of the program, written to control the acquisition and output of data from the pulsed laser experiment, is included as an Appendix at the end of this thesis. No fast permanent data storage was available, so all output was displayed in real time as the experiment progressed. Before the firing of the laser depicted in Figure 25, the computer program resets both integrators, gates both integrators, measures offsets or dark signals off of both integrators, and resets the integrators again. A few microseconds after this last reset, the trigger signals are produced and the sequence in Figure 25 takes place. Then, the data are taken from both integrators via an ADC interface to the computer. The integrators are reset again. After that, the control routine awaits the next clock generated interrupt (400 millisecond intervals) to begin the cycle again.

During the interval between reading of the data from the integrators and the second reset signal, the computer tests whether the laser fired successfully. If the reference signal level is below a certain value, the routine discards the data and waits for the next interrupt. A higher reference level indicates a successful firing of the laser and initiates the calculation of a normalized scaled value for display.

The fundamental purpose was to obtain values for I_f/I_0 at each wavelength as explained in equation (3). However, the matter is

somewhat complicated. Due to offsets on the outputs of the integrators, noise, and possible ground loops, the offset of both integrators must be measured and subtracted to obtain useful intensity values. The need for real time display requires that the normalized intensity values be multiplied by a scaling factor to obtain a number large enough to give a response on the strip chart. Also, when one is looking at low concentration constituents, the background may be many times more intense than the sharp signal lines. This requires that a DC offset be subtracted from the signals so that the ZPLs can be observed. A DC offset may need to be added when using a delayed gate to gate out very large short lived signals. Such signals cause reflections in the coaxial cable between the anode and the gates resulting in delayed fluorescence which occurs coincident with the negative portion of the ringing from the earlier signal. The function chosen is represented in equation (5) and can be seen in the program if one traces through the math for the normalized mode:

$$(\text{DC offset}) + \left[\frac{(\text{Signal})-(\text{Signal offset})}{(\text{Reference})-(\text{Reference offset})} \times (\text{Scaling factor}) \right] \quad (5)$$

The scaling factor and the DC offset to be used are entered at the teletype during set-up. The calculation in equation (5) is done after every successful firing of the laser.

Several steps are taken to improve the precision of the computer output from the experiment. When the data are read from the ADC, the voltage is measured eight times and accumulated. This sum is converted

to floating point and divided by eight to give an average value. This improves on the ±1 precision of a single ADC conversion. All calculations after initial data acquisition are carried out in floating point with 24 bit precision. The final value, after calculations with equation (5) are complete, is converted back to an integer just before display on a 12 bit -10 to +10 volt DAC onto the strip chart recorder.

From the outset, the pulsed fluorescence experiment suffered from high noise levels. Thus, to obtain useful spectra, such as those near the detection limits, Figures 13 and 14, some way of dealing with the noise had to be found. Only for the most intense spectra, e.g., 100 ppb perylene, could an output based on equation (5) give useful spectra. Some reasons for these problems are given in the next section. However, at the completion of this work, the noise had to be dealt with by the computer program. Simply averaging the data as they arrived was unsatisfactory. An average large enough to give smooth data also required extremely slow accumulation of data. An average small enough to allow no compromise in resolution of the dispersed spectra would actually make the data appear worse than no average at all. The eye can discriminate and discard spurious data and still recognize real trends in the data. Simple averaging cannot.

The answer to this type of noise lies in filtering, not in averaging or smoothing. Filtering more closely approximates the action of the human mind when viewing noisy data. The empirically developed filter used in this work and shown in the program in the Appendix effectively reduces noise in output of the program. The top spectrum

in Figure 27 was produced by photographing an oscilloscope display of the output without the usual smoothing. To extract the data from the noise, the program does a median weighted average.

The way that the median weighted average acts as a filter can be understood from the following description. The data are taken and calculations with equation (5) carried out. The data are then stored in order of accumulation in a fifteen point running stack. This preserves the temporal relationship of the data so that the real spectral intensity changes in time are preserved. Each time a new point is obtained, it is added to the bottom of this stack and a point from the top is discarded. To obtain the output point after the addition of a new input point, a second stack of numbers is constructed from the first. The second stack is ordered from largest to smallest number with total disregard to the order of occurrence in the running stack.

Once ordered, the numbers in the second stack are multiplied by a symmetric set of fifteen coefficients[24] (0, 0, -5, -30, 50, 100, 200, 300, 200, 100, ...). The number obtained after dividing by the total is fixed (changed to integer representation) and displayed at the output DAC. This entire process is repeated from the updated running stack each time a new input value is obtained. For data not requiring

---

[24]The particular values for these coefficients were chosen in an intuitive nonrigorous manner. Experimentation with arbitrary data sets convinced the author that these numbers produced a better filter than any of the least-squares derived sets of coefficients.

Figure 27. A. Raw data from a scan in the region of the benzo(e)pyrene origin at a concentration near the detection limit.

Figure 27. B. The same data after filtering

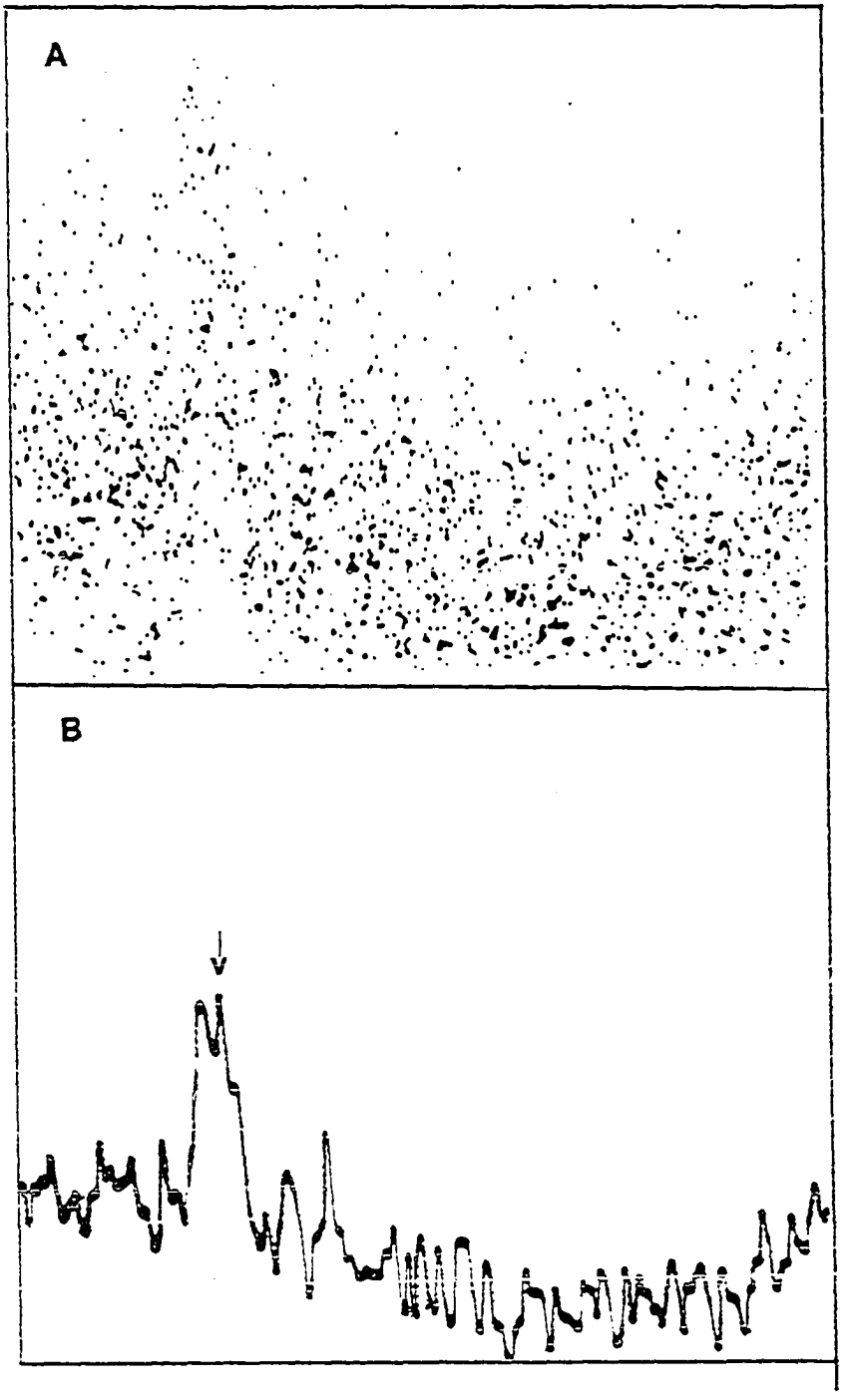
A
B

filtering, this heavy weighting on the median results in good preservation of the data. Points widely divergent from the median, however, receive zero weight serving only to determine the median and not contributing to the weighted average.

Since 15 points is about as large a resolution element as the analyst would want to contend with in a 25 Hz experiment, the ideal smooth might involve a cascade of two or more of the above filter routines. However, the sorting of the running stack taken a lot of processor time. Thus, one 15 point filter is all that there is time for before the next interrupt arrives. The compromise used in the program listed in the Appendix is to follow a fifteen point filter routine with a running average. The lower data set in Figure 27 is the result of doing a 15 point filter followed by a 15 point running average on the data set in the top half of the figure. The arrow in Figure 27B marks the benzo[e]pyrene ZPL. This structure is real and reproducible.

E. Suggested Improvements

1. In data handling and computer control

With Figure 27 in mind, an immediate improvement can be suggested. The filter routine implemented for the data in this thesis was adopted out of desperation because the author was mistakenly using smooth as the key word to search the literature for filters. Since this work was finished, it was found that a mathematically more elegant filter routine based on a digital implimentation of a Butterworth filter could do as

good a job of extracting data as the empirical filter. Programs utilizing Butterworth filters have been written (72,74) and shown to give results comparable to Figure 27B at a fraction of the computer calculation time. Thus, two or more Butterworth filter routines could be cascaded to give greatly improved data extraction in real time.

Another, even more obvious, improvement can be made. When normalizing, filtering, scaling, and outputting data as the experiment is taking place, any error in scan speed filtering, DC offset, or scale factor can ruin the stripchart representation of the data. The remedy for this is to add a permanent data storage device to the computer system. The I_f/I_o versus λ[25] data could then be stored permanently. After all of the data have been taken and the laser turned off for a particular spectrum, the optimal smoothing, scaling, and DC offset values could be chosen at leisure. The running time of any filter routine would be of no consequence and several stripchart displays could be made of a single spectrum to feature several chosen elements of the data in an optimal manner. With permanent storage of the normalized data, the only errors which would make a spectral data set worthless would involve the wrong excitation wavelength, too fast of a scan rate, or the wrong gate width and delay settings.

When using FLNS for routine PAH analysis, increased automation of the instrumentation could greatly decrease the skill demanded of the

---

[25]Lambda, λ, usually expressed in nanometers (nm) or angstroms (Å) is the common symbol for wavelength.

operator. Control of the laser wavelength and monochromator scan speed could be made automatic by installing stepping motors or similar devices to the wavelength drives of these two instruments. The computer under program control could then select the proper excitation wavelength for the compound being determined, tell the operator which laser dye to use, and verify that the laser was lasing at the proper wavelength with a reasonable intensity. During a scan, the computer program could be made to sample the signal levels and to select a scan speed (or number of scans to average) which would optimize both the signal-to-noise ratio of the data and the speed of the experiment.

The gate width and delay could also be easily automated. The potentiometers which act as variable current sources and adjust the response time of the monostable multivibrators could be replaced with current DACs. This would give the computer program digital control over gate width and delay. The computer could then produce temporal profiles for any or all luminescence signals in a spectrum. Such capabilities would greatly aid the experimentalist when choosing the best conditions for determining a new compound. Also, such automation would remove the possibility of operator mistakes when doing routine analyses. Essentially every aspect of this experiment is amenable to computer control.

2. Increased laser power

Data presented in this dissertation show that FLNS is a sensitive technique. However, any means of decreasing the limits of detection holds great attraction. An order-of-magnitude increase in signal intensity translates to a comparable decrease in the detection limit and, concomitantly, a higher probability that a target compound present in a sample can be determined. The direct proportionality between fluorescence intensity and excitation beam intensity, shown in equation 1, indicates that increased laser power should improve the technique.

Improved lasers for increased excitation intensity should be readily available. Contemporary laser designs, some touted highly by manufacturers and others recommended by fellow investigators (70), could be expected to offer improved performance over the laser used for most of the work reported herein. Further FLNS work in Dr. Small's research group will be facilitated by the use of a Nd:YAG pumped dye laser system, one of the more attractive laser systems for flexibility, power and stability. Following is a discussion of the extent to which increased power can increase signals. Also presented are some changes in the technique that will have to be adopted to take full advantage of the possible improvements.

A more accurate model of the photophysics of fluorescent molecules involves terms not included in equation 1. Some of these terms become increasingly important as excitation power densities are increased. The effects associated with these terms are presented in many works,

including some referenced herein (17,18,52,75,76). Only those effects most important to the analytical application of FLNS to organic glasses will be discussed here. Ultimately, power-related phenomena are expected to impose limits to the signal increases obtainable by increasing laser power.

An important effect to consider is the saturation of the absorption transitions. Saturation occurs for a one-molecule system when the photon density is so high that more than one photon interacts in a period of time shorter than the natural lifetime of the upper state of the absorption transition. The second interacting photon is likely to cause a stimulated de-excitation, returning the molecule to the ground state and adding a photon back into the excitation beam. For the entire FLNS sample population,[26] this means that beyond a certain point increased power density will not result in increased signal levels. This maximum signal occurs at power densities which equalize the populations of molecules in the ground and upper levels of the absorption transition.

An approximation of the power density required for saturation of a transition can be easily calculated from the absorption cross-section and the natural lifetime of the upper state. Origin band excitation in PAHs seems most likely to experience this effect due to the relatively

---

[26]The sample population includes those sample molecules in the excitation region whose transition energies within the inhomogeneously broadened absorption profiles allow them to absorb the excitation beam.

long lifetimes of the zero-point vibrational levels of the S_1 electronic states in these molecules. Using typical values for PAH species (absorption cross-section = 2×10^{-18} cm^2 and $S_{1,0}$ lifetime = 20 ns), the power for saturation is about 10^7 watts cm^{-2}. Note that the laser used for this work (10 milliwatts average power, 25 Hz repetition rate, 5 ns pulse duration, and 10^{-2} cm^2 excitation volume cross section) at maximum output gave power densities of about 8×10^6 watts cm^{-2} or about equivalent to that necessary for saturation of a PAH 0→0 transition.

Nearly all of the work in this dissertation was done utilizing excitation into a vibrational band of S_1. The lifetimes of the vibrationally excited states of molecules are on the order of picoseconds or less under solid state conditions (17,31). This allows excitation power densities several orders of magnitude higher than that required for the 0→0 transition before saturation occurs. Saturation of the absorption transitions of PAHs during FLNS analysis is much less likely than is the following phenomenon.

At power densities well below saturation, the zero point vibrational level of S_1 begins to act as a reservoir, or "sink", for a significant fraction of the sample population. After relaxing rapidly from the pumped vibrational level, molecules can reside in the $S_{1,0}$ state long enough to let one or more additional photons pass without the absorption interactions that would have occurred had the molecule had time to relax completely to the ground state. This depletion of the sample population results in a lower than expected absorption of the excitation beam and a nonlinear relationship between increases in excitation beam intensity and increases in fluorescence intensity.

Simple calculations show that on the order of 10% of the ground state population is depleted for a typical PAH species during optimum[27] performance of the laser used here. There are two implications of this population depletion effect that are of great importance to analytical FLNS. Ground state depletion sets a limit above which signal intensities cannot be increased by increasing laser power. Secondly, the signal normalization explicit in equations 3 and 5 will degrade analytical results at the power densities necessary for maximum signal levels.

Laser power increases can augment FLNS signals in two ways. Increasing peak power of the laser pulses has just been shown to offer little more than a factor of ten increase in signal for most PAHs. However, the pulse repetition rate could be increased substantially from 25 Hz. If high peak powers are maintained, a factor of ten increase in repetition rate should yield an order of magnitude increase in total signal. Continued increases in repetition rate would soon become counterproductive due to an increasing importance of the triplet state as a sink and to the improbability of maintaining high peak powers. Maximum peak signal levels are desirable for optimum differentiation of signal from random noise.

---

[27] Losses due to reflection from lens and window surfaces and from helium bubble scattering along with laser alignment problems, ensured that power densities near 8×10^6 watts cm^{-2} were rarely achieved during the FLNS experiments presented in this work.

Even under conditions of maximum fluorescence intensity from a sample, FLNS signals will remain linearly proportional to analyte concentration at a fixed excitation power density. The molecules making up the sample population must be well isolated for line narrowing of analytical utility to occur. This fact manifests itself as a flattening of the calibration curve at concentrations no higher than 10 ppm for most PAH species in the organic glasses used here. Also, no more than 10% of the analyte molecules in the excitation volume are involved with the excited isochromats during FLNS. This means that the effective excited state population never exceeds about 5×10^{-6} Molar during FLNS of PAHs in organic glasses. These maximum expected levels for this technique are about an order of magnitude lower than the excited state population densities reached during laser pumping of an intense quasi-line of perylene at 10^{-4} Molar in a Shpolskii matrix. These LESS conditions have been reported to produce superradiant emission (38,52, 70). Although the greatly simplified appearance of the spectra taken under these conditions is intriguing, the nonlinear relationship between intensity and concentration may relegate the technique to the status of an interesting anomaly.

The relatively low excited state population densities obtainable under analytical FLNS conditions preclude the possibility of amplified spontaneous luminescence (52,75,76). A photon from spontaneous fluorescence of a molecule in the excited volume has an insignificant chance of encountering a resonant excited state as it exits from the sample. Thus, there should be no mechanism for effecting a change in

the relationship between concentration and signal intensity as power levels are increased. The isolated molecules act independently so that an increase in the number of molecules in the sample volume will increase the observed signal.

The above arguments indicate that a one-hundred-fold increase in FLNS signals should be obtainable by improving the laser power. The only changes necessary to take advantage of the improved signal levels arise from the nonlinear relationship between laser and signal intensity. Abandoning the normalization step would actually cause little trouble since higher power lasers are also usually more stable. Also, the associated high power densities would make fluorescence intensity nearly independent of small changes in laser power. The reference beam measurements could best be used to insure that the laser power does not drift during a run and to detect and discard the occasional missed shot.

In summary, an improved linear working range for FLNS in organic glasses should be made possible by utilizing a laser optimally suited to the task. Projecting from the data presented in other sections, it should be possible to determine many PAHs at concentrations anywhere between 1 ppm and 0.01 pptr in the glass.

3. Gated integrator improvements

Increasing laser power by more than about 100 times would probably be undesirable. Everything from multiphoton photochemistry and power induced physical changes in the sample to all sorts of nonlinear absorption, luminescence, and Raman effects could begin to cause

problems as power densities are increased. Another aspect of this instrumentation could use a great deal of improvement. The gated integrators used in this work were hastily adapted from the commercial product with little attention to several operating parameters that are quite important for optimum operation.

A more careful implementation of the gate and integrator circuitry on a printed circuit board designed especially for this application would eliminate many of the problems encountered in these experiments. A newly designed gated integrator could utilize the best modern gate transistors, gate drivers, low leakage operational amplifiers, and timing circuits. Some of the present problems that could be eliminated are temporal jitter of delay and gate width, signal reflections, and leaky gates.

Temporal resolution as already described would require gate delays that can be set with better than one nanosecond reproducibility. Gate widths must be just as reproducible, especially when selecting early temporal components. In the instrument used for the work reported here, the same signal that triggered the laser was used to trigger the delay circuit. This trigger event occurs about 1.5 microseconds before arrival of the laser pulse at the sample. This requires stability in the gate delay circuits of better than one part per thousand! It is doubtful that the trigger-to-pulse output reproducibility is that good. Preliminary attempts to circumvent this obvious problem by using an electrical trigger produced by the actual discharge of the nitrogen laser cavity were unsatisfactory because the

necessary electrical connection served as a pathway for the conducting of massive noise signals into the integrator circuits. This intense radiofrequency interference (RFI) is generated by the firing of the thyratron and the subsequent discharge in the laser cavity. RFI tends to scramble the states of the gate logic.

Both the long delay and the RFI problems could be eliminated by using a trigger generated photoelectrically from a portion of the nitrogen laser beam. This redesign of the experiment would also require that the gate logic be redesigned to make it respond faster. The 74121 monostable multivibrators and much of the gate driving logic could be replaced by one of the new Schottley integrated circuits of similar function. This could reduce trigger-to-gate delay from the present minimum of 1.5 μs to less than 50 ns. This reduced delay, along with elimination of any electrical contact between either the computer or laser and the trigger circuit, should reduce gate jitter tremendously. The increased temporal resolution afforded by this means should allow exclusion of Raman and reflected light interferences from all but the shortest lived PAH fluorescence signals.

Another of the most troublesome problems encountered involved signal reflections within the twelve to twenty inches of coaxial cable used to connect the PMT anode to the gates. This problem's most obvious manifestation was the appearance of negative regions in the dispersed spectra of delayed emission from mixtures. The negative regions corresponded to spectral segments where intense short lived optical signals were being gated out. Observations with an oscilloscope

showed that large short lived signals tended to produce oscillations in the electrical potential up and down the coaxial cable. For delayed gates, the integrals of these reflections are negative in many instances.

Several stop-gap measures were taken to allow data to be taken under these circumstances. Something had to be done because the computer ADC interface could not measure negative signals. These temporary solutions included the addition of a relatively large positive offset to the output amplifier in the integrator circuit and rudimentary attempts at impedence matching using 50 ohm terminators and small (5 and 10 ohm) resistors in series with the gates. These measures tended to degrade the overall performance of the instrumentation by limiting the dynamic range at the integrator output and by providing competing circuits to ground which decrease the signal observed at the analyzing capacitor.

A much more attractive answer is to eliminate the offending length of cable. All such reflections could be eliminated by placing the gate and gate driver circuits inside the PMT housing as close as possible to the anode. This should also allow for greater electrical shielding. Such a change has been advocated by another researcher since the beginning of these experiments (70).

A third major problem associated with performance of the integrator design involves "leaky" gates. The complementary FET current gates used could not handle all of the signal from the most intensely fluorescent samples. The source to drain resistance of the "on" gate measures about 50 ohms. The sample PMT, at maximum signal response, can produce

more than 40 volts across 50 ohms. This high potential on the inputs to the FETs tends to turn both gates "on" and divide all signals above a certain level between ground and the analyzing capacitor. This division takes place regardless of the intended state of the gates. Thus, very large signals can neither be gated out nor measured accurately.

The same consultant mentioned above (70) has investigated this problem and has concluded that a greater immunity to problems with leaking gates can be designed into a fast response gated charge integrator. Several alternate FET transistor types are available which are more rugged with respect to high currents, have higher off-to-on resistance ratios, and are just as fast in response as the FETs used in this work, with comparable charge injection properties. In particular, gate arrays are available which would allow design of circuits with two or more FETs in parallel to replace either or both of the FETs used in the present gate design. Such an arrangement would decrease the effective on-resistance of the gates via the $R = (\frac{1}{R_1} + \frac{1}{R_2} + \ldots)^{-1}$ rule. This decreased impedance would decrease the potential produced at the gate inputs and reduce the likelihood of leaky gates.

Rather than the 0 and +6 volt off and on signals used to drive the present FETs, a redesigned circuit might better use a larger voltage swing, say -3 to +12 volts. This should also help to improve the off-to-on resistance ratio and make the gates operate better. Better gates located at the PMT anode driven by improved gate drivers and timing elements triggered from a photodiode output would be a great advance.

The only remaining elements in the integrator are the analyzing capacitor and the op-amps, cf., Figure 23. The main objective in their design is that they be able to hold signals with very little loss due to current leakage. As already mentioned, high speed is not necessary. Any convenient stable low inductance capacitor and high input resistance integrated circuit op-amp should serve the purpose.

4. Miscellaneous improvements

The liquid helium cryostat was used in these experiments because of the artifically low cost of liquid helium at this institution. Boiling helium in the optical paths no doubt causes substantial noise problems which could be eliminated by substituting a closed cycle helium refrigerated optical cryostat for the present Dewar. The temperature of the sample in a conduction-cooled holder could be controlled for a more reproducible cool-down procedure. Thus, all guess work could be eliminated from glass formation procedures.

There are no doubt many more areas that could be improved. Many of these involve procedures inappropriate for inclusion here. One important problem, noticed by other investigators (77) after the experiments reported here were concluded, is that the microscope slide reference beam splitting technique is highly polarization-dependent. Thus, the polarization of the laser must be stable to give useful reference beam measurements.

V. RESULTS AND DISCUSSION

A. Introduction

This chapter presents data from experiments designed to demonstrate the power of FLNS as an analytical technique. These data show that FLNS in practice fulfills the expectations indicated by examination of the physical principles. An examination of the following results will show that FLNS satisfies the requirements listed for an ideal analytical method.

Three different sets of experimental runs are presented. After a brief description of the behavior of the specific glass mixutres used, a set of reference spectra are presented. These representative FLN spectra were taken from glasses to which a single PAH compound had been added. The reference spectra characterize the FLN behavior of individual species at the selected wavelengths. The next section demonstrates resolution of thirteen of the components in a mixture of fourteen polycyclic aromatic compounds. The last section presents the results of real sample analyses for several PAH species. Many spectra are presented throughout this chapter to compensate for the scarcity of FLNS spectra in published literature.

B. Glasses Used

Only two glass forming solvent mixtures were used for most of these studies. Subsequent to the completion of this work, other investigators in the same research group began to investigate new glass forming

organic solvent mixtures for molecular FLNS (78) as well as totally new types of glasses for inorganic FLNS (79). A major goal at the initiation of this project was to find glasses containing substantial amounts of water. Such glasses should greatly facilitate water analysis for PAH species by allowing direct incorporation of water samples.

Development of the first glass grew from the observation that 2-methyltetrahydrofuran (MTHF) mixed with ethanol (ETOH) at ratios between 1:4 and 1:2.5 formed better glasses than either solvent alone. It was also found that the 1:4 MTHF-ETOH mixture could be made more stable and more compatible with the sample cells[28] by adding about 5% water to the mixture. This 1:4 MTHF in ETOH solvent mixture with 5-10% water was used to form the glass in many early experiments. Because of its properties as a good solvent and its miscibility with the other glass, this mixture was used as the solvent for diluting all standards and real samples.

Most of the spectra were taken using a water-glycerol glass mixture. This glass was developed after systematic investigation of several possible glasses indicated that many combinations of glycerol, ethanol, and water form stable clear glasses in the clear plastic sample cells. Mixtures of ethanol and glycerol from nearly pure ethanol to a ratio of about 1:1 were found to be satisfactory as long as no more than 40% water or 10% MTHF were added. Starting with water and glycerol,

---

[28]Thin walled transparent polystyrene culture tubes manufactured by Falcon, Oxnard, California.

investigations showed that initial volume ratios of 4:5 water-glycerol allowed addition of up to 40% ethanol and/or up to 10% MTHF.

The glass mixture used for most experiments was formulated by diluting 4:5 water-glycerol by 20% with 1:4 MTHF-ETOH. This mixture was chosen because it formed stable glasses, was less viscous than mixtures containing more glycerol, and allowed great flexibility for sample introduction.

Samples incorporated into this glass mixture were routinely cooled from room temperature to 4.2K in about fifteen minutes. The proper cooling rate was achieved by lowering the samples slowly through the region within the neck of the Dewar that was level with the surface of the liquid nitrogen in the outer jacket. Once the samples were below the level of the liquid nitrogen, after between 10 and 20 minutes of cooling, the glasses were completely formed and could then be rapidly lowered into position below the liquid helium level.

Addition of water and ethanol to the glycerol to levels well above the minimum required for stable glass formation was important. The less viscious solutions could be readily mixed to introduce samples or standard solutions. Water samples could be added by using the sample in place of all or part of the water in the 4:5 water-glycerol component. Organic samples were introduced into the glass by diluting or dissolving them into the 4:1 ethanol-MTHF component before formulation of the complete glass solvent mixture.

When utilizing this glass mixture, the most bothersome samples were those that had already been diluted in a hydrocarbon solvent such as

hexane. Hydrocarbon solvents form a separate phase when added to this highly polar glass. For those instances where samples in hexane were used, the hexane solution was first added to a flask containing one half the final desired volume of completely formulated 20% (4:1 ETOH-MTHF) 80% (4:5 water-glycerol). This mixture in an open flask was then placed in a warm ultrasonic bath until the hexane had evaporated and a homogeneous solution formed. This solution was then diluted to the desired volume with fresh glass solvent mixture and was ready to use.

C. Reference Spectra

1. Experimental

This section contains one or more FLN spectra for each of 18 different polycyclic aromatic compounds. Spectra at "ideal" FLNS excitation wavelengths are shown for triphenylene, pyrene, 1-methylpyrene, 1-ethylpyrene, 1-butylpyrene, benzo(e)pyrene, anthracene, benzo(a)anthracene, 9-phenylanthracene, 9-methylanthracene, benzo(g,h,i)perylene, 9,10-dimethylanthracene, benzo(k)fluoranthene, 9,10-dibromoanthracene, benzo(a)pyrene, 3,4,9,10-dibenzpyrene, and perylene. The spectra of these compounds are presented in order of increasing excitation wavelength. A broad range of FLNS behavior is represented both by those compounds whose spectra are presented and those whose behavior is only mentioned.

Unless otherwise stated, these spectra are all plots of normalized fluorescence intensity, cf., equation 5, versus wavelength in nanometers (nm). Most spectra include wavenumber (cm^{-1}) energy designations along

the abcissa, in addition to the linear wavelength designations. For most of these spectra, the highest energy fluorescence ZPL has been assigned as the origin and the energy splittings between this line and the strong vibrational ZPLs shown. This facilitates comparison of these narrow line spectra with those published from mixed crystal, Shpolskii, or other FLNS work. Where possible, reference is made to literature spectra.

All of the following FLN spectra were taken from standard solutions diluted in the 4:5 water in glycerol glass. The standard solutions were prepared by weighing small quantities (a milligram or so) of the solid compound using a microgram balance in a climate controlled room.[29] The solid was then dissolved and diluted to either 10 or 25 ml using the 1:4 MTHF in ethanol solvent mixture. Small amounts of these solutions were then diluted into the final glass mixture to give 1.0 to 0.1 ppm PAH. The solid PAH compounds were used as obtained from various sources without further purification. All of the reference materials were purported to be of 98% or greater purity. It was reasoned that it should be easy to differentiate between major and minor PAH constituent fluorescence, thus making rigorous purification unnecessary.

---

[29]Use of this sensitive balance in the special weighing room was graciously permitted by J. Steve Gibson and Mike Hadka of Professor Harvey Diehl's research group.

For all of these reference compounds, excitation wavelengths in low lying vibronic bands of S_1 were selected. As described earlier, this allows observation of origin band fluorescence and leads to useful analytical lines in region II. The spectral regions within which to search for ideal excitation wavelengths were chosen by a simple empirical method. Collections of classical fluorescence and absorption spectra such as Birks (17), Berlman (80), and Porro et al. (81), along with any specific references, were consulted to gain clues to the location of the fluorescence origin.

With the compound in a glass at 4.2K, a more exact location of the broad band origin was determined with high energy excitation using the Ar laser, N_2 laser, or a high energy dye in the dye laser. If, in the broad band fluorescence spectra thus produced, a well-resolved vibronic band with a small (<2 nm) displacement from the origin could be observed, this fluorescence band was used to predict the location of a well-resolved low lying vibrational band in absorption. After choosing a dye for the laser to give tunability in the predicted region, the search began for the best wavelength setting in this region. By repeatedly scanning over the fluorescence origin while making small changes in the excitation wavelength, the author could rapidly locate a narrow ($\sim$0.5 nm) region which gave maximum intensity and a minimum number of ZPLs. Although several such ideal excitation wavelengths should exist for each compound, the author chose to stop after finding only one such wavelength for most of the following compounds.

Rather than discussing special problems or unusual behavior in a separate chapter, these special discussions are included in the subsections associated with the spectra which best illustrate the phenomena. For completeness, the author has endeavored to mention his conclusions from the results of every compound investigated during the more than four years spent on these studies.

2. Triphenylene

Figure 28 shows a FLN spectrum of triphenylene produced by excitation with the 333-336 nm multiplet from the argon ion laser. The dye laser system used does not produce wavelengths short enough to excite FLNS from this compound. Unfortunately, the N_2 laser at 337.1 nm has not yet been tried. The 335.8 nm line of the Ar ion laser seems to be the one producing the good FLN spectra shown. This spectrum generally resembles the published broad band spectra (80) and Shpolskii spectra (38).

Triphenylene is one of several compounds which exhibits a weak fluorescence origin line. The vibrational line at (0,0) minus 1160 cm^{-1} is by far the strongest line in the spectrum. This spectrum represents the most pronounced manifestation of the Herzberg-Teller false origin in this dissertation. The vibrational line at 365.3 nm arises from fluorescence transitions so strongly allowed that transitions into vibrational states building on this state can be observed. This compound as well as benzo(e)pyrene are molecules for which excitation into the 0-0 band may give the best analytical lines. Note that the two

Figure 28. FLN spectrum of triphenylene excited with the argon ion laser

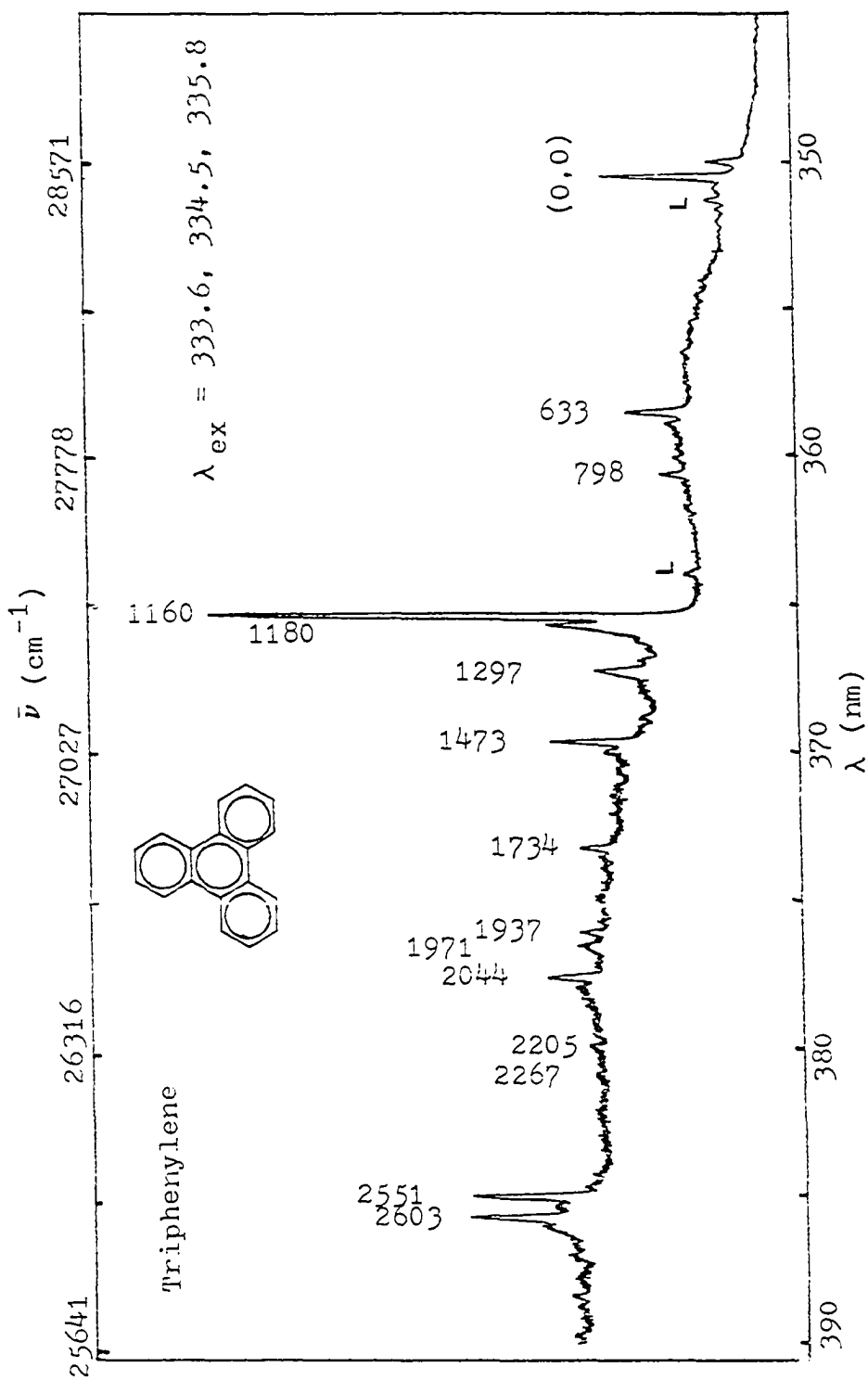
Triphenylene
λ_{ex} = 333.6, 334.5, 335.8
(0,0)
L
633
798
L
1160
1180
1297
1473
1734
1937
1971
2044
2205
2267
2551
2603
$\bar{\nu}$ (cm^{-1})
28571
27778
27027
26316
25641
350
360
370
380
390
λ (nm)

lines marked "L" are due to scattered light from the 351.1 and 363.8 nm lines of the argon ion laser.

3. Phenanthrene, chrysene and azulene

These compounds were investigated during the course of this work. Spectra are not included because the quality of the line narrowed spectra at the accessible excitation wavelengths were unacceptable for resolution of complex mixtures. Excitation of phenanthrene with the 337.1 nm N_2 laser produced a weak multisite (more correctly, multi-isochromat) spectrum with the origin near 346 nm. Useful FLN from phenanthrene would require tunability in the 336 to 346 nm range which could not be achieved with the laser used.

Excitation of chrysene with the 351.1 nm argon line gave weak fluorescence with three distinct ZPLs between 362.5 and 364.0 nm. Using a different glass formulation, McColgin (55) obtained higher quality FLNS spectra of chrysene using the same 351.1 nm laser line. Drastic differences in solvent composition cause slight spectral shifts in a molecules' absorption bands. When using a fixed frequency laser, the glass solvent used can mean the difference between observing and not observing an intense narrow line fluorescence spectrum.

This same effect seems to have allowed McColgin (55) to observe FLN for azulene. Efforts to excite FLN from azulene using the water-glycerol glass and the 363.8 nm argon ion laser line produced only low intensity phonon dominated fluorescence. Tunability between 330 and 366 nm should allow observation of excellent FLNS for all three of these compounds. Azulene is of particular interest because of its low natural abundance.

This PAH is an attractive candidate for inclusion as an internal standard for studying interferences or various proposed extraction procedures.

4. Pyrene

The bottom spectrum in Figure 29 shows a typical FLNS spectrum for pyrene. This molecule is very well behaved yielding an intense ZPL from a single isochromat when excited at 363.5 nm. Besides its exemplary FLN behavior and high natural abundance, the most striking thing about pyrene's fluorescence is its unusually long lifetime. In the water glycerol glasses,[30] pyrene fluorescence signals persist so long that measurable levels exist after more than an 850 nm delay. These spectral line locations (45,82) and lifetimes (17) agree quite well with the literature.

5. Benzo(e)pyrene

The middle spectrum in Figure 29 shows an FLN spectrum of benzo-(e)pyrene (BeP) excited at 365.6 nm. As in the case of triphenylene, one of the vibrational bands (at 387.2 nm) is as strong as the fluorescence origin at 375.8 nm. The emission is also not very intense. Note that these three spectra were taken during the same run so that the equation 5 type scale factors listed are a good way to

---

[30]Laboratory observations seemed to show, surprisingly, that the fluorescence lifetime of pyrene in 4:1 ETOH-MTHF solution at room temperature was very short. No fluorescence intensity persisted more than 10 ns after the laser pulse.

Figure 29. FLN spectra of pyrene, benzo(e)pyrene and 1-methylpyrene

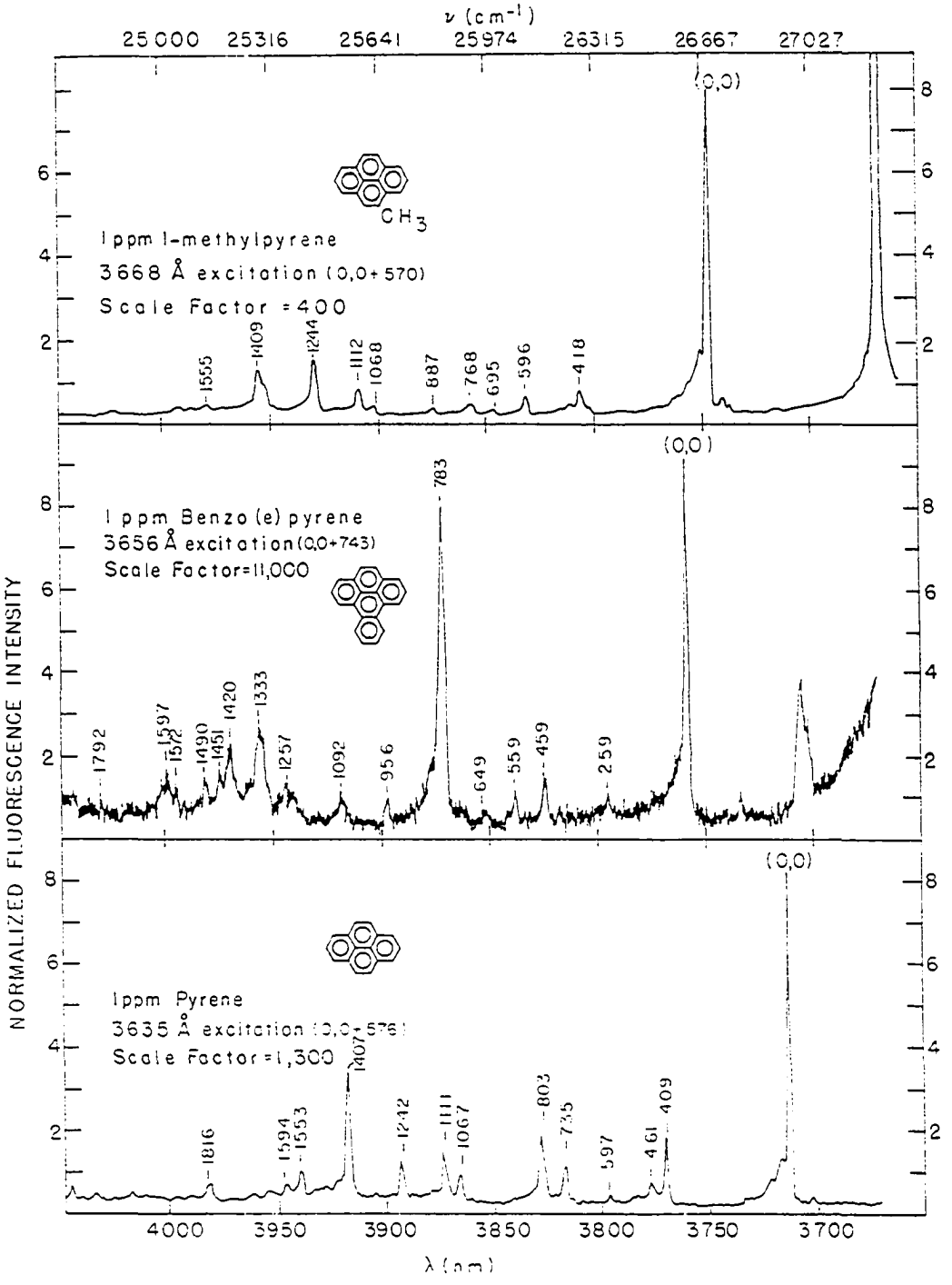
ν (cm⁻¹)
25000 25316 25641 25974 26315 26667 27027
(0,0)
CH3
1 ppm 1-methylpyrene
3668 Å excitation (0,0+570)
Scale Factor = 400
1555
1409
1244
1112
1068
887
768
695
596
418
(0,0)
1 ppm Benzo (e) pyrene
3656 Å excitation (0,0+743)
Scale Factor=11,000
783
1792
1597
1572
1490
1451
1420
1333
1257
1092
956
649
559
459
259
(0,0)
1 ppm Pyrene
3635 Å excitation (0,0+578)
Scale Factor = 1,300
1407
1816
1594
1553
1242
1111
1067
803
735
597
461
409
NORMALIZED FLUORESCENCE INTENSITY
4000 3950 3900 3850 3800 3750 3700
λ (nm)

compare fluorescence intensities. The scale factor used to get the BeP spectrum is 8.5 times as large as the one used for pyrene (P).

BeP was studied more than any other molecule during the final days of this research. Analysis for this molecule was given high priority because of the need to show that it could be determined independently of its carcinogenic isomer benzo(a)pyrene (BaP). Other problems were encountered besides the lack of intensity.

Figure 30 is included to show more of BeP's spectrum than is shown in Figure 29. This spectrum, along with others, was used to produce the information shown in Table 1. Table 1 verifies that the line at 387.2 nm is indeed a Herzberg-Teller false origin of BeP. This table shows the vibrational energy spacings of the vibrations building on both the origin and the false origin and demonstrates the correspondence. The group of lines near 410 nm bears the same energy relationship to the false origin at 387.2 nm that the group of lines at 398 nm does to the origin at 375.8 nm. The abnormally intense line at 395.6 nm can be seen from the table to be an accidental overlap of a (0,0) - 1335 cm^{-1} state and a (784) - 550 cm^{-1} state. The 1335 cm^{-1} transition building on the false origin appears at 408.4 nm or (0,0) - 2124 cm^{-1}.

The worst interference problem encountered during these investigations was between BeP and the 1-alkylpyrenes. As can be seen on the top two spectra in Figure 29, the origins of B(e)P and 1-methylpyrene (1-MP) largely overlap. Overlap under these conditions would not always cause problems. However, in this case, the 365.6 nm excitation wavelength chosen for BeP excites a strong ZPL for 1-MP which exactly

Figure 30. FLN spectrum of benzo(e)pyrene to show enough lines for vibrational analysis

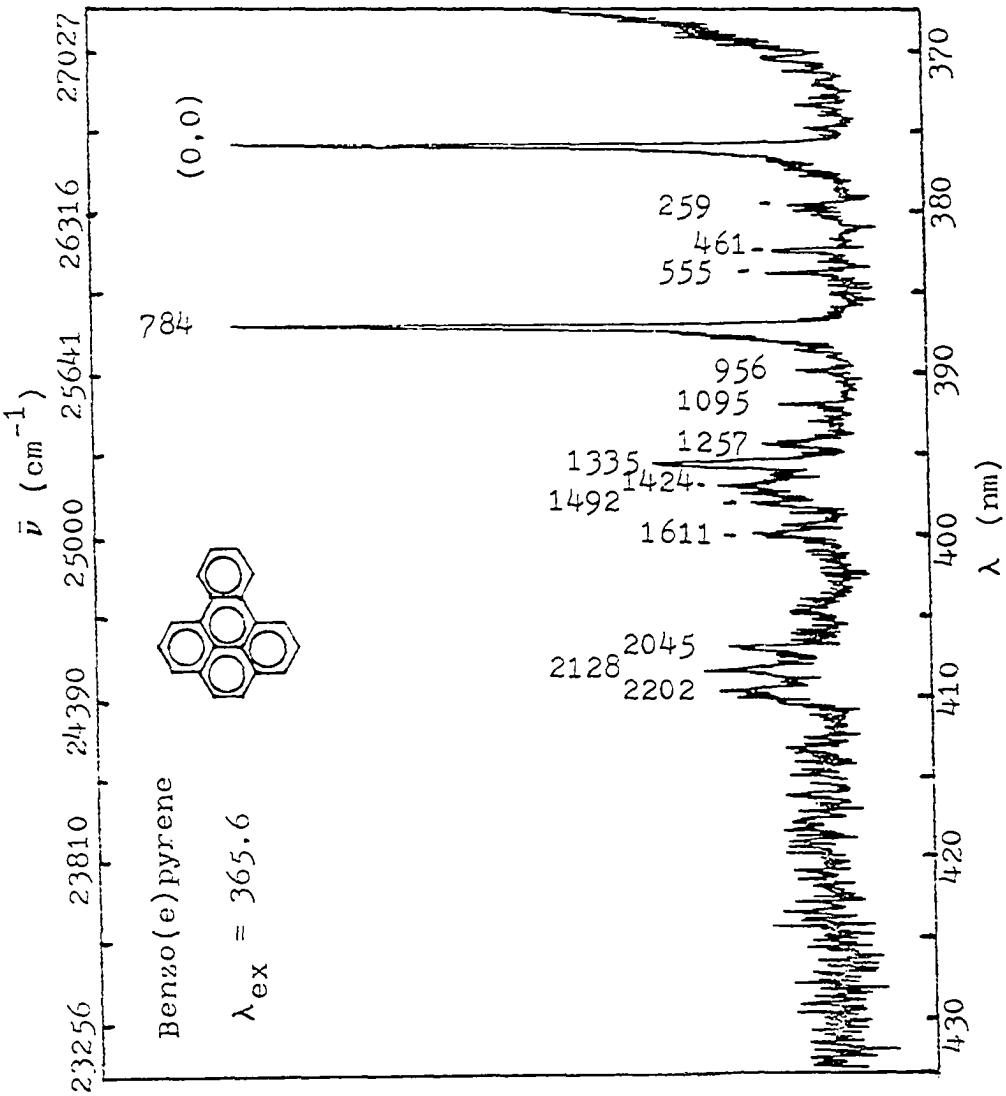
Benzo(e)pyrene
λ_{ex} = 365.6
(0,0)
784
259
461
555
956
1095
1257
1335
1424
1492
1611
2045
2128
2202
$\bar{\nu}$ (cm^{-1})
23256
23810
24390
25000
25641
26316
27027
λ (nm)
430
420
410
400
390
380
370

Table 1. Vibrational energy spacings in benzo(e)pyrene. Excitation is at 365.6 nm or (0,0) + 743 cm^{-1}

Wavelength in nm	Energy Relative to (0,0) in cm^{-1}	Intensity Relative to (0,0)	Energy Relative to False Origin in cm^{-1}	Intensity Relative to False Origin
375.8	0.00	1.00	---	---
379.5	259	0.06	---	---
382.4	461*[a]	0.12	---	---
383.9	555*	0.09	---	---
385.2	649	0.02	---	---
387.2	783*	0.83	0	1.00
389.8	956	0.08	173	---
391.9	1092	0.09	309	---
394.4	1257*	0.05	474*	0.06
395.6	1335*	0.24	550*	0.29
397.0	1420*	0.14	637	0.17
397.5	1451	0.05	668	---
398.1	1490	0.06	707	---
399.4	1572	0.06	789*	0.11
399.8	1597	0.07	814	---
404.8	1906	0.06	1123	0.07
407.0	2040	0.13	1257*	0.16
408.4	2124	0.14	1341*	0.17
409.7	2202	0.14	1419*	0.17

[a]Note that the marked, *, vibrations building on (0,0) have corresponding lines within experimental error building on the false origin.

overlaps the origin of BeP at 375.8 nm as shown in the top spectrum of Figure 31.

Referring to this figure, mixture 81-1 contains 200 ppb each of pyrene, benzo(e)pyrene, 1-methylpyrene, anthracene, benzo(a)pyrene (BaP), and perylene. Resolution of every component except BeP was so trivial that the complete series of spectra is not shown. The lower spectrum in Figure 31 is from a mixture containing 1.0 ppm pyrene, 0.10 ppm BeP, 0.10 ppm BeP, and 0.01 ppm acridine. In the top spectrum, containing 1-MP, the only discernable BeP line is the false origin at 387.2 nm. The bottom spectrum shows that, as long as there is no 1-MP present, the BeP ZPLs can be quite easily observed.

The mistaken choice of 365.6 nm for BeP excitation was not discovered until after the first spectra in the SRC-II analysis run had been taken, cf., Figure 40. However, during later analyses, cf., Figure 47, the author noticed the interference and changed to use of origin band excitation for BeP. Investigations during the final experimental run to check the results of the SRC-II analysis, vide infra, confirmed that 375.8 nm excitation for BeP with observation of the false origin at 387.4 eliminates 1-MP interference.

6. 1-Alkylpyrene

The top spectrum in Figure 29 is of 1-methylpyrene. From the low scale factor, its fluorescence intensity can be seen to be approximately three times greater than pyrene at the same concentration. Interestingly, the fluorescence lifetime of 1-MP in this glass is even longer than that for pyrene, with signals observable after one

Figure 31. FLNS of two mixtures showing effect of 1-methylpyrene interference with benzo(e)pyrene

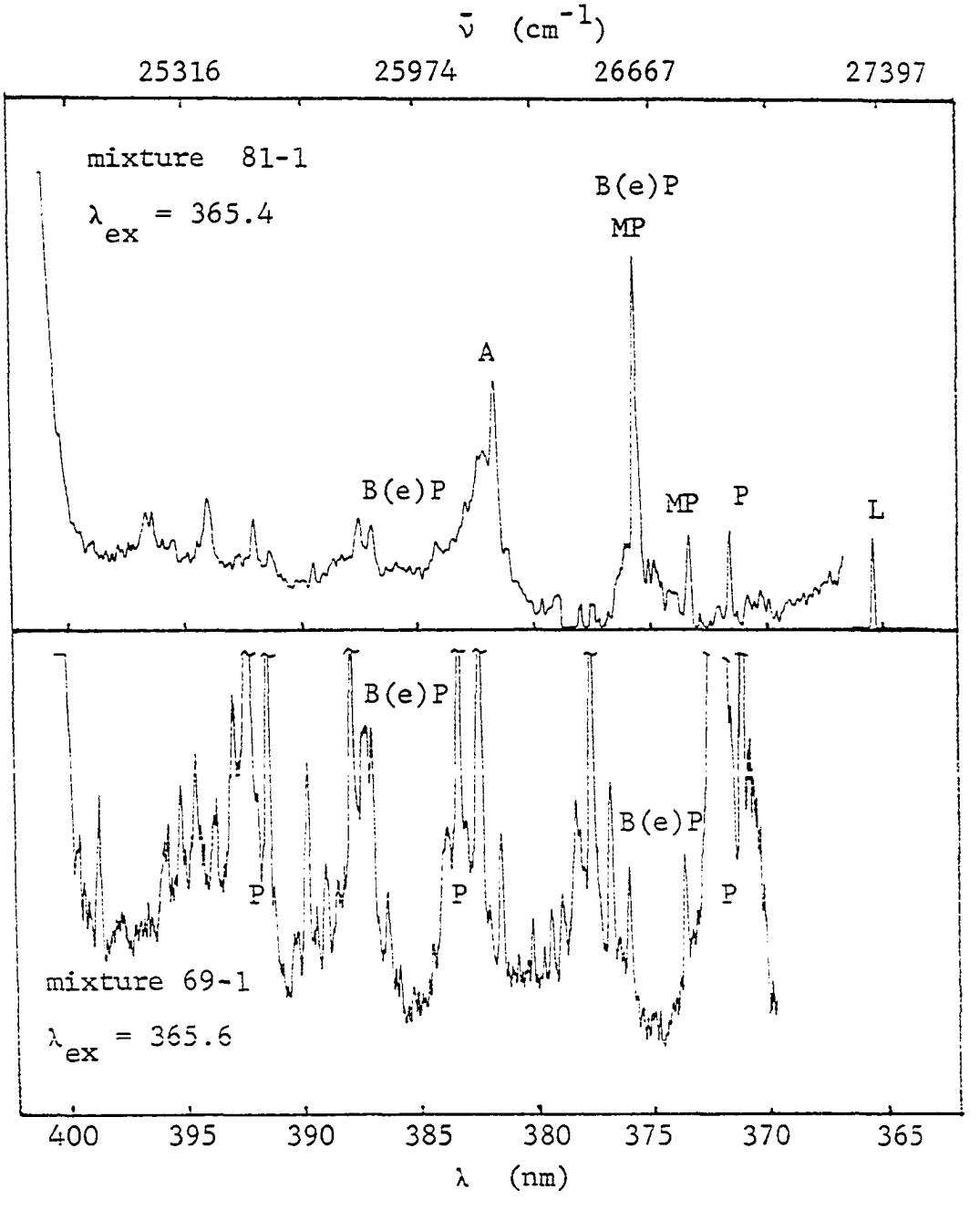
ν̄ (cm⁻¹)
25316
25974
26667
27397
mixture 81-1
λex = 365.4
B(e)P
MP
A
B(e)P
MP
P
L
B(e)P
B(e)P
P
P
P
mixture 69-1
λex = 365.6
400
395
390
385
380
375
370
365
λ (nm)

microsecond. The general appearance of the spectrum is very similar to that of pyrene. Differences include the addition of extra lines in the (0,0) - 695, -768, and -887 regions. As one might expect, adding the methyl group has little effect on the spectroscopy of pyrene other than lowering the energy of the excited states.

In fact, the addition of any alkyl group to the one position would be expected to have about the same effect in this polar glass solvent mixture. The polar solvent probably exerts most of its affect on the molecule's spectroscopy by interacting with the polarizable π clouds of the pyrene ring. All alkyl substituents at the same ring position should have about the same effect on the π cloud of the ring. Figure 32 confirms that the different size alkyl substituents have no real effect on the spectroscopy observed under these conditions.

The only differences discernible in these spectra of 1-methyl, 1-ethyl, and 1-butylpyrene involve the peak shapes. Figure 33 further confirms the lack of significant differences at 363.5 nm excitation. The bottom spectrum in Figure 33 shows 1-MP using excitation resonant with the origin band. Notice that this greatly sharpens and intensifies the vibrational lines.

There are several important considerations to contend with while assessing the implications of the near exact coincidence of the 1-alkylpyrene spectra. First, the biological activity of PAH species which are differentiated only by the size of an alkyl substituent at a single ring location may well be identical. The general consensus is that the carcinogenic or mutagenic mechanisms of PAHs involve the

Figure 32. FLN spectra of some 1-alkylpyrenes

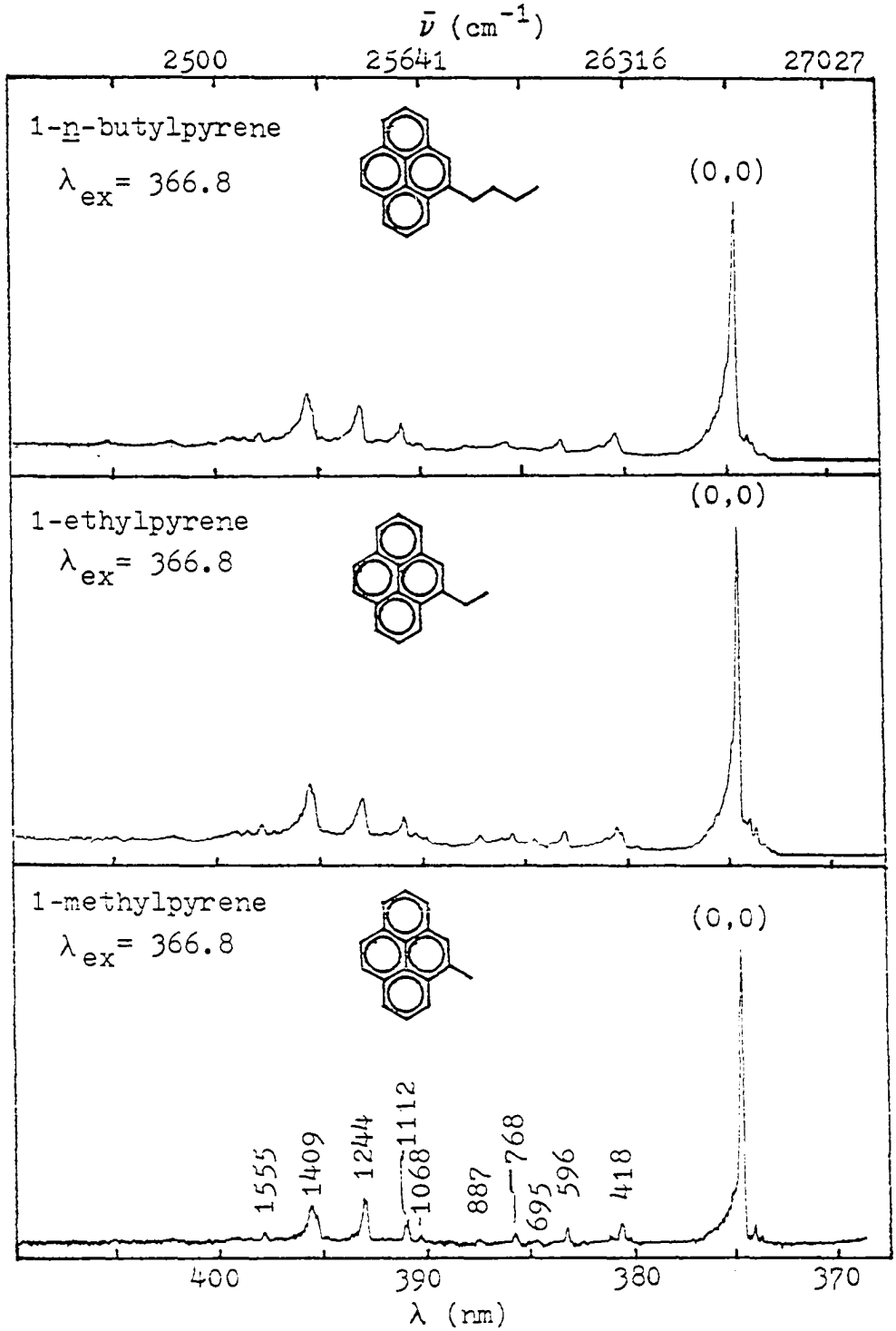
$\bar{\nu}$ (cm^{-1})
2500
25641
26316
27027
1-n-butylpyrene
λ_{ex}= 366.8
(0,0)
1-ethylpyrene
λ_{ex}= 366.8
(0,0)
1-methylpyrene
λ_{ex}= 366.8
(0,0)
1555
1409
1244
1112
1068
887
768
695
596
418
400
390
380
370
λ (nm)

Figure 33. FLN spectra of the 1-alkylpyrenes with an expanded intensity scale to show vibrational structure. Note that the bottom spectrum utilizes excitation into the origin band

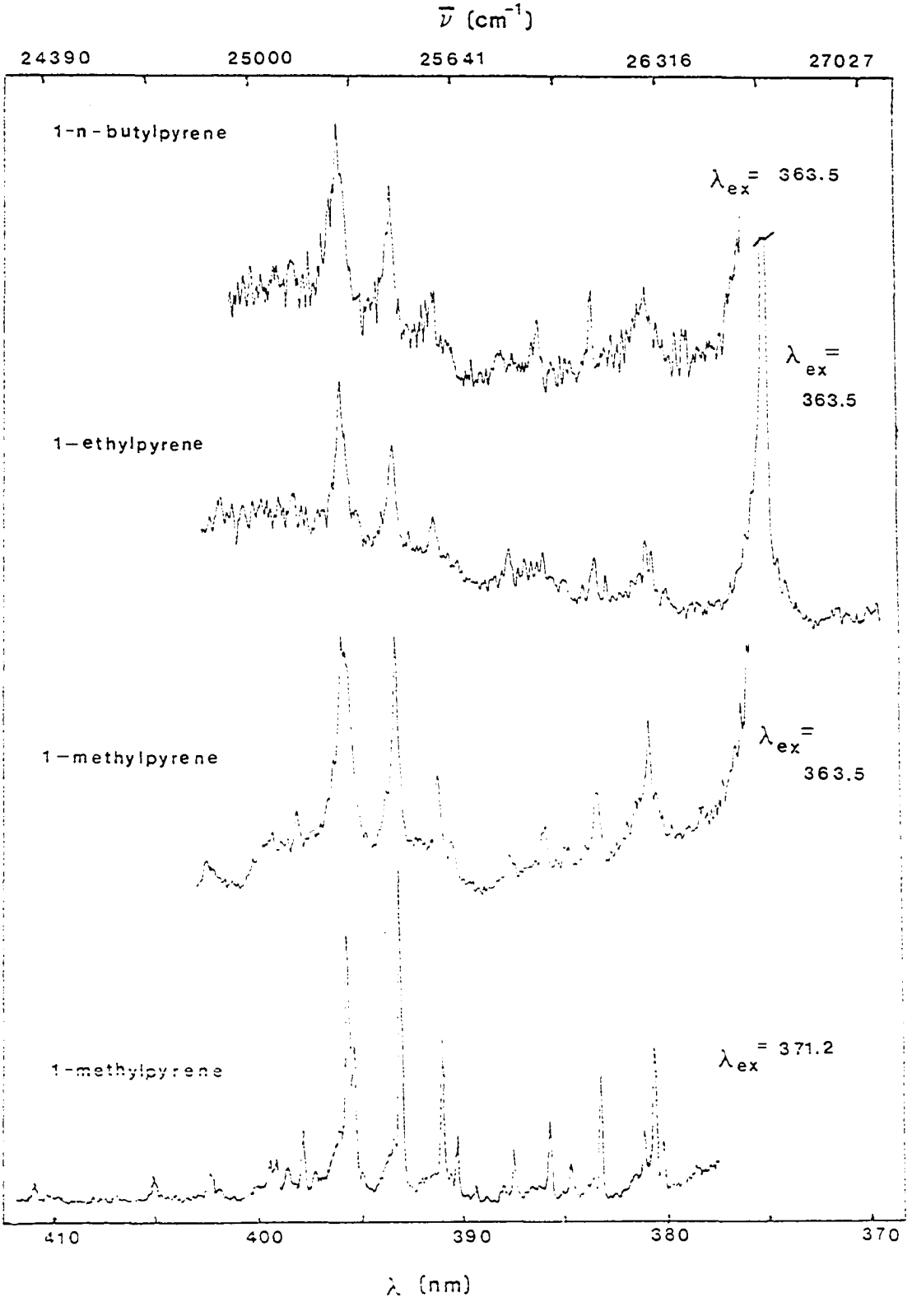
$\bar{\nu}$ (cm^{-1})
24390
25000
25641
26316
27027
1-n-butylpyrene
λ_{ex} = 363.5
λ_{ex} = 363.5
1-ethylpyrene
1-methylpyrene
λ_{ex} = 363.5
1-methylpyrene
λ_{ex} = 371.2
410
400
390
380
370
λ (nm)

enzymatic pathway that the cell chooses when metabolizing the ring structure. Other enzymatic pathways may metabolize all alkyl substituents to the same moiety before the ring metabolizing steps. There may well be no need to differentiate between methyl, ethyl, propyl or longer alkyl groups. Only the position of the substituent on the ring structure may be important in selecting those pathways that lead to adverse biological activity. Fortunately, the position of a substituent has a relatively large effect on a PAH compound's spectroscopy.

There is hope, even if the investigator must resolve a homologous series of alkyl PAH species. By formulating a glass mixture so that it more strongly interacts with the hydrophobic alkyl groups, the affects of these substituents can be amplified. A hydrocarbon glass, for example, may shift the spectra of different alkyl substituted compounds enough to facilitate resolution. Differences in the bands associated with the alkyl group ((0,0) - 695, -768 and -887, for example) may allow spectral separation. If necessary, the resolution of the technique can be increased by utilization of narrower bandpass lasers and monochromators to allow splitting of the unresolved multiplet ZPLs. At 0.1 nm resolution, the coincidence of the 1-alkylpyrene spectra may well be a blessing since it simplifies the spectra of natural mixtures with little loss in the meaning of the results.

7. Anthracene

The spectrum of anthracene shown in the lower part of Figure 34 indicates the well-behaved nature of this compound in this glass. At

an excitation wavelength of 373.8 nm, only one prominent isochromat is observed at each transition. Unlike some compounds, the phonon side bands of anthracene are well resolved from the ZPLs and are easily observed. The spectra of anthracene used in this dissertation appear much as would be expected from previous Shpolskii (34) and mixed crystal (83,84) work. The fluorescence lifetime was observed to be short, ca., 5 ns, as expected from Birks (17). The excitation wavelength shown here and used in the remainder of this dissertation is quite different from the 363.8 nm wavelength used in the earlier concentration studies, cf., Figures 15 and 16. This 373.8 nm wavelength, nearer the origin, yields a simplified spectrum with intensities just as high as the old wavelength. The wavelength shown in Figure 34 should be better for anthracene analysis in mixtures.

8. Benz(a)anthracene

The compound from which the spectrum in the middle of Figure 34 was obtained is an interesting case. In this spectrum, there is some multi-site emission and the bands appear with some underlying phonon structure. This solution was made up from a standard solid labeled 2,3-benzophenanthrene, which had been dissolved to 68.4 ppm in 1:4 MTHF-ETOH stock. Another sample, from a solid labeled 1,2-benzanthracene, was made up into an 83.2 ppm stock in 1:4 MTHF-ETOH solution. These are two different names for the same compound. Yet, glasses containing both 1.0 and 0.10 ppm of the 1,2-benzanthracene from the 83.2 ppm stock gave only broad band fluorescence with the bands located at about the same

Figure 34. FLN spectra of anthracene, benzo(a)anthracene and 9-phenylanthracene

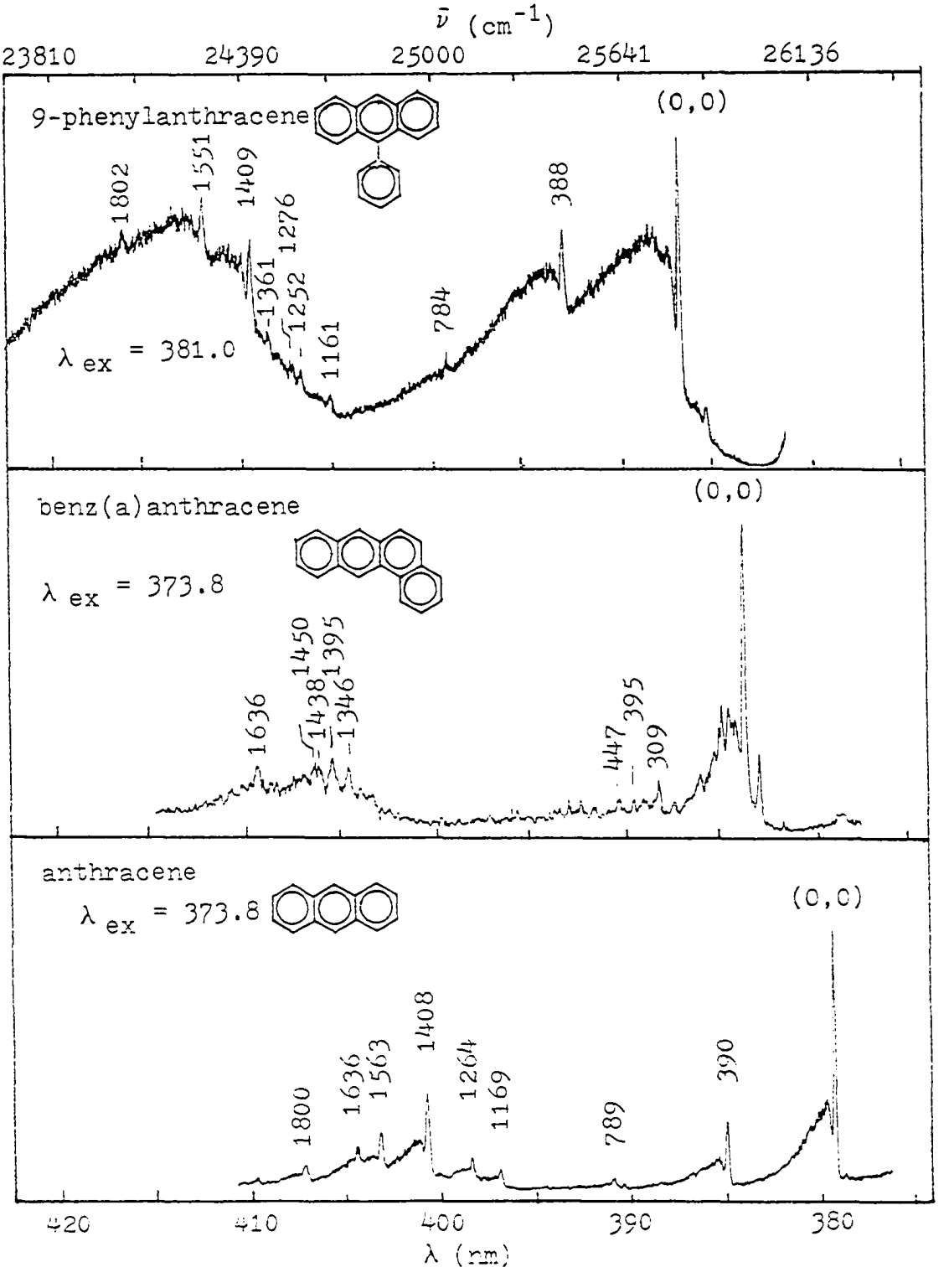
$\bar{\nu}$ (cm^{-1})
23810
24390
25000
25641
26136
9-phenylanthracene
(0,0)
1802
1551
1409
1361
1276
1252
1161
784
388
λ_{ex} = 381.0
benz(a)anthracene
(0,0)
λ_{ex} = 373.8
1636
1450
1438
1395
1346
447
395
309
anthracene
λ_{ex} = 373.8
(0,0)
1800
1636
1563
1408
1264
1169
789
390
420
410
400
390
380
λ (nm)

place as in the sharp line spectrum shown in Figure 34. The general appearance of both the broad band and sharp line spectra agrees quite well with LESS spectra (37). It seems unlikely that the spectrum in Figure 34 is an impurity.

The broad structure beneath the ZPLs in the spectrum of benz(a)-anthracene shown in Figure 34 may well be a remnant of the broad structure that was seen in the other spectra mentioned above. Other examples of this behavior were observed. The author believes that the broad structure is due to the spectroscopy of oligomers. Due to poor solvation, the PAH molecules tend to associate with one another in small groups rather than remaining dispersed throughout the solution. In the 68.4 ppm stock, the predominant form of benz(a)anthracene seems to be as completely solvated and isolated molecules. In the 83.2 ppm stock, oligomeric associations or aggregates seem to prodominate. The interesting fact is that the aggregates seem to persist through dilution into the water-glycerol and the following several days of standing before the experiments in which the data were taken. This phenomenon will be discussed in more detail under the 2-methylanthracene subheading.

9. 9-Phenylanthracene

The top spectrum in Figure 34 shows the best FLNS that could be obtained for 9-phenylanthracene in this glass mixture. The PSBs are very prominent. However, this broad structure may present no problems in mixture analysis since it drops rapidly in intensity at excitations

different from that used here and since it should be easy to distinguish sharp ZPLs on top of these broad bands. This seems to be an intensely fluorescent compound which should be easy to determine in mixtures.

10. 2-Methylanthracene

The spectra of this compound which appear in Figures 35 and 36 are included to discuss the effect of aggregate formation in FLNS investigations. As discussed in the Theory chapter and in references 35, 60 and 61, if the attractions between molecules of a guest species are for some reason stronger than the interactions between the guest molecules and the host, the guest molecules may congregate into groups that range in size from dimers and larger oligomers to microcrystals. Oligomeric aggregates, although not large enough to exhibit any Tyndall effect, can cause a lot of trouble. The molecules in an aggregate tend to act as a unit absorbing and radiating photons as a group rather than as the distinct matrix isolated molecules required for effective line narrowing.

Figure 35 is a laser excited fluorescence spectrum from a sample exhibiting an aggregate problem. At concentrations in the glass down to 0.10 ppm, no choice of excitation wavelength would give fluorescence spectra without the broad structure. Figure 36 shows a series of spectra taken with different excitation wavelengths in the region of the origin band of an 0.10 ppm 2-methylanthracene doped glass. The broad structure centered at about 387 nm persists in its approximate location and changes only in intensity as the excitation is scanned

Figure 35. Laser excited broad band fluorescence of 2-methylanthracene

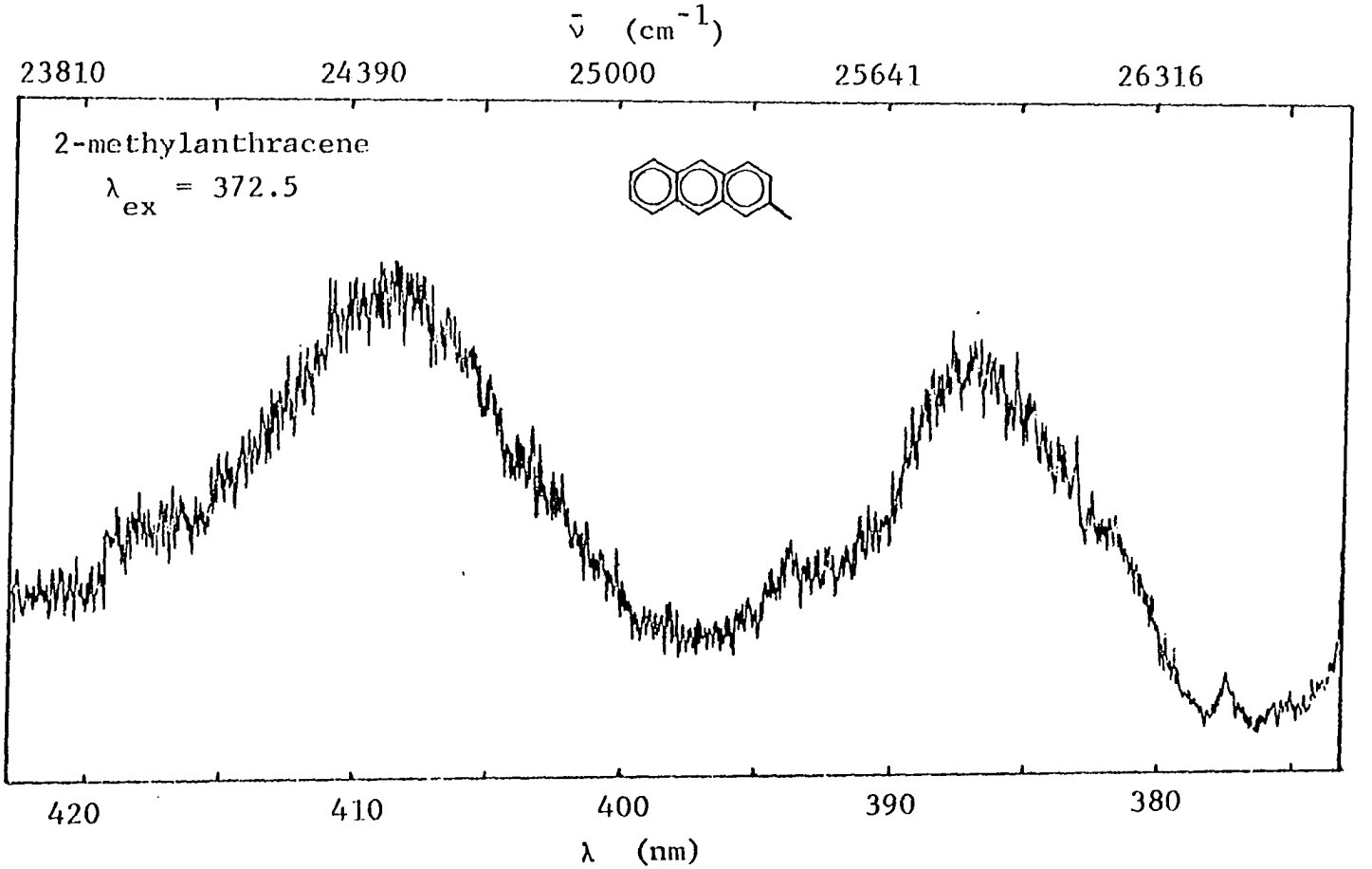
$\bar{\nu}$ (cm^{-1})
23810
24390
25000
25641
26316
2-methylanthracene
λ_{ex} = 372.5
420
410
400
390
380
λ (nm)

Figure 36. Broad band and sharp line components in fluorescence of a 2-methylanthracene sample

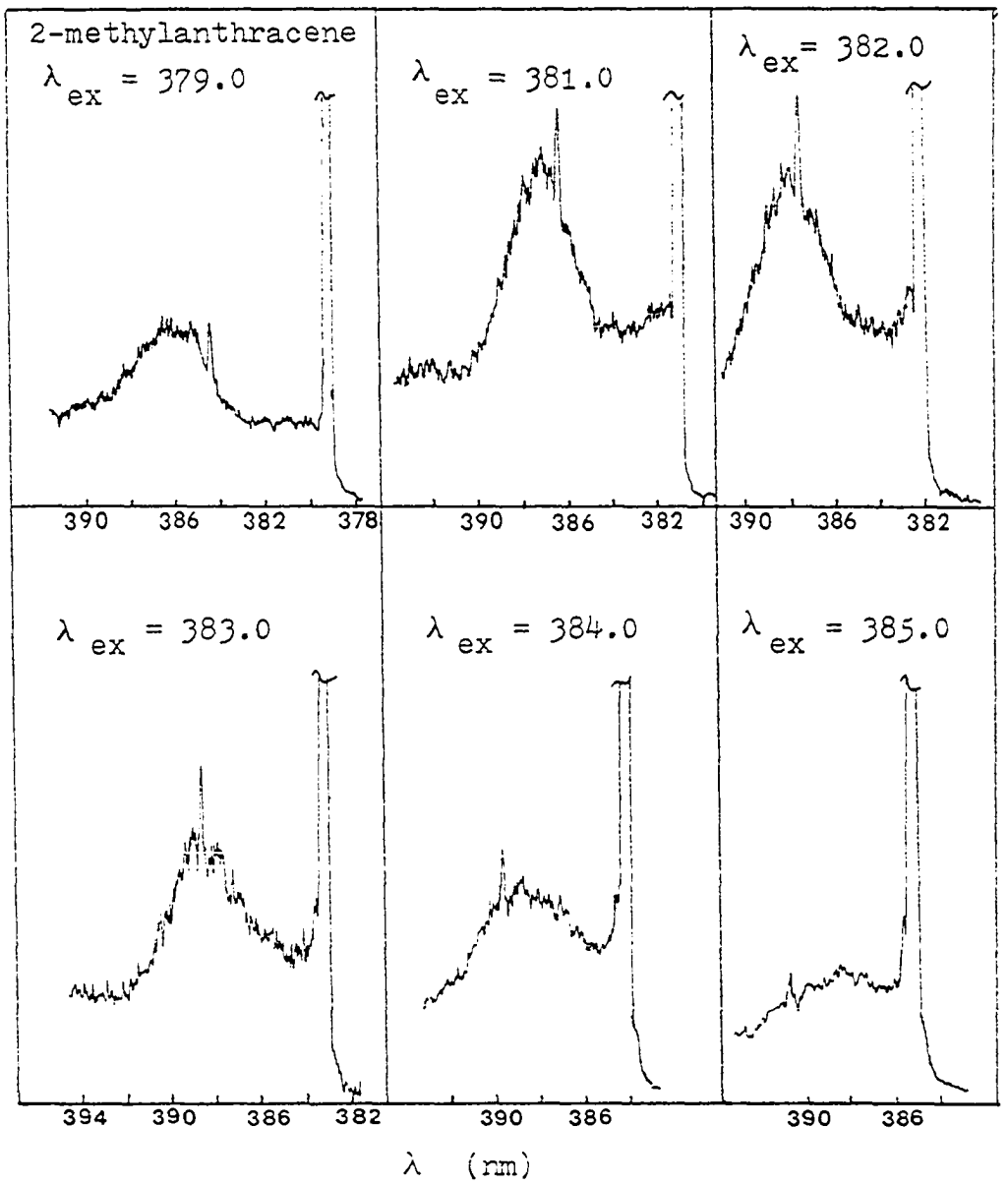
2-methylanthracene
λ ex = 379.0
λ ex = 381.0
λ ex = 382.0
λ ex = 383.0
λ ex = 384.0
λ ex = 385.0
390 386 382 378
390 386 382
390 386 382
394 390 386 382
390 386
390 386
λ (nm)

over a range of 6.0 μm. Some fraction of the 2-methylanthracene exists as isolated molecules and accounts for the small sharp ZPL that can be observed in each spectrum. The ZPL behaves just as predicted in the theory chapter. The aggregate band behaves as an independent structure whose intensity depends only on the extinction coefficient at the laser wavelength.

The fact that the aggregate emission is in the same region as the FLNS emission tends to indicate that there are only two or a few molecules in each oligomer. Further investigations indicated that the aggregates definitely exist in the 4:1 ETOH-MTHF stock solutions since shattered glasses made by rapid freezing of the stock solutions gave the same behavior. The problem is in the choice of solvents. As a wider range of glass formulations comes into routine use, better solvents can be chosen to solvate samples and break up the aggregates. Preliminary observations indicate that aggregate formation also prevented the author from obtaining FLN from picene and coronene as well as 2-methylanthracene.

11. 9-Methylanthracene

The bottom spectrum in Figure 37 is of 9-methylanthracene (MA). The reader will note that this spectrum looks nearly identical to that of the parent compound, anthracene. The major vibrational lines of MA have the same energy separations from the MA origin that anthracene vibrations do from the anthracene origin. With a few added or missing lines and differences in intensities of both ZPLs and PSBs, the same thing could be said of all the substituted anthracenes. This is

Figure 37. FLN spectra of 9-methylanthracene, benzo(ghi)-perylene and 9,10-dimethylanthracene

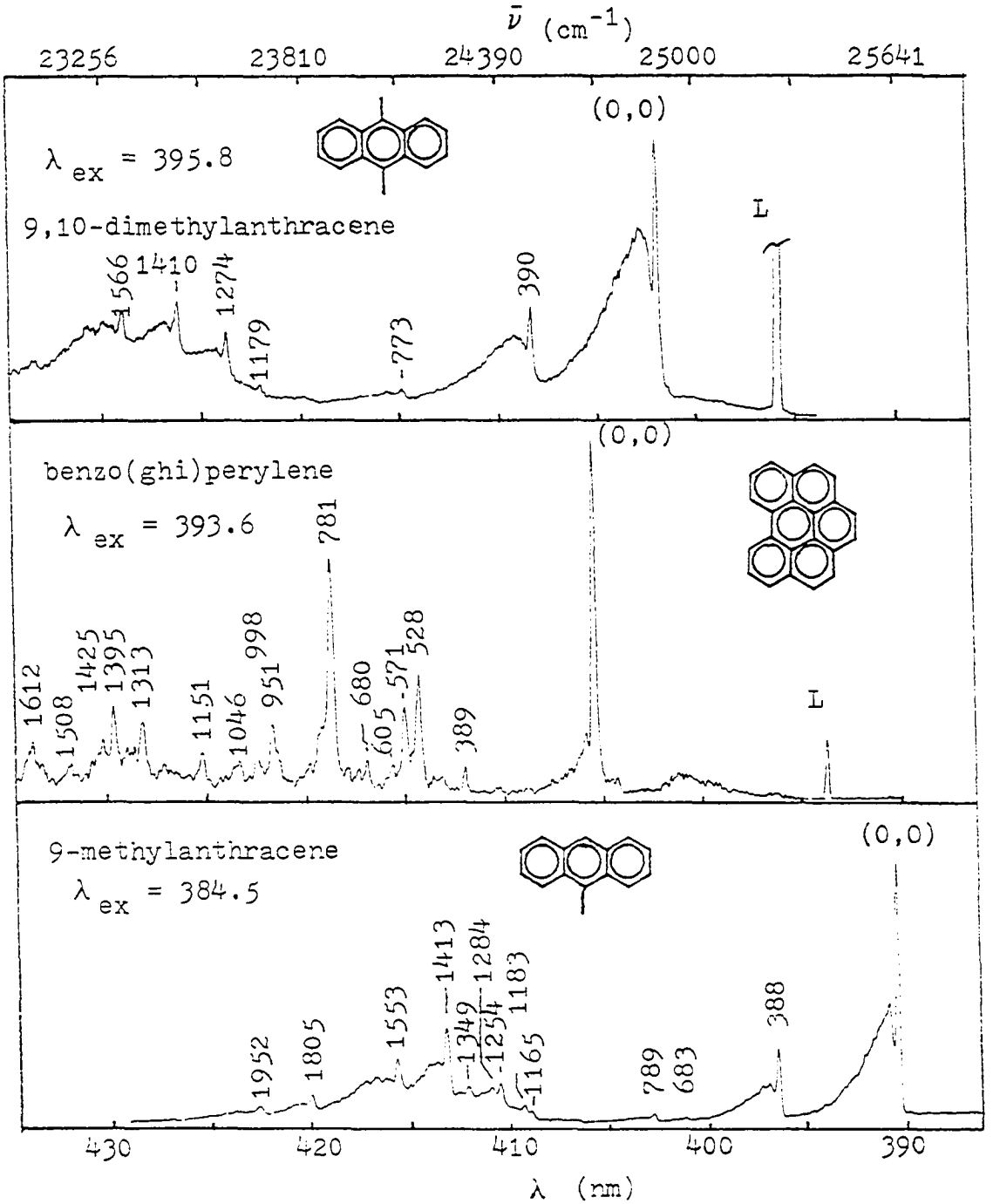
$\bar{\nu}$ (cm^{-1})
23256
23810
24390
25000
25641
(0,0)
λ_{ex} = 395.8
9,10-dimethylanthracene
1566
1410
1274
1179
773
390
L
(0,0)
benzo(ghi)perylene
λ_{ex} = 393.6
781
1612
1508
1425
1395
1313
1151
1046
998
951
680
605
571
528
389
L
9-methylanthracene
λ_{ex} = 384.5
(0,0)
1952
1805
1553
1413
1349
1284
1254
1183
1165
789
683
388
430
420
410
400
390
λ (nm)

illustrated in Table 3 which summarizes the vibrational analysis of all the anthracenes for which FLN was observed. The difference between these molecules which makes resolution by FLNS trivial is the spectral shifts of the origin region. These spectral shifts are all much larger than the 0.1 nm resolution afforded by FLNS with the instrumentation used here.

12. Benzo(ghi)perylene

The FLN spectrum in the middle of Figure 37 was taken from a standard solution of benzo(ghi)perylene (BghiP). This standard solution spectrum has an unusually large number of lines. However, the similar appearance of the phonon structure on all of the lines tends to indicate that all of the lines are of BghiP. As added evidence of this, the weak BghiP spectrum excited from a standard coronene solution (not shown) looked very similar to this one. The question of a contaminant could be cleared by tuning the laser to the 410 or 420 nm region and seeing if any of these ZPLs remain.

13. Coronene, picene, 9-vinylanthracene, pentacene and acridine

These five compounds were also briefly investigated. None of these were found to give spectra containing prominent ZPLs when incorporated into the water-glycerol glass and excited at various wavelengths with the lasers used. Coronene, picene, and pentacene all seemed not to dissolve at all in the 4:1 ETOH-MTHF stock solutions. Any spectra which could be observed when the saturated stock solutions were incorporated into glasses contained only broad structure.

Table 2. Comparison of vibrational energies in substituted anthracenes

A	PA	MA	DMA	DBrA
---	---	---	---	210
390	388	388	390	405
---	---	---	---	614
---	---	683	---	654
789	784	789	773	811
---	---	---	---	1038
---	---	---	---	1065
1169	1161	1165	---	---
---	---	1183	1179	1181
---	1252	1254	---	---
1264	1276	1284	1274	1263
---	---	1349	---	---
1408	1409	1413	1410	1388
---	---	---	---	1474
1563	1551	1553	1566	1543
1636	---	---	---	---
---	---	---	---	1754
1800	1802	1805	---	1795
---	---	1952	---	1945

A = Anthracene
PA = 9-Phenylanthracene
MA = 9-Methylanthracene
DMA = 9,10-Dimethylanthracene
DBrA = 9,10-Dibromoanthracene

Note that energies are expressed in wavenumbers (cm^{-1})

The other two compounds seemed to present other problems. 9-Vinylanthracene did dissolve to form a brilliantly fluorescent solution after several minutes in a warm ultrasonic cleaning bath. No sharp ZPLs could be found in the dispersed fluorescence spectra of a glass containing this compound. It seems possible that the 9-vinylanthracene was highly aggregated or even partially polymerized so that FLN from isolated molecules could not be observed. No fluorescence of any kind could be observed from acridine in the water-glycerol glass.

14. 9,10-Dimethylanthracene

An FLN spectrum of this compound (DMA) is shown at the top of Figure 37. This compound behaves much like the other anthracene derivatives as detailed under the discussion of MA and in Table 2.

15. Benzo(k)fluoranthene

Benzo(k)fluoranthene (BkF), as shown in the bottom spectrum of Figure 38, presents one of the simplest FLN spectra of any molecule investigated. Except for an energy shift, this spectrum appears identical to the LESS spectrum shown in reference 43 as would be expected considering the aforementioned similarities of these techniques.

16. 9,10-Dibromoanthracene

DBrA again exhibits the recognizable anthracene fluorescence pattern as discussed earlier. From the spectrum of this compound

Figure 38. FLN spectra of benzo(k)fluoranthene, 9,10-dibromoanthracene and benzo(a)pyrene

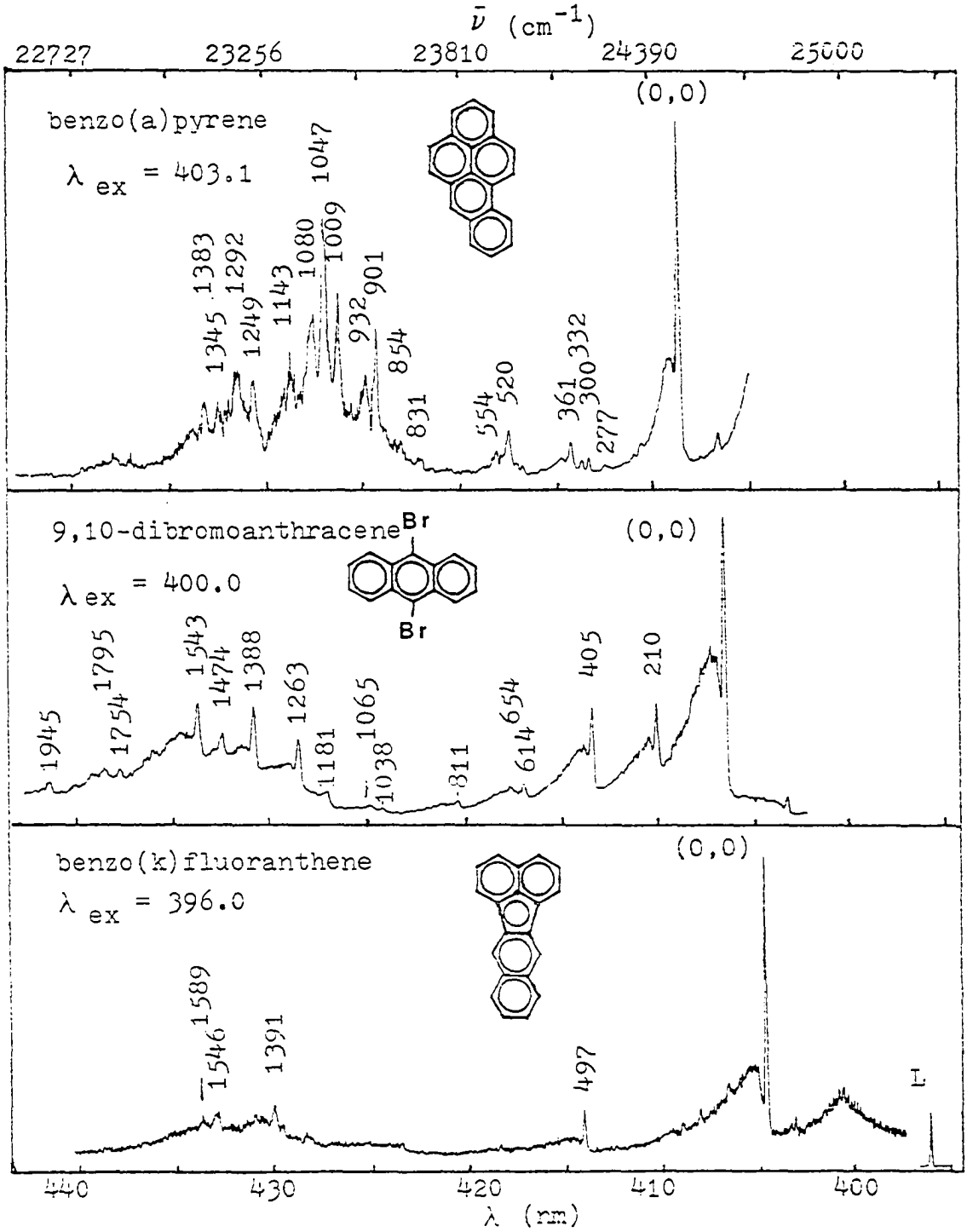
$\bar{\nu}$ (cm^{-1})
22727
23256
23810
24390
25000
benzo(a)pyrene
λ_{ex} = 403.1
(0,0)
1383
1292
1249
1345
1143
1080
1047
1009
932
901
854
831
554
520
361
332
300
277
9,10-dibromoanthracene
Br
Br
λ_{ex} = 400.0
(0,0)
1945
1795
1754
1543
1474
1388
1263
1181
1065
1038
811
654
614
405
210
benzo(k)fluoranthene
λ_{ex} = 396.0
(0,0)
1589
1546
1391
497
L
440
430
420
410
400
λ (nm)

shown in the middle of Figure 38, it can be seen that even the phonon structure looks the same as the parent.

17. Benzo(a)pyrene

Benzo(a)pyrene (BaP) is a compound of great interest because of its recognized wide occurrence and carcinogenicity. Almost every analytical technique in the literature for PAH analysis gets applied to analysis for this compound. The spectrum shown at the top of Figure 38 for BaP is quite normal for a FLN spectrum of a PAH. The origin stands out in a relatively open area of the spectrum. The relatively uncomplicated structure in the low lying vibrational region and the increasing congestion at more than 850 cm^{-1} from the origin are also typical of many FLN spectra of PAH species. The particulars of analysis for BaP with FLNS will be discussed more in later sections.

18. 3,4,9,10-Dibenzpyrene

The spectrum of DBP shown in the lower part of Figure 39 is, no doubt, the simplest FLN spectrum of any in this dissertation. The origin dominates the spectrum with only three vibrational lines observable on the same sensitivity scale.

19. Perylene

Perylene (Pe) possesses the lowest energy S_1 state of any species for which FLN was observed. This molecule is perhaps the most studied fluorescent PAH species. The first reported organic FLNS (44,57) experiments utilized this compound. The fluorescence quantum yield

Figure 39. FLN spectra of 3,4,9,10-dibenzpyrene and perylene

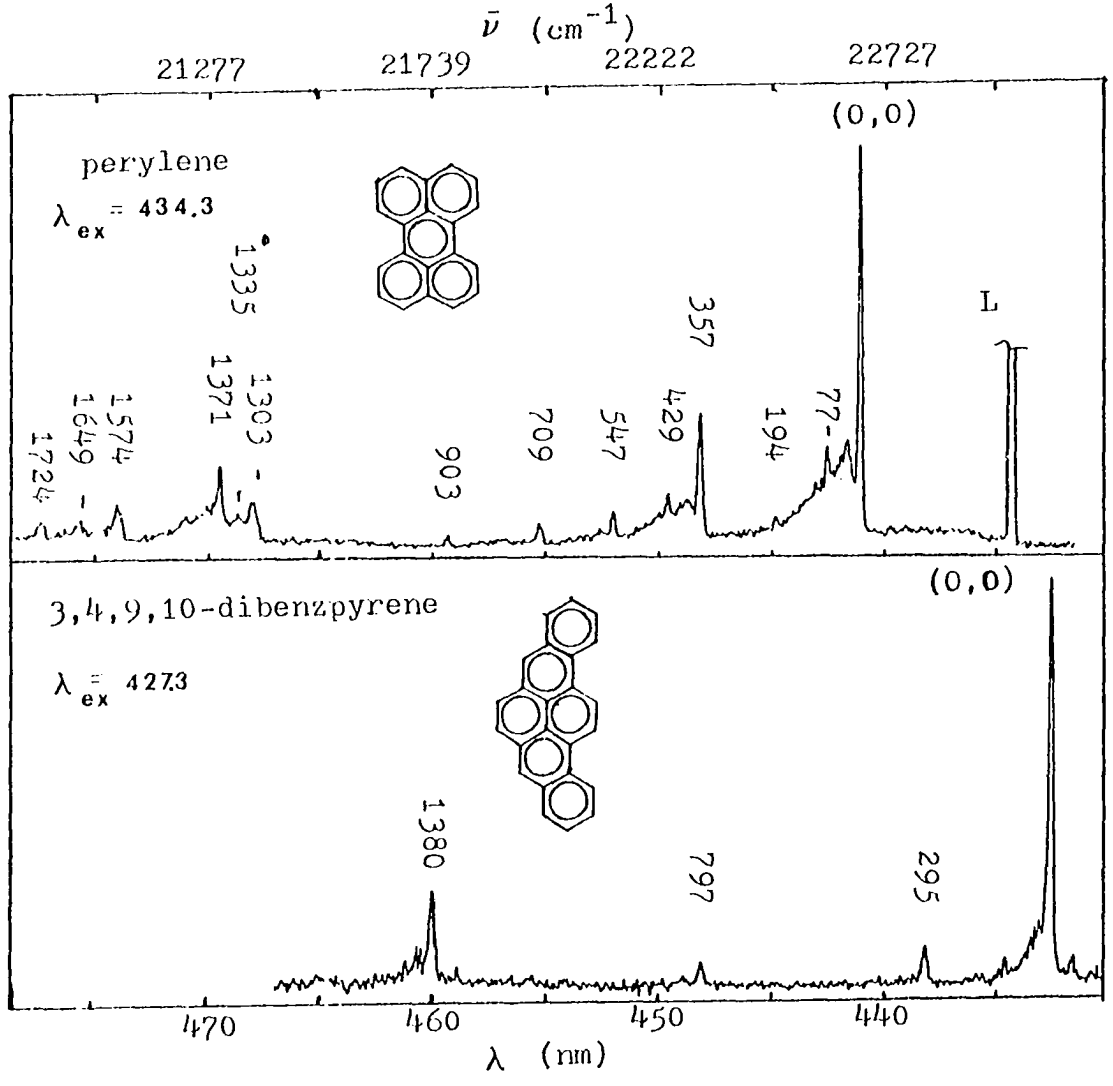
$\bar{\nu}$ (cm^{-1})
21277
21739
22222
22727
(0,0)
perylene
λ_{ex} = 434.3
1335
357
L
1371
1303
1574
1649
1724
903
709
547
429
194
77-
3,4,9,10-dibenzpyrene
λ_{ex} = 427.3
(0,0)
1380
797
295
470
460
450
440
λ (nm)

for perylene is so high that an 0.10 ppm stock solution looks blue from fluorescence in room light. Because of this, spectra of Pe appear in many of the papers on sharp line fluorescence (37,40,56).

The Pe spectrum in the top half of Figure 39 appears typical of the FLNS spectra presented in this section. The origin is the most intense line with the next most intense ZPL occurring at (0,0) - 357 cm^{-1}. The ZPLs at (0,0) - 77 and -429 cm^{-1} are probably from a second isochromat that is not as efficiently pumped by the laser line. Excitation into the origin at about 441 nm would make the 357 vibration a good analytical line and eliminate the minor isochromat contributions. However, the spectrum of Pe is so intense that its situation in the low energy region of the uv-visible spectrum should prevent significant interferences.

D. Resolution of an Artificial Mixture

The next six figures demonstrate resolution of thirteen of the components from an artificial mixture containing fourteen polycyclic aromatic compounds. These spectra were all taken during one run from a single glass which had been doped with stock solutions so as to contain each of the following compounds at 200 ppb: pyrene (P), benzo(e)pyrene (BeP), 1-methylpyrene (MP), anthracene (A), benz(a)-anthracene (BaA), 9-phenylanthracene (PA), 9-methylanthracene (MA), benzo(*ghi*)perylene (BghiP), 9,10-dimethylanthracene (DMA), 9,10-dibromoanthracene (DBrA), benzo(a)pyrene (BaP), 3,4,9,10-dibenzpyrene (DBP), perylene (Pe) and acridine.

These fourteen compounds were not carefully selected. They represent all of the species on hand that were found to be compatible with the water-glycerol glass. Acridine was included in this mixture and in several less complicated samples which were among the seven samples analyzed during one night. During this brief experiment, no acridine spectrum could be obtained and it is not likely that any acridine fluorescence appears in any of these spectra.

Most of the spectra were taken using the preselected excitation wavelengths for the compound desired. The excitation wavelength used is listed with each of the spectra. Since all of the compounds were in the same glass being analyzed one after the other with the same optical alignment, the intensities in these spectra help indicate relative sensitivities for the various species. The scale factors used to produce the displays are, therefore, listed on each spectrum. Recall from the section on computer control and data reduction that the scale factor is inversely proportional to fluorescence yield, I_{fl}/I_L. Among the most intense spectra is that for perylene in Figure 45 with a scale factor of 120. Among the least intense signals are those for BeP and BaA in Figures 40 and 41 which show only small ZPLs in displayed spectra at scale factors of 1800.

For several of these spectra, temporal resolution was utilized to help simplify the spectra. In those spectra for which no delay or gate [width] are listed, the integrators were opened to signals at the arrival of the laser pulse and gated off after the maximum, 850 ns, gate width. In other words, unless a delay and gate are listed, no

temporal resolution was used. Temporal resolution was applied mostly for cosmetic reasons in these spectra since it was not really required for observation of any of these signals.

The three spectra in Figure 40 demonstrate resolution of the FLN signals for pyrene, benzo(e)pyrene, and 1-methylpyrene from the mixture. The middle spectrum of BeP was taken before the aforementioned interference by 1-methylpyrene was noticed. Thus, only the false origin ZPL for BeP occurs without major interference. Better resolution of BeP from solutions containing MP are shown in later figures. One of the most remarkable features of the spectra in this figure is the high intensity of the MP spectrum even after the delayed gate.

Anthracene, benz(a)anthracene, 9-phenylanthracene and 9-methylanthracene are shown resolved in the three spectra of Figure 41. As will be recalled from the reference spectra, the best apparent excitation wavelength for both A and BaA occurs at 373.8 nm. Thus, spectra from these two species together appear in the bottom spectrum of this figure. This spectrum was scaled for optimum display of the anthracene fluorescence. The insignificance of the BaA ZPL on this scale illustrates both the difference in fluorescence intensity and the need for permanent data storage so that such spectra can be displayed with scale factor, smoothing, and dispersion optimized for the feature desired.

For many of the spectra, the laser line is recorded. Often, to get the laser on scale so that its lineshape and exact position can be

Figure 40. FLN spectra showing resolution of pyrene, benzo(e)pyrene and 1-methylpyrene from the mixture

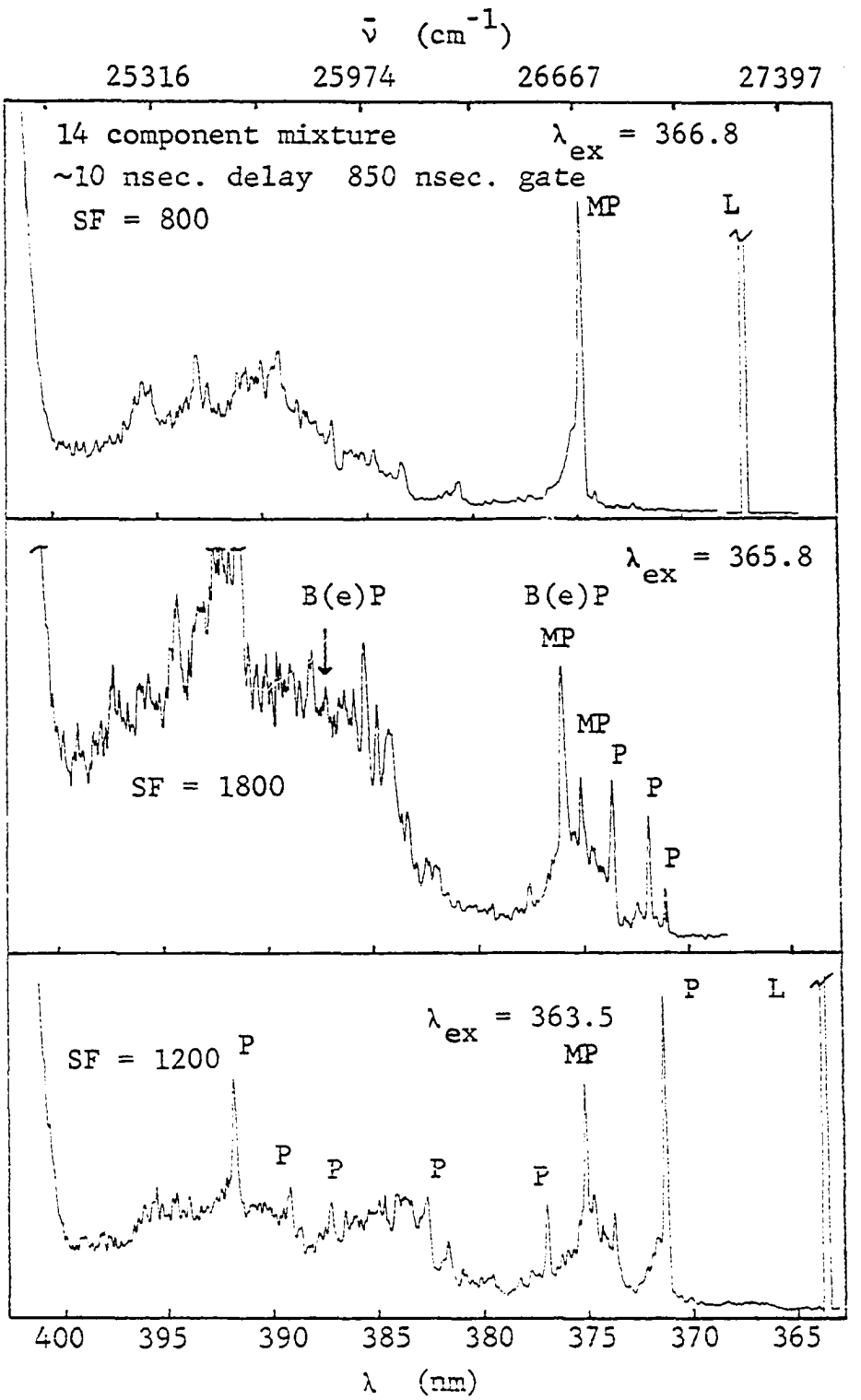
$\bar{\nu}$ (cm^{-1})
25316
25974
26667
27397
14 component mixture
~10 nsec. delay 850 nsec. gate
SF = 800
λ_{ex} = 366.8
MP
L
λ_{ex} = 365.8
B(e)P
B(e)P
MP
MP
P
P
P
SF = 1800
P
L
λ_{ex} = 363.5
SF = 1200
P
MP
P
P
P
P
400
395
390
385
380
375
370
365
λ (nm)

Figure 41. FLN spectra showing resolution of anthracene, benz(a)anthracene, 9-phenylanthracene and 9-methylanthracene from the mixture

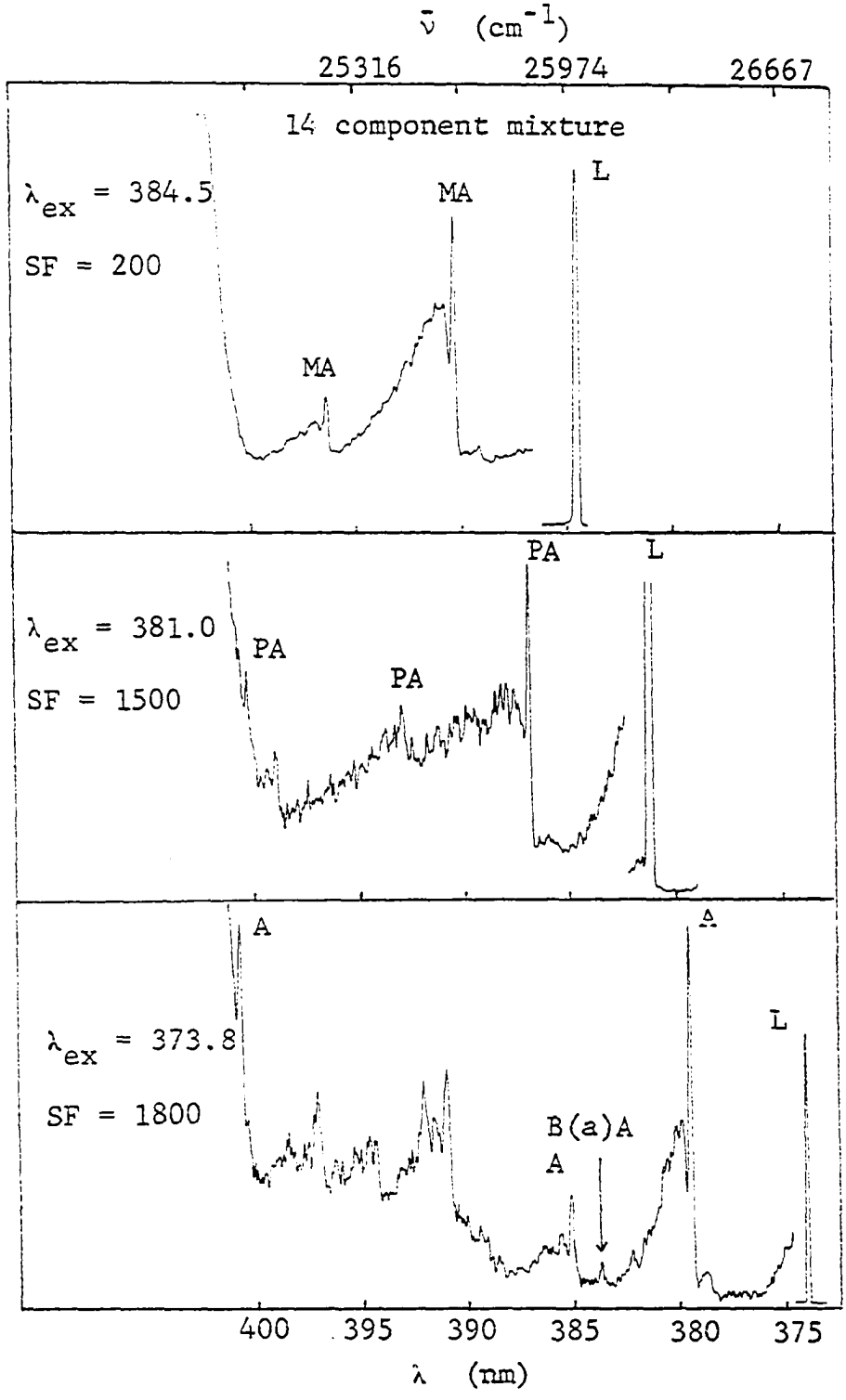
$\bar{\nu}$ (cm^{-1})
25316
25974
26667
14 component mixture
λ_{ex} = 384.5
SF = 200
MA
MA
L
λ_{ex} = 381.0
SF = 1500
PA
PA
PA
L
λ_{ex} = 373.8
SF = 1800
A
A
L
B(a)A
A
400
395
390
385
380
375
λ (nm)

seen, a stack of neutral density filters was inserted into the collection optics path as the monochrometer scanned through the laser wavelength. The three spectra reproduced in Figure 41 were all taken this way and exhibit clearly all three of the spectral regions mentioned in the Theory chapter. Notice that as the wavelength is advanced to lower energy, from bottom to top in these figures, the simple spectra in region II change dramatically. The only observable ZPLs in region II of the spectra in Figure 41 are due to the compounds whose ideal excitation regions had been chosen.

Figure 42 shows spectra of benzo(ghi)perylene, 9,10-dimethyl-anthracene, and 9,10-dibromoanthracene. The B(ghi)P spectrum at the bottom of this figure is quite intense and easily recognized by comparison to the reference spectrum. However, there seems to be a lot of extra broad structure associated with each of the transitions. The apparent broadening may be due to aggregate formation induced by the heavy, 2.8 ppm, total PAH concentration in this polar glass. An 850 ns wide delayed gate was used to minimize interference in this region by intense nine substituted anthracene fluorescence.

The middle section of Figure 42 shows a spectrum excited at the wavelength chosen for 9,10-dimethylanthracene. Multiple isochromat emission in the region of the B(ghi)P and DBrA origins dominate the spectrum. However, careful examination shows two definite lines due to DMA. There needs to be a way to redisplay such spectra. The noise level is quite low indicating that the DMA ZPLs could have been displayed at full scale deflection.

Figure 42. FLN spectra showing resolution of benzo(ghi)perylene, 9,10-dimethylanthracene and 9,10-dibromoanthracene from the mixture

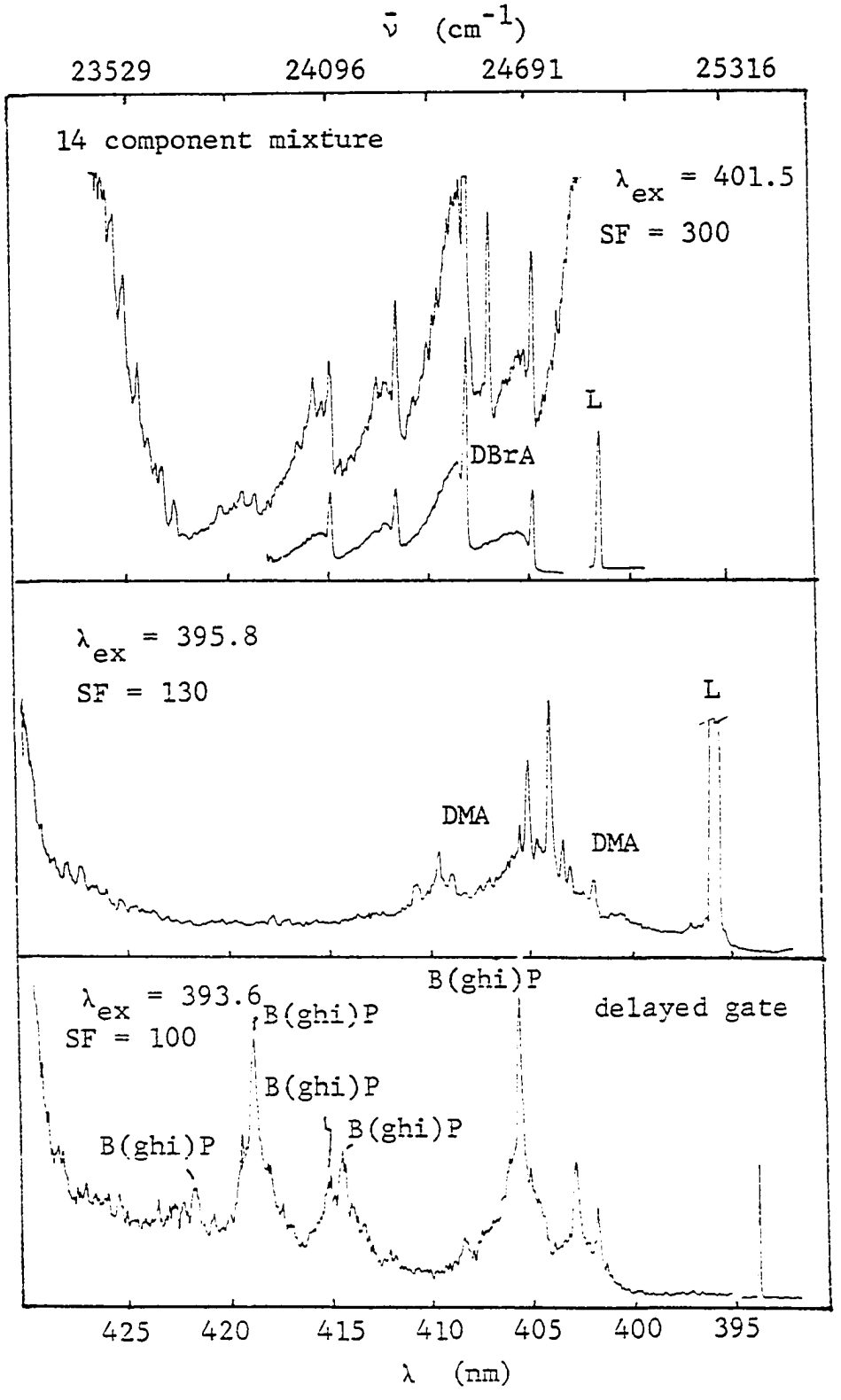
$\bar{\nu}$ (cm^{-1})
23529
24096
24691
25316
14 component mixture
λ_{ex} = 401.5
SF = 300
DBrA
L
λ_{ex} = 395.8
SF = 130
DMA
DMA
L
λ_{ex} = 393.6
SF = 100
B(ghi)P
B(ghi)P
B(ghi)P
B(ghi)P
B(ghi)P
delayed gate
425
420
415
410
405
400
395
λ (nm)

The top section of Figure 42 shows two spectra at the 401.5 nm excitation wavelength. The top trace is taken from the mixture. Since the reference spectrum for 9,10-dibromoanthracene was taken at 400.0 nm, a 401.5 nm excited DBrA standard spectrum is shown as the lower trace. This allows identification of the DBrA lines in the mixture spectrum. The strong ZPL with little phonon structure which appears between the two highest energy DBrA lines is probably due to benzo(a)pyrene. The mixture spectrum is reproduced again in Figure 43 with a smaller scale factor to show that all of the major DBrA lines can be identified.

Figure 44 shows the FLN spectrum of benzo(a)pyrene excited from the mixture. Again, note that region II is very simple with only B(a)P giving prominent lines. This is true in spite of the seemingly close proximity of this excitation line to that chosen for DBrA. The complicated perylene and 3,4,9,10-dibenzpyrene spectra appearing in region III are so intense due to the fact that the excitation line is in a congested region of the absorption spectra exciting many isochromats and thus a larger fraction of the total molecules.

The last figure in this series, Figure 45, presents spectra excited from the mixture of 3,4,9,10-dibenzpyrene (DBP) and perylene (Pe). The 427.4 nm line excites both species with DBP being easily resolved from Pe. Excitation at 433.8 nm excites fluorescence only from perylene. This low energy line is below the origins of every species except perylene. The perylene spectrum generated from the mixture contains no

Figure 43. FLN spectrum of 9,10-dibromoanthracene excited from the mixture

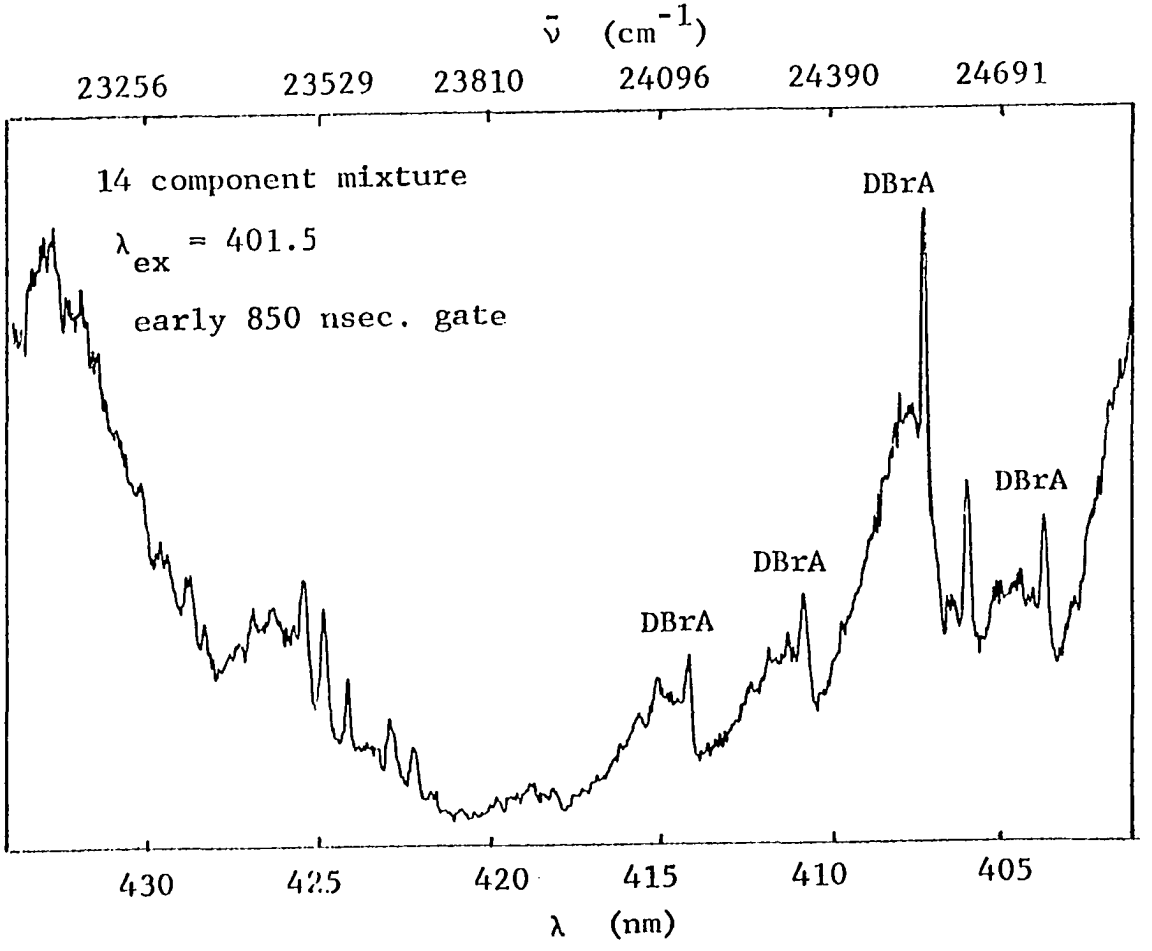
$\bar{\nu}$ (cm^{-1})
23256
23529
23810
24096
24390
24691
14 component mixture
λ_{ex} = 401.5
early 850 nsec. gate
DBrA
DBrA
DBrA
DBrA
430
425
420
415
410
405
λ (nm)

Figure 44. FLN spectrum showing resolution of benzo(a)pyrene from the mixture

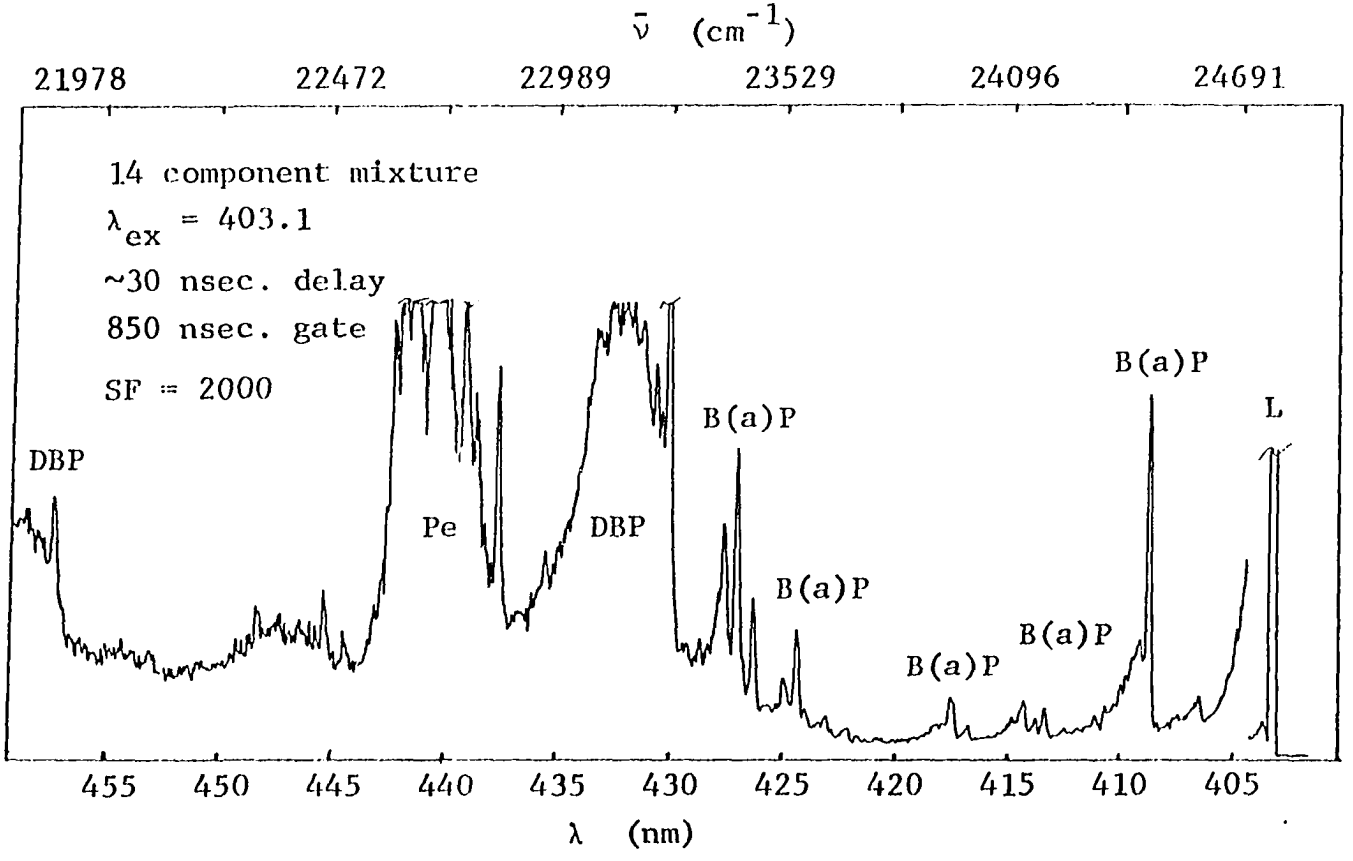
$\bar{\nu}$ (cm^{-1})
21978
22472
22989
23529
24096
24691
14 component mixture
λ_{ex} = 403.1
~30 nsec. delay
850 nsec. gate
SF = 2000
DBP
Pe
DBP
B(a)P
B(a)P
B(a)P
B(a)P
B(a)P
L
455
450
445
440
435
430
425
420
415
410
405
λ (nm)

Figure 45. FLN spectra showing resolution of 3,4,9,10-dibenzpyrene and perylene from the mixture

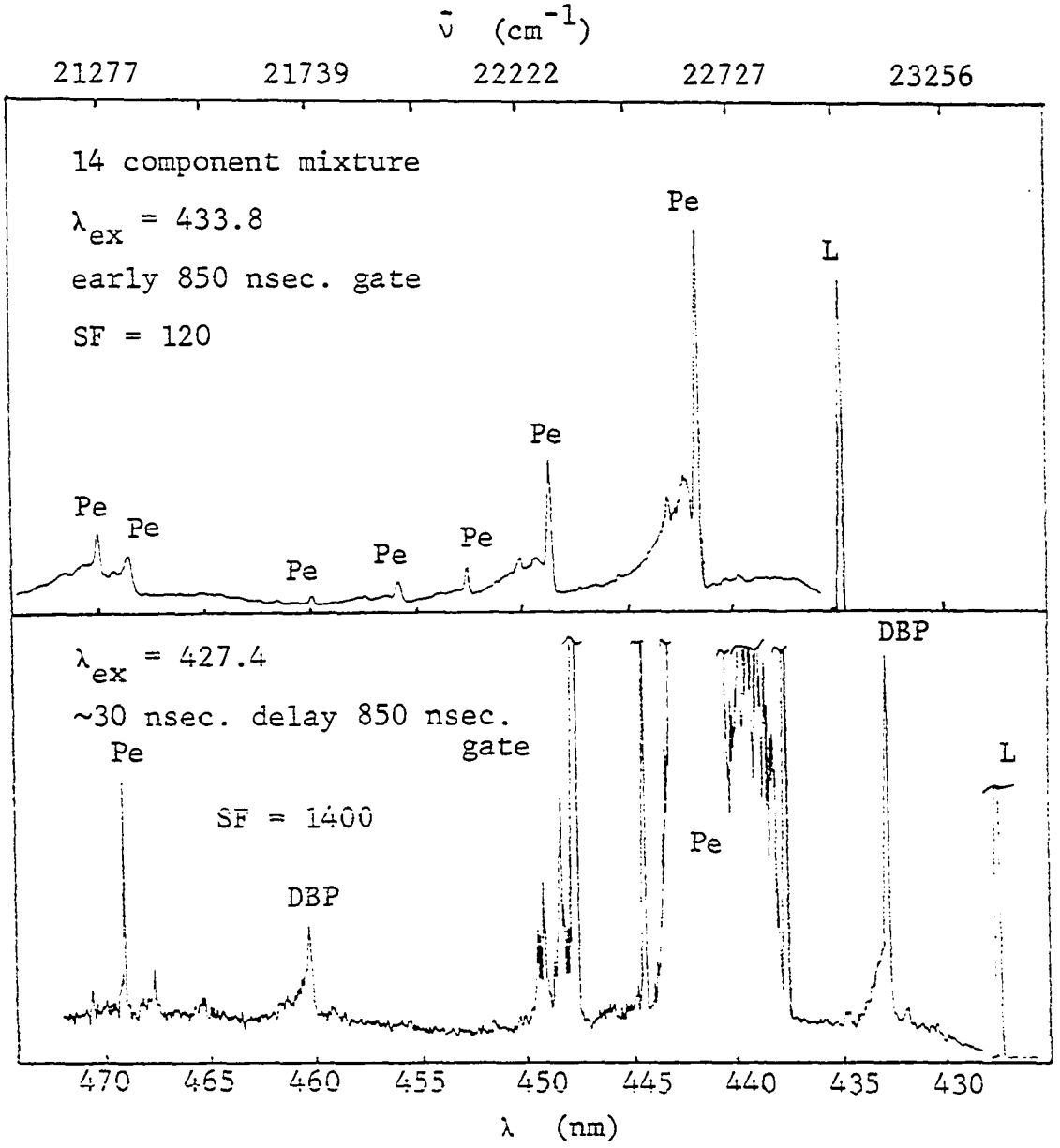
ν̃ (cm⁻¹)
21277
21739
22222
22727
23256
14 component mixture
λex = 433.8
early 850 nsec. gate
SF = 120
Pe
Pe
Pe
Pe
Pe
Pe
Pe
L
λex = 427.4
~30 nsec. delay 850 nsec. gate
SF = 1400
Pe
DBP
Pe
DBP
L
470
465
460
455
450
445
440
435
430
λ (nm)

other fluorescence features and looks very similar to the reference spectrum.

E. Analysis of SRC-II Samples

1. Direct dilution

The true test of any technique for PAH analysis is its application to real samples. Natural PAH mixtures generally contain hundreds of PAH species and vast quantities of other organic material. The problem is compounded by the fact that in many natural samples, the total PAH concentrations may be in the pptr range (1). Even a technique like FLNS, with its low pptr detection limits for each species, would require an extraction and preconcentration step in procedures for PAH determination in ground water, for example. Rather than develop and test such procedures, a natural sample with relatively high PAH concentrations was chosen.

The products from the solvent refined coal processes are high in PAH material content. In fact, the high concentrations of PAHs along with compounds in other classes make SRC-II a very potent carcinogen. A sample of this coal liquification product, SRC-II, was supplied to Ames Laboratory as a surrogate reference material by the National Bureau of Standards. A small sample of this material was obtained by the author from Dr. C. Chriswell (10) and used in these investigations. Although it is suspected that the composition of the SRC-II samples change with time, even while refrigerated, several groups analyzed the sample during the fall and winter of 1979. The results of several of

the other analyses are summarized along with the results of the following experiments in Table 4 at the end of this section.

The SRC-II sample as obtained was a very dark golden brown oil. The optical density or total absorbance of this material was so high that it had first to be diluted with 1:4 MTHF-ETOH to give final dilutions in the water-glycerol glass of 10^4 and 10^5 to one. This dilution insured an optical density low enough to minimize the inner filter effect and other problems caused by high concentrations in this glass. At the same time, these dilutions were not so high as to preclude observation of rather intense PAH FLN from the glasses, cf. Figures 46 through 49.

As can be seen in these spectra, regions I and III are very pronounced. Yet, in Figures 46 and 49, the analytical lines for the species sought appear just as clean and free of interference as they did in the artificial mixture. No doubt, the temporal resolution used in the pyrene and 1-alkylpyrene spectra shown in Figure 46 contributed greatly to the clean appearance of these spectra.

Earlier results discussed in the Theory chapter and published in reference 45 had shown that direct absolute calibration yielded linear intensity to concentration relationships for more than three decades in PAH concentration. To insure that this held true when doing FLNS with the pulsed laser and gated detection systems using computer normalization and smoothing, a series of quantitation experiments was conducted. A series of solutions containing pyrene, benzo(e)pyrene, 1-methylpyrene, anthracene, benzo(a)pyrene, and perylene at

concentrations from 1 ppm to 2.0 pptr (six decades) were prepared. These quantitation standards were prepared in two groups, one with all concentrations equal and the other with concentrations of the various species varying over three orders of magnitude. Glasses from these groups of samples were used to obtain the detection limit and temporal resolution spectra discussed earlier, Figures 13, 14, 19, and 20. These mixtures were also used as concentration standards all through the SRC-II runs.

By measuring the height above background for the chosen analytical ZPL and taking into account the scale factors and recorder sensitivities used, it is possible to calculate a response factor for the compound being monitored in each of the glasses in the cryostat. Equation 6 expresses this relationship. In essence, Equation 6 takes into account the effects of computer scaling, Equation 5, to produce a number proportional to I_{Fl}/I_L in Equation 3.

$$RF = \frac{PH}{FSH} \times \frac{\text{Rec. Att.}}{1000} \times \frac{1}{SF} \tag{6}$$

RF = Response factor (proportional to I_{Fl}/I_L, Equation 3)

PH = Measured peak height of chosen ZPL

FSH = Height of full scale response in same units as PH

Rec. Att. = Full scale response of the recorder in millivolts

SF = Scale factor selected in Equation 5

Two or three samples whose concentrations were to be compared were inserted into the cryostat. The laser was then tuned to the correct excitation wavelength for one of the species and optical alignment and

integrator gating optimized. The samples were then turned one at a time into alignment on the optical axis so that only the factors in Equation 12 were variable. Thus, an RF for the compound in each of the glasses was determined. Several experimental runs using a wide range of concentrations of the six compounds were made. The results verified that within about 10% error over at least three decades, the RF values were indeed proportional to concentration.

Rather than present any of the data from the quantitated standards, aspects of the SRC-II analyses will be used to verify quantitative linear response. By including at least one of the six component standard mixtures in each set of samples cooled during the SRC-II analyses, the concentration of the PAHs in the unknown could be determined as shown in Equation 7.

$$C_{unk} = RF_{unk} \times \frac{C_{std}}{RF_{std}} \tag{7}$$

RF_x = Response factor, Equation 6

C_x = Concentration

Using the above computational methods, several compounds in the SRC-II dilutions were quantitated. The spectrum for pyrene in the $1{:}10^4$ dilution shown at the bottom of Figure 46 indicates a concentration in the glass of 71 ppb. A similar spectrum taken of the $1{:}10^5$ dilution of SRC-II gave 9.6 ppb pyrene in the glass. Similar calculations were run on all six compounds with results as summarized in Table 3.

Figure 46. FLN spectra showing resolution of pyrene, 1-alkylpyrene and anthracene from SRC-II

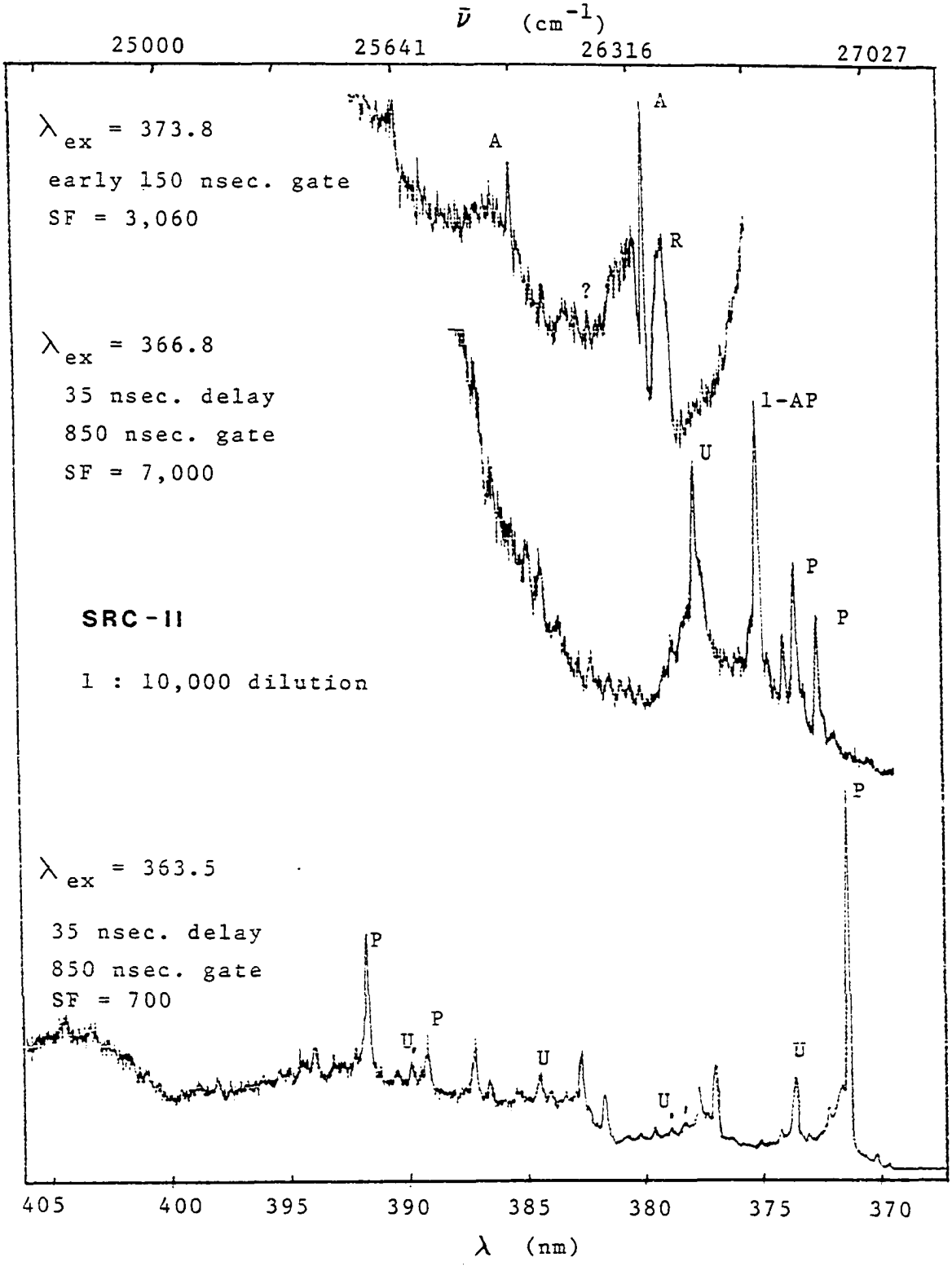
$\bar{\nu}$ (cm^{-1})
25000
25641
26316
27027
λ_{ex} = 373.8
early 150 nsec. gate
SF = 3,060
A
A
R
?
λ_{ex} = 366.8
35 nsec. delay
850 nsec. gate
SF = 7,000
1-AP
U
P
P
SRC-II
1 : 10,000 dilution
P
λ_{ex} = 363.5
35 nsec. delay
850 nsec. gate
SF = 700
P
U
P
U
U
U
405
400
395
390
385
380
375
370
λ (nm)

The middle and top spectra in Figure 46 are quite similar to the corresponding spectra from the artificial mixture run. The 1-alkylpyrene ZPL is intense and well resolved with no indication of any likely interference. A prominent unknown emission occurs in the FLN spectrum excited with the 366.8 nm laser line. This is apparently a species with long lived fluorescence and could well be pyrene with an alkyl substituent at another location. The two intense ZPLs in the top spectrum are from anthracene. The line directly below the question mark in this top trace is in the right place to be due to benz(a)anthracene.

As evidence of the extreme sensitivity of FLNS, consider the spectra of benzo(e)pyrene presented in Figure 47. As mentioned in the preceding section, these three spectra are the only ones taken of B(e)P with excitation into the origin band. Also recall that this compound could just give a detectable response on the same scale as the MP and P fluorescence in Figure 40. The wavelength scales of the three spectra in Figure 47 are carefully lined up for comparison. The B(e)P peak in the $1{:}10^{4}$ dilution of SRC-II (at the top of the figure) is easily observed. The sharp intense structures of P and 1-AP shown in Figure 40 are absent here due to the lower energy excitation line. The B(e)P in the $1{:}10^{5}$ dilution spectrum is a little harder to see, as is the B(e)P peak in the 200 pptr standard that was in the cryostat at the same time as the two SRC-II dilutions. Careful comparison on the original strip chart recordings showed that the three marked lines are in the correct positions. Other scans also demonstrated that the gross structure of the background was reproducible.

Figure 47. FLN spectra showing resolution of benzo(e)pyrene from SRC-II using 375.8 nm (origin band) laser excitation

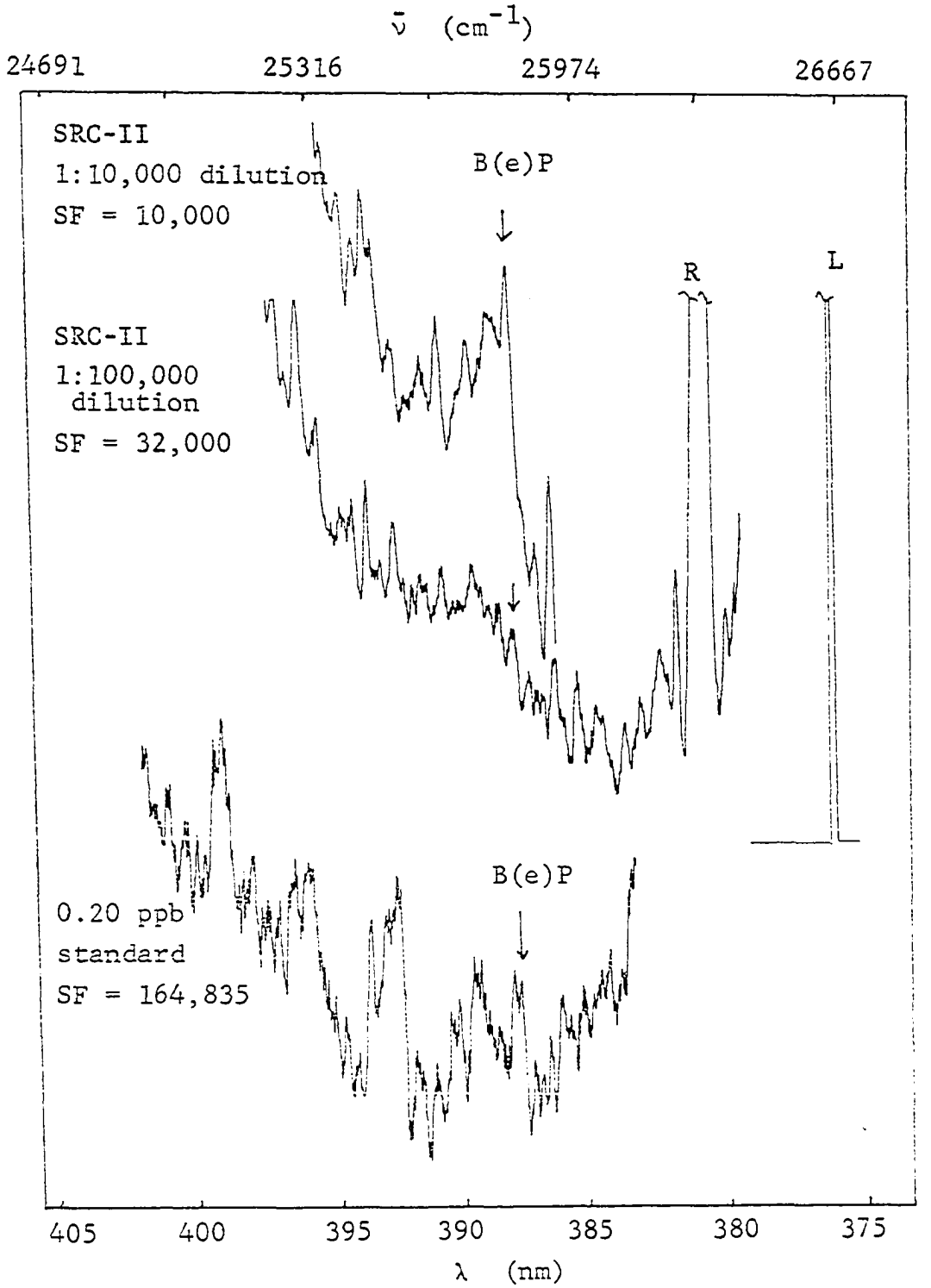
$\bar{\nu}$ (cm^{-1})
24691
25316
25974
26667
SRC-II
1:10,000 dilution
SF = 10,000
B(e)P
R
L
SRC-II
1:100,000
dilution
SF = 32,000
0.20 ppb
standard
SF = 164,835
B(e)P
405
400
395
390
385
380
375
λ (nm)

The most convincing proof that the marked lines are B(e)P ZPLs is the fact that the concentrations calculated from these three spectra agree closely with each other and with later determinations of B(e)P in another glass using a higher concentration standard, cf., Table 3. These three spectra were taken at very slow scan speeds with maximum filtering and averaging of the data. The background structure for the most part is real and reproducible. Careful comparison of the middle and top spectra show that most of the features in one spectrum have a counterpart in the other. Keep in mind that sharp structures due to the solvent and scatter of the reflected laser line inside the monochrometer will not change with dilution of the dopant in the glass. The standard spectrum shown at the bottom of this figure compares quite well with the structure in the spectrum shown in Figure 27. The spectrum in Figure 27 was taken from a glass containing a similar low B(e)P concentration using a faster scan speed.

In addition to the six compounds from the concentration study, benzo(k)fluoranthene (BkF) was determined in the SRC-II sample. After obtaining a sample of BkF late in this series of experiments, a solution containing BkF and BaP was prepared to check for possible interference. Resolution of these compounds was no problem at all with FLNS. For this reason, the solutions prepared were used as quantitation standards for BkF in the SRC-II sample. The left hand spectrum in Figure 48 was the result, indicating 1.9 ppb BkF in the $1{:}10^4$ SRC-II dilution.

Figure 48. FLN spectra showing resolution of benzo(k)fluoranthene and benzo(a)pyrene from SRC-II

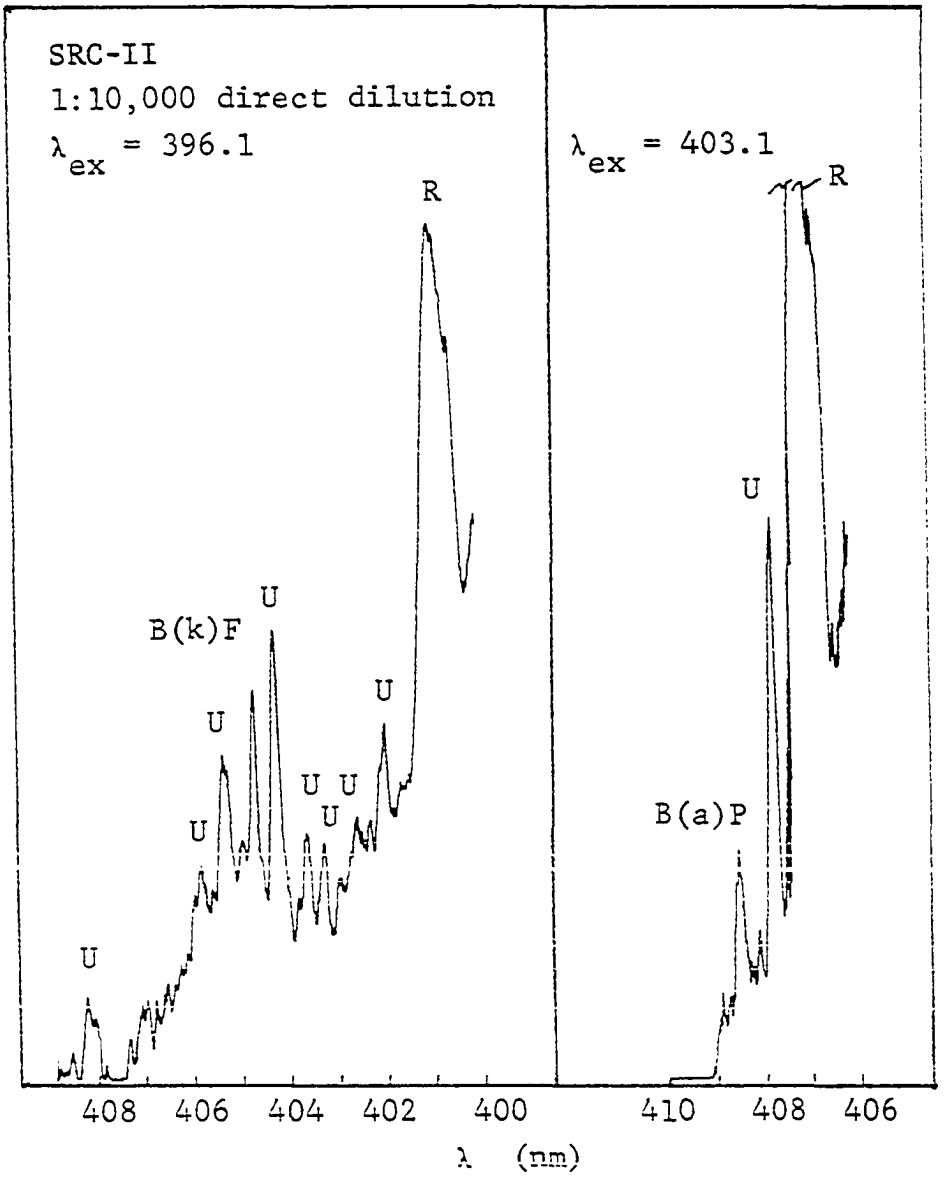
SRC-II
1:10,000 direct dilution
λex = 396.1
R
U
B(k)F
U
U
U
U
U
U
U
λex = 403.1
R
U
B(a)P
408
406
404
402
400
410
408
406
λ (nm)

The B(a)P and B(k)F spectra are included together in Figure 48 partly because they, along with anthracene in Figure 46, illustrate a problem encountered when working at low concentrations. The excitation wavelengths chosen (at higher concentrations) for these compounds are quite close to the origins. In the cases of B(a)P and B(k)F, this means that the chosen analytical lines occur on the rapidly falling low energy side of region I. This rapidly changing baseline distorts the appearance of PSBs and makes the spectra hard to recognize at low concentrations. The intense Raman emission seen near the ZPLs of A, B(k)F and B(a)P further complicate matters. Raman problems can be partially eliminated by improved temporal resolution while the sloping baselines can be improved by choosing excitation wavelengths that move the analytical ZPLs farther into region II.

Over a month after the data in Figures 46 through 49 were taken, the SRC-II sample was analyzed again for pyrene and benzo(e)pyrene. This time, rather than the standard glass formulation previously described, the SRC-II sample was diluted with dimethylsulfoxide (DMSO) and used to formulate glasses by diluting a 5:4 glycerol-water mixture to 120% original volume. A single $1:5 \times 10^4$ dilution of SRC-II in this glass, along with two standard solutions in a similar glass, were inserted into the cryostat and analyzed. Two concentrations for both pyrene and benzo(e)pyrene in the SRC-II sample were calculated from the FLN results. These values were averaged and included with the calculated average deviation in the bottom line of Table 3. Although less care was taken (the deviations are unusually large), both concentration values agree quite well with earlier data.

Figure 49. FLN spectrum showing resolution of perylene from SRC-II

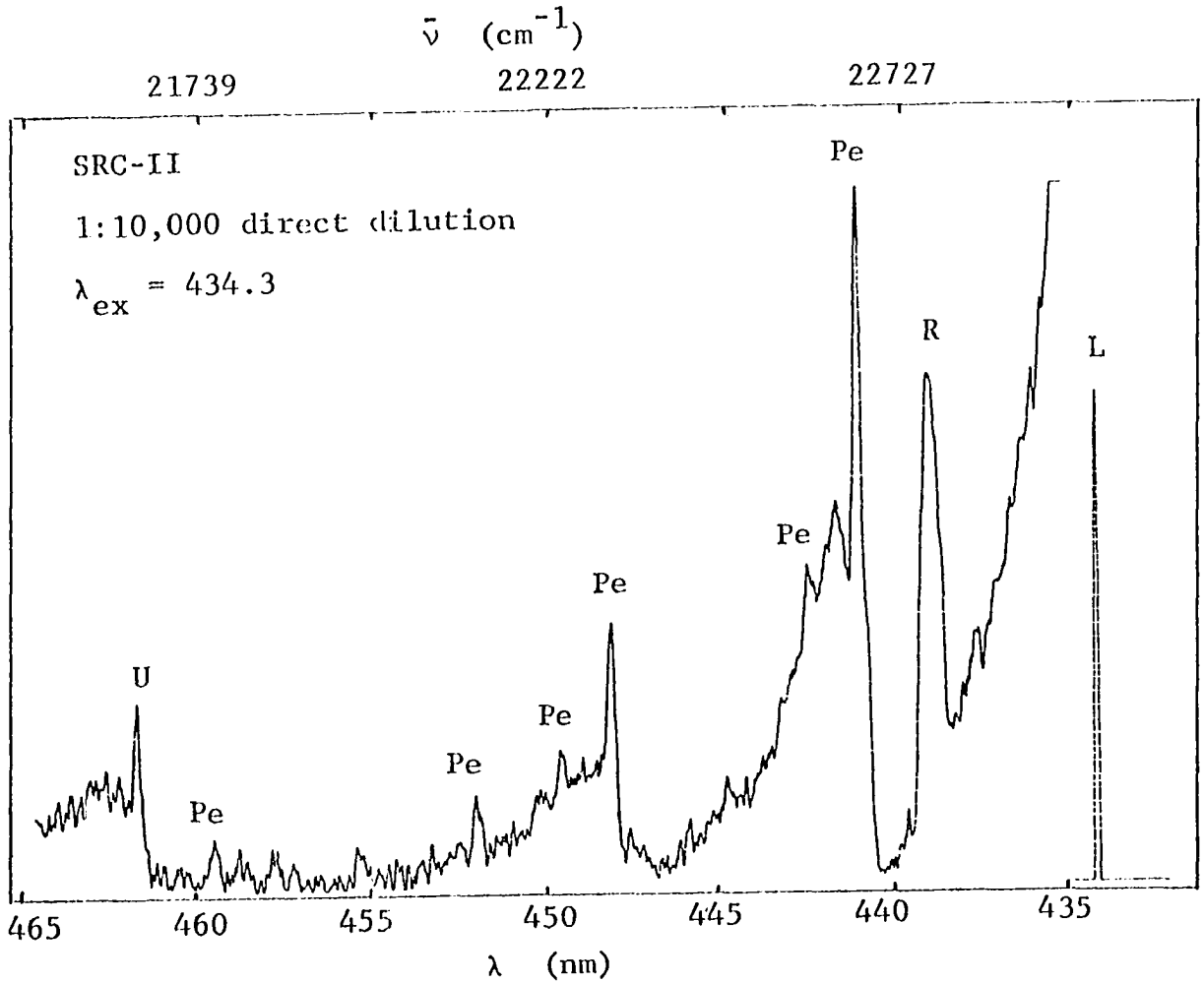
$\bar{\nu}$ (cm^{-1})
21739
22222
22727
SRC-II
1:10,000 direct dilution
λ_{ex} = 434.3
U
Pe
Pe
Pe
Pe
Pe
Pe
R
L
465
460
455
450
445
440
435
λ (nm)

Table 3. Summary of results for FLNS analysis of SRC-II. The values represent concentration in the undiluted SRC-II

Compound	Pyrene	1-Alkylpyrene	Benzo(e)pyrene
$1:10^4$ dilution	711 ppm	83.5 ppm	57 ppm
$1:10^5$ dilution	958 ppm	81.5 ppm	56 ppm
$1:5 \times 10^4$ dilution with 20% DMSO	780 ± 13%	---	56 ± 12%

Anthracene	Benzo(k)fluoranthene	Benzo(a)pyrene	Perylene
290 ppm	19.2 ppm	95 ppm	18.5 ppm
320 ppm	18.2 ppm	---	---
---	---	---	---

The summary presented in Table 3 illustrates several important points about the determination of PAHs in diluted SRC-II. While the spectra (Figures 46 through 49) demonstrate qualitative analysis with FLNS, this table supports the contention that FLNS is a valid quantitative technique for PAH analysis in a complicated natural sample. Note that in every case where multiple determinations were carried out, the concentrations determined agree quite well. The agreement between B(e)P analyses is particularly striking. Surprisingly, pyrene seems to give the worst numbers from SRC-II. The problem must not lie in detection of the signal since pyrene gives very nice signals.

Notice that with pyrene, the higher the dilution used, the higher the concentration determined. Also note that the pyrene concentration is very high in the SRC-II sample. The fact that FLNS will only detect dispersed PAH molecules suggests a logical explanation. The very high pyrene concentrations in the SRC-II oil may approach saturation.

At these high levels, pyrene may exist largely as aggregates or as some other sort of chemical complex. The analyte may also be associated with the surfaces of particulate inclusions within the SRC-II. These associations, formed in the neat oil, may persist through dilution into the glass. The higher the dilution, the greater the extent to which these associations would break up. Thus, in more dilute solutions, a higher fraction of the total pyrene would exist as the detectable free solvated molecules. This hypothesis would be interesting to investigate using such variations as a hydrocarbon glass and greater care to solvate the oily sample.

2. Pyrene in HPLC fractions

During the SRC-II analyses, Chriswell and Ogawa (85) supplied this investigator with the fractions from one HPLC run of the SRC-II sample. Some of these fractions were marked to indicate that they contained pyrene, benzo(e)pyrene, or benzo(a)pyrene. Preliminary investigations showed no B(e)P in the marked fractions. The spectra obtained for B(a)P in the fractions were similar though more intense than the one shown on the right side of Figure 48. Spectra from the pyrene fractions were also obtained and are included in Figures 50 and 51.

The fractions were labeled in order of their elution; H-1, H-2, etc. Only fractions H-10 and H-11 seemed to contain pyrene. The spectra are included here to illustrate several facts. First note that, as the chromatographers would have expected, no pyrene signal appears in H-9. Fraction H-10 contains a large amount of pyrene as does H-11. No pyrene signal at all could be seen in H-12.

The spectrum of H-10 shows nothing significant except pyrene. The H-11 fraction shows mostly pyrene peaks with at least one other contributing species marked U. Because the U origin region shown at the top of Figure 50 corresponds quite well with the 1-alkylpyrene origin, the spectrum in Figure 51 was taken. This spectrum shows that excitation at the 1-alkylpyrene ideal wavelength gives the 1-alkylpyrene analytical line at the predicted location. This indicates, as expected, that 1-alkylpyrene elutes after pyrene.

The bottom spectrum in Figure 50 is that of the H-9 fraction when excited with the 363.5 nm line for pyrene. Even with the 28 times

Figure 50. FLN spectra of pyrene HPLC fractions taken with the pyrene excitation wavelength

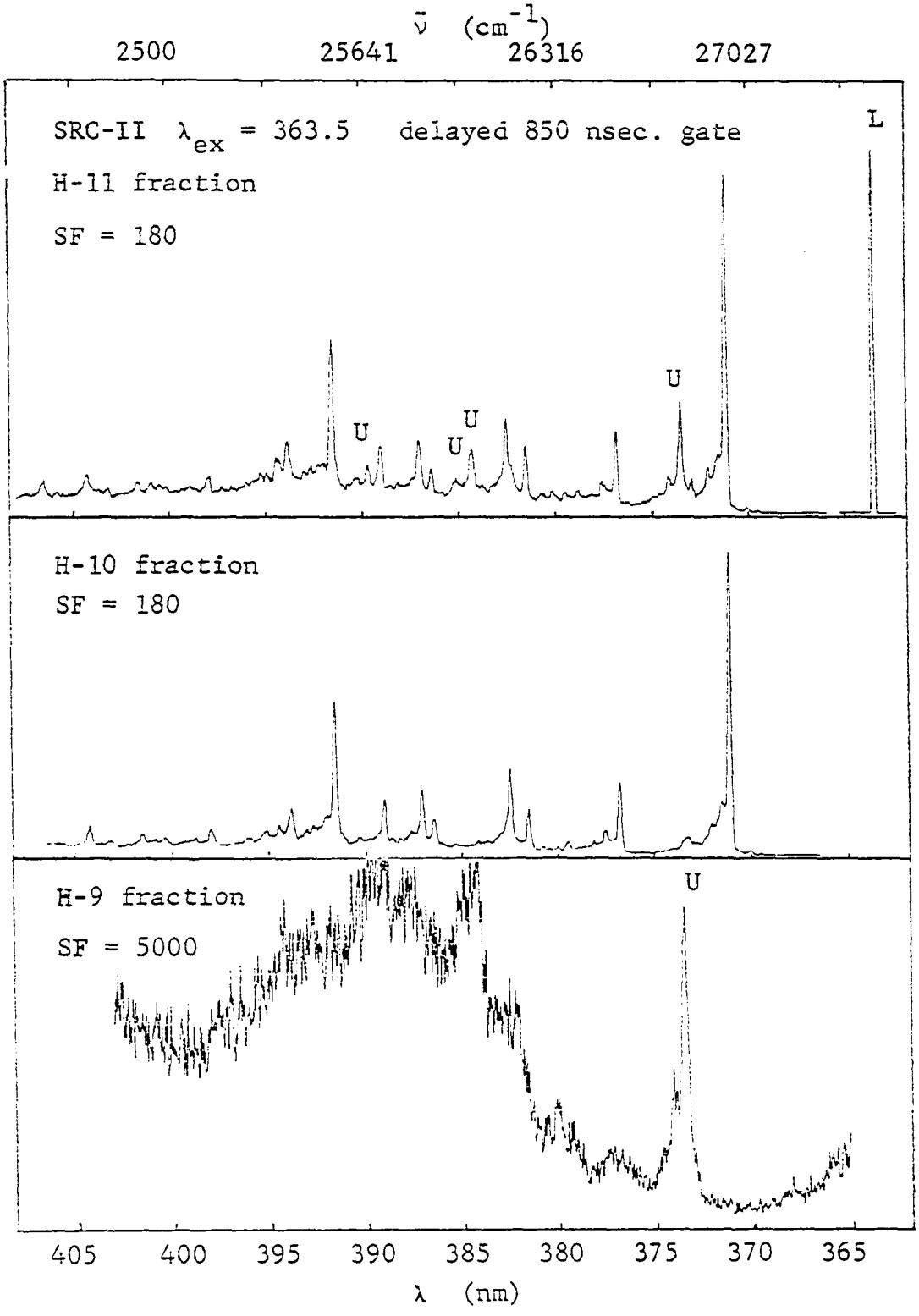
$\bar{\nu}$ (cm^{-1})
2500
25641
26316
27027
SRC-II λ_{ex} = 363.5 delayed 850 nsec. gate
H-11 fraction
SF = 180
L
U
U
U
U
H-10 fraction
SF = 180
H-9 fraction
SF = 5000
U
405
400
395
390
385
380
375
370
365
λ (nm)

Figure 51. FLN spectra of HPLC fraction taken using the 1-alkylpyrene excitation wavelength

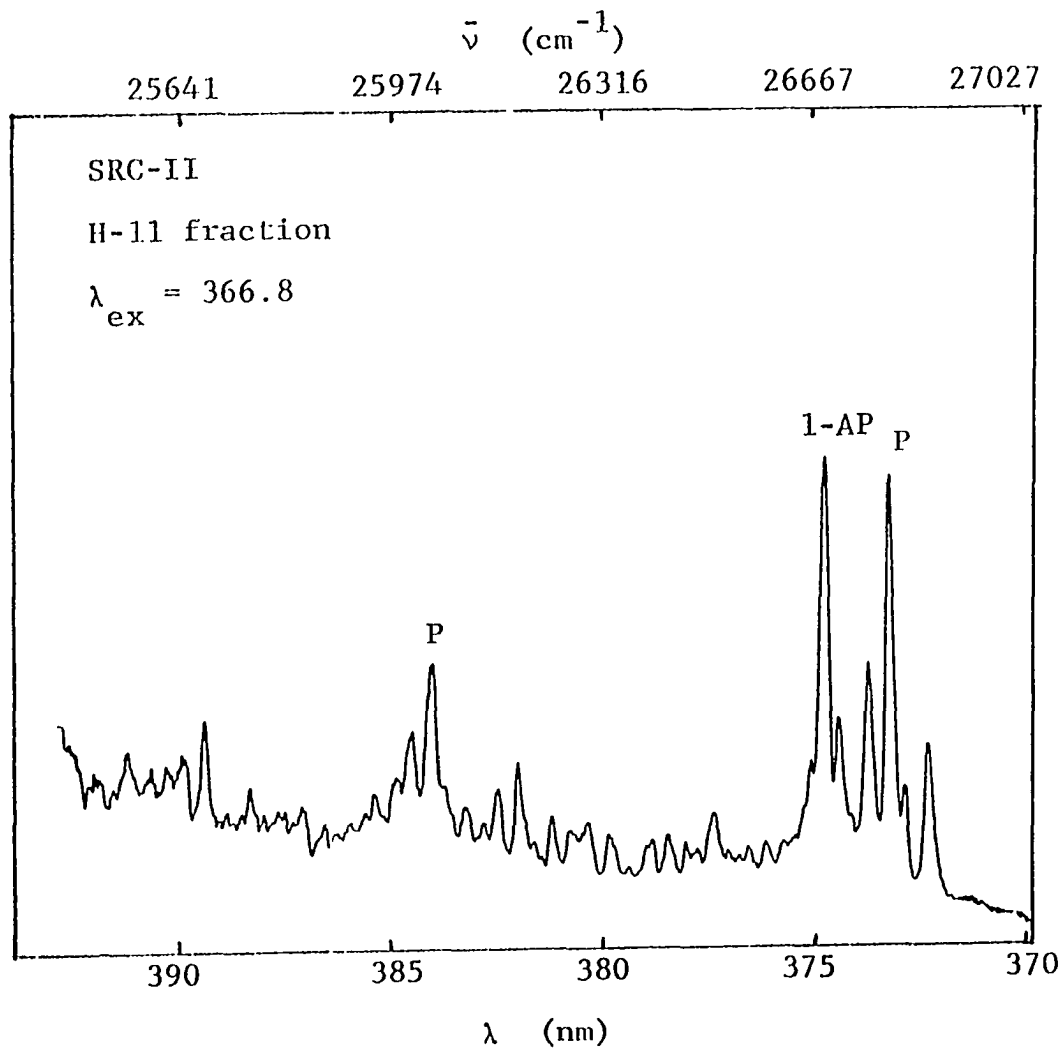
$\bar{\nu}$ (cm^{-1})
25641
25974
26316
26667
27027
SRC-II
H-11 fraction
λ_{ex} = 366.8
1-AP
P
P
390
385
380
375
370
λ (nm)

increase in sensitivity used, no pyrene fluorescence can be observed. However, this spectrum aptly illustrates one of the problems pointed out in the instrumentation section. Observation on an oscilloscope showed that the very intense signals from the H-9 fraction were short lived. Nearly all fluorescence signals had decayed before the opening of the gates to the integrator, yet a signal was obtained. This spectrum is due to the problem earlier referred to as leaky gates. The improvements in the gated integrators that have been suggested, vide supra, should eliminate this type of signal.

Concentrations of pyrene and benzo(a)pyrene in the fractions were determined using the previously described quantitation standards. By estimating the volumes of the fractions, total elution volume and injection volume, the concentrations of these two species were estimated in the SRC-II sample. The results of these calculations are included with the summary in Table 4. The B(a)P concentration thus determined was 179% higher than that determined from direct dilution. Also, the pyrene concentration determined was 551% higher than the direct dilution value. Speculations about the significance of this are included in the next section.

3. Comparison to other methods

The averaged results from Table 3 are compared to results when using other techniques to analyze SRC-II in Table 4. As was mentioned earlier, several other groups analyzed the SRC-II material. Chriswell and Ogawa (85) used HPLC with a modern variable excitation fluorescence

Table 4. Comparison of SRC-II analysis results

Investigator:	Chriswell (10,78)	Junk (8)	Junk (8)	Yang (38)	---	---	---
Technique: / Compound	HPLC	GC/MS	HPLC/ GC/MS	LESS	FLNS	HPLC/ FLNS	Average
Dibenzophenone	620	197 ± 90	2657	---	---	---	1160 ppm
Benzo(a)pyrene	130	84 ± 57	---	145	95	160	123 ppm
Benzo(e)pyrene	270	29 ± 5	---	126	56	---	120 ppm
Pyrene	4100	1031 ± 234	3926	4605	816	4500	3200 ppm
Carbazole	2440	239 ± 38	---	---	---	---	1300 ppm
Acridine	80	118 ± 87	---	---	---	---	99 ppm
Benzo(k)fluoranthene	---	---	---	77.5	18.2	---	48 ppm

detector. Greg Junk and his associates used capillary column GC/MS both for direct injection of the SRC-II and for analysis of HPLC fractions (8). Yang and Fassel (38) and Yang et al. (43) used laser excited Shpolskii spectroscopy as described earlier. FLNS results are included both from analysis of direct dilutions and HPLC fractions.

The data in Table 4 show a rather wide variation in the results of the various SRC-II analyses. The FLNS results agree most closely with the CC-GC/MS data. The similarity between the FLNS and GC/MS results extends to the analysis of the HPLC fractions for pyrene. Both techniques show more pyrene by a factor of about four in the HPLC fractions. HPLC, HPLC/GC/MS, and LESS are all consistently higher than the corresponding results for direct analysis using GC/MS or FLNS. Much more quantitative work remains to be done before much significance can be placed on any of these numbers.

VI. SPECULATION

A. Limits to Sensitivity

FLNS should be able to achieve ultra low detection limits. The one pptr detection limit projected in earlier sections would mean that the integrators would be measuring signals from about 10^5 molecules in the excitation region. The achievable factor of one hundred increase in signal levels projected by the instrumentation improvements section could lower this to about one thousand molecules in glass concentrations of .01 pptr or 10^{-11} g per liter.[31]

The ultimate achievable sensitivity limit will occur when the signal ZPL cannot be discriminated against optical and electrical noise. FLNS being a nondestructive technique, the background signal levels can be integrated to any desired precision. Thus, theoretically, any desired low detection limit can be achieved. The fluorescence from one molecule measured and integrated enough times will eventually show above noise in a well-designed experiment based on a nondestructive technique.

The conventional monochrometer with an exit slit and PMT detector rapidly places practicality limits on low signal detection. Considering

---

[31] For those who would demand, "Yes, but, what is the smallest amount of analyte that gives a response?", note that 10^{-11} g per liter corresponds to about three hundred attograms of analyte in the excitation region.

that the band pass through the exit slit is about 0.1 nm and that the region of interest, region II, is about 20 nm wide indicates that all but 0.5% of the desired signal is being wasted at any given time.

By buying or making a monochrometer which can be set to focus any 10 nm to 20 nm region of the uv-visible region onto a high density photosensitive array, the FLNS technique could be greatly improved. By imaging a 10 nm spectral region about the analytical ZPL onto a 1000 element linear photodiode array, the amount of signal measured in a given length of time could be increased by 100 times. This increased signal precision could be used to increase sensitivity for small signals or to decrease the analysis time. Using such a spectrometer for determining a series of species in a sample would simply require moving the spectral region to be analyzed along in front of the laser as it is brought to bear at the excitation wavelengths selected for each analyte.

B. Sampling

Development of and understanding of proper sampling techniques are just as important as developing the ultimate instrumentation. Consider, for example, PAHs in natural waters. Analysis for PAH materials in natural waters was given high priority consideration until the completion of the work reported herein. While the occurrence of PAH species in water may be very important (1), the solubility of these species in water is quite low (86). Thus, the question arises: in what form do PAH compounds occur in natural or polluted waters and

what effect does their physical and chemical form have on their detection by FLNS?

Polycyclic aromatic materials often occur in water samples at concentrations above saturation (1, 87). Besides dissolved PAH, such water samples must contain microcrystalline precipitates, PAH absorbed on organic and inorganic particulates (87), and PAH adsorbed to or dissolved in micelles (88). The cell walls of living and dead micro-organisms suspended in the water have been shown to have a powerful affinity for PAH species (87). Speculation that much of the excess PAH concentration may exist in association with micelles has lead to investigation of the effects of surfactant solutions on PAH fluorescence (88).

Any physical state other than dispersed isolated single molecules would probably prevent FLN from occurring. As already mentioned, microcrystals and aggregates do not contribute to FLN signals. PAH molecules adsorbed onto particulates may still be able to exhibit line narrowing if there are no molecules around capable of coupling strongly with their excited electronic states. Likewise, molecules of PAH existing inside micelles are probably also capable of exhibiting FLN. The absorption and fluorescence intensities of PAH species inside a micelle may well be quite different from those for PAH molecules in the bulk solution due to differences in effective solvent polarity (88).

To summarize, any sample likely to contain PAH materials as particulates needs to be carefully treated in preparation for FLNS

analysis. Simple extraction and solvation procedures need to be developed to insure that all of the PAH material in the glass is in the form of completely solvated isolated molecules. These adsorption and precipitation phenomena may account for the low pyrene concentrations determined by FLNS when compared to the results for LESS. It would be most instructive to undertake a series of experiments to see if a glass based on a better solvent gives higher values. Experiments using internal standards and standard additions with artificial mixtures made up similar to those used by Herbes (87) could test whether a given extraction and/or glass formulation technique was solvating adsorbed PAH species.

C. Some Variations

Fluorescence line narrowing spectroscopy is still a new technique for analytical chemists. As such, there can be no doubt but that there are many related avenues open for further research. Applications to other types of compounds and other types of samples could be many and varied. Many instrumentation variations present themselves, as does a wide variety of investigations utilizing FLNS, to study the occurrence and chemistry of low level environmental pollutants. Even such exciting ideas as utilization of two photon excitation in fluorescence line narrowing seem likely fertile research areas. To be frank, the author is fortunate to have been involved so early in the development of this new methodology.

VII. SUMMARY

This dissertation highlights the importance and need for a new powerful PAH analysis technique. Fluorescence line narrowing spectrometry from organic glasses has the potential to fulfill the requirements for an ideal PAH analysis method. In the Theory chapter, the reasons why FLNS should be highly selective are given and then demonstrated in the sections on analysis of both an artificial mixture and of the complex SRC-II samples. The high sensitivity, broad working range, and quantitative response of the technique are demonstrated in the Theory chapter and the section on SRC-II analysis. The simplicity of the instrumentation and the ease with which most of the data in this dissertation were taken demonstrate the practicality of the technique. By virtue of the fact that laser excited fluorescence does not consume the samples once they are incorporated into the glasses, FLNS offers great flexibility for maximizing selectivity and quantitative response.

VIII. LITERATURE CITED

1. Andelman, J. B.; Suess, M. J. Bull. Wld. Hlth. Org. 1970, 43, 479.

2. Lee, M. L.; Novotny, M.; Bartle, K. D. Anal. Chem. 1976, 48(2), 405.

3. Lee, M. L.; Novotny, M.; Bartle, K. D. Anal. Chem. 1976, 48(11), 1566.

4. Tokousbalides, P.; Hinton, E. R.; Dickinson, R. B.; Bilotta, P. V.; Wehry, E. L.; Mamontov, G. Anal. Chem. 1978, 50(8), 1189.

5. Hecht, S. S.; Bondinell, W. E.; Hoffman, D. J. Natl. Cancer Inst. 1974, 53, 1121.

6. Allen, R. E.; Vickroy, D. G. Sonderdruck aus: Beiträge zur Tobakforshung. 1976, 8(7), 430.

7. Lee, M. L.; Vassilaros, D. L.; White, C. M.; Novotny, M. Anal. Chem. 1979, 51(6), 768.

8. Junk, G. A. Ames Laboratory-USDOE, Ames, Iowa. Private communication.

9. Ryan, J. P. Ames Laboratory-USDOE, Ames, Iowa. Private communication.

10. Chriswell, C. D. Ames Laboratory-USDOE, Ames, Iowa. Private communication.

11. Das, B. S.; Thomas, G. H. Anal. Chem. 1978, 50(7), 967.

12. Wise, S. A.; Chesler, S. N.; Hertz, H. S.; Hilpert, L. R.; May, W. E. Anal. Chem. 1977, 49(14), 2306.

13. Brown, J. C.; Hayes, J. M.; Small, G. J. In "Lasers and Chemical Analysis", Hieftje, G. M.; Lytle, F. E.; Travis, J. C., Eds.; The Humana Press: Clifton, NJ, 1980.

14. Wehry, E. L., presented in part at the 32nd Annual Summer Symposium on Analytical Chemistry, Purdue, Indiana, June 1979.

15. Reddy, G. T.; Bourne, S.; Cunningham, P. T. Anal. Chem. 1979, 51(9), 1535.

16. King, D. S.; Stephenson, J. C. IEEE J. Quantum Electronics 1979, QE-15(19), 14D.

17. Birks, J. B. "Photophysics of Aromatic Molecules"; Wiley-Interscience: New York, 1970.

18. Herzberg, G. "Molecular Spectra and Molecular Structure, III. Electronic Spectra and Electronic Structure of Polyatomic Molecules"; Van Nostrand and Reinhold Co.: New York, 1966, Chapter II.

19. Brophy, J. H.; Rettner, C. T. Optics Letters 1979, 4(10), 337.

20. Klimcak, C. M.; Wessel, J. E. Anal. Chem. 1980, 52(8), 1233.

21. Mamantov, G.; Wehry, E. L.; Kemmerer, R. R.; Hinton, E. R. Anal. Chem. 1977, 49(1), 86.

22. Skoog, D. A.; West, D. M. "Fundamentals of Analytical Chemistry", 3rd ed.; Holt, Rinehart and Winston: New York, 1976; Chapter 24.

23. Richardson, J. H.; Ando, M. E. Anal. Chem. 1977, 49(7), 955.

24. Vo-Dinh, T. Anal. Chem. 1978, 50(3), 396.

25. Vo-Dinh, T.; Gammage, R. B. Anal. Chem. 1978, 50(14), 205.

26. Latz, H. W.; Ullman, A. H.; Winefordner, J. D. Anal. Chem. 1978, 50(14), 2148.

27. Wehry, E. L.; Mamantov, G. Anal. Chem. 1979, 51(6), 643A.

28. Stroupe, R. C.; Tokousbalides, P.; Dickinson, R. B.; Wehry, E. L.; Mamantov, G. Anal. Chem. 1977, 49(6), 701.

29. Dickinson, R. B.; Wehry, E. L. Anal. Chem. 1979, 51(6), 778.

30. Maple, J. R.; Wehry, E. L.; Mamantov, G. Anal. Chem. 1980, 52(6), 920.

31. Small, G. J. Ames Laboratory-USDOE and Iowa State University, Ames, Iowa. Private communications.

32. Burke, F. P.; Small, G. J. Chem. Phys. 1974, 5, 198.

33. Burke, F. P.; Small, G. J. J. Chem. Phys. 1974, 61, 4588.

34. Shpolskii, V. E.; Bolotnikova, T. N. Pure Appl. Chem. 1974, 37(1), 183.

35. Richards, J. L.; Rice, S. A. J. Chem. Phys. 1971, 54(5), 2014.

36. Personov, R. I.; Osad'ko, I. S.; Godyaev, E. D.; Al'shits, E. I. Soviet Physics Solid State 1972, 13(9), 2224.

37. Kirkbright, G. F.; DeLima, C. G. Analyst 1974, 99, 338.

38. Yang, Y.; Fassel, V. A. Thesis research, Iowa State University, Ames, Iowa, unpublished.

39. Colmsjö, A.; Stenberg, U. Anal. Chem. 1979, 51(1), 145.

40. D'Silva, A. P.; Ostreich, G.; Fassel, V. A. Anal. Chem. 1976, 48(6), 915.

41. Woo, C. S.; D'Silva, A. P.; Fassel, V. A. Anal. Chem. 1980, 52(1), 159.

42. Ostreich, G. Ph.D. Dissertation, Iowa State University, Ames, Iowa, 1979.

43. Yang, Y.; D'Silva, A. P.; Isles, M.; Fassel, V. A. Anal. Chem. 1980, 52(8), 1350.

44. Personov, R. I.; Al'shits, E. I.; Bykovskaya, L. A. Optics Commun. 1972, 6(2), 169.

45. Bykovskaya, L. A.; Personov, R. I.; Kharlamov, B. M. Chem. Phys. Letters 1974, 27(1), 80.

46. Brown, J. C.; Edelson, M. C.; Small, G. J. Anal. Chem. 1978, 50(9), 1394.

47. Brown, J. C.; Duncanson, J. A.; Small, G. J. Anal. Chem. 1980, 52(11), 1711.

48. Szabo, A. Phys. Rev. Letters 1970, 25(14), 924.

49. Eberly, J. H.; McColgin, W. C.; Kawaoka, K.; Marchett, A. P. Nature 1974, 251, 215.

50. Cunningham, K.; Morris, J. M.; Fünfshilling, J.; Williams, D. F. Chem. Phys. Letters 1975, 32(3), 581.

51. Fünfshilling, J.; Williams, D. F. Photochem. Photobiol. 1975, 22, 151.

52. Abram, I.; Auerbach, R. A.; Birge, R. R.; Kohler, B. E.; Stevenson, J. M. J. Chem. Phys. 1974, 61(9), 3857.

53. Marchetti, A. P.; McColgin, W. C.; Eberly, J. H. Phys. Rev. Letters 1975, 35(6), 387.

54. DeVries, H.; Wiersma, D. A. Phys. Rev. Letters 1976, 36(2), 91.

55. McColgin, W. C. Ph.D. Dissertation, The University of Rochester, Rochester, N.Y., 1975.

56. Kohler, B. E. In "Chemical and Biochemical Applications of Lasers"; More, C. B., Ed.; Academic Press: New York, 1979; Vol. IV, p. 30.

57. Personov, R. I.; Kharlamov, B. M. Optics Commun. 1973, 7(4), 417.

58. Abram, I. I.; Auerbach, R. A.; Birge, R. R.; Kohler, B. E.; Stevenson, J. M. J. Chem. Phys. 1975, 63(6), 2473.

59. Flatsher, G.; Friedrich, J. Chem. Phys. Letters 1977, 50(1), 32.

60. Pfister, C. Chem. Phys. 1973, 2, 171.

61. Pfister, C. Chem. Phys. 1973, 2, 181.

62. Martinand, M.; Kottis, Ph. J. Phys. Chem. 1978, 82(13), 1497.

63. Al'shits, E. I.; Personov, R. I.; Kharlamov, B. M. Chem. Phys. Letters 1971, 40(1), 116.

64. Al'shits, E. I.; Personov, R. I.; Kharlamov, B. M. JETP Lett. 1977, 26(11), 586.

65. Williamson, R. L.; Kwiram, A. L. J. Phys. Chem. 1979, 83(26), 3393.

66. Wright, J. C.; Gustafson, F. J. Anal. Chem. 1978, 50(12), 1147A.

67. Weber, M. J.; Paisner, J. A.; Sussman, S. S.; Yen, W. M.; Riseberg, L. A.; Brechev, C. J. Lumin. 1976, 12(13), 729.

68. Riseberg, L. A. Phys. Rev. A 1973, 7(3), 671.

69. Harris, J. M.; Lytle, F. E.; McCain, T. C. Anal. Chem. 1976, 48(14), 2095.

70. Isles, M. K. Ames Laboratory-USDOE, Ames, Iowa, private communication.

71. Edelson, M. Ames Laboratory-USDOE, Ames, Iowa, private communication.

72. Johnson, C. Ames Laboratory-USDOE, Ames, Iowa, unpublished research.

73. Lytle, F. E. Anal. Chem. 1974, 46(6), 545A.

74. Skank, H.; Flatten, J. Ames Laboratory Instrumentation Services Department, USDOE, Ames, Iowa, private communication.

75. Yariv, A. "Quantum Electronics"; John Wiley & Sons, Inc.; New York, 1975; Chapters 8 & 12.

76. Schäfer, F. P. In "Topics in Applied Physics, Vol. I, Dye Lasers"; Schäfer, F. P., Ed.; Springer-Verlag: New York, 1973, Chapter 1.

77. Duncanson, J. A.; McGlade, M. J. Ames Laboratory-USDOE, Ames, Iowa, unpublished research.

78. Chiang, Iris; McGlade, M. J. Ames Laboratory and Iowa State University, Ames, Iowa, unpublished research.

79. Stout, R. P. Ames Laboratory and Iowa State University, Ames, Iowa, unpublished research.

80. Berlman, Isadore B. "Handbook of Fluorescence Spectra of Aromatic Molecules"; Academic Press: New York, 1965.

81. Porro, T. J.; Anacreon, R. E.; Flandreau, P. S.; Fagerson, I. S. J. Ass. Off. Anal. Chem. 1973, 56(3), 607.

82. Bree, A.; Vilkos, V. V. B. Spectrochimica Acta 1971, 27A, 2333.

83. Bree, A. V.; Katagiri, S. J. Molec. Spectros. 1965, 17, 24.

84. Small, G. J. J. Chem. Phys. 1970, 52(2), 656.

85. Chriswell, C.; Ogawa, I. Ames Laboratory-USDOE, Ames, Iowa, 1979.

86. Davis, W.; Krahl, M.; Clowes, G. J. Am. Chem. Soc. 1942, 64, 108.

87. Herbes, S. E. Water Research, 1977, 11, 493.

88. Nakajima, A. Photochem. Photobiol. 1977, 25, 593.

IX. ACKNOWLEDGEMENTS

This work was supported by the Assistant Secretary for Environment, Office of Health and Environmental Research, without whose gracious monitary support this work would not have been possible (contract No. W-7405-Eng-82).

Many of my colleagues within the Ames Laboratory and Iowa State University made invaluable contributions to this work. Nothing of value could have been accomplished without the aid given by the many professionals on both the Ames Lab and ISU support staffs. Except for the special guidance offered by Professor Gerald J. Small and many of the other members of his and Professor Edward S. Yeung's research groups, I consider it impossible to begin offering specific acknowledgements other than those already in the text. To be just, such an effort would significantly lengthen this already oversize document.

X. APPENDIX. FLNS SOFTWARE: EXPERIMENTAL CONTROL AND DATA ACQUISITION

```
MLFS:    .CSECT
;;&&&&&&&&&&&&&&&&&&&&&&&&&&&&&&&&&&&&&&&&&&&&&&&&&&&&&&&&&&&&&&&&&&&
;; MOLECTRON EVANS BOX GATED FLUORESCENCE ROUTINE, ALLOWS DISPLAY
;; OF SIGNAL ONLY, REFERENCE ONLY, OR NORMALIZED SPECTRA.  DATA
;; MAY BE DISPLAYED DIRECTLY OR AFTER A FIVE POINT OR 15 POINT
;; MEDIAN WEIGHTED BAD POINT REJECTING SMOOTH AND ANY SIZE AVERAGE.
;; ONLY SINGLE POINT ACCUMULATION AT THE EVANS BOX IS ALLOWED.
;;&&&&&&&&&&&&&&&&&&&&&&&&&&&&&&&&&&&&&&&&&&&&&&&&&&&&&&&&&&&&&&&&&&&
;;  BOX GATE TRIGGER  . . . . . . . = CSR0 OF PAPER-TAPE INTERFACE
;;  LASER TRIGGER . . . . . . . . . = CSR1 OF PAPER-TAPE INTERFACE
;;  EVANS BOX RESET TRIGGER . . . . = CSR0 OF STEPPING MOTOR INTERFACE
;;  SIGNAL ANALOG INPUT . . . . . . = ADC0
;;  REFERENCE ANALOG INPUT  . . . . = ADC1
;;  REAL-TIME OUTPUT TO STRIPCHART= DAC1
;;&&&&&&&&&&&&&&&&&&&&&&&&&&&&&&&&&&&&&&&&&&&&&&&&&&&&&&&&&&&&&&&&&&&
;;

          R0=%0   ;GENERAL REGISTER DEFINITION
          R1=%1
          R2=%2
          R3=%3
          R4=%4
          R5=%5
          R6=%6
          R7=%7
          SP=R6
          PC=R7
          SWR=177570
          PS=177776
         $CONSL
TKS=177560        ;CONSOLE KEYBOARD STATUS
TKB=177562        ;CONSOLE KEYBOARD BUFFER
TPS=177564        ;CONSOLE PRINTER STATUS
TPB=177566        ;CONSOLE PRINTER BUFFER
TKIAD=60          ;VECTOR ADDRESS OF CONSOLE KEYBOARD INTERRUPT
TPIAD=64          ;VECTOR ADDRESS OF CONSOLE PRINTER INTERRUPT
```

```
37 =            ADCSR=176770            ; ANALOG TO DIGITAL CONVERTER STATUS REGISTER
38 =            ADCDT=176772            ; ADC DATA BUFFER
39 =            ADCINT=130              ; ADC INTERUPT VECTOR
40 =            ADCIS=132               ; ADC INTERUPT HANDLER PS WORD
41 =            LTCI=100                ; LINE TIME CLOCK INTERUPT VECTOR
42 =            LTCIS=102
43 =            DAC1=176760             ; DIGITAL TO ANALOG CONVERTER # 1
44 =            SEC=72
45 =            V=126
46 =            CC=003                  ; CONTROL C
47 =            KWCSR=172540            ; CLOCK STATUS REGISTER
48 =            KWPB=172542             ; CLOCK PRESET BUFFER
49 =            KWCT=172544             ; CLOCK COUNTER
50 =            KWINT=104               ; CLOCK INTERUPT VECTOR
51 =            KWINS=106               ; INTERUPT STATUS
52 =            DAC2=176762             ; DIGITAL TO ANALOG CONVERTER # 2
53 =            RDAT=300
54 =            AT=100
55 =            NUL=000
56 =            N=116
57 =            G=107
58 =            Y=131
59    ;
60 =            STOP=174
61 =            CR=015
62 =            LF=012
63 =            SPC=040
64 =            MINUS=055
65 =            BELL=007
66 =            PLUS=053
67 =            TIMES=130
68 =            DIVIDE=057
69 =            EQUAL=075
70 =            PT4=23420               ; POWERS OF TEN FOR GETDICIMAL ROUTINE
71 =            PT3=1750
72 =            PT2=144
73 =            PT1=12
```

```
=               PT0=1
        ;;
        ;;&&&&&&&&&&&&&&&&&&&&&&&&&&&&&&&&&&&&&&&&&&&&&&&&&&&&&&&&&&&&&&&&&&&&&
        ;; MAIN CONTROLING SECTION OF THE PROGRAM
        ;;&&&&&&&&&&&&&&&&&&&&&&&&&&&&&&&&&&&&&&&&&&&&&&&&&&&&&&&&&&&&&&&&&&&&&
        ;;
                CLR     INITMSG         ; INITIALIZE FOR INTRO MESSAGE
        BGNG:   MOV     #1000,SP        ; INITIALIZE PROCESSOR STACK
                MOV     #EVH,@#LTCI     ; INITIALIZE LINE TIME CLOCK VECTOR
                CLR     @#LTCIS
                MOV     #CLKIH,@#KWINT  ; INITIALIZE REAL TIME CLOCK VECTOR
                CLR     @#KWINS         ; ALLOW FOR OTHER INTERUPTS
                MOV     #7611,@#KWPB    ; SET PRESET BUFFER FOR 25.1 HERTZ
                MOV     #110,@#KWCSR    ; INIT. FOR REPEATED INT COUNT DOWN
                MOV     #-1,FCR         ; SET FOR NOT FIRING
                MOV     #3,HZ           ; SET FOR 3 60THS OR 20 Hz
                MOV     #1,BLUBL        ; INITIALIZE BELL FOR BELL
                MOV     HZ,EVCTR        ; INITIALIZE EVENT COUNTER
                CLR     DM              ; SET FOR DISPLAY MODE ZERO
                CLR     SM              ; SET FOR SMOOTHING MODE ZERO
                MOV     #1,SF           ; SET INITIAL SCALING FACTOR TO ONE
                MOV     #-1,NOISY       ; INITIALIZE FOR NOISY DATA SMOOTH
                MOV     SF,ITOF         ; FLOAT NEW SCALING FACTOR
                JSR     PC,NFLOAT
                MOV     HP,SFHP         ; SAVE FLOATED SCALING FACTOR
                MOV     LP,SFLP
                JSR     PC,COEFNT       ; CALCULATE SMOOTHING COEFFICIENTS
                JSR     PC,TOFS         ; TAKE INITIAL OFFSET
                TST     INITMSG         ; SHOULD FIRST TIME MSG BE PRINTED?
                BNE     SKPMSG          ; NO, SKIP MESSAGE.
                INC     INITMSG         ; SET SO MESSAGE WON'T PRINT AGAIN.
                MOV     #MSG1,R3        ; POINT TO HEADING MESSAGE
                JSR     PC,PNEXT        ; PRINT HEADING MESSAGE
        SKPMSG: MOV     #47600,FSO      ; INITIALIZE ORDERED FLOATING POINT STACK
                MOV     #35000,PADB     ; INITIALIZE SCRATCH PAD POINTER
        ;;
                MOV     #50000,FS       ; INITIALIZE BEGINNING OF STACK POINTER
```

```
111   L1:     JSR     PC,TCHR         ; WAIT FOR NEXT CHARACTER OR INTERUPT
112           CMP     SP,#1000        ; HALT IF THE PROGRAM IS MESSING UP
113           BEQ     T
114           HALT
115   T:      JSR     PC,PKL          ; ECHO ANY CHARACTER
116           CMP     #NUL,R0         ; IS CHARACTER A NULL ?
117           BNE     A               ; NO, CHECK FOR OTHERS
118           JSR     PC,CRLF         ; YES, ACKNOWLEGE RECIEPT OF CONTROL
119           MOV     #MSG2,R3
120           JSR     PC,PNEXT
121           JSR     PC,GTDCML       ; TAKE NEW DISPLAY MODE
122           MOV     R1,DM           ; SAVE NEW DISPLAY MODE
123           JSR     PC,CRLF         ; ACKNOWLEGE END OF CONTROL COMMAND
124           BR      L1
125   A:      CMP     #CC,R0          ; IS CHARACTER A CONTROL C ?
126           BNE     B               ; NO, CHECK FOR OTHERS
127           MOV     #50000,FS       ; REINITIALIZE SEQUENTIAL STACK POINTER
128           JSR     PC,CRLF         ; YES, ACKNOWLEGE CONTROL CHARACTER
129           MOV     #MSG3,R3
130           JSR     PC,PNEXT
131           JSR     PC,GTDCML       ; TAKE NEW SMOOTHING MODE
132           MOV     R1,SM           ; SAVE NEW SMOOTHING MODE
133           JSR     PC,CRLF         ; ACKNOWLEGE END OF CONTROL SEQUENCE
134           BR      L1
135   B:      CMP     #AT,R0          ; IS CHARACTER AN AT SIGN ?
136           BNE     C               ; NO, RETURN
137           JSR     PC,CRLF         ; ACKNOWLEGE RECIEPT OF CONTROL CHARACTER
138           MOV     #MSG4,R3
139           JSR     PC,PNEXT
140           JSR     PC,GTDCML       ; TAKE NEW SCALING FACTOR
141           MOV     R1,SF           ; SAVE SCALING FACTOR
142           MOV     R1,ITOF         ; FLOAT SCALING FACTOR
143           JSR     PC,NFLOAT
144           MOV     HP,SFHP         ; SAVE SCALING FACTOR IN FLOATING
145           MOV     LP,SFLP         ; POINT.
146           JSR     PC,CRLF         ; SHOW END OF CONTROL
147           JMP     L1
```

```
148   C:      CMP     #BELL,R0        ; IS CHARACTER A BELL ?
149           BNE     E               ; NO, CHECK FOR NEXT CONTROL CHARACTERS
150           NEG     BLNBL           ; YES, CHANGE STATE IN BLNBL FLAG
151           JSR     PC,CRLF         ; ACKNOWLEDGE RECIEPT OF CONTROL
152           JMP     L1              ; RETURN FOR NEXT CHARACTER
153   E:      CMP     #N,R0           ; IS CHARACTER AN N ?
154           BNE     F               ; IF NOT, GO ON
155           NEG     NOISY           ; YES, CHANGE STATE OF NOISY FLAG
156           BLT     MEC             ; IF NOW NOT SET, RETURN
157           MOV     #NMSG,R3        ; IF SET, PREPARE TO PRINT MESSAGE
158           JSR     PC,PNEXT        ; ASK FOR NUMBER OF POINTS TO AVERAGE
159           JSR     PC,GTDCML       ; TAKE NUMBER OF POINTS IN DECIMAL
160           MOV     R1,NPTA         ; SAVE NUMBER OF POINTS TO AVERAGE
161           MOV     #20000,R0       ; POINT TO TOP OF STACK
162           MOV     R0,NDISPS       ; REINITIALIZE STACK POINTER
163           ASL     R1              ; MULTIPLY NPTA BY 2 AND
164           ASL     R1              ; BY 2 AGAIN TO GET SIZE OF BUFFER NEEDED
165           SUB     R1,R0           ; CALCULATE END OF BUFFER
166           MOV     R0,NDISPE       ; SAVE NEW END OF BUFFER
167           MOV     NPTA,ITOF       ; PREPARE TO FLOAT NPTA
168           JSR     PC,NFLOAT       ; FLOAT NUMBER OF POINTS TO AVERAGE
169           MOV     HP,NPTAHP       ; SAVE FLOATED NPTA
170           MOV     LP,NPTALP
171   MEC:    JSR     PC,CRLF         ; ACKNOWLEDGE END OF CONTROL
172           JMP     L1              ; RETURN FOR NEXT CHARACTER
173   F:      CMP     #G,R0           ; IS CHARACTER A  G ?
174           BNE     H               ; NO, GO ON.
175           MOV     #MSG5,R3        ; POINT TO REINIT MSG.
176           JSR     PC,PNEXT        ; PRINT REINITILIZATION MESSAGE.
177           JMP     BGNG            ; REINITIALIZE PROGRAM.
178   H:      CMP     #PLUS,R0        ; IS CHARACTER A PLUS SIGN ?
179           BNE     J               ; IF NOT RETURN
180           JSR     PC,CRLF         ; IF SO, ACKNOWLEDGE RECEIPT OF CONTROL CHR
181           MOV     #MSG6,R3        ; PREPARE TO PRINT
182           JSR     PC,PNEXT        ; PRINT MESSAGE
183           JSR     PC,GTDCML       ; TAKE NEW VOLTAGE OFFSET
184           MOV     R1,VOFS         ; SAVE NEW VOLTAGE OFFSET
```

```
                JSR     PC,CRLF          ; ACKNOWLEGE END OF CONTROL
                JMP     L1               ; RETURN FOR NEXT CHARACTER
J:              CMP     #DIVIDE,R0       ; IS CHARACTER A SLASH ?
                BNE     K                ; IF NOT, GO ON.
                JSR     PC,CRLF          ; ACKNOWLEDGE RECEIPT OF CONTROL CHR.
                NEG     FCR              ; IF SO, NEGATE FIRE CONTROL ?
                BLT     JC               ; IF FCR IS NOW NEG STOP INTERRUPTS.
                MOV     #7611,@#KWPB     ; MAKE SURE PRESET IS SET FOR 25.1 HZ
                MOV     #111,@#KWCSR     ; START THE CLOCK INTERUPTS
                BR      K                ; AND RETURN
JC:             MOV     #110,@#KWCSR     ; STOP THE CLOCK
K:              JMP     L1               ; RETURN FOR NEXT CHARACTER.
BLNBL:          .WORD   1                ; WORD FOR BELL-NO-BELL STORAGE
NOISY:          .WORD   -1               ; NOISY FLAG
FCR:            .WORD   1                ; LASER FIRING STATUS WORD
;;
;;&&&&&&&&&&&&&&&&&&&&&&&&&&&&&&&&&&&&&&&&&&&&&&&&&&&&&&&&&&&&&&&&&&&&&&
;; EVENT LINE INTERUPT HANDLER ROUTINE;  FIRES LASER AT
;;  25 HZ AND TAKES AND DISPLAYS DATA EACH TIME THE LASER FIRES
;;&&&&&&&&&&&&&&&&&&&&&&&&&&&&&&&&&&&&&&&&&&&&&&&&&&&&&&&&&&&&&&&&&&&&&&
;;
EVH:            INC     EVCTR            ; INCREMENT EVENT COUNTER
                RTI                      ; LTC INTERUPTS ONLY SET STATUS
CLKIH:          TST     EVCTR            ; IS LASER IN STATUS TO FIRE ?
                BNE     FIRE             ; IF SO GO ON TO FIRE EXPERIMENT.
                RTI                      ; IF NOT JUST RETURN UNTIL LTC SET TO ON
FIRE:           CLR     EVCTR            ; CLEAR STATUS AND FIRE EXPERIMENT
                JSR     PC,RESET         ; RESET THE BOX
                JSR     PC,TOFS          ; TAKE OFFSETS
                BIS     #3,@#177550      ; FIRE THE LASER AND BOX
                BIC     #3,@#177550
                TST     SM               ; CHECK SMOOTHING MODE.
                BMI     EA               ; IF NEGATIVE DO FIVPS
                BEQ     EB               ; IF 0 DO NOT SMOOTH
                JSR     PC,ONESEC        ; IF POSITIVE DO FIFTEEN  POINT SMOOTH
                BR      EC               ; RESTORE RETURN
EA:             JSR     PC,FIVPS         ; DO FIVE POINT SMOOTH
```

```
222             BR      EC                      ; RESTORE RETURN
223     EB:     JSR     PC,ONEPS                ; TAKE SINGLE POINT
224             TST     RERROR                  ; WAS REFERENCE A ZERO IN NORMALIZED MODE ?
225             BNE     EC                      ; IF SO DO NOT DISPLAY
226             JSR     PC,DISPLY               ; DISPLAY POINT WITHOUT SMOOTHING
227     EC:     JSR     PC,RESET
228             CLR     RERROR                  ; CLEAR ERROR IN REFERENCE FLAG
229     ER:     RTI                             ; RETURN TO COMMAND MONITOR
230     ;;
231     ;;&&&&&&&&&&&&&&&&&&&&&&&&&&&&&&&&&&&&&&&&&&&&&&&&&&&&&&&&&&&&&&&&&&&&&&&
232     ;;   S U B R O U T I N E S     F O R     M L F S
233     ;;&&&&&&&&&&&&&&&&&&&&&&&&&&&&&&&&&&&&&&&&&&&&&&&&&&&&&&&&&&&&&&&&&&&&&&&
234     ;;
235     ;; TPT, TAKE POINT, A SUBROUTINE TO TAKE A POINT FROM AN ADC CHANEL
236     ;; POINTED TO BY THE INSTRUCTION STORED AT WADC.  THE CONVERSION
237     ;; IS STORED AT HPA AND LPA
238     ;;
239     TPOINT:     $SAVE
240                 MOV     R5,-(SP)    ;SAVE REGISTERS R5-R0 ON THE STACK
241                 MOV     R4,-(SP)
242                 MOV     R3,-(SP)
243                 MOV     R2,-(SP)
244                 MOV     R1,-(SP)
245                 MOV     R0,-(SP)
246                 CLR     R0                  ; CLEAR INITIAL # STORAGE
247     TPTL1:      MOV     WADC,@#ADCSR        ; START CONVERSION
248     TPTL2:      TSTB    @#ADCSR             ; IS CONVERSION COMPLETE
249                 BPL     TPTL2               ; NO, KEEP LOOKING
250                 MOV     @#ADCDT,R3          ; YES, READ VALUE
251                 SUB     R3,R0               ; FIND DIFFERENCE
252                 BGE     TPTC                ; IF POSITIVE PROCEED WITH TEST
253                 NEG     R0                  ; IF NEGATIVE NEGATE DIFFERENCE
254     TPTC:       CMP     R0,#2               ; IS DIFF > 2 ?
255                 BLE     TPTC1               ; NO, CONTINUE
256                 MOV     R3,R0               ; YES, SAVE LAST CONVERSION AND
257                 BR      TPTL1               ; GET ANOTHER POINT
258     TPTC1:      MOV     #1,R5               ; TAKE AVERAGE OF NEXT 8 POINTS
```

```
TPTL3:   MOV     WADC,@#ADCSR
TPTL4:   TSTB    @#ADCSR
         BPL     TPTL4
         ADD     @#ADCDT,R3
         INC     R5
         CMP     R5,#10
         BLT     TPTL3
         MOV     R3,ITOF
         JSR     PC,NFLOAT
         MOV     HP,HPA
         MOV     LP,LPA
         MOV     HP8,HPB             ; DIVIDE BY 8
         MOV     LP8,LPB
         MOV     #HPB,R5
         FDIV    R5
         $RESTORE
          MOV    (SP)+,R0      ;RESTORE REGISTERS R0-R5 FROM THE STACK
          MOV    (SP)+,R1
          MOV    (SP)+,R2
          MOV    (SP)+,R3
          MOV    (SP)+,R4
          MOV    (SP)+,R5
         RTS     PC                  ; RETURN
;;
;;&&&&&&&&&&&&&&&&&&&&&&&&&&&&&&&&&&&&&&&&&&&&&&&&&&&&&&&&&&&&&&&&&&&
;;
;; OFFSET TAKING SUBROUTINE, FIRES ONLY EVANS BOX THROUGH CSR0
;; OF THE TAPE READER INTERFACE, AND STORES THE OFFSETS
;;
TOFS:    BIS     #1,@#177550         ; FIRE THE EVANS BOX
         BIC     #1,@#177550
         MOV     #401,WADC           ; SET TO CONVERT REFERENCE CHANEL
         JSR     PC,TPOINT           ; TAKE REFERENCE OFFSET
         MOV     HPA,ROFHP           ; SAVE REFFERENCE OFFSET
         MOV     LPA,ROFLP
         MOV     #1,WADC             ; SET FOR CHANEL ZERO
         JSR     PC,TPOINT           ; TAKE SIGNAL CHANEL OFFSET
```

```
                MOV     HPA,SOFHP           ; SAVE NEW SIGNAL OFFSET
                MOV     LPA,SOFLP
                JSR     PC,RESET            ; RESET THE EVANS INTEGRATORS
                RTS     PC                  ; RETURN TO CALLING ROUTINE
;;
;;&&&&&&&&&&&&&&&&&&&&&&&&&&&&&&&&&&&&&&&&&&&&&&&&&&&&&&&&
;;
;; ONE POINT SMOOTH,  SINGLE OUTPUT POINT PASSING PROGRAM
;; RETURNS UNSCALED NORMALIZED (AS SPECIFIED BY DM) VALUE
;; BACK TO CALLING PROGRAM IN FLOATING POINT STACK LOCATION 1
;;
ONEPS:          $SAVE
                 MOV    R5,-(SP)        ;SAVE REGISTERS R5-R0 ON THE STACK
                 MOV    R4,-(SP)
                 MOV    R3,-(SP)
                 MOV    R2,-(SP)
                 MOV    R1,-(SP)
                 MOV    R0,-(SP)
                MOV     #401,WADC           ; CONVERT ON REFERENCE CHANEL
                JSR     PC,TPOINT           ; READ VALUE OF REFERENCE CHANEL
                MOV     ROFHP,HPB           ; RECALL REFERENCE OFFSET
                MOV     ROFLP,LPB
                MOV     #HPB,R5
                FSUB    R5                  ; REF - REF OFFSET
                TST     DM                  ; TEST DISPLAY MODE
                BNE     OPSA                ; BRANCH IF MODE NOT ZERO
                MOV     #C1,R0              ; IF ZERO
                MOV     (R0)+,HP2           ; MOVE ONE INTO REFERENCE
                MOV     (R0),LP2            ; REGISTER
                BR      OPSD                ; AND GO ON TO TAKE SIGNAL CHANEL
OPSA:           BGT     OPSB                ; IF DM NOT NEG IT IS POSITIVE
                MOV     HPA,HP1             ; IF NEG RETURN ONLY REFERENCE CHANEL
                MOV     LPA,LP1
                BR      OPSR1
OPSB:           CMP     HPA,C12             ; IS IT A GOOD SHOT FOR NORMALIZATION ?
                BPL     OPSC                ; YES, GO ON TO NORMALIZE
                INC     RERROR              ; IF NOT, SET ERROR FLAG
```

```
            TST     BLNBL             ; SHOULD I RING THE BELL ?
            BMI     OPSR1             ; IF NOT I WON'T
            MOV     #BELL,R0
            JSR     PC,PKL            ; RING BELL TO INDICATE MISFIRE
            BR      OPSR1             ; AND BRANCH OUT
OPSC:       MOV     HPA,HP2           ; MOVE REFERENCE INTO PLACE FOR DIVIDE
            MOV     LPA,LP2
OPSD:       MOV     #1,HADC           ; POINT ADC TO SIGNAL CHANEL
            JSR     PC,TPOINT         ; TAKE SIGNAL READING
            MOV     SOFHP,HPB         ; MOVE SIG OFFSET IN FOR SUBTRACT
            MOV     SOFLP,LPB
            MOV     #HPB,R5
            FSUB    R5                ; SIGNAL - SIGNAL OFFSET
            MOV     HPA,HP1
            MOV     LPA,LP1
            MOV     #HP2,R5
            FDIV    R5                ; SIGNAL DIVIDED BY REFERENCE IN ONE
OPSR1:      JSR     PC,RESET          ; RESET BOX
OPSR:       $RESTORE
             MOV    (SP)+,R0      ;RESTORE REGISTERS R0-R5 FROM THE STACK
             MOV    (SP)+,R1
             MOV    (SP)+,R2
             MOV    (SP)+,R3
             MOV    (SP)+,R4
             MOV    (SP)+,R5
            RTS     PC
;;
;;&&&&&&&&&&&&&&&&&&&&&&&&&&&&&&&&&&&&&&&&&&&&&&&&&&&&&&&&&&&&&&&&&&&
;;
;; FIVE POINT SMOOTH, USES STACKS AT 50000, AND 47700
;; KEEPS A CONSTANTLY UPDATED INCOMMING DATA STACK
;; AND PRODUCES AN ORDERED STACK FROM WHICH A
;; -3,12,17,12,-3  SMOOTH IS DONE EACH TIME THE
;; LASER FIRES
;;
FIVPS:      $SAVE
             MOV    R5,-(SP)      ;SAVE REGISTERS R5-R0 ON THE STACK
```

```
370             MOV     R4,-(SP)
371             MOV     R3,-(SP)
372             MOV     R2,-(SP)
373             MOV     R1,-(SP)
374             MOV     R0,-(SP)
375             JSR     PC,ONEPS        ; TAKE NEXT POINT
376             TST     RERROR          ; TEST ERROR FLAG
377             BNE     FVPR            ; IF SET BRANCH OUT
378             MOV     FS,R0           ; IF NOT POINT TO INCOMMING DATA STACK
379             MOV     LP1,-(R0)       ; SAVE NEW POINT ON INCOMMING
380             MOV     HP1,-(R0)       ; POINT STACK
381             MOV     R0,FS           ; SAVE UPDATED POINTER
382             CMP     R0,#47754       ; IS INPUT STACK FULL ?
383             BGT     FVPR            ; IF NOT BRANCH TO RETURN
384             MOV     #47754,FLPORE   ; POINT TO END OF INCOMMING DATA BUFFER
385             MOV     #50000,FLPORB   ; POINT TO BEGINNING OF BUFFER
386             MOV     #47554,FSOE     ; POINT TO END OF ORDERED BUFFER
387             JSR     PC,FLPOR        ; MAKE FLTING POINT ORDERED STACK AT FSO
388             MOV     FSO,R0          ; POINT TO BEGINNING OF ORDERED STACK
389             MOV     -(R0),LP1
390             MOV     -(R0),HP1
391             MOV     #CM3,R1
392             MOV     (R1)+,HP2
393             MOV     (R1)+,LP2
394             MOV     #HP2,R5
395             FMUL    R5              ; P1 TIMES -3
396 FVPL1:      MOV     -(R0),LP2
397             MOV     -(R0),HP2
398             MOV     (R1)+,HP3
399             MOV     (R1)+,LP3
400             MOV     #HP3,R5
401             FMUL    R5              ; P2 TIMES C
402             FADD    R5              ; ACCUMULATE
403             CMP     R1,#C35         ; END OF COEFFICIENT LIST ?
404             BLT     FVPL1           ; NO, KEEP ACCUMULATING
405             MOV     (R1)+,HP2
406             MOV     (R1),LP2
```

```
407             MOV      #HP2,R5
408             FDIV     R5                  ; SUM DIVIDED BY 35
409             JSR      PC,DISPLY           ; DISPLAY SMOOTHED NUMBER
410             MOV      #50000,FLPORB
411             MOV      #47754,FLPORE
412             JSR      PC,MVDNST           ; MOVE DOWN STACK FOR NEXT POINT
413   FVPR:     CLR      RERROR              ; CLEAR ERROR FLAG
414             $RESTORE
415              MOV     (SP)+,R0     ;RESTORE REGISTERS R0-R5 FROM THE STACK
416              MOV     (SP)+,R1
417              MOV     (SP)+,R2
418              MOV     (SP)+,R3
419              MOV     (SP)+,R4
420              MOV     (SP)+,R5
421             RTS      PC
422   ;;
423   ;;EEEEEEEEEEEEEEEEEEEEEEEEEEEEEEEEEEEEEEEEEEEEEEEEEEEEEEEEEEEEEEEEEEEEEEEEEEEEE
424   ;;
425   ;; ONESEC, 0.6 SECOND TIME CONSTANT ON OUTPUT
426   ;; DOES A 1/930 * ( 0, 0, -5, -30, 50, 100, 200,
427   ;;  300, ..... ) 15 POINT MEDIAN WEIGHTED AVERAGE
428   ;; TYPE SMOOTH ON A RUNNING STACK AND DISPLAYS EACH TIME THE
429   ;; LASER IS FIRED.  USES STACKS AT 50,000 AND 47600.
430   ;;
431   ONESEC:   $SAVE
432              MOV     R5,-(SP)     ;SAVE REGISTERS R5-R0 ON THE STACK
433              MOV     R4,-(SP)
434              MOV     R3,-(SP)
435              MOV     R2,-(SP)
436              MOV     R1,-(SP)
437              MOV     R0,-(SP)
438             JSR      PC,ONEPS            ; TAKE A POINT
439             TST      RERROR              ; WAS THERE A REFERENCE ERROR ?
440             BNE      ONSCR               ; IF YES, IGNORE POINT AND RETURN
441             MOV      FS,R0               ; IF NOT SAVE POINT.
442             MOV      LP1,-(R0)
443             MOV      HP1,-(R0)
```

```
444             MOV     R0,FS           ; SAVE UPDATED STACK POINTER.
445             CMP     R0,#47704       ; IS STACK FULL YET ?
446             BGT     ONSCR           ; IF NOT, JUST GO ON.
447             MOV     #47704,FLPORE   ; IF FULL SET UP TO ORDER STACK.
448             MOV     #50000,FLPORB
449             MOV     #47600,FSO      ; INITIALIZE  ORDERED STACK POINTER
450             MOV     #47504,FSOE
451             JSR     PC,FLPOR        ; MAKE A NEW ORDERED STACK.
452             MOV     FSO,R0          ; POINT TO TOP OF ORDERED STACK.
453             SUB     #10,R0          ; SKIP FIRST TWO NUMBERS
454             MOV     -(R0),LP1       ; MOVE FIRST NUMBER ONTO WORKING STACK
455             MOV     -(R0),HP1
456             MOV     #CM5,R1         ; POINT TO FIRST COEFFICIENT.
457             MOV     (R1)+,HP2       ; LOAD COEFFICIENT ONTO WORKING STACK
458             MOV     (R1)+,LP2
459             MOV     #HP2,R5         ; POINT TO FLOATING POINT WORKING STACK
460             FMUL    R5              ; MULTIPLY FIRST PAIR ON STACK
461   ONSCL1:   MOV     -(R0),LP2       ; LOAD NEXT NUMBER
462             MOV     -(R0),HP2
463             MOV     (R1)+,HP3       ; LOAD NEXT COEFFICIENT
464             MOV     (R1)+,LP3
465             MOV     #HP3,R5         ; POINT TO TOP OF WORKING STACK
466             FMUL    R5              ; MULTIPLY NUMBER COEFFICEENT PAIR
467             FADD    R5              ; AND ACCUMULATE
468             CMP     R1,#C930        ; END OF STACK YET ?
469             BLT     ONSCL1          ; NO, MULTIPLY AND ACCUMULATE NEXT PAIR.
470             MOV     (R1)+,HP2       ; LOAD DIVISOR
471             MOV     (R1),LP2
472             MOV     #HP2,R5
473             FDIV    R5              ; DIVIDE FOR WEIGHTED AVERAGE
474             JSR     PC,DISPLY       ; CALL DISPLAY ROUTINE
475             MOV     #50000,FLPORB   ; LOAD BEGINNING OF STACK
476             MOV     #47704,FLPORE   ; LOAD END OF STACK
477             JSR     PC,MVDNST       ; MOVE DOWN STACK FOR NEXT POINT
478   ONSCR:    CLR     RERROR          ; MAKE SURE ERROR IS CLEARED
479             $RESTORE
480              MOV    (SP)+,R0    ;RESTORE REGISTERS R0-R5 FROM THE STACK
```

```
                MOV     (SP)+,R1
                MOV     (SP)+,R2
                MOV     (SP)+,R3
                MOV     (SP)+,R4
                MOV     (SP)+,R5
                RTS     PC                      ; RETURN TO INTERUPT HANDLER.
;;
;;&&&&&&&&&&&&&&&&&&&&&&&&&&&&&&&&&&&&&&&&&&&&&&&&&&&&&&&&&&&&&&&&&&&&&&
;;
;; FLOATING POINT STACK ORDERING PROGRAM.  INPUT STACK
;; FROM FLPORB TO FLPORE.  OUTPUT STACK STARTS AT FSO
;;
FLPOR:  $SAVE
                MOV     R5,-(SP)        ;SAVE REGISTERS R5-R0 ON THE STACK
                MOV     R4,-(SP)
                MOV     R3,-(SP)
                MOV     R2,-(SP)
                MOV     R1,-(SP)
                MOV     R0,-(SP)
        MOV     FLPORB,R0               ; POINT TO START OF STACK
        MOV     PADB,R1                 ; POINT TO START OF SCRATCH PAD
FLPR1:  MOV     -(R0),-(R1)             ; MAKE COPY OF BUFFER
        CMP     R0,FLPORE               ; END OF BUFFER ?
        BGT     FLPR1                   ; NO, KEEP COPYING
        MOV     R1,PADE                 ; YES, SAVE END OF SCRATCH PAD
        MOV     FSO,R5                  ; POINT TO TOP OF ORDERED STACK
FLPR2:  MOV     PADB,R4                 ; POINT TO START OF SCRATCH PAD
        SUB     #4,R4                   ; POINT TO FIRST HP IN SCRATCH PAD
        MOV     R4,R3
        SUB     #4,R3                   ; POINT TO SECOND HP IN SCRATCH PAD
FLPR3:  CMP     (R4),(R3)               ; IS NUMBER IN (R4) BIGGER THAN NUMBER IN R3
        BGT     FLPRB                   ; NO, JUST GO ON
        BLT     FLPRA                   ; IF LESS THAN REPLACE R4
        CMP     +2(R4),+2(R3)           ; IF EQUAL HP COMPARE LP'S
        BGT     FLPRB                   ; IF R4 LP LARGER, KEEP IT
FLPRA:  MOV     R3,R4                   ; POINT TO BIGGER NUMBER
FLPRB:  CMP     R3,PADE                 ; END OF SCRATCH PAD
```

```
        BLE     FLPRC           ; IF SO SAVE LARGEST NUMBER
        SUB     #4,R3           ; IF NOT, POINT TO NEXT HP IN PAD
        BR      FLPR3           ; AND KEEP COMPARING FOR LARGEST NUMBER
FLPRC:  MOV     +2(R4),-(R5)    ; SAVE LP OF LARGEST # IN ORDERED STACK
        MOV     (R4),-(R5)      ; SAVE HP ALSO
        CMP     R5,FSOE         ; IS ORDERED STACK FULL ?
        BLE     FLPRRT          ; YES, BRANCH EXIT
        MOV     #100001,(R4)    ; PUT LARGE NEG INTEGER IN VACANT HOLE
        BR      FLPR2           ; AND GO BACK TO FIND THE NEXT LARGEST NUMBER
FLPRRT: $RESTORE
         MOV    (SP)+,R0    ;RESTORE REGISTERS R0-R5 FROM THE STACK
         MOV    (SP)+,R1
         MOV    (SP)+,R2
         MOV    (SP)+,R3
         MOV    (SP)+,R4
         MOV    (SP)+,R5
        RTS     PC
;;
;;&&&&&&&&&&&&&&&&&&&&&&&&&&&&&&&&&&&&&&&&&&&&&&&&&&&&&&&&&&&&&&&&&&&&&&
;;
;; ROUTINE TO MOVE DOWN A FLOATING POINT STACK THAT
;; IS LOCATED BETWEEN FLPORB AND FLPORE , RESETS FS TO FSE-4
;;
MVDNST: $SAVE
         MOV    R5,-(SP)    ;SAVE REGISTERS R5-R0 ON THE STACK
         MOV    R4,-(SP)
         MOV    R3,-(SP)
         MOV    R2,-(SP)
         MOV    R1,-(SP)
         MOV    R0,-(SP)
        MOV     FLPORB,R0       ; POINT TO START OF STACK
        MOV     #-4,R1
        ADD     R0,R1           ; POINT TO SECOND LP IN STACK
MDS1:   MOV     -(R1),-(R0)     ; MOVE DOWN LOW PARTS
        MOV     -(R1),-(R0)     ; MOVE DOWN HIGH PARTS
        CMP     R1,FLPORE       ; END OF STACK YET ?
        BGT     MDS1            ; NO, KEEP SHIFTING
```

```
555             MOV     R0,FS           ; SET BACK STACK POINTER
556             $RESTORE
557              MOV    (SP)+,R0    ;RESTORE REGISTERS R0-R5 FROM THE STACK
558              MOV    (SP)+,R1
559              MOV    (SP)+,R2
560              MOV    (SP)+,R3
561              MOV    (SP)+,R4
562              MOV    (SP)+,R5
563             RTS     PC
564     ;;
565     ;;EEEEEEEEEEEEEEEEEEEEEEEEEEEEEEEEEEEEEEEEEEEEEEEEEEEEEEEEEEEEEEEEEEEEEEEEEEEE
566     ;;
567     ;; SUBROUTINE TO GENERATE FLOATING POINT COEFFICIENTS FOR SMOOTH
568     ;;
569     COEFNT: $SAVE
570              MOV    R5,-(SP)    ;SAVE REGISTERS R5-R0 ON THE STACK
571              MOV    R4,-(SP)
572              MOV    R3,-(SP)
573              MOV    R2,-(SP)
574              MOV    R1,-(SP)
575              MOV    R0,-(SP)
576             MOV     #NM3,R1         ; POINT TO FIXED POINT LIST
577             MOV     #CM3,R2         ; POINT TO FLOATING POINT LIST
578     CF1:    MOV     (R1)+,ITOF      ; FETCH NUMBER TO FLOAT
579             JSR     PC,NFLOAT       ; FLOAT NUMBER
580             MOV     HP,(R2)+        ; SAVE HIGH PART OF FLOATED NUMBER
581             MOV     LP,(R2)+        ; SAVE LOW PART OF FLOATED NUMBER
582             CMP     R1,#CM3         ; HAVE ALL NUMBERS BEEN FLOATED
583             BLT     CF1             ; NO, FLOAT NEXT NUMBER
584             $RESTORE                ; YES, RESTORE REGISTERS
585              MOV    (SP)+,R0    ;RESTORE REGISTERS R0-R5 FROM THE STACK
586              MOV    (SP)+,R1
587              MOV    (SP)+,R2
588              MOV    (SP)+,R3
589              MOV    (SP)+,R4
590              MOV    (SP)+,R5
591             RTS     PC
```

```
;;
;;&&&&&&&&&&&&&&&&&&&&&&&&&&&&&&&&&&&&&&&&&&&&&&&&&&&&&&&&&&&&&&&&&&&&&&&&&&&&
;;   P A R A M E T E R S    F O R    M L F S    P R O G R A M
;;&&&&&&&&&&&&&&&&&&&&&&&&&&&&&&&&&&&&&&&&&&&&&&&&&&&&&&&&&&&&&&&&&&&&&&&&&&&&
;;
NM3:        .WORD   -3                  ; INTIGER COEFFICIENTS
N12:        .WORD   14
N17:        .WORD   21
            .WORD   14
            .WORD   -3
N35:        .WORD   43
N1:         .WORD   1
N8:         .WORD   8.
NM5:        .WORD   -5.
NM30:       .WORD   -30.
N50:        .WORD   50
N100:       .WORD   100.
N200:       .WORD   200.
N300:       .WORD   300.
            .WORD   200.
            .WORD   100.
            .WORD   50.
            .WORD   -30.
            .WORD   -5.
N930:       .WORD   930.
CM3:        .WORD   0                   ; FLOATING POINT COEFFICIENTS
            .WORD   0
C12:        .WORD   0
            .WORD   0
C17:        .WORD   0
            .WORD   0
            .WORD   0
            .WORD   0
            .WORD   0
            .WORD   0
C35:        .WORD   0
            .WORD   0
```

```
629   C1:       .WORD   0
630             .WORD   0
631   HP8:      .WORD   0
632   LP8:      .WORD   0
633   CM5:      .WORD   0
634             .WORD   0
635   CM30:     .WORD   0
636             .WORD   0
637   C50:      .WORD   0
638             .WORD   0
639   C100:     .WORD   0
640             .WORD   0
641   C200:     .WORD   0
642             .WORD   0
643   C300:     .WORD   0
644             .WORD   0
645             .WORD   0
646             .WORD   0
647             .WORD   0
648             .WORD   0
649             .WORD   0
650             .WORD   0
651             .WORD   0
652             .WORD   0
653             .WORD   0
654             .WORD   0
655   C930:     .WORD   0
656             .WORD   0
657   ;;
658   HZ:       .WORD   3               ; FREQUENCY OF PULSES, 60THS/PERIOD
659   EVCTR:    .WORD   0               ; EVENT COUNTER
660   DM:       .WORD   0               ; DISPLAY MODE
661   SN:       .WORD   0               ; SMOOTHING MODE
662   SF:       .WORD   1               ; SCALING FACTOR
663   SFHP:     .WORD   040000          ; FLOATED SCALING FACTOR
664   SFLP:     .WORD   0
665   WADC:     .WORD   1               ; ADC COMMAND
```

```
629   C1:       .WORD   0
630             .WORD   0
631   HP8:      .WORD   0
632   LP8:      .WORD   0
633   CM5:      .WORD   0
634             .WORD   0
635   CM30:     .WORD   0
636             .WORD   0
637   C50:      .WORD   0
638             .WORD   0
639   C100:     .WORD   0
640             .WORD   0
641   C200:     .WORD   0
642             .WORD   0
643   C300:     .WORD   0
644             .WORD   0
645             .WORD   0
646             .WORD   0
647             .WORD   0
648             .WORD   0
649             .WORD   0
650             .WORD   0
651             .WORD   0
652             .WORD   0
653             .WORD   0
654             .WORD   0
655   C930:     .WORD   0
656             .WORD   0
657   ;;
658   HZ:       .WORD   3               ; FREQUENCY OF PULSES, 60THS/PERIOD
659   EVCTR:    .WORD   0               ; EVENT COUNTER
660   DM:       .WORD   0               ; DISPLAY MODE
661   SM:       .WORD   0               ; SMOOTHING MODE
662   SF:       .WORD   1               ; SCALING FACTOR
663   SFHP:     .WORD   040000          ; FLOATED SCALING FACTOR
664   SFLP:     .WORD   0
665   WADC:     .WORD   1               ; ADC COMMAND
```

```
666   ROFHP:    .WORD   0               ; REFERENCE OFFSET
667   ROFLP:    .WORD   0
668   SOFHP:    .WORD   0               ; SIGNAL OFFSET
669   SOFLP:    .WORD   0
670   INITMSG:  .WORD   0
671   ;;
672   HPC:      .WORD   0               ; FLOATING POINT STACK
673   LPC:      .WORD   0
674   HPB:      .WORD   0
675   LPB:      .WORD   0
676   HPA:      .WORD   0
677   LPA:      .WORD   0
678   HP3:      .WORD   0
679   LP3:      .WORD   0
680   HP2:      .WORD   0
681   LP2:      .WORD   0
682   HP1:      .WORD   0
683   LP1:      .WORD   0
684   ;;
685   ETST:     .WORD   0               ; ERROR FP STACK TEST WORD
686   FS:       .WORD   50000           ; START OF SEQUENTIAL STACK
687   FSO:      .WORD   47600           ; START OF ORDERED STACK
688   RERROR:   .WORD   0               ; ERROR IN REFERENCE FLAG (BAD SHOT)
689   FLPORB:   .WORD   50000
690   FLPORE:   .WORD   50000
691   PADB:     .WORD   35000           ; BEGINNING OF SCRATCH PAD
692   PADE:     .WORD   0               ; END OF SCRATCH PAD
693   FSOE:     .WORD   0               ; END OF ORDERED BUFFER
694   NPTA:     .WORD   1               ; NUMBER OF POINTS TO AVERAGE
695   NPTAHP:   .WORD   040000          ; FLOATED NUMBER OF POINTS
696   NPTALP:   .WORD   0
697   ;;
698   ;;&&&&&&&&&&&&&&&&&&&&&&&&&&&&&&&&&&&&&&&&&&&&&&&&&&&&&&&&&&&&&&&&&&&&&&&&
699   ;;  M E S S A G E    B U F F E R   F O R    M L F S
700   ;;
701   MSG1:     .BYTE   CR,LF,LF,LF,LF
702             .ASCII  ' Molectron Laser/ Evans Box Fluorescence Program'
```

```
703             .BYTE   CR,LF
704             .ASCII  'Type  NUL  to enter new  Display Mode'
705             .BYTE   CR,LF,SPC,SPC,SPC
706             .ASCII  'zero for signal only,-1 for reference only, and'
707             .ASCII  ' +1 for normalized fluorescence'
708             .BYTE   CR,LF
709             .ASCII  'Type  CONTROL C  to enter new smoothing mode'
710             .BYTE   CR,LF,SPC,SPC,SPC
711             .ASCII  'zero for unaveraged, -1 for five point smooth'
712             .ASCII  ', and +1 for fifteen point smooth'
713             .BYTE   CR,LF
714             .ASCII  'Type  0  to enter new scaling factor'
715             .BYTE   CR,LF
716             .ASCII  'Type  +  to enter a new DC offset for disply'
717             .BYTE   CR,LF,LF
718             .ASCII  ' Type slash,  /  , and turn on LTC to start laser'
719             .ASCII  ', Type slash or turn off LTC to turn off laser'
720             .BYTE   CR,LF,LF
721             .ASCII  ' Type  N  to change states of the noisy flag'
722             .ASCII  ' or to enter number of points to average '
723             .BYTE   CR,LF
724             .ASCII  ' Type  G  to reinitialize the program to signal'
725             .ASCII  ' only, no smooth, scale factor =1, and  N not set'
726             .BYTE   CR,LF,LF,LF,LF,LF,LF,LF,LF,STOP
727   NMSG:     .BYTE   CR,LF
728             .ASCII  'Enter number of points to average .. '
729             .BYTE   STOP
730   MSG2:     .ASCII  ' NEW DISPLAY MODE .. '
731             .BYTE   STOP
732   MSG3:     .ASCII  ' NEW SMOOTHING MODE .. '
733             .BYTE   STOP
734   MSG4:     .ASCII  ' NEW SCALING FACTOR .. '
735             .BYTE   STOP
736   MSG5:     .BYTE   CR,LF
737             .ASCII  ' Program Reinitialized. '
738             .BYTE   CR,LF,LF,LF,STOP
739   MSG6:     .ASCII  ' NEW DC-OFFSET .. '
```

```
                .BYTE   STOP
                .EVEN
;;
;;&&&&&&&&&&&&&&&&&&&&&&&&&&&&&&&&&&&&&&&&&&&&&&&&&&&&&&&&&&&&&&&&&&&&&&
;;
;;   G E N E R A L    S U B R O U T I N E S
;;
;;&&&&&&&&&&&&&&&&&&&&&&&&&&&&&&&&&&&&&&&&&&&&&&&&&&&&&&&&&&&&&&&&&&&&&&
;; DISPLAY ROUTINE, TO OUTPUT NUMBER CONTAINED IN FLOATING POINT
;; LOCATION ONE TO DAC1 AFTER ADDITIONAL AVERAGING AND ADDITION
;; OF OFFSETS AS REQUIRED.  OUTPUT IS RESTRICTED TO BETWEEN ZERO
;; AND +5 VOLTS.
;;
DISPLY:         MOV     R5,-(SP)        ; SAVE R5
                TST     NOISY           ; TEST THE NOISY FLAG
                BLE     MVCC            ; IF NOT SET JUST DISPLAY NUMBER
                JSR     PC,NSYDISP      ; IF SET, DO AVERAGE OF DISPLAYED POINTS
MVCC:           MOV     SFHP,HP2        ; RECALL SCALE FACTOR
                MOV     SFLP,LP2
                MOV     #HP2,R5
                FMUL    R5              ; POINT TIMES SCALE FACTOR
                MOV     HP1,HP          ; PREPARE TO FIX VALUE OF AVERAGE
                MOV     LP1,LP
                JSR     PC,FIX
                ADD     VOFS,FIXED      ; ADD IN ANY IMPOSED OFFSET
                CMP     FIXED,#3777
                BLE     MVCA
                MOV     #3777,FIXED
MVCA:           TST     FIXED
                BGE     MVCB
                CLR     FIXED
MVCB:           MOV     FIXED,@#DAC1    ; DISPLAY #
                MOV     (SP)+,R5
                RTS     PC
;;
;;&&&&&&&&&&&&&&&&&&&&&&&&&&&&&&&&&&&&&&&&&&&&&&&&&&&&&&&&&&&&&&&&&&&&&&
;; ROUTINE TO DO RUNNING AVERAGE ON OUTPUT DATA, PARAMETERS ARE
```

```
777   ;; CALCULATED FROM KEYBOARD ENTRY BY COMMAND MONITOR, E, WITH
778   ;; DATA RECIEVED AND PASSED IN FLOATING POINT STACK LOCATION ONE
779   ;;
780   NSYDISP: $SAVE
781              MOV     R5,-(SP)     ;SAVE REGISTERS R5-R0 ON THE STACK
782              MOV     R4,-(SP)
783              MOV     R3,-(SP)
784              MOV     R2,-(SP)
785              MOV     R1,-(SP)
786              MOV     R0,-(SP)
787             MOV      NDISPS,R0        ; RETRIEVE STACK POINTER
788             MOV      LP1,-(R0)        ; SAVE LAST POINT ON STACK
789             MOV      HP1,-(R0)
790             MOV      R0,NDISPS        ; SAVE UPDATED STACK POINTER
791             CMP      R0,NDISPE        ; ARE WE AT END OF STACK ?
792             BGT      NDSPR            ; IF NOT, BRANCH OUT
793             MOV      #20000,R0        ; IF SO, PREPARE TO TAKE AVERAGE OF STACK
794             MOV      -(R0),LP1        ; RETRIEVE FIRST POINT INTO FP STACK
795             MOV      -(R0),HP1
796   NDSPL1:   CMP      R0,NDISPE        ; END OF STACK YET ?
797             BLE      NDSPC            ; IF SO DEVIDE BY NPTA
798             MOV      -(R0),LP2        ; IF NOT GET NEXT POINT
799             MOV      -(R0),HP2
800             MOV      #HP2,R5          ; PREPARE TO ADD
801             FADD     R5               ; ACCUMULATE POINT FOR AVERAGE
802             BR       NDSPL1           ; GET NEXT POINT
803   NDSPC:    MOV      NPTAHP,HP2       ; RETRIEVE NUMBER OF POINTS
804             MOV      NPTALP,LP2
805             MOV      #HP2,R5          ; PREPARE TO DIVIDE
806             FDIV     R5               ; FIND AVERAGE, LEAVE IN ONE
807             MOV      FS,-(SP)         ; SAVE OLD FS POINTER
808             MOV      #20000,FLPORB    ; LOAD BEGINNING OF STACK
809             MOV      NDISPE,FLPORE    ; AND ITS END FOR MOVE DOWN
810             JSR      PC,MVDNST        ; MOVE STACK DOWN FOR NEXT POINT
811             MOV      FS,NDISPS        ; SAVE UPDATED STACK POINTER
812             MOV      (SP)+,FS         ; RESTORE OLD FS
813   NDSPR:    $RESTORE
```

```
814             MOV     (SP)+,R0    ;RESTORE REGISTERS R0-R5 FROM THE STACK
815             MOV     (SP)+,R1
816             MOV     (SP)+,R2
817             MOV     (SP)+,R3
818             MOV     (SP)+,R4
819             MOV     (SP)+,R5
820             RTS     PC                  ; RETURN TO CALLING ROUTINE
821     ;;
822     NDISPS: .WORD   20000               ; BEGINNING OF RUNNING AVERAGE STACK
823     NDISPE: .WORD   17774               ; END OF RUNNING STACK
824     ;;
825     ;;&&&&&&&&&&&&&&&&&&&&&&&&&&&&&&&&&&&&&&&&&&&&&&&&&&&&&&&&&&&&&&&&&&&&
826     ;; RESET TO SEND A RESET PULSE AT CSR0 OF 167770 OF STEPPING MOTOR INTERFACE
827     ;;
828     RESET:  BIS     #1,@#167770
829             BIC     #1,@#167770
830             RTS     PC
831     ;;&&&&&&&&&&&&&&&&&&&&&&&&&&&&&&&&&&&&&&&&&&&&&&&&&&&&&&&&&&&&&&&&&&&&
832     ;;&&&&&&&&&&&&&&&&&&&&&&&&&&&&&&&&&&&&&&&&&&&&&&&&&&&&&&&&&&&&&&&&&&&&
833     ;;
834     ;;  V E R Y   G E N E R A L     S U B R O U T I N E S
835     ;;
836     ;;&&&&&&&&&&&&&&&&&&&&&&&&&&&&&&&&&&&&&&&&&&&&&&&&&&&&&&&&&&&&&&&&&&&&
837     PKL:    TSTB    @#TPS               ; SUBROUTINE TO PRINT R0
838             BPL     PKL
839             MOV     R0,@#TPB
840             RTS     PC
841     ;;
842     ;;&&&&&&&&&&&&&&&&&&&&&&&&&&&&&&&&&&&&&&&&&&&&&&&&&&&&&&&&&&&&&&&&&&&&
843     ;;
844     PNEXT:  MOV     R0,-(SP)            ; SUBROUTINE TO PRINT MESSAGES
845     PNEXTE: MOVB    (R3)+,R0            ; GET CHARACTER
846             JSR     PC,PKL              ; PRINT CHARACTER
847             CMPB    (R3),#STOP          ; LAST BYTE OF MESSAGE ?
848             BNE     PNEXTE              ; NO, GET NEXT BYTE.
849             MOV     (SP)+,R0
850             RTS     PC                  ; YES, RETURN.
```

```
;;
;;&&&&&&&&&&&&&&&&&&&&&&&&&&&&&&&&&&&&&&&&&&&&&&&&&&&&&&&&&&&&&&&&&&&&&&&&
;;
CRLF:    MOV    #TAM3,R3         ; SUBROUTINE TO PRINT CR LF
         JSR    PC,PNEXT
         RTS    PC
TAM3:    .BYTE  CR,LF,STOP
         .EVEN
;;
;;&&&&&&&&&&&&&&&&&&&&&&&&&&&&&&&&&&&&&&&&&&&&&&&&&&&&&&&&&&&&&&&&&&&&&&&&
;; A ROUTINE TO GET A DECIMAL NUMBER FROM KEYBOARD TO R1
;;
GTDCML:  MOV    R5,-(SP)
         MOV    R4,-(SP)
         MOV    R3,-(SP)
         MOV    R2,-(SP)
         MOV    R0,-(SP)
GDCMLE:  CLR    R0               ; CLEAR WORKING REGISTER
         CLR    R1               ; CLEAR ACCUMULATER
         CLR    R3               ; CLEAR SIGN POINTER
         MOV    #5,R2            ; SET UP DIGIT COUNTER
DGDT:    JSR    PC,TCHR          ; TAKE CHARACTER
         CMPB   #MINUS,R0        ; IS CHARACTER A MINUS SIGN
         BNE    DC1              ; NO, GO ON.
         INC    R3               ; YES, INCRIMENT R3 AS SIGN POINTER
         BR     DC3              ; GO BACK FOR NEXT CHARACTER
DC1:     CMPB   #PLUS,R0         ; IS THE CHARACTER A POSITIVE SIGN ?
         BNE    DC2              ; NO, CONTINUE
         CLR    R3               ; INDICATE POSITIVE # IN SIGN POINTER
         BR     DC3              ; GO GET NEXT CHARACTER
DC2:     CMPB   R0,#SPC          ; IS CHARACTER A CARRIAGE RETURN ?
         BEQ    DRTRN            ; YES, RETURN.
         SUB    #60,R0           ; DECODE, IS IT TOO SMALL ?
         BMI    DERR             ; YES, TYPE ILLEGAL DIGIT.
         CMP    R0,#11           ; IS DIGIT TOO LARGE ?
         BGT    DERR             ; YES , TYPE ILLEGAL DIGIT
         DEC    R2               ; DECRIMENT DIGIT COUNTER
```

```
              BLT     DTMD                ; IF TOO MANY DIGITS ERROR END
              CLC
                                          ; SHIFT ACCUMULATOR FOR NEW DIGIT
              MUL     #12,R1
              BCS     DTMD                ; NOTIFY IF # TOO LARGE
              BLT     DTMD                ; IF IT HAS BECOME NEG IT IS TOO LARGE
              ADD     R0,R1               ; ADD NEW DIGIT TO ACCUMULATER
              BMI     DTMD                ; JUST SLIGHTLY ILLEGAL #'S GET TO HERE
              ADD     #60,R0              ; RECODE DIGIT
      DC3:    JSR     PC,PKL              ; PRINT DIGIT
              BR      DGDT
      DRTRN:  TST     R3                  ; TEST SIGN
              BEQ     DRTRN2              ; IF PLUS GO ON
              NEG     R1                  ; IF NEGATIVE NEGATE MAGNITUDE
      DRTRN2: MOV     #SPC,R0
              JSR     PC,PKL
              MOV     (SP)+,R0
              MOV     (SP)+,R2
              MOV     (SP)+,R3
              MOV     (SP)+,R4
              MOV     (SP)+,R5
              RTS     PC
      DERR:   MOV     #DEM1,R3            ; GET STARTING ADDRESS OF MESSAGE
              ADD     #60,R0              ; RECODE BAD CHARACTER
              JSR     PC,PKL              ; ECHO BAD CHARACTER
              JSR     PC,PNEXT
              BR      GDCMLE
      DTMD:   MOV     #DEM2,R3
              ADD     #60,R0              ; RECODE DIGIT
              JSR     PC,PKL              ; ECHO LAST DIGIT
              JSR     PC,PNEXT
              BR      GDCMLE
      ;;
      ;;&&&&&&&&&&&&&&&&&&&&&&&&&&&&&&&&&&&&&&&&&&&&&&&&&&&&&&&&&&&&&&&&&&&&&&
      ;;  TAKE CHARACTER SUBROUTINE, WAITS IN LOOP FOR CHARACTER THEN
      ;;  RETURNS IT IN R0 AFTER STRIPPING OFF PARITY
      ;;
```

```
TCHR:   INC     @#TKS
TCHRL:  TSTB    @#TKS
        BPL     TCHRL
        MOV     @#TKB,R0
        BIC     #177600,R0
        CLR     @#TKB
        CLR     @#TKS
        RTS     PC
;;
DEM1:
        .BYTE  CR,LF
        .ASCII  ' ILLEGAL DECIMAL DIGIT,  RETYPE '
        .BYTE  CR,LF
        .BYTE  STOP
        .EVEN
;;
DEM2:
        .BYTE  CR,LF
        .ASCII  ' NUMBER TOO LARGE ,RETYPE '
        .BYTE  CR,LF,STOP
        .EVEN
;;
;;&&&&&&&&&&&&&&&&&&&&&&&&&&&&&&&&&&&&&&&&&&&&&&&&&&&&&&&&&&&&&&&&&&&&&&&&&&&&&&&&&&&
;; FIXN, A PROGRAM TO FIX AN OCTAL INTIGER FROM A NORMALIZED
;; FLOATING POINT NUMBER.
;; TAKES THE FLOATING POINT NUMBER FROM HP AND LP AND PUTS
;; THE SINGLE PRECISION INTIGER INTO FIXED.
;; EXPECTS CALLS OF THE FORM  JSR PC,FIX
;;
FIX:    $SAVE
         MOV    R5,-(SP)      ;SAVE REGISTERS R5-R0 ON THE STACK
         MOV    R4,-(SP)
         MOV    R3,-(SP)
         MOV    R2,-(SP)
         MOV    R1,-(SP)
         MOV    R0,-(SP)
        CLR     R0                  ; CLEAR SIGN POINTER
```

```
962             MOV     HP,R1           ; READ  HP TO DECIFER EXPONENT
963             BPL     FIXC1           ; IF POSITIVE GO ON
964             INC     R0              ; IF NEGATIVE SET SIGN POINTER
965     FIXC1:  ASH     #-7,R1          ; SHIFT EXPONENT INTO POSITION
966             BIC     #177400,R1      ; STRIP OFF SIGN BIT
967             SUB     #200,R1         ; DECODE EXPONENT
968             BLE     ZERON           ; IF EXP <1 NUMBER IS ZERO
969             CMP     #17,R1          ; IS # TOO LARGE ?
970             BLT     MAXN            ; YES , SHOW MAX
971             MOV     HP,R4           ; RETREAVE HIGH PART
972             MOV     LP,R5           ; RETREAVE LOW PART
973             BIC     #177600,R4      ; STRIP OFF EXPONENT AND SIGN
974             BIS     #000200,R4      ; PUT IN HIDDEN BIT
975             SUB     #10,R1          ; ACCOUNT FOR PREDISPLACEMENT OF BITS
976             ASHC    R1,R4           ; SHIFT BITS INTO PLACE WITH EXPONENT
977     FRTN:   TST     R0
978             BEQ     FIXC2           ; IF POS DON'T NEGATE
979             NEG     R4              ; IF NEG NEGATE MAGNITUDE
980     FIXC2:  MOV     R4,FIXED
981             $RESTORE
982              MOV    (SP)+,R0     ;RESTORE REGISTERS R0-R5 FROM THE STACK
983              MOV    (SP)+,R1
984              MOV    (SP)+,R2
985              MOV    (SP)+,R3
986              MOV    (SP)+,R4
987              MOV    (SP)+,R5
988             RTS     PC
989     ZERON:  CLR     R4
990             BR      FIXC2
991     MAXN:   MOV     #77777,R4
992             BR      FRTN
993     FIXED:  .WORD   0
994     ;;
995     ;;&&&&&&&&&&&&&&&&&&&&&&&&&&&&&&&&&&&&&&&&&&&&&&&&&&&&&&&&&&&&&&&&&&&&&&&&
996     ;; SUBROUTINE NFLOAT TO FLOAT SINGLE PRECISION OCTAL NUMBERS
997     ;; EXPECTS CALLS OF THE FORM  JSR  PC,NFLOAT
998     ;; THE NUMBER TO FLOAT IS STORED IN ITOF AND THE RESULTS ARE RETURNED
```

```
 999    ;; IN HP AND LP
1000    ;;
1001    NFLOAT:  CLR      HP                ; CLEAR LOCATION FOR HIGH PART
1002             $SAVE
1003               MOV     R5,-(SP)      ;SAVE REGISTERS R5-R0 ON THE STACK
1004               MOV     R4,-(SP)
1005               MOV     R3,-(SP)
1006               MOV     R2,-(SP)
1007               MOV     R1,-(SP)
1008               MOV     R0,-(SP)
1009              CLR      LP                ; CLEAR LOCATION FOR LOW PART
1010              MOV      ITOF,R3           ; READ IN INTEGER TO FLOAT
1011    ;;
1012              ASL      R3                ;TEST SIGN, IS NUMBER ZERO OR NEGATIVE?
1013              BNE      NOTZER            ;NOT ZERO, CONTINUE
1014              CLR      R2                ;ZERO, PUT ZERO IN R2,
1015              CLR      R3
1016              BR       NFRTN             ;AND RETURN
1017    NOTZER:   MOV      #220,R2           ;NO, SET STARTING VALUE OF EXPONENT
1018              BCC      SHIFT             ;NOT NEGATIVE, CONTINUE.
1019              BIS      #400,R2           ;NEGATIVE, SET SIGN BIT IN R2,
1020              NEG      R3                ;AND GET A POSITIVE MANTISSA
1021    SHIFT:    ASL      R3                ;SHIFT NUMBER, LOOK FOR HIGHEST DIGIT
1022              DEC      R2                ;CORRECT EXPONENT FOR SHIFTED NUMBER
1023              BCC      SHIFT             ;CARRY NOT SET, LOOK AT NEXT BIT
1024              ASHC     #7,R2             ;ASHC 2,#7,  SHIFT FLOATED WORD
1025    ;;
1026    NFRTN:    MOV      R3,LP             ; STORE LOW PART
1027              MOV      R2,HP             ; STORE HIGH PART
1028              $RESTORE
1029               MOV     (SP)+,R0      ;RESTORE REGISTERS R0-R5 FROM THE STACK
1030               MOV     (SP)+,R1
1031               MOV     (SP)+,R2
1032               MOV     (SP)+,R3
1033               MOV     (SP)+,R4
1034               MOV     (SP)+,R5
1035              RTS     PC
```

```
ITOF:     .WORD   0
HP:       .WORD   0
LP:       .WORD   0
;;
;;&&&&&&&&&&&&&&&&&&&&&&&&&&&&&&&&&&&&&&&&&&&&&&&&&&&&&&&&&&&&&&&&&&&
;;
VOFS:     .WORD   0                  ; VOLTAGE OFFSET
          .END
```

CROSS-REFERENCE LISTING = MEANS EQUATED %=REGISTER '=GLOBAL

SYMBOL		VALUE	DEF	REFERENCES													
A		000306	125	117													
ADCDT	=	176772	38	250	262												
ADCINT	=	000130	39														
ADCIS	=	000132	40														
ADCSR	=	176770	37	247	248	259	260										
AT	=	000100	54	135													
B		000354	135	126													
BELL	=	000007	65	148	335												
BGNG		000004	81	177													
BLNBL		000734	197	90	150	333											
C		000442	148	136													
CC	=	000003	46	125													
CF1		002706	578	583													
CLKIH		000750	208	84													
CM3		003022	617	391	577	582											
CM30		003066	635														
CM5		003062	633	456													
COEFNT		002662	569	100													
CR	=	000015	61	701	703	705	708	710	713	715	717	720	723	726	727	736	738
				857	935	937	942	944									
CRLF		005376	854	118	123	128	133	137	146	151	171	180	185	189			
C1		003052	629	322													
C100		003076	639														
C12		003026	619	330													
C17		003032	621														
C200		003102	641														
C300		003106	643														
C35		003046	627	403													
C50		003072	637														
C930		003136	655	468													
DAC1	=	176760	43	771													
DAC2	=	176762	52														
DC1		005456	877	874													
DC2		005470	881	878													

```
MAXN        006142   991  970
MDS1        002626   551  554
MEC         000570   171  156
MINUS   =   000055    64  873
MLFS        000000     1
MSG1        003254   701  105
MSG2        004575   730  119
MSG3        004623   732  129
MSG4        004653   734  138
MSG5        004703   736  175
MSG6        004742   739  181
MVCA        005070   768  766
MVCB        005102   771  769
MVCC        005002   757  755
MVDNST      002600   541  412  477  810
N       =   000116    56  153
NDISPE      005320   823  166  791  796  809
NDISPS      005316   822  162  787  790  811
NDSPC       005220   803  797
NDSPL1      005172   796  802
NDSPR       005300   813  792
NFLOAT      006152  1001   97  143  168  267  579
NFRTN       006242  1026 1016
NHSG        004525   727  157
NM3         002752   597  576
NM30        002774   606
NM5         002772   605
NOISY       000736   198   95  155  754
NOTZER      006214  1017 1013
NPTA        003246   694  160  167
NPTAHP      003250   695  169  803
NPTALP      003252   696  170  804
NSYDIS      005114   780  756
NUL     =   000000    55  116
N1          002766   603
N100        003000   608
N12         002754   598
N17         002756   599
N200        003002   609
N300        003004   610
N35         002764   602
```